
THE UNIVERSITY
*of* EDINBURGH

# The effect of cortical bone decollagenisation on fracture biomechanics at low strain rate

Khalid Ghassan Al-Hourani


Doctor of Medicine (M.D.)

The University of Edinburgh

2020

## ABSTRACT

### Introduction

The ability of bone to resist failure is directly dependant on the intrinsic properties, namely the inorganic (hydroxyapetite) and organic (collagen) contents. Traditionally, inorganic content has been associated with stiffness of bone, whereas organic content has been associate with toughness. The aim of this research is to study the biomechanical effects of staged demineralisation and decollagenisation of femoral cortical segments. The staged protocol for decollagenisation should be considered a novel component of this study.

A clinical correlation study to complement the biomechanical work was also undertaken. Femoral shaft fracture patterns in all ages were clinically and radiologically assessed to delineate if any correlation exists with the biomechanical findings of manipulated bone.

### Methods

Ovine femoral cortical bone specimens were demineralised in 10% EDTA under ultrasonic assistance. Decollagenisation was achieved using 5M and 10M NaOH solution at 44 degrees celsius. Bone processing was undertaken at time points 0, 6, 12, 24 and 48 hours. Samples were mechanically tested under low strain four-point bending. ANOVA testing was undertaken to compare groups with $p<0.05$ significant.

This biomechanical data was correlated with clinical data analysing femoral shaft fractures in three age groups; (paediatric (0-16), adult (17-54) and older age (>55)) to reflect immature, peak bone age and osteoporotic bone respectively. Binary logistic analysis was used to assess significance of bone age with respect to fracture pattern (p-value <0.05 was significant).

**Results**

Demineralised bone demonstrated a reduction of ultimate strength, yield strength and elastic modulus at 48 hours ($p<0.05$). There was significant increase in toughness at 48 hours.

Decollagenised bone showed a reduction in ultimate and yield strength at 12 hours. There was an initial increase in elastic modulus at 6 hours after immersion in both NaOH solutions ($p<0.05$), followed by progressive reduction. There was over 70% decrease in toughness in decollagenised samples at 48 hours ($p<0.05$).

A total of 163 patients with femoral shaft fractures were analysed. Paediatric, adult and older groups included 38, 37 and 88 patients respectively. One hundred and two (102) fractures were simple and 61 comminuted. Paediatric and older groups were more likely to sustain a simple fracture, with the adult group more likely to sustain a high energy comminuted fracture.

**Conclusion**

Demineralised bone develops an increased ability to deform under bending with an increase in yield strain, ultimate strain and post-yield strain. This makes it tougher, behaving as a ductile material.

In contrast, decollagenised cortical bone behaves as a brittle material. There is a progressive decrease in yield and ultimate properties of stress and strain. Post-yield properties are almost zero with greater rates of decollagenisation.

This study demonstrates an association between degree of fracture comminution and physiological age, with simple fractures being significantly associated with immature and osteoporotic bone. High energy mechanism trauma was directly related to fracture comminution at peak bone age.

## LAY SUMMARY

Bone is dependant on its natural constituents for its strength. Within bone is a smaller set of elements (inorganic and organic). The inorganic content is mainly composed of calcium and the organic content is mainly composed of a protein called collagen. The collagen is thought to convey the property of resistance to breaking, whereas the inorganic content conveys resistance to bone being bent. This thesis aimed to remove the collagen content of sheep thigh (femur) bone in a staged fashion, and to study the effect of this on its bending behaviour until it breaks (fracture). This is considered the novel component. This study also aimed to see if laboratory results correlated with real-life injuries to this same bone in human beings.

If bone can be manipulated in staged way, this can allow the scientific community to better study how bone breaks. This information can be used to help design electronic models that can help predict how bone will behave as opposed to testing this on animals or cadaveric human bone. This will also aid in the prevention of fracture, and design of stronger devices to fix fractures in weaker bone.

The calcium and collagen content was removed in stages (over time) using specific solutions. At this point, the segments of femoral shaft were tested using a machine that bends the bone and records the measurements electronically. This was done at a low bending force. Patients who sustained a thigh fracture, were also analysed to record how their bone broke. The assumption was that children's bone had less calcium and elderly bone less collagen.

In bone in which the calcium was removed, this resisted bending better, and became more bendable in nature (ductile). In bone with collagen removed, this showed an initial increased resistance to bending, however as further collagen removal occurred, this decreased. Collagen removed bone also showed a gradual decrease in the resistance to breaking until it was extremely susceptible to breaking under the smallest force.

Decollagenised bone behaves as a material more closely linked to elderly bone behaviour. The more collagen is removed from bone, the easier it breaks. Child and elderly bone is more likely to break into two parts under force. Adult bone is more likely to shatter into many pieces under force.

**Declaration**

I, Khalid Ghassan Al-Hourani, declare that this thesis and the work presented in it are my own and has been generated by me as the result of my own original research. This work was done wholly whilst in candidature for a research degree at the University of Edinburgh. Where I have consulted the published work of others, this is always clearly attributed and where I have quoted the work of others, the source is always referenced. With the exception of such references, this thesis is entirely my own work. The material contained in this thesis has not been submitted in whole or any part for any other degree or qualification at this university or any other.

Khalid Ghassan Al-Hourani

April 2020

**Acknowledgements**

I would like to give thanks to:

Firstly my supervisors, Professor Hamish Simpson and Dr Robert Wallace for their invaluable direction, advice and support throughout.

I would like to thank the radiology department at the Royal Infirmary of Edinburgh for helping me process the radiographs. Additionally, a special mention to AP Jess Abattoirs, for providing ovine bone for the study.

I would like to thank my mother Zaida, my father Ghassan, my brother Ammar and my sister Dania for their continued love and support throughout my life, without which I would not succeed. Last but not least, I am grateful to my loving wife Maria for her kindness and belief.

”وَأَن لَّيْسَ لِلإِنسَانِ إِلاَّ مَا سَعَى“

“One can have only that for which they make the effort”

# Contents

# List of tables

# List of figures

# 1. INTRODUCTION

## 1.1 Aims

Bone is a composite material, that has structural, biochemical, endocrine and haematopoietic responsibilities in the human body [1]. It consists of cellullar, extracellular and water components [1]. The cellular components include osteocytes, osteoblasts and osteoclasts, with the extracellular components consisting of an inorganic (calcium hydroxyaptetite) and organic (mainly collagen type I) phase. Alongside water, these three components form a three-dimensional matrix that is in essence a mineralised collagen fibril [2].The inorganic content imparts bone stiffness especially in compression [3, 4]. The organic content is important for bone toughness or the energy required to fracture [5-7].

A simplified analogy of bone could be thought of in the form of a cheesecake. In order to understand how the cheesecake bends as a whole structure, it is essential to understand how the constituents, namely the cheese and the digestive base, behave. The reason this is essential is that it is presumed that the cheese will impart different biomechanical properties to that of the digestive base, and in combination, these will dictate how the cheesecake behaves under bending. The cheesecake in this analogy is the femoral shaft as a macro-structure (extrinsic properties), with the cheese and the digestive base forming the micro-structure - or the organic (collagen) and inorganic properties (calcium hydroxyapatite). These are otherwise referred to as the intrinsic properties.

To date, removing collagen from bone has been done with a starting point and an end point of decollagenisation, with little ability to stage this process in between. For example - let us assume a linear line graph with the x-axis representing time and the y axis representing force required to fracture, under a bending load. If the only two studied time points of decollagenisation on the x-axis are at 0 and 100 hours, it is not scientific enough to assume that the force at 50 hours can be predicted in a linear fashion. The reason for this is that bone has not been decollagenised to 50 hours, only at 0 and 100 hours, and therefore it is impossible to delineate this information with confidence.

Additionally, whilst the literature (which will be explored in the subsequent review), has extensively studied the effect of staged demineralisation on cortical bone, this has been reserved for whole bone measurements and synthetically staged experimentation on bone segments remains scarce. This skews the results significantly given it cannot isolate the intrinsic contribution of mineral, on the biomechanical behaviour of bone. It is these deficiencies in the literature that this thesis aims to address.

This research aims to devise a novel staged protocol for the demineralisation and decollagenisation of ovine femoral shaft cortical segments. This research will examine the effects of varying degrees of mineral and collagen disruption on bending behaviour of cortical ovine bone at a low strain rate as baseline. It is intended that the findings from this thesis are to be used to predict behaviour in fragility fractures, and in particular osteoporotic fracture modelling, as this condition affects both the mineral and collagen components.

The epidemiology of femoral shaft fractures is well studied. However, what is less known is the fracture patterns that occur under varying mechanisms of energy across all ages. Furthermore, there is no clear evidence in the literature to suggest a physiological age at which bone behaviour changes in clinical practice. This thesis aims to address these deficiencies in the literature. This thesis also aims to delineate wether bone behaviour findings at the nanostructure, relate to macro-structure whole bone behaviour in a clinical setting.

## 1.2 Research questions

The following research questions will be addressed in this thesis:

1. Does cortical bone biomechanical behaviour change with disruption of the mineral content at a low strain rate?
2. Does cortical bone biomechanical behaviour change with disruption of the collagen content at a low strain rate?
3. Is there a correlation between the behaviour of demineralised ovine cortical bone segments and femoral shaft fractures in clinical practice?
4. Is there a correlation between the behaviour of decollagenised ovine cortical bone segments and femoral shaft fractures in clinical practice?

Research questions 1 and 2, are primarily laboratory based questions. Ovine cortical bone segments will be processed to allow demineralisation and decollagenisation as will be described later in this thesis. The segments will then be mechanically tested to delineate values under bending behaviour until failure.

Research questions 3 and 4, are primarily clinical questions. Femoral shaft fractures will form the basis of this component to allow a more valid comparison to ovine femoral cortical bone. Bone behaviour will be analysed to delineate wether with increasing age, there is an effect on fracture pattern (simple or comminuted shaft fractures) under a low or high energy mechanism.

## 1.3 Null hypotheses

1. Staged demineralisation of ovine bone cortical segments has no effect on the mechanical properties of these segments under bending load applied at low strain rate.
2. Staged decollagenisation of ovine bone cortical segments has no effect on the mechanical properties of these segments under bending load applied at low strain rate.
3. Increasing physiological age has:
    1. No effect on the incidence of femoral shaft fracture in a local population
    2. No effect on fracture pattern (simple versus comminuted femoral shaft fracture)
4. The mechanism energy (low versus high energy) leading to the femoral shaft fracture has no effect on the fracture pattern (simple versus comminuted femoral shaft fracture)

## 1.4 Novel aspects

Following on from section 1.1, it is important to clarify the novel components of this research. To the best of the author's knowledge, there is an absence in the literature of research which has devised a staged protocol for the demineralisation and decollagenisation of ovine cortical bone segments that then undergo mechanical testing, to delineate the effects of a staged process on intrinsic bone behaviour. This forms a novel aspect of this research.

The above process will therefore intentionally manipulate bone quality, namely demineralise (leading to a proportionally higher organic ratio), or decollagenise (leading to proportionally higher inorganic ratio). This manipulated bone will be tested mechanically under bending under a low strain rate.

Paediatric, young adult and older adult femoral shaft fracture has not been assessed in the literature prior to this study, utilising age as an independant predictor of fracture pattern with a low or high mechanism of energy. The paediatric, adult, and older ages are intended to be used as surrogates for de-mineralised, control and decollagenised bone respectively. These findings will then be assessed against laboratory findings to delineate whether a clinical correlation exists.

Justification for the above statements of novel aspects shall be explored in the literature review.

# 2. LITERATURE REVIEW

To best understand the behaviour of bone, one should understand the basic composition of bone with regards to intrinsic elements, how this forms a macro-structure and how this influences biomechanical behaviour.

Building on this understanding, one can identify methodology which will enable the manipulation of certain properties in isolation in order to isolate their mechanical influence. To this effect, the various methodological choices related to the research will be justified, such as previous work on demineralisation and decollagenisation and choice of animal model.

Finally, the elements of the clinical component of this study shall be covered under two broad headings: physiological change in bone with age (including the effect of ageing on both extrinsic and intrinsic properties), and pathological conditions relating to the inorganic and organic content of bone.

## 2.1 Defining bone

Bone can be defined based on its composition, structure and function. In essence, bone is a composite crystalline material, with structural, biochemical, endocrine and haematopoietic responsiblities.

### 2.1.1 Bone Composition

Bone extracellular matrix is a composite connective tissue consisting of an organic collagen phase, inorganic mineral phase and structural water.

The inorganic carbonated hydroxyapatite and collagen fibres are the basic building blocks. Hydroxyapetite is a naturally occuring mineral with the formula $Ca_5$, ($PO_4$, $Ca_3)_3$ (OH). This carbonated hydroxyapatite unit comprises two entities; hydroxyl and apatite (phosphate mineral). The carbonated hydroxyapatite mineral (also known as a dahllite) has a hexagonal crystallographic symmetrical structure.

This was discovered as a result of pioneering work by Robinson et al as a result of the advent of transmission electron microscopy, where a beam of electrons was transmitted through a micro-structure to form an image. This was able to provide the observations seen with regards to the arrangement [8, 9].

Weiner and Traub extensively studied the organisation of crystals in collagen fibrils utilising electron diffraction. The mineral content was found to be arranged in a parallel latticed tightly packed layer, in a staggered array model on and within the collagen fibrils, forming a collagen-crystal composite. The collagen itself is not the crystal, the mineral is, however the mineral-collagen composite is crystallised [10-13]. It is this homogenous structure of elements, arranged in a lattice, that provides the notion that bone, at its core, is a crystal.

The collagen fibrils form the organic content of bone, primarily formed by collagen type I. Collagen is a fibrous scleroprotein, a proline rich tripeptide, with glycine being the most abundant amino acid found within this. Collagen is one subdivision of scleroproteins, with others being keratin, elastic and fibroin [14].

Collagen type I is the main collagen found in bone, although other collagens do exist such as collagen type II, IV, V and XI [15, 16]. This is a fibrillar protein 300nm long and 1.5nm wide (modulated in part by types III and V collagen which are found in low levels in bone) [17]. It consists of a coiled subunit - with two alpha-1 and one alpha-2 collagen chains. These three subunits coil together into a right handed triple helical structure. The unique mechanical properties of type 1 collagen is owed to the fact its rod like triple helices form lateral interactions. Covalent aldol cross-links form (through the action of lipo-oxygenase enzyme) between the helices stabilising the side-to-side packaging of collagen molecules, forming a strong construct; the collagen fibre [18-21]. In combination with the mineral phase, this forms the strong mineralised collagen fibre construct. The other type of cross link is non-enzymatic, and are either glycation or oxidation induced, otherwise known as advanced glycation end-products (AGE) [22-25]. Initially these cross-links are immature (divalent), however, through a continuous maturation process are converted into a mature trivalent cross-link. The formation of these trivalent cross-links remains poorly understood [19, 26-28]. However, other studies suggest this may be to do with ageing and tissue lifespan which will be explored later in this thesis [29].

The third vital component of this composite is water. This forms around 15-25% of the contents of the extracellular metric (inorganic/organic composite forming upto 75%) [30]. As part of the extra-cellular complex, water occupies the the intra-cortical pores, including the vascular spaces (Haversian and Volkmann's systems) as well as the lacuno-canalicular network [31]. Water naturally affiliates with collagen molecules given certain amino acids within collagen are hydrophilic, such as lysine and arginine. Water can exist as either loose or tightly bound to the mineralised collagen fibril. The initial osteoid laid down by the osteoblast is a hydrated collagen molecule, and as this collagen crystallises, water is displaced [32]. The remaining water content exists between the mineralised collagen planes as a fluid layer [32].

### 2.1.2 Bone structure

Bone has a varied arrangement of structures, at many scales, which work in concert to exert its function on the human body. It is a complex five level hierarchical structure consisting of the macrostructure, the microstructure, the sub-microstructure, the nanostructure and the sub-nanostructure [33].

Figure 1 shows relative size of each level. The macrostructure, which is visible to the human eye, is the cancellous and cortical element of bone. The microstructure and sub-microstructure consists of haversian systems and lamellae respectively. The nanostructure and sub-nanostructure consists of the mineralised collagen fibre and fibril respectively, with the molecular structure consisting of the mineral crystal and the organic proteins forming the collagen as discussed earlier [33]. This structure, with its arrangement and orientation, is a core determinant of the mechanical function of bone (Figure 1).

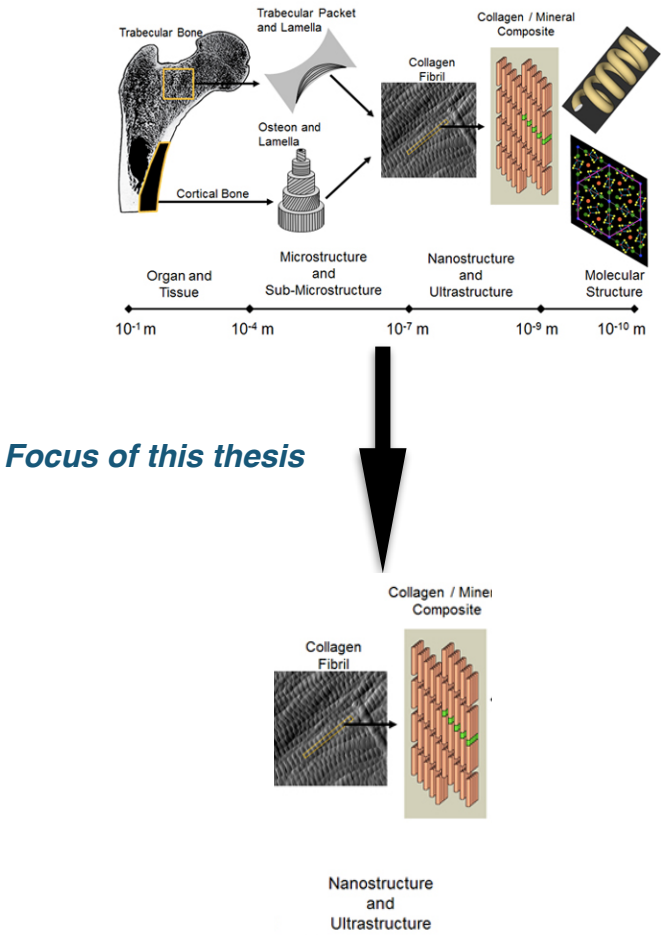


**Figure 1. Hierarchical structure of bone.** ***Modified from http://www.iupui.edu/***

For the purposes of this research, the nanostructure shall be the focus. The most prominent structure seen at the nanostructure is the mineralised collagen fibre. The identification of this structure started with the pioneering work of Robinson et al, who used transmission electron microscopy to study bone, identifying plate-shaped, rather than needle shaped mineral crystals [8]. Furthermore, it was at this stage that the first documentation of mineral crystals existing within a collagen framework occurred. Hodge et al expanded on this almost a decade later, utilising electron microscopy via a negative contrast method, observing a tropocollagen molecule, and being the first to describe the staggered array effect of mineral crystal both within and on collagen fibrils [34]. The understanding of this composite material has allowed the scientific community to further their understanding, particularly on the mechanical properties of the mineral phase. However, much of the collagen phase remains misunderstood, as will be explored below.

### 2.1.3 Structure formation

Bone is anisotropic as its arrangement leads to directionally dependant biomechanical properties [35, 36]. The mechanical axis of the axial skeleton is in the longitudinal plane and is therefore strongest in that plane. This is an important concept to explore as mechanical testing is often performed through a bending load, perpendicular to the mechanical axis.. Work by Bonfield et al on bovine cortical femora loaded at different angles showed a decrease in elastic modulus (resistance to bending), when loaded at angles of 20 degrees and above to the mechanical axis, and in particular if loaded at 90 degrees [37]. This corroborated by earlier work from Dempster et al on cadaveric tibia, who showed that ultimate tensile strength of bone loaded across the lamellar orientation, was less than that when bone is loaded parallel to lamellar orientation [38].

Bend testing therefore simulates a load pattern at right angles to the norm. If bone is assumed to be at its weakest when loaded at a non-physiological angle (90 degrees), then by extension, intrinsic behaviour at its weakest can also be delineated.

The pioneering principle behind this thought process is known as Wolff's law. In the late 19th century, the German anatomist and surgeon, Julius Wolff, proposed a theory on the alignment of bone; that is, that trabecular bone (specifically proximal femur) oriented and aligned itself at areas of principle stress experienced by bone [39, 40].

The proposed mechanism by which bone is selectively deposited in areas of stress remains incompletely understood. However, “strain generated potential” is one mechanism which is thought to occur. This works by two main mechanisms, piezoelectricity and streaming potential. Friedenberg et al is credited for the understanding of the piezoelectric process. White rabbits were used as an animal model to measure in vivo current across fracture sites in the femora and tibiae. Th mechanical stimulation was induced through the fracture and was measured via electrodes which were connected to an electrometer. An electric current was visualised from stressed bone, dependant on the rate and magnitude of stress; piezoelectricity [41].

Fukada et al has also explored this concept, observing the concave (compression) side being more negative than the convex (tension) side [42]. In his study, bovine and human cadaveric femora were thinly cut and exposed to a shear stress. In addition to the findings by Friedenberg, it was noted that the piezoelectric effect mainly applied to collagen fibres, which led to their slippage past each other. The magnitude of this effect was dependant on the angle between the applied load and the axis of the long bone.

These electric signals are carried within extra-cellular fluid otherwise known as streaming potential. Pinkowski et al used whole bone tibia and four-point bending to test streaming potential in a sodium chloride solution. A negative relationship was observed with increasing solution concentration, or viscosity [43]. These results have been supported in the literature in more recent studies [44-46].

The cellular component of bone, mainly osteocytes, play a central role by sensing this mechanical stimulation, all of which results form the initial mechanical force. Osteoblasts seem to follow the more negative charge, laying down new bone and this is where remodelling mainly occurs [47-50].

## 2.2 Mechanical properties

It is important to study the mechanical properties (the effect of a force on a structure) of bone, as this allows us to delineate its susceptibility to failure. To do this there are several engineering principles that should be explored and understood, in order to draw a scientific conclusion. The mechanical properties of bone are determined by the same engineering principles required to study those of metals, wood and glass.

### 2.2.1 Extrinsic structural properties

Strength is a loose term in biomechanics, but is generally defined by the ultimate force which can be withstood by a structure before failure, or in the case of bone, fracture. It is a measure of the extrinsic property of a structure. A force causes an object to either accelerate or decelerate. It also has magnitude (strength) and acts in a specific direction, and therefore it is termed a vector force. Within the context of the femur, there are many force vectors acting across it, as a result of mechanical load through body weight, muscle and ligamentous forces. Therefore the overall magnitude and direction is termed the resultant force. When a force causes an object to rotate (as opposed to linear motion), it is termed a “moment”. This moment force will have a “moment arm”, and this is a the lever against which the force acts in order to produce this rotation [51].

There are basic forces which act across a structure; compression, transverse loading, torsion and bending, and these cause the structure to behave in certain ways. The bending force is most relevant to this thesis, causing a compression and a tension surface, or bowing of the structure (Figure 2). The concave side constitutes the compressive force (where the force is applied), with the tension side being the convex side [52]. One can imagine, the tension side begins to elongate as it bends, and it is therefore easier for a crack to appear if under greater tension.

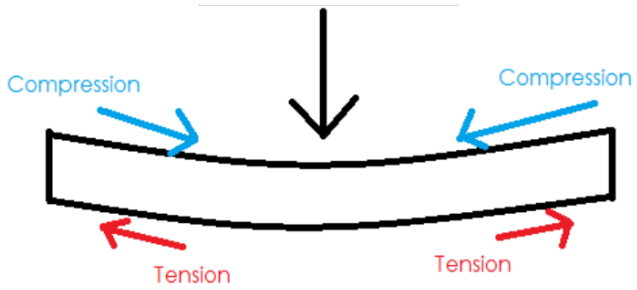


**Figure 2. Demonstrating load applied (black arrow) and resulting forces across the structure. *Modified from Truss Bridge Design Project.***

As a result of the force acting across a structure, it will undergo deflection, which is the degree to which a structural element is displaced from its central axis. This is usually a distance measurement, but can be an angular measurement.

If the force and deflection were plotted on a graph, it would generate a graph similar to that shown in Figure 3. The “stiffness” of an object can then be measured.

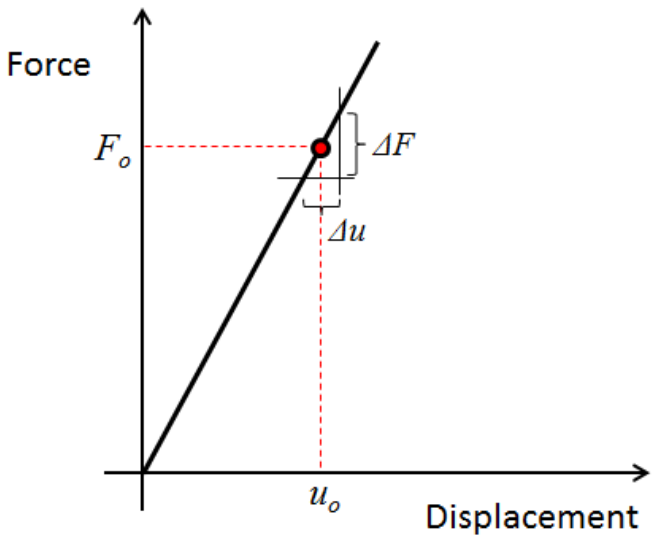


**Figure 3. Stiffness of an object. *Modified from www.comsol.com.***

Stiffness is a measure of the extrinsic resistance to bending of a macro-structure eg the whole bone [53]. The stiffness of an object is determined by the displacement of that object as increasing force is applied. If this is plotted as a graph then the gradient represents the stiffness (Force/Deflection) of an object. The area under the graph represents "work done to fracture" ie the energy required to failure of the macro-structure under bending [54].

### 2.2.2 Intrinsic material properties

Stress is the force applied on an object divided by the area upon which it acts. It is in effect, normalised force, and measures the strength of the intrinsic components that form a structure. In a similar manner, the deflection can also be normalised to the area, and this is called strain, or change in size of bone in relation to its original length. It is essential that these measures are used, as the beams to be studied will not all be of exactly the same size. For example, if a force is applied across two beams, one of which is thicker than the other, it would not be clear which is the "weaker" structure based on the force applied to failure alone [55]. To analyse strength, the force should be geometrically adjusted to the cross sectional area of the bone, therefore measuring stress, and one may find the ultimate stress to failure across both beams in this way would be the same. As a result of stress and strain, one could plot a graph similar to that for force and deflection as shown in Figure 4.

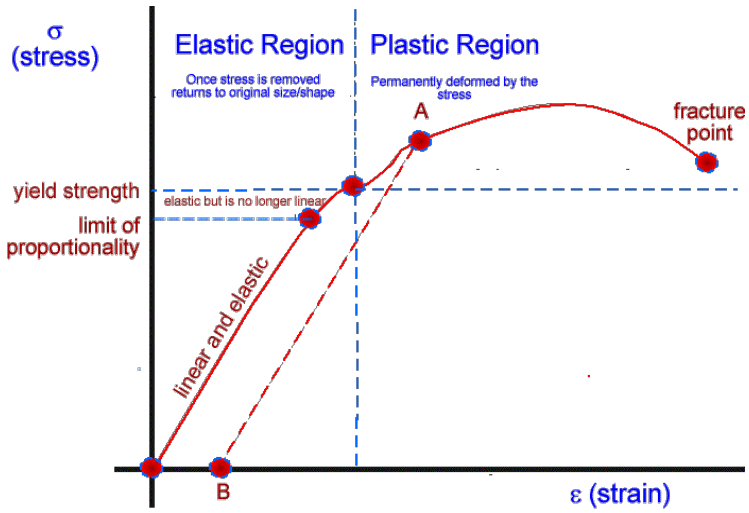


**Figure 4. Young's modulus of an object.** ***Modified from www.cyberphysics.com***

The elastic modulus or Young's modulus is an intrinsic material property that is delineated from a stress versus strain curve of a material. The elastic range is a non-permanent deformation and the plastic range is a permanent deformation. The elastic modulus is the linear gradient of a stress versus strain graph in the elastic zone, with the area under this whole graph being the toughness or the energy required to fracture (elastic and plastic ranges) [54, 56].

The initial constant proportionality of the slope is as a result of Hooke's law. This states that the deformation of an object is directly proportional to the force applied. Therefore removing the initial stress will return the structure to its original shape. Hooke's law will hold upto a maximal stress, known as the limit of proportionality [57]. This is similar to a spring mechanism whereby it initially deforms under load, then returning to its original shape when the load is removed. Following this, the structure is maintained in the elastic phase until the "yield point" is achieved. This is the point above which any additional stress will cause the substance to remain permanently deformed; the plastic phase [51].

Viscoelasticity is the property of a material that exhibits both viscous and elastic characteristics under varying rate and duration of strain. It is characterised by both recoverable elastic deformation, as well as permanent viscous deformation. Viscoelasticity has three main characteristics; creep, stress relaxation and load-rate dependance of stiffness (hysteresis) [58, 59].

Creep is a property where if a constant stress is applied, then a structure will continue to deform. Stress relaxation is observed as a decrease in stress when a constant strain is generated. Hysteresis describes the energy lost during both loading and unloading, and as bone is not a purely elastic structure, a degree of energy will be lost during this process [60].

It is important to note that normal bone viscoelasticity is loading rate dependant, exhibiting greater viscoelastic properties (increased strength and elastic modulus) at a faster loading rate. In 1974, Crowninshield et al examined this effect on bone segments from the tibial diaphysis of freshly slaughtered beef cattle and these were loaded at various strain rates ranging from 0.001 strains per second, to 1000 strains per second, with the higher strain rates achieved with a drop hammer. Crowninshield demonstrated that elastic modulus increased (0.0167 to 250GPa) with increasing strain rates. This also applied to ultimate

stress, with a maximum value of 2.5N/m$^2$ compared to 0.25N/m$^2$ at the lower strain rate [61]. Wright et al conducted a similar bovine study, using larger cylindrical segments of bovine bone under a tension load with strain rate varying from 0.00053 strains per second, to 237 strains per second. Elastic modulus also increased from 17.7 GN/m$^2$ to 40.4GN/m$^2$ at the highest strain rate. Similarly, ultimate strength followed, with a range of ultimate strength of 99.2MN/m$^2$ to 271.4MN/m$^2$ [62]. Further studies have found similar findings, in both torsional loads [63], as well as bone of varying mineralisation levels [64].

### 2.2.3 Bone toughness

Traditionally toughness has been thought of as the ability of a structure to dissipate energy applied through deformation, without the initiation or propagation of a crack [65]. As it is a parameter relating to the ability of absorption and release of energy, simply speaking it is therefore the ability of a structure to resist failure (eg fracture in bone). Toughness is a multi-scale process that is related to each hierarchy in bone, with the assumption being that each level provides its relative optimal toughness [66]. Therefore there are intrinsic and extrinsic toughening mechanisms as will be explored later in this chapter. Essentially however, the intrinsic ability relates to “crack-dilatation”, or the ability to inhibit crack-growth, by increasing the surface area at the crack tip. The extrinsic mechanism is derived from crack-bridging, which acts to reduce the crack-driving force through a shielding mechanism [67, 68].

There is no standard method for the measurement of toughness [69]. The majority of studies focus on measuring the energy to initiate a crack ($K_c$). However, other methods do exist, such as the additional contribution of the inelastic phase until failure ($J_c$), with R-curves utilised for the the resistance to crack propagation. These methods are all defined by the American Society for Testing and Materials (ASTM), however there is no clear recommendation by this group on the optimum application in bone or other biological materials. Furthermore, to derive the Kc and Jc values separately requires a strict protocol with the careful machining of bone to idealised geometrical standards. This is then followed by careful micro-notching at the bone surface before testing [70].

For the purposes of this study, bone was tested to failure, which includes both the initial crack and crack propagation to fracture ($K_c$ and $J_c$). This provides a complete picture of the "work-done" to include both the elastic and plastic phase and is in line with much of the literature [2, 5, 64, 71].

### 2.2.4 Fluid theory

Comprising around 20% of bone volume, water is a key component and determinant of mechanical behaviour of bone. It occupies the porosities within bone (pore-water), the lacuno-canalicular spaces (free/mobile water), and moves according to pressure gradients upon locomotion of the skeleton. Water tends to associate with the hydrophilic amino acids of collagen type 1, namely lysine, arginine and hydroxyproline, and initial unmineralised osteoid laid down by osteoblasts is in effect hydrated collagen. As the osteoid is mineralised, water is displaced. However, a water component remains within the sheets of the mineralised collagen fibres, which add to the mechanical properties of bone - this is referred to as structural water (Figure 5) [72].

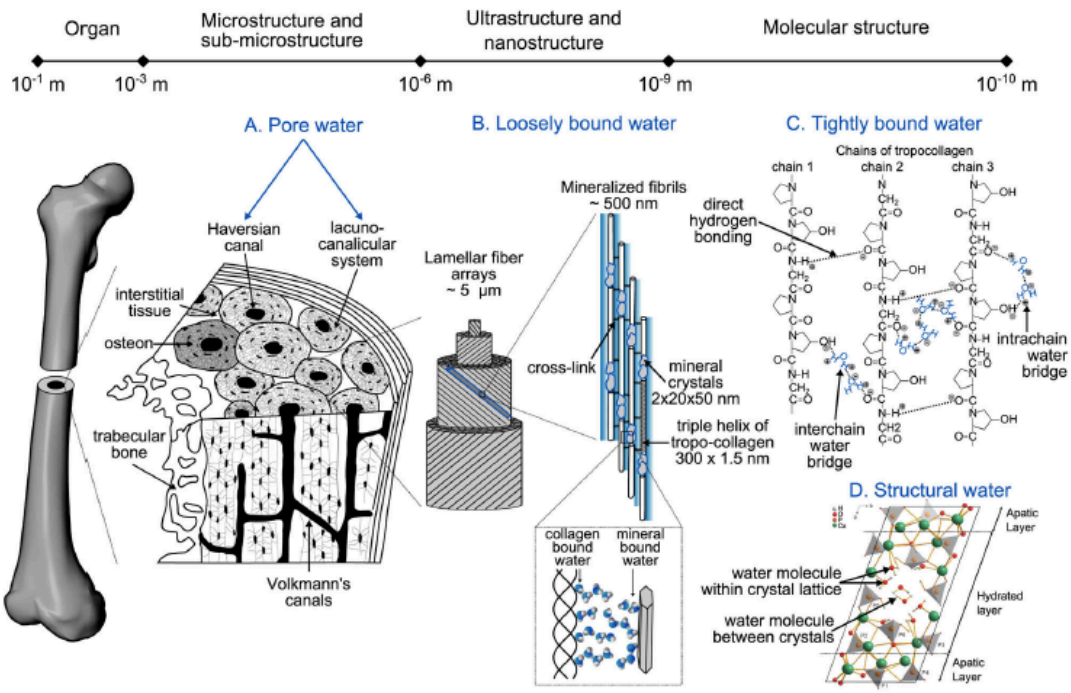


**Figure 5. Water at each hierarchical level.** ***Taken from Davies et al.***

Structural water affects similar mechanical properties as collagen, such as ductility, or the amount of post-yield strain that is achieved (in the plastic phase).

Biomechanical effects of loss of water are mainly undertaken through thermal dehydration of bone (air drying, or vacuum oven drying). Wess et al looked at the effect of dehydration on rat tendon samples which were periodically heated in an oven to 120 degrees celsius. Through x-ray diffraction imaging, which assesses proton distribution patterns within a structure, a change was observed in the collagen patterns. There was a collapse between the fibrils with shortening of the segments, with shearing of the cell units (Figure 6) [73].

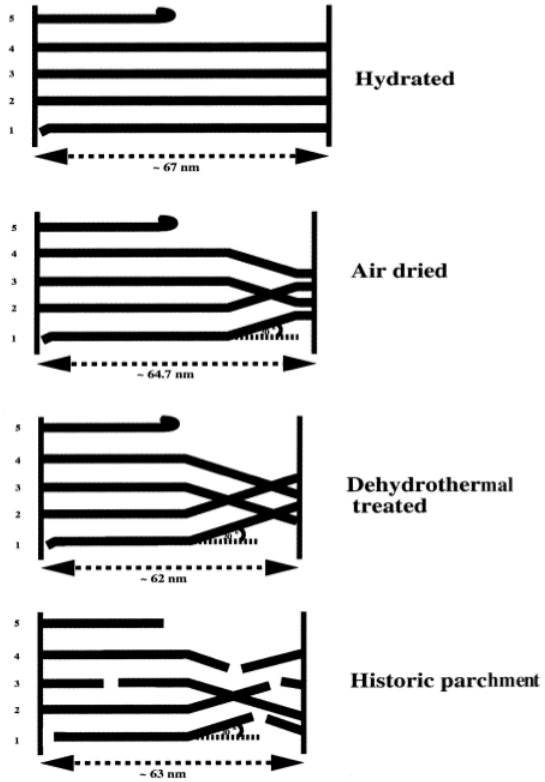


**Figure 6. Changes in collagen structure following dehydration.** ***Taken from Wess et al.***

Specific to bone, changes in dehydration on mechanical values have been observed since the early 1950's, when Smith et al observed the effects of temperature on bone from various species including tibia, horse and ox. Smith observed an inverse linear relationship between temperature and elastic modulus [74]. More recently, Faingold et al built on this understanding and tested hydrated and dehydrated cortical equine metacarpal bonbon segments.

The dehydrated samples were oven dried upto 100 degrees celsius. Mechanical testing was undertaken using nano/micro-indentation and atomic force microscopy (testing the molecular osteonal level), to provide a global assessment of elastic modulus. The modulus at osteonal, mineralised fibril and lamellar levels were all found to be upto 50% higher in the dehydrated samples. This suggested that in addition to the findings by Wess et al, that there is re-orientation of the mineralised fibrils in the lattice structure, which renders the structure stiffer in the elastic phase, but less ductile with a reduced resistance to fracture in the plastic phase [75].

The thought behind this stiffening mechanism reflects work by Wenger et al, who mechanically tested rat tail tendon, and found that air-dried tendon increased in elastic modulus from 3.7GPa to 11.5GPa. The increased stiffness was theorised to be as a result of the a higher mineral to collagen ratio, with the stiffening process being overtaken in effect by the mineral phase. This seems to be achieved by the compaction of mineralised fibres, and as a result the mineral also, leading to a stiffer unit [76]. Other studies, through a combination of indentation and bend testing have corroborated these findings. Broz et al dehydrated whole bone mouse femora and following three-point bending observed higher stiffness and reduced ductility in the dehydrated specimens [77]. Nyman et al used cadaveric human femoral segments which were oven-dried and also noted similar findings [2, 78].

At the material level, or that which forms the enquiry level of this thesis, in addition to the stiffening process that occurs with dehydration, there seems to be an effect on the toughening mechanisms. Nyman et al studied cortical bone specimens of human femoral diaphysis. Vacuum oven drying was used to dehydrate the specimens for upto 4 hours at temperature of 110 degrees celsius, after which the wet and dry specimens were three-point bend tested. A loss of bone toughness (resistance to fracture) was observed with increased dehydration. The reason for this remained unclear, however it was suggested that disruption of the collagen phase, which is thought to be the main determinant of bone toughness, was a significant contributing factor [78]. Nyman himself further supported his own work with another cadaveric human cortical femoral study, with partial air dehydration of segments, to simulate presumed water content changes with ageing. A significantly reduced toughness, as a result of decreased post-yield strain was observed, with mean values of 1.559 $MJ/m^3$ (wet bone) to 0.341 $MJ/m^3$ (dehydrated bone) [79].

This is further supported by Yan et al who took bovine cortical bone and thermally dehydrated it in a vacuum oven at 60 degrees celsius. The specimens underwent 4-point flexural testing under a constant strain rate, finding a 45% reduction in fracture toughness in the dehydrated samples [80]. A higher 60% reduction in toughness was observed by Melvin et al in a similar study, however the discrepancy in toughness loss is likely due to the method of mechanical testing, with Yan utilising four-point bending, whereas Melvin utilised single notch bend testing, which does not test to failure, but rather is a measure of crack-propagation [81].

### 2.2.5 Bone mechanics

Previous work by Rho et al has shown that cortical and cancellous bone differ mechanically. Cadaveric human tibiae were isolated and prepared in a standardised fashion, and cut into cubes of cortical and cancellous specimens respectively. These specimens were subject to both micro-tensile as well as ultrasonic testing. Young's modulus of cortical bone was significantly higher than cancellous bone (20.7GPa v 14.8GPa) [82].

This was further backed by Bayraktar et al, using cadaveric human femoral cortical and cancellous which were machined into segments and imaged using micro-computed tomography (micro-CT). Segments were mechanically tested, with extrapolation of the mechanical values obtained into a finite element analysis model. The study concluded that elastic modulus and yield strains were approximately 10% lower for cancellous bone in comparison to cortical, with ultimate strength approximately 25% lower [83]. Further previous studies by Choi et al and Kuhn et al have shown that cortical bone had a higher elastic modulus by 19% [84] and 28% [85] respectively.There does however seem to be a large span of values in the literature, from as little as 1.0GPa [86] to as much as 20.0GPa [82]. This is likely to be as a result of a few confounding factors. Firstly there is a great variation in the type of bone studied, such as human cadaveric femora to bovine tibia. Secondly, there is a range of testing methods that have been employed in the literature, with Rho et al utilising three-point bending, whereas Choi et al utilised four-point bending. This brings in a significant confounding factor owing to the varying amounts of shear stress that must be factored into three-point bending [87].

The addition of shear would be expected to yield lower values, as there is an additional external force, as opposed to pure bending.

It is perhaps unsurprising that different mechanical properties exist between the two types of bone, as cancellous bone is more porous. A previous biomechanical theory of this by Choi et al posits that as cancellous bone is a more mosaic structure than cortical (cement lines, porosity, orientation) then greater stress risers exist lending itself to weakness [84]. The plastic phase is prolonged as trabecular bone collapses and “re-compacts” thereby increasing stiffness again. This can explain why energy absorbed by trabecular bone can exceed that of cortical bone in compression. This also means that cancellous bone is relatively more ductile, or is able to incur greater post-yield strain.

Additionally, cortical bone is able to withstand greater stress but relatively lower strain than cancellous bone. At a strain rate greater than 2%, cortical bone will fail [88], whereas cancellous bone can withstand higher strains[89]. Due to the tightly packed structure of cortical bone, it does not have the same prolonged plastic phase as cancellous bone, and cannot store as much fracture energy as cancellous bone as it is not as porous or fluid filled [89]. A graphical representation of basic mechanical properties of cortical and cancellous bone is shown below in figure 7 [90-92].-

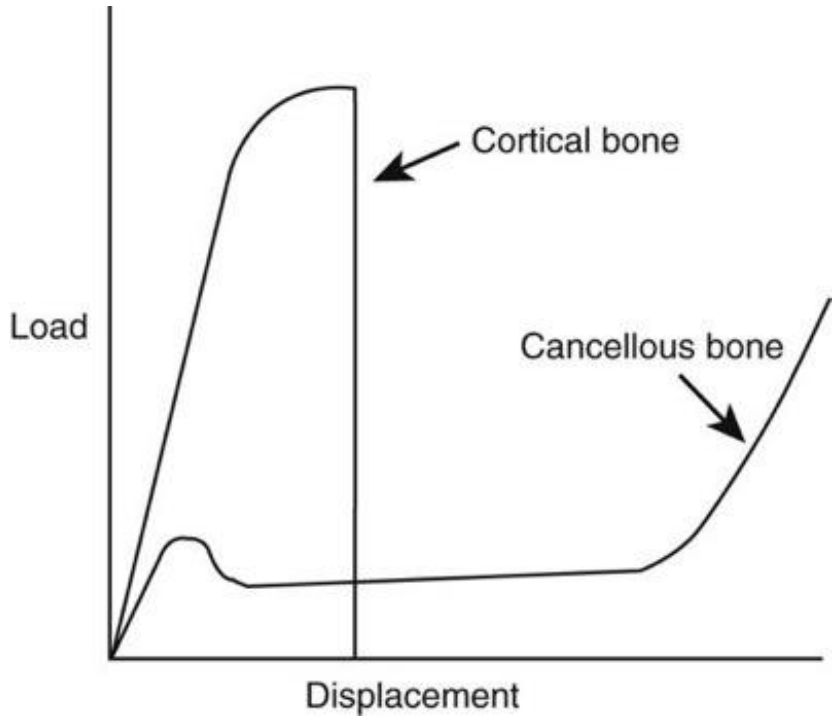


**Figure 7. Load displacement curves for cortical and cancellous bone. *Taken from veteriankey.com***

The definition of bone viscoelasticity is the behavioural response of bone depending on strain rate and duration. This means that bone becomes stiffer, or, Young's modulus increases at faster strain rates and these increasing rates are likely to affect mechanical properties [59, 93, 94]. This is important as cortical bone fatigue failure is likely as a result of exposure to higher orders of magnitude of strain rates under bending [95]. It is useful to divide these properties into pre and post yield categories. The consensus of opinion from a number of the relevant studies is that higher strain rates have a proportional relationship to pre-yield properties [96-106]. This is particularly evident in studies by Crowninshield et al and Wright et al. Crowninshield et al. in their study, were able to load fresh bovine bone progressively at increased strain rates, resulting in progressively positive increases in elastic modulus and ultimate properties [98]. Wright et al. in their study, also looked at these findings, by standardised tensile longitudinal mechanical testing of compact bovine bone at increasing strain rates. A significant positive correlation was found between strain rate and ultimate strength, as well as ultimate strength and density [102].

There is a disagreement in these two studies however, with Crowninshield reporting a maximal energy absorption capability of compact bone at a defined strain rate, with Wright unable to back this result. A reason for this discrepancy could be due to the difference in strain rates used by the two studies. Crowninshield et al tested cortical tibial diaphyseal bone of freshly slaughtered beef cattle, which would be assumed to have greater water retention given the fresh nature. This is in comparison to bone segments used by Wright et al, which were not. Furthermore, the variation in strain rate between the two studies were significant, with Crowninshield testing upto 1000 strains per second, compared to 237 strains per second in the study by Wright et al. These two factors could have a confounding impact on the variation in results seen, with a maximum elastic modulus of 250GPa for Crowninshield's study, compared to 40.4GN/$m^2$ for that by Wright et al. However what remains clear is the message across both studies, that is, that strain rate affects mechanical properties [64, 97]. Whilst one explanation of this includes fluid theory and its contribution to viscoelasticity, it is possible the mineral and collagen content contributes also. Yamashita et al thermally denatured collagen type I in mineralised cortical bone segments machined from human femoral diaphysis. Alpha-chymotrypsin was then applied to these bone segments in order to digest denatured, and not intact collagen type I. The content of intact collagen remaining was measured using liquid chromatography.

Some of these samples were then rehydrated to evaluate level of denatured collagen as well as water content effect. Three-point bending tests were conducted following this, and the loss factor measured (amount of energy stored and lost during mechanical deformation). A higher loss factor value implies greater viscoelasticity, which was seen in wet compared to dry samples, with no significant difference in matched hydration samples with varying levels of denatured collagen [107].

The effect of strain rate on post-yield properties is less clearly agreed upon. Hansen et al, using cadaveric human cortical femoral bone, under rigorous mechanical testing, was able to back up previous findings on pre-yield and yield point association with strain rate. Strain rates varying from 0.14 strain per second to 29.1 strains per second were applied, finding a linear relationship with rate and yield point. However despite concluding that post-yield effects were less clearly understood, it was demonstrated that strain rate had a greater post-yield deformation effect than previously thought [108]. These findings were consistent with other studies involving cadaveric human and animal bone [103, 105, 106]. This was thought to be due to a sharper ductile to brittle transition at moderate to higher strain rates. These results are more clearly shown in Figure 8.

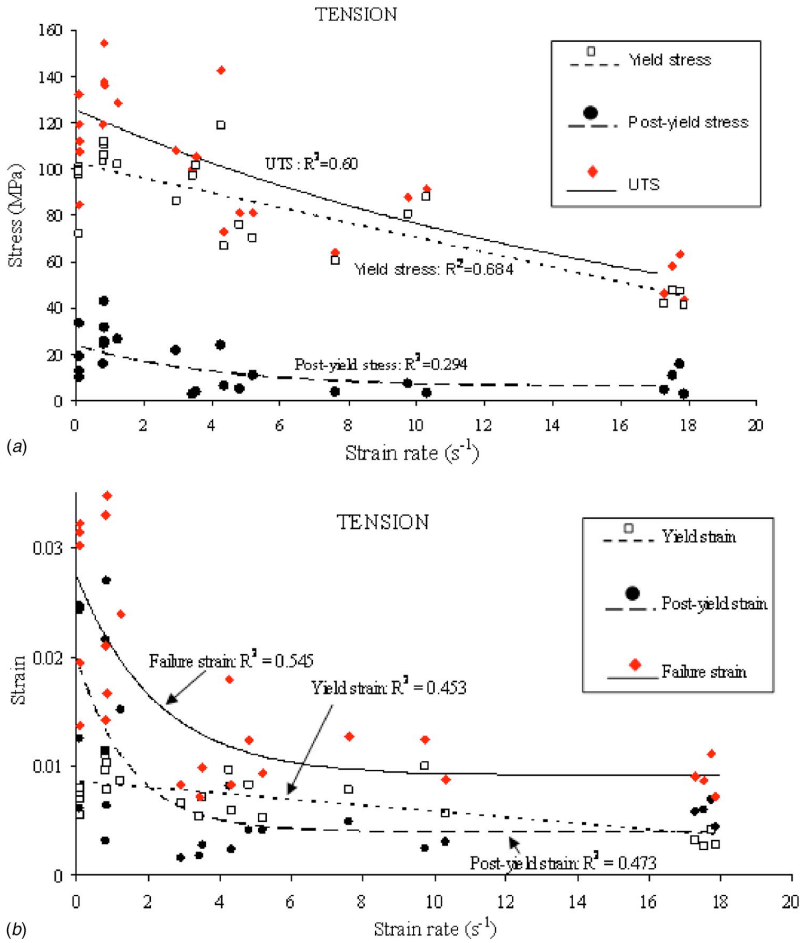


**Figure 8. Stress v Strain rate (top diagram) and Strain v Strain rate showing post yield properties. *Modified from Hansen et al.***

### 2.2.6 Tension and compression

The distribution of lamellar bone and the orientation of the collagen fibres within them correspond to their function and strength. The collagen fibres are oriented in the weight-bearing axis according to Wolff's law as explored earlier, which is the longitudinal mechanical axis. Subsequently strength under a longitudinal load is greater than that under transverse loading. This helps bone to withstand the forces it is required to undergo during locomotion [109, 110].

Bone seems to adapt to the direction of loading as suggested by Reilly et al in his mechanical studies of equine bone [111]. An example of this is the femur, which has a slight anterior curvature, meaning that slight bending of the femur is produced during longitudinal loading. This leads to tension on the anterior cortex and compression on the posterior cortex. Subsequently, it is more likely to fail on the tension surface in healthy bone. This is based on the elastic theory of bending, which states that the outermost fibres of a beam, which are furthest from the neutral axis, will fail first. Detailed histology of both anterior and posterior cortices has shown that mineral and collagen orientation is more longitudinal in the anterior cortex, and more transverse in the posterior cortex, which optimises the mechanical strength at each cortex. This explains why the femur is more likely to fail on the anterior surface [112-114]. The anterior surface would be subjected to a tensile load, whereas the posterior cortex would be subjected to a more compressive load posteriorly. The posterior cortex is therefore strengthened reinforced by the re-orientation of lamella along compressive lines. Small angle x-ray scattering in a study by Fratzl et al confirmed the above mentioned findings [115].

Various mechanical studies have demonstrated the difference in mechanical values of Young's modulus and ultimate stress of cortical and cancellous bone in tension and compression as shown in tables 2.4.1 and 2.4.2.

**Table 2.4.1. Showing mechanical values in cortical bone**

| | **Elastic modulus (x10 E9 $N/m^2$)** | **Ultimate stress (x10 E6 $N/m^2$)** |
|---|---|---|
| **Tension** | 11.4 - 19.1 | 107 - 146 |
| **Compression** | 15.1 - 19.7 | 156 - 212 |

**Table 2.4.2. Showing mechanical values in cancellous bone**

| | **Elastic modulus (x10 E9 $N/m^2$)** | **Ultimate stress (x10 E6 $N/m^2$)** |
|---|---|---|
| **Tension** | 0.2 - 5 | 3 - 20 |
| **Compression** | 0.1 - 3 | 1.5 - 50 |

Values for cortical bone in table 2.4.1 are taken from Evans , Kotani and Wright [102, 116, 117]. Values for cancellous bone in table 2.4.2 are taken from Currey, Carter, Weaver and Galante [99, 100, 118, 119].

Both types of bone are stronger in compression than in tension. However, this is not always the case, particularly in bone which has suboptimal collagen to mineral ratio such as that in paediatric bone or osteoporotic bone. Examples of compression fractures in paediatric and osteoporotic populations include torus and spinal wedge fractures respectively [120, 121].

This knowledge is invaluable in implant design, such as plates being used as tension bands. In essence, the tension side of bone can be re-inforced by applying a plate on the side of eccentrically loaded bone such as a femur. By pre-bending the plate it also allows tension resistance on the convex surface and compression on concave aspect of loaded bone.

## 2.3 Modes of biomechanical testing

A surrogate for the assessment of bone quality is biomechanical strength. This is due to the notion that bone mass, bone composition, geometry and material properties all contribute to its structural integrity [122]. Modes of testing can be subdivided into those that assess mechanical properties, those that assess bone geometry and those that analyse bone micro-architecture (Figure 9) [123]. Specific to the level of hierarchy studied in this thesis includes microbeam, micro-indentation and nano-indentation testing.

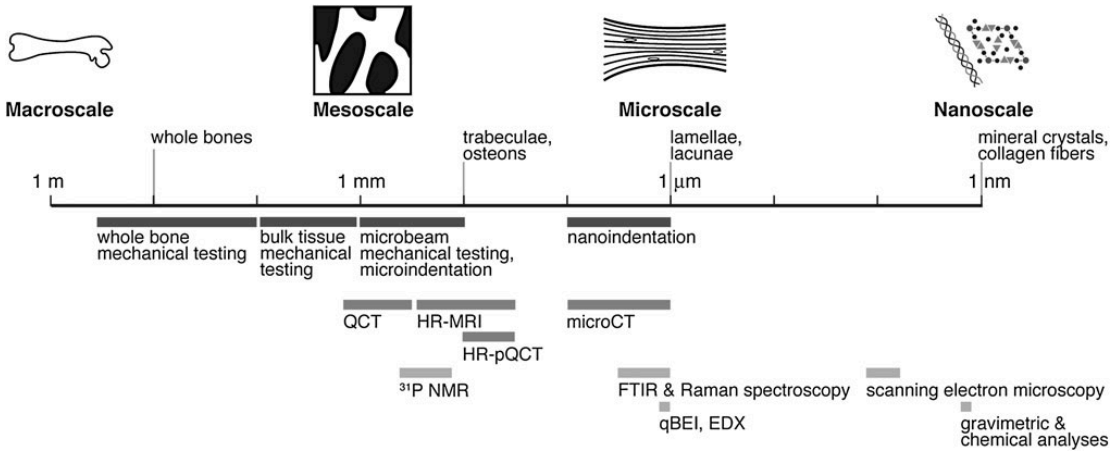


**Figure 9. Describes methods of testing at structural levels. Dark grey bars - mechanical testing, medium grey bars - micro-architectural and light grey bars - compositional tests.** ***Taken from Donnelly, 2010.***

### 2.3.1 Microbeam

This is conducted to isolate the material intrinsic properties of bone. In these tests a section of bone as small as 200 x 200 x 2000 micrometers, are derived from either cortical or cancellous bone, and then loaded in a fashion to allow bending or tension loads to occur. Traditionally this has occurred through 3-point bending popularised by Kuhn et al [85], however more recently there has been a drive towards 4-point bend testing [84]. This is shown in Figure 10 [124].

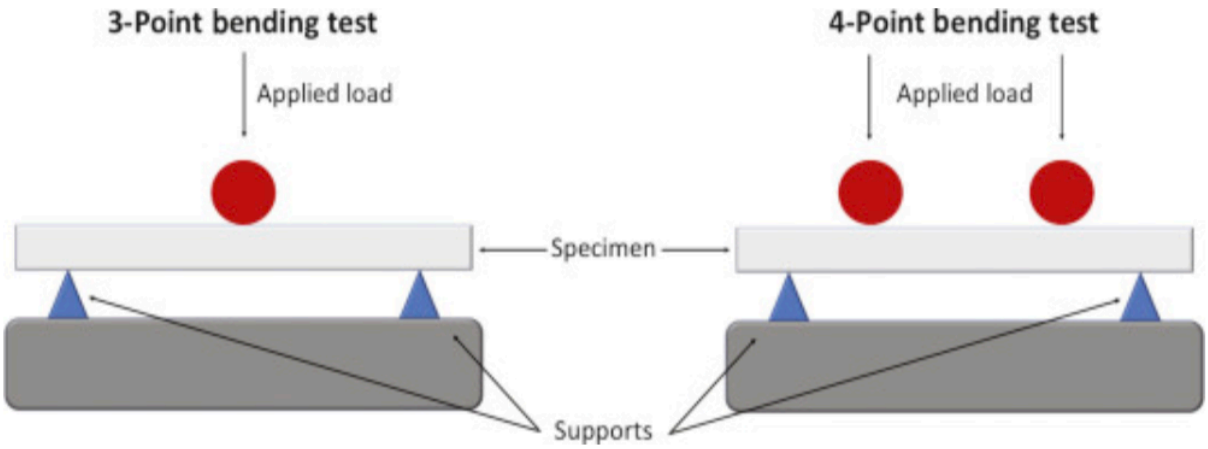


**Figure 10. Three-point and four-point bending tests with difference in applied load.** ***Taken from Khan et al.***

In 1989, Kuhn et al, studied human cadaveric trabecular and cortical iliac crest segments using a Leitz microscope body and stage, which was modified. A load was applied through a head attached to the stationary body tube of the converted microscope (vertical movement controlled by the stepper motor). Force and deflection data was acquired from a load cell set on a stage and a linear transformer was used to convert mechanical into electronic data (Figure 11).

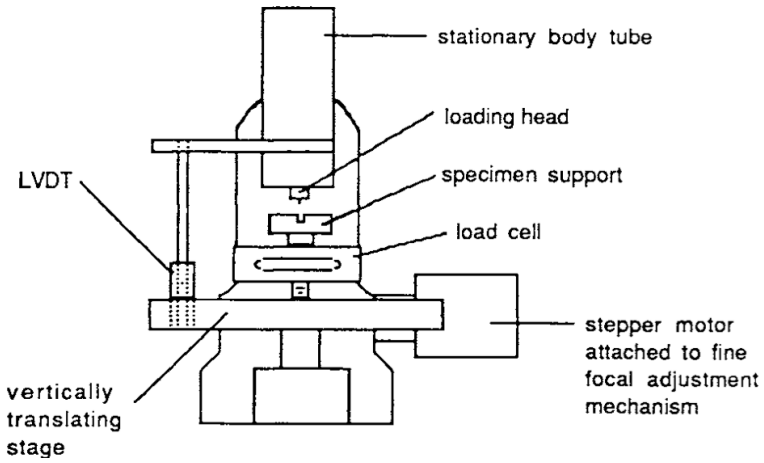


**Figure 11. Modified Leitz microscope designed by Kuhn et al for three-point bend testing.**

Choi et al, built on this idea and a year later, configured the loaded head to a four-point bending system, in his study analysing human cancellous subchondral and trabecular bone from a tibia [84]. The move away from three-point bending has been as a result of an acknowledgement that the stress applied in such a test is very concentrated into a focal area, which leads to micro-shear forces, that can lead to premature failure of bone [87]. Four-point bending therefore, gives a “purer” test, with the elimination of shear forces. The deflection in such a set up is commonly measured using an electronic set up, where a sensor crosshead is centred on the central neutral axis of the structure being tested, with the cross-head measuring the furthest deflection. Four-point bending is also particularly useful where there has been a compromise of bone quality, such as bone which is likely to exhibit brittle behaviour, as this cannot withstand shear stress as well as physiologically normal bone [125]. From microbeam bend testing, certain mechanical results indicative of

intrinsic properties can be derived such as that described above (stress, strain, elastic modulus, toughness). This was thought to be the most suitable form of mechanical testing in this thesis.

### 2.3.2 Microindentation

Indentation testing can be used to test the material properties at the microscale or bone structural unit. This consists of pressing a hard tip with a known force into an object, with measurements at the contact area recorded. As a result the “hardness” of a material is measured. This is a material surface property defined by the force divided by the imprint area, and it characterises resistance to plastic deformation. The theory being that in structures with higher hardness, there is an increased elastic modulus. One such study utlising micro indentation is that by Hodgskinson et al who conducted a study in 1989 on cancellous and compact bone. Bone specimens underwent micro-indentation testing, and it was shown that in cancellous bone (mean 10% mineral content), that hardness and by extension Young’s modulus was reduced by a mean 12% [126].

Depth sensing technology is utilised to measure tip displacement. Tips are often made from diamond and are commonly spherical, four-sided pyramidal or asymmetric pyramidal shapes. Spherical tips are often most commonly used however they are most difficult to manufacture.
They allow minimisation of plastic deformation and damage to the structure outwit the experimented region. This is an advantage over micro-beam testing which damages the whole micro-structure as it loads to failure. Other advantages include ease of testing and the ability to conduct multiple experiments on various sections of the beam to be tested. Conversely however, if the study methodology requires testing to failure, then micro-indentation alone is not sufficient, and either whole bone, body tissue or microbeam testing should be utilised.

More recently there has been development of micro-indentation testing for in vivo specimens utilising a hypodermic needle [127]. However this has not been validated.

### 2.3.3 Nanoindentation

This was introduced by Oliver et al, with six types of beams used including silica, glass, aluminium, tungsten, quartz and sapphire. This was designed to solve the problem of “collateral damage” that occurs to the area surrounding the indentation when micro-indentation is used. Oliver et al utilised a three-sided pyramidal shaped indenter was sequentially loaded and unloaded to allow elastic followed by plastic deformation and the contact area measured. This provides a sum of displacement in the loading/unloading curves [128]. The result is a more precise measure of indentation area than previously utilised with micro-indentation, which relied on making an indentation to plastic deformation and then measurement of this area using a microscope (Figure 12).

Nanoindentation is capable of analysing an even smaller scale (nano scale as opposed to microscale), to the level of the individual lamellae to within a 5% error rate [129]. In addition to the indentation tip, a scanning probe microscope is also utilised to detect an even smaller area of indentation. This method can also be utilised to detect subtle mechanical changes in diseased bone pr that subject to drug treatment. However this requires the need for specialist instrumentation at some cost.

Additionally the specimens would have to be accurately machine prepared in order to deliver the smoothest surface possible for testing, not visible to the human eye. The economic burden as a result of this in addition to the level of investigation conducted in this thesis meant that this method of testing was not required or appropriate.

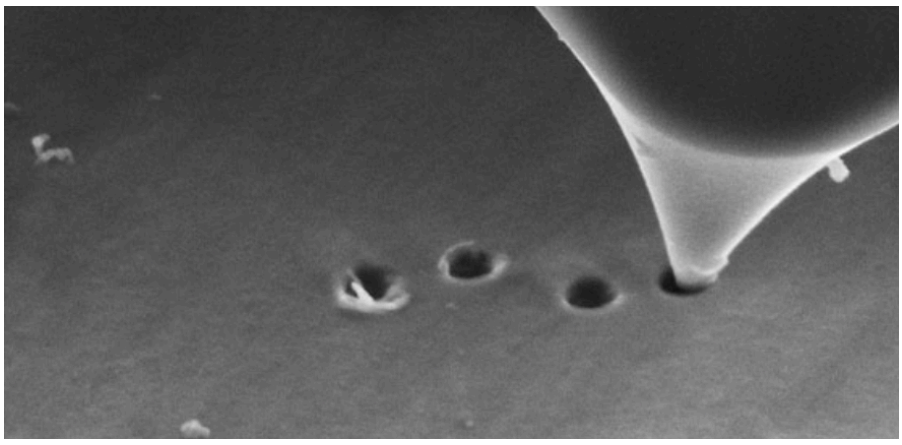

**Figure 12. Image of nano-indent created on a surface using a pyramidal indenter.**
***Taken from www.nanotechnik.com***

### 2.3.4 Finite Element Analysis (FEA)

Initially theorised in the 1940's by Hrennikoff [130] and Courant [131], this is a technological development that allows for the prediction of how a structure will behave under load, by breaking the structure into "finite elements", or ultrastructure nodes. The subdivision into finite elements allows for accurate representation of complex material geometry, capture of local effects and inclusion of all elements within a cubic structure eg mineral, collagen fibrils and cross-links in bone.

The most commonly applied method is the voxel-conversion technique, where a voxel is the 3-dimensional equivalent of a pixel (2-dimensional). The idea is to firstly image the specimen in question, using micro-computed tomography (micro-CT) or micro-magnetic resonance imaging (micro-MRI). This image is then uploaded onto computed software which creates a mesh of nodes to "fill" the geometrical structure being tested (comprising the elements in the block). As there are intrinsic values for bone that are available in the literature, a simulated "load" can then occur on simulation software, to predict how the structure will behave. One disadvantage of this model is that the "known" values in the literature are not absolute, with significant variation. This is based on confounding factors, such as type of bone used, location in the bone, size of segments, mechanical testing methods and unstandardised bone quality which will be explored later in this chapter.

More recently, the voxel-based FEA model has been validated in the literature by Chevalier et al, in order to reduce the level of assumption in the literature. Human trabecular bone was extracted from proximal femora and underwent uniaxial mechanical testing utilising nano-indentation. A parallel FEA model utilising the same bone was simulated alongside the biomechanical study. An excellent correlation was observed in density and mechanical testing results [132]. A significant limitation of FEA remains that the model is only as good as the operator who generates the geometrical images for the model. Any error is therefore amplified in bone of varying quality eg osteoporotic bone. Furthermore, it does not take into account the influence of the soft tissue envelope, which can cary both the magnitude, as well as the direction of the external force being applied to load [132].

For the purposes of this research, FEA is unsuitable. This is due to the fact that there are no known values for a staged model for demineralisation and decollagenisation, which forms a novel aspect of this thesis. Therefore, it would only be suitable for FEA following the generation of results.

## 2.4 Modes of bone failure

Much of the understanding of fracture biomechanics is based on the understanding that bone is strongest in compression and weakest in tension. The simplest example is a long bone undergoing a pure bending load; there is a concave compression side and a convex tension side as explored earlier. The tension side undergoes progressive elongation until a crack appears.

### 2.4.1 Crack initiation/propagation

Fractures originate through the initiation of a crack. A crack is a volume-less defect in an osteon. This is due to certain interfaces within an osteon that provides structurally weak areas, providing the path of least resistance for a crack to appear and propagate. This is particularly true when bone is not loaded along physiological lines such as in pure bending.

In cortical bone, the weakest point is along the “cement lines”, first described by Von Ebner in 1875. These are thin lines that around the haversian systems (vascular supply) in bone. In the early 1900’s these cement lines were examined to delineate their components, with Weidenreich et al finding that there was an absence of collagen fibres, with the mineral having a more granular structure under histological staining [133]. Schmidt et al, under polarised light, found no evidence of any specific “cement” or grout structure that differed to the micro-structure of bone [134]. Philipson et al, examined bone sections from orangutan and whales under x-ray diffraction, finding low values of collagen, but noted there was upto 50% increase in mineral in these regions (hypermineralised) [135].

Cement lines result from the area in bone where there is a reversal of the absorption phase during remodelling, to a bone formation phase, and is why there is a relative hypermineralisation. This reflects the overactivity of osteoblasts in phase two of remodelling [136, 137].

The cement lines form areas of weakness compared to surrounding lamellar bone. Dong et al investigated the cement line interfacial strength in human humeral diaphyseal cortical bone by performing osteon push-out tests. The cement line interfaces tested were 1) between osteon and interstitial bone and 2) between bone tissue lamellae. The shear strength between lamellae were found to have an average of 73.71MPa, whereas the shear strength of cement lines in interstitial bone were much lower at a mean of 7.21MPa [138]. Bigley et al conducted a similar study but on equine cortical bone, whilst the mean interstitial cement line was lower (30.7MPa), than lamellar (32.7MPa) [139], the values differed significantly to the study from Dong et al. Several causes for this discrepancy are possible. Firstly the bone from different species were tested (human v equine). Secondly, humeral non-weight bearing bone was used for one study, whereas third metacarpal bone was used for another. Different bone block measurements and thicknesses were used which can confound the intrinsic properties of bone under testing. Additionally, Bigley et al used one standardised push out tray and hole for mechanical testing, whereas this was varied by Dong et al, where multiple smaller holes were used for the interstitial cement line interface.

It is therefore at the interstitial cement line interface, where a crack is likely to initiate, as this reaches its yield point at a lower load than that of the surrounding bone. With repetitive loading, or with an excessively high primary load, the crack is able to progress transversely along cement lines through the material, and this progresses to the outer layers until the cortex fails.

### 2.4.2 Delamination failure

This is best described as a critical failure mechanism in laminated fibre reinforced polymer matrix composites. [140] Examples of fibres used include fibreglass, carbon fibre, basalt and aramid (Figure 13)

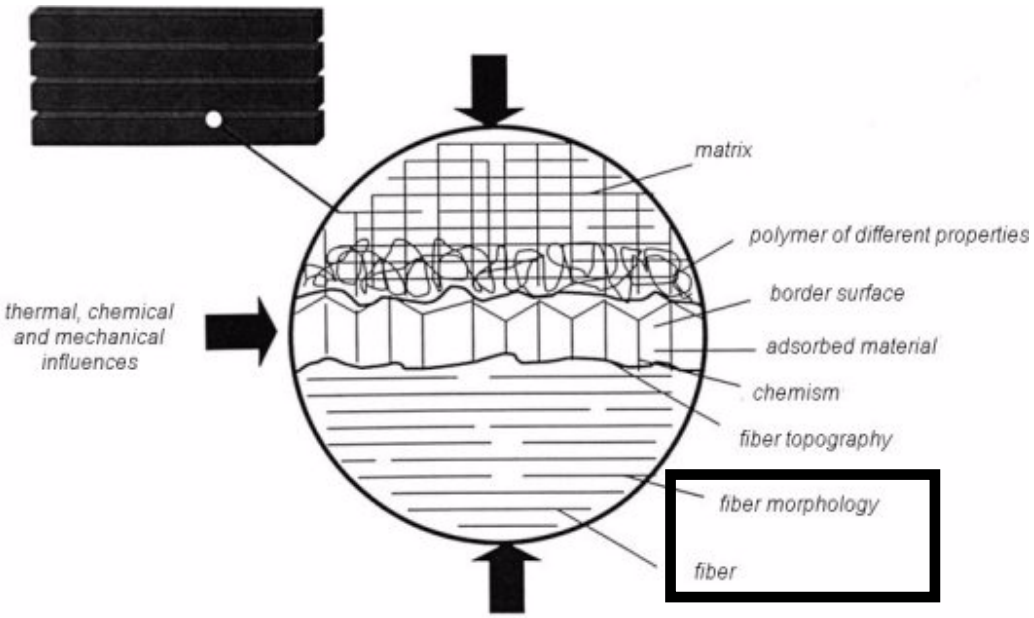


**Figure 13. Fibre reinforced polymer composite. *Modified from kenzgerlessmanhand.id.st.***

Fibre-reinforced material do not fail by initiation or propagation of a single crack, but rather the accumulation of these. Once the fibre fails, strength is dependant on the individual laminated sheets which were reliant on the fibre. The high inter-laminar stresses exceed the through thickness strength of the relatively weaker individual sheets. Failure of this polymer occurs as a result of an initial fibre fracture [141]. Cyclic fatigue or loading out of plane are examples of mechanisms which can induce this initial failure. Specifically, three ways are known for fibre failure:

1. Crack propagation as a result of undue stress at the crack tip
2. Yield of matrix around the crack tip leading to an invagination of the fibre into the matrix
3. Shear failure of the interfacial region [142]

These three mechanism all lead to a reduced toughness of the composite [143]. Cross-link contribution to delamination failure in bone remains unclear. The most comprehensive study on the delimitation effect in bone was conducted by Fantner et al, utilising trabecular human and bovine vertebral bone samples. Atomic force microscopy was utilised to study the mechanical effects at the fibrillar level, with electron microscopy used to delineate the changes seen. A delamination effect was noted between collagen fibrils in bundles, with a shearing effect observed at the cross-links (Figure 14) [144].

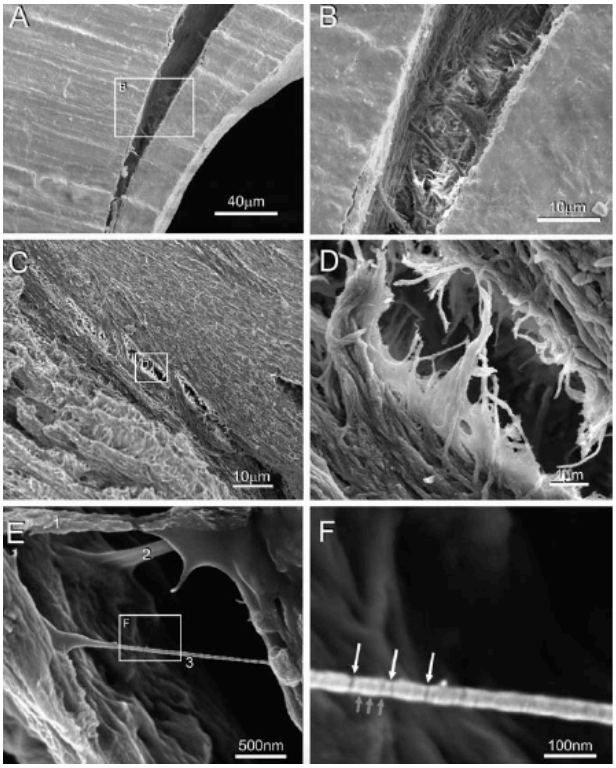


**Figure 14. Delamination effect noted on a trabecular level (A) ranging to a fibrillar level (F) where cross-link shearing is noted between bundles.** ***Taken from Fantner et al.***

### 2.4.3 Fragility failure

Fragility fracture is defined by the World Health Organization as "a fracture caused by injury that would be insufficient to fracture a normal bone as a result of reduced compressive and/or torsional strength of bone" [145].

As explored above, the tendency is for bone to fail on the tension side of an applied load as opposed to compression. This is based on the knowledge that bone is anisotropic and stronger in compression. However, fragility fractures fail partly as a result of bone that is

weaker in compression. Leng et al analysed the post-yield behaviour of cadaveric tibiae from middle aged (over 53 years old) and elderly age groups (over 83 years old). The bones were from donors that were not known to have bone disease. Cylindrical specimens from the diaphysis were mechanically tested in cyclic loading-relaxation at a low strain rate of 0.001 strains per second. It was found that in the elderly bone, there was progressive reduction in elastic modulus, yield point, stress relaxation and energy dissipation under compression [146]. The most recent study to analyse bone behaviour with age is that by Zioupos et al in 2020. This was mainly looking at the effects of ductile to brittle transition.

A ductile material is one that exhibits a degree of post-yield strain, whereas a brittle material is one that fails in the elastic phase and exhibits little to no post-yield behaviour. Zioupos analysed cadaveric donor femora in those following skeletal maturity (aged 15 and over), and those long after skeletal maturity (aged 55 years and over). Over 100 samples of bone were machined into segments from the mid-diaphysis and loaded along the mechanical axis of the femur. These were then notched in order to test work to fracture (surrogate of toughness) and loaded in three-point bending. In addition to supporting the findings of Leng et al, a progressive shift was seen from the young to the older bone, from a ductile to more brittle type behaviour. It was also shown that older bone required a smaller change in strain rate in order for it to exhibit a duct to brittle transition in behaviour compared to the younger bone, which maintained its ductile properties until much high strain rates (from ~ 9 × 10 micro-strains per second for young to ~0.7 × micro-strains per second for the elderly bone) [147].

This is an important concept that contributes towards our understanding of fractures that fail in compression, otherwise known as insufficiency fractures, such as that seen in the vertebra and sacrum. The causes of compression failure and thereby fragility fracture is likely multifactorial. However, it has been postulated by visualisation using electron microscopy that the mineral and collagen phases have varying relaxation rates, whereby the mineral component relaxed immediately ready for another load cycle, compared to the collagen phase which requires additional time to reach maximum relaxation in time for another load. This therefore transfers the load for a brief period almost exclusively onto the mineral phase, thereby stiffening the construct. This effect is amplified in rapid cyclic loading [147].

### 2.4.4 Fracture types

The importance of identifying the fracture type is related to its treatment. A clinical example of this includes paediatric femoral fractures, with long oblique fractures being more “length unstable” than transverse fractures. Subsequently, the oblique fracture may merit treatment other than flexible nailing, compared to a transverse fracture, which is relatively more length stable and where flexible nailing suffices for stability [148, 149]. In order for a fracture to reduce appropriately and heal, the forces need to be reversed and anatomy restored. Failure to understand this renders inappropriate treatment, and combined with early rehabilitation can lead to a recurrence or failure, as the forces which created the fracture are not held in check.

Fractures types vary according to the traumatic vector which is applied to bone. This is also dependant on the surrounding soft tissues which can often absorb energy (change magnitude) and the loading direction (overall vector) [150]. Figure 15 shows the common fracture types in clinical practice.

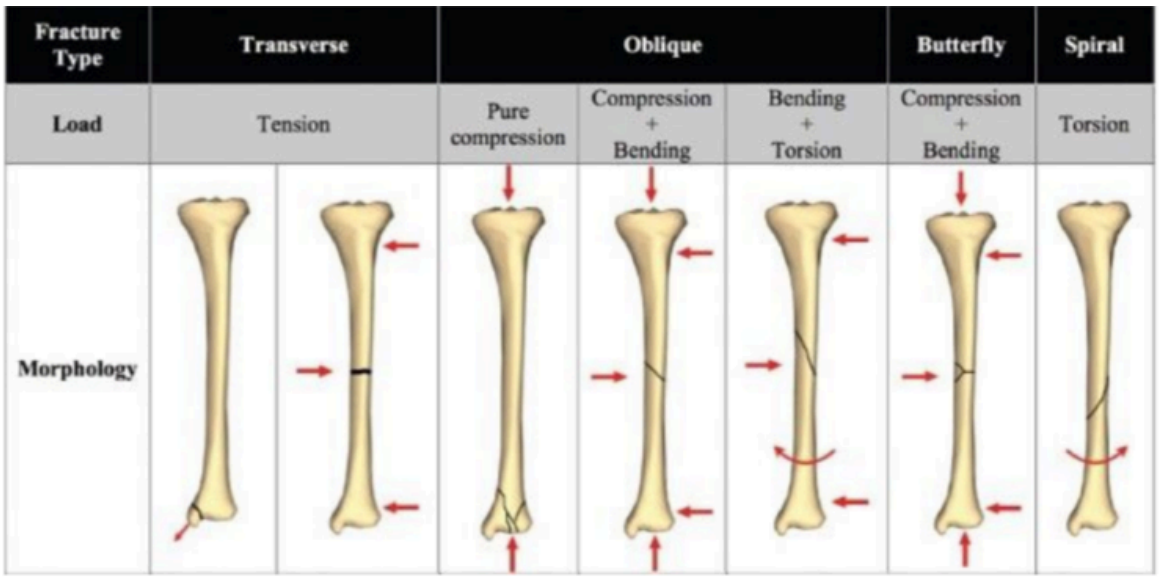


**Figure 15. Fracture types resulting from applied loads.**
***Taken from Rockwood and Green’s.***

Transverse fractures are tension fractures, with a primary load applied perpendicular to the long axis of the bone. They may also occur as a result of internal loading tension such as the case with medial malleolar injuries [151]. These are typically lower in energy [152] due

to the fact these are primarily tension failures, with crack propagation along lines of least resistance in the transverse plane.
The bending load need not be purely perpendicular for a transverse fracture to occur, particularly if there is no compressive component [153].

Oblique fractures, as the name suggests, occur obliquely or diagonally to the long axis of the bone. They can occur as a result of a pure axial loading (where the bone's natural compression and tension surfaces come into play) [151], as a result of of a combined bending and axial loading, or combined torsion and bending [153]. In a pure axial load, a shear force comes into play at 45 degrees to the axial load, with a shear force being when two forces enact in opposing directions across the bone. Where a torsional force is dominant along with a bending force, a long oblique fracture will occur as opposed to a short oblique [150].

Spiral fractures occur almost exclusively through torsional forces [154]. This fracture type has a distinct vertical component and sharp ends. Depending on the orientation of the rotational force, either a right-handed or left-handed spiral occurs [150].

## 2.5 Role of mineral in bone

The mineral content of bone has been has been shown to confer strength and stiffness [155]. The ratio of bone mineral to collagen content is very important as this helps determine the degree of stiffness and toughness. Increasing mineral content in bone makes bone "stiffer", however this is balanced against the fact it becomes more brittle.

To understand the effect of mineral variation, exaggerated biomechanical models of hypermineralisaion or hypomineralisation can be explored. Interesting examples of structures with hypermineralised content include the fin bulla of a whale or ossicles of the auditory canal. The high mineral content increases their stiffness, however both are not designed for their strength, rather for their acoustic properties. In contrast, deer antlers are relatively hypomineralised and have a reduced Young's modulus. However this means they can withstand a higher ultimate strain and require exceedingly more stress to fracture [156]. Figure 16 demonstrates the mechanical properties of these bones.

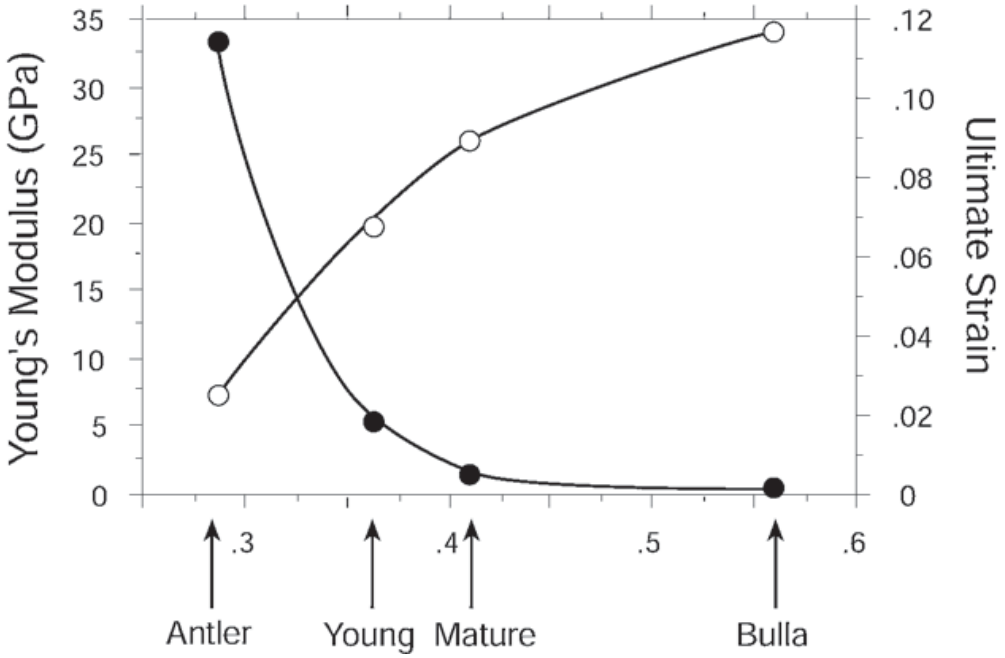


**Figure 16. Relationship between Young's modulus and strain in various structures. *Taken from Turner et al***

A biomechanical model for increasing stiffness in more mineralised bone has also been proposed by Currey et al. One such study involved immature rabbit metatarsals, and these were dynamically loaded in three-point bending. Ash content (a crude measure of mineral content) and elastic modulus were elicited to observe for any correlation. Low values of ash content were found to be reflective of lower elastic modulus and vice versa [157]. In a an annotation article, Currey argues that bone with increased mineral content has longer apatite crystals without a corresponding increase in thickness and it is this length to thickness ratio that affects stiffness. In addition, as more mineralised bone is more saturated with apatite crystals, this leads to end to end fusion of said crystals, also contributing to their stiffness, almost as one mega-structure. This was based on observations of bone under electron microscopy [158]. This work is supported by Kubala and Vose, who tested the strength of cadaveric femora. Using a make-shift hydraulic loading device, the whole bone shaft was loaded to failure and measurements of deflection taken. Bone strength was mathematically determined against a constant load. The ash content was determined by pulverising a segment of bone, and running an x-ray beam through this, with a percentage x-ray transmittance recorded. Ash content ranged from 63% - 71%, finding a positively linear relationship from 6.5 - 24 kg/mm$^2$ of stress to failure required [159].

## 2.6 Role of collagen in bone

The organic content of bone plays an important role in the mechanical properties of bone. The importance of collagen fibres on mechanical properties has previously been explored [109, 110, 160-163]. Collagen fibre orientation has been shown to be of great importance in the toughening mechanism of bone [164-167]. The energy absorbed which confers degree of toughness, is absorbed in three ways [7]:

1. In the form of diffuse damage prior to the generation of a crack.
2. Energy required to start the “final crack” that propagates into fracture.
3. Energy required to “drive” the crack into a final fracture leading to two or more distinct fragments.

One of the first to study this was Gebhardt (1905) who was able to show that collagen fibres oriented longitudinally showed tensile strength and those oriented transversely showed compressive strength [168]. This work was further corroborated by Ascenzi et al, who studied tensile and compressive properties in single osteons. In addition to Gebhardt’s findings, it was shown that the stress-strain curve and therefore modulus of elasticity differed in osteons with a higher collagen to mineral ratio, with said osteons being less stiff [3, 169].

The anisotropy of collagen type 1 seems to result from the alignment of sub fibrils along the fibril axis. Varying biomechanical values have been given for the collagen type 1 fibril. Graham et al stretched in vitro assembled type 1 collagen from human fibroblasts using atomic force microscopy and obtained a Young’s modulus of 32MPa [170]. Eppell et al mechanically tested the sea cucumber, which contain collagen fibrils similar to those found in vertebrates, and showed a Young’s modulus of 550MPa.[171] Yang et al, tested collagen fibrils from bovine achilles tendon using a home-built atomic force microscope, and found varying Young’s modulus for dry (5 GPa) and wet (0.2-0.5 GPa) collagen fibrils [172, 173]. The varying values found in these studies indicate lack of standardisation in mechanical testing as well as condition of collagen fibril on testing. Atomic force microscopy cannot provide more than low strain rates and this therefore fails to provide accurate information with regards to rate dependant properties of a fibril.

Furthermore, testing collagen away from its natural habitat renders it susceptible to cyclic fatigue and dehydration induced embrittlement, thereby skewing the values [171].

Viguet-Carrin et al considered the structure of the collagen fibre of vital importance to properties such as bone ductility and toughness [16]. It is known that conditions in which there is a mutation in collagen formation, such as Osteogenesis imperfecta, are associated with fracture fragility. Changes in collagen orientation and content can therefore affect fracture mechanics and susceptibility. In the more common condition of osteoporosis, collagen cross-links are affected leading to fragility and previous investigation of this effect on rats has been tested showing changes in mechanical properties [174, 175]. Kovach et al has shown, using a laser autofluorescence technique employed on ageing baboon cortical bone specimens, that bone toughness is significantly reduced[176]. Further work on baboon cortical bone by Wang et al supported this. In his study, cortical bone was enzymatically denatured in an effort to replicate ageing bone, and in this he showed that fracture toughness was  up to 20% lower (Figure 17).

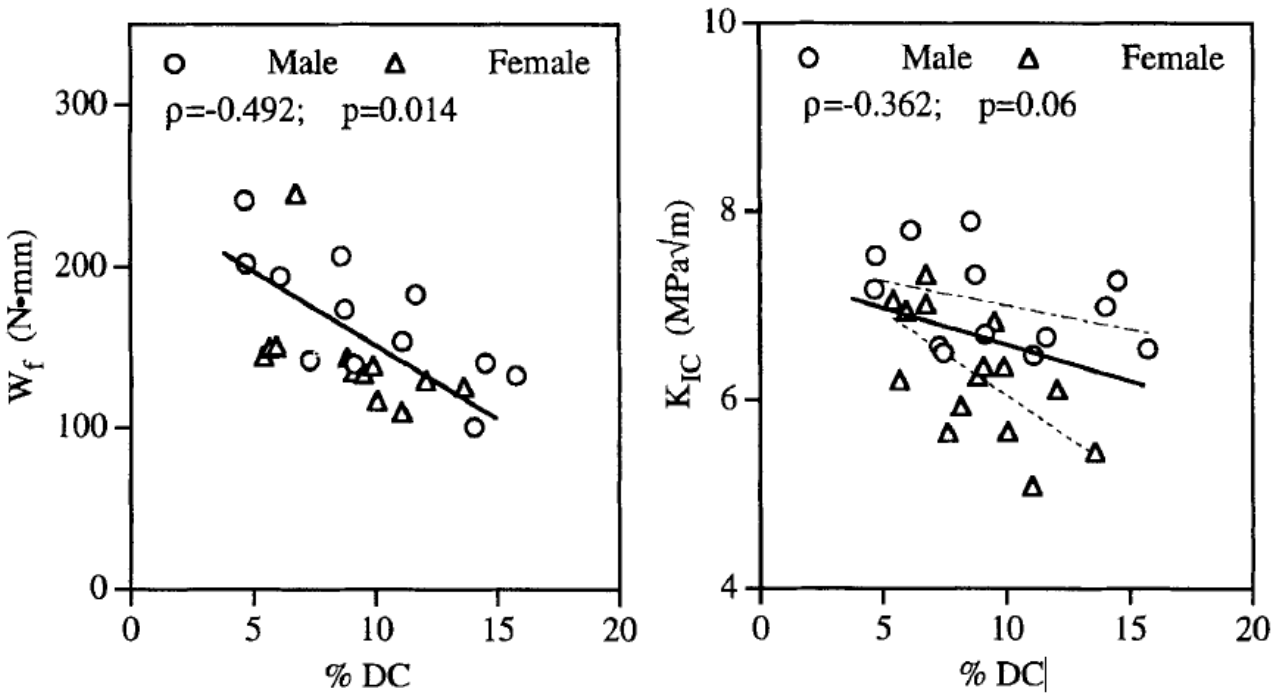


**Figure 17. Fracture toughness reduction in denatured collagen in male and female baboon cortical bone.** ***Taken from Wang et al.***

In a further study by Wang et al, human cadaveric femoral cortical segments were thermally denatured to affect the organic phase. Mechanical testing of bone using three-point bend testing showed that fracture toughness reduced to a few percent of original, and interestingly, bone stiffness remained minimally affected [177]. The main limitation to these results however was the inability to specifically target bone collagen fibres without affecting the surrounding mineralised framework. Additionally three-point bending only provided mechanical properties in one mode of failure.

The reason for this reduction in toughness is not entirely clear in humans, however, Jonas et al has previously shown in copper deficient rat bone that collagen cross-links are directly related to bone strength [178]. This has been backed by Lees et al in a further study on rat bone [179]. It is also important to note that other mechanisms have been shown to affect fracture toughness. These mechanisms are micro-cracking and crack-bridging, which are vital toughening mechanism in bone [180].

Vashishth et al showed that intrinsic micro-cracks were a major factor associated with the toughening of human and bovine bone. A proposed mechanism was microcrack tip dilatation in ductile bone leading to a re-distribution of the stresses around the fracture tip by lowering bone stiffness [181, 182]. Further studies on this by Wang et al proposed a further detailed extension to this mechanism at the nanocrack level [183].

In contrast, Nalla et al argued that the extrinsic crack-bridging mechanism was the main contributing factor to toughening in large crack sizes, and that micro-cracks alone were insufficient to increase fracture toughness. The role of crack-bridging is to lower compliance (by increasing stiffness) through bridging collagen fibres as shown in Figures 18 (a) and (b) respectively. The untracked ligament bridges result from either a nonuniform crack extension or where the main crack attempts to link up with the small crack [184]. This is further backed by other studies which provide similar conclusions [185-187].

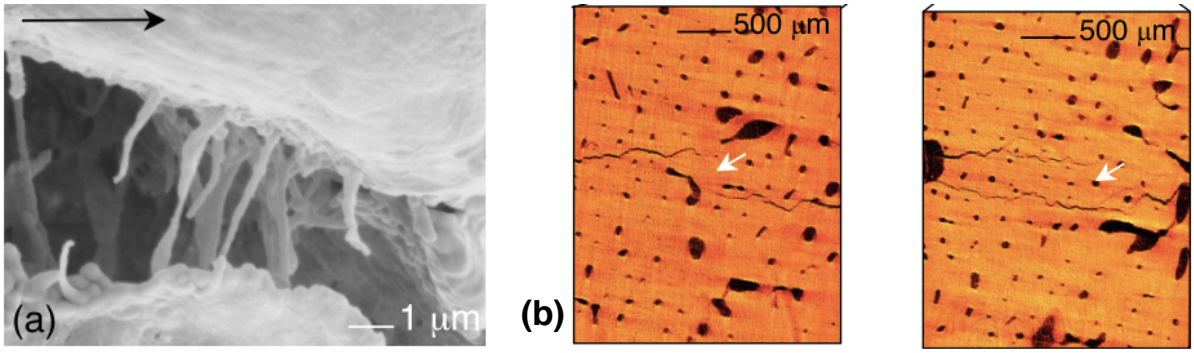


**Figure 18. Histological images of (a) bridging collagen fibers and (b) untracked ligament bridges. *Taken from Nalla et al***

The relevance of the toughening mechanisms can be related to the hierarchical structure to be explored in this thesis, which addresses the nanostructure of bone. A previous section of this chapter has addressed methods of failure, one of which involved delamination failure [144]. Whilst the cross-links in themselves are part of the ultra-structure, these do link the mineralised collagen fibrils which form the nano/micro-structure. Failure of the micro-structure does not occur independently to the failure of the structures which link them, and in fact, they seem to work in concert [143]. Failure of the micro-structure therefore needs to take into account that the collagen fibres in themselves can be disrupted.

## 2.7 Physiological changes in ageing

An ageing population is one that is distinguished by a growing number and proportion of older individuals, with a rising average population age. According to the United Kingdom Office for National Statistics in 2019, the average age of the population continues to rise as a result of greater life expectancy, exceeding the birth rate. In the next 50 years, it is estimated that there will be an additional 8.2 million people aged 65 years and over in the UK. Additionally, the over 65 year age group is the fastest growing age-group [188]. This is important to know as in order to match the challenges of an ageing population in the form of fragility fracture prevention and treatment, it is essential the scientific community is aware of the physiological changes of ageing bone at a micro-structural level.

### 2.7.1 Micro-structural change

Wang et al has previously reported that there is an optimal mineralisation density that leads to maximal bone toughness before brittle behaviour commences [189]. Seeman et al has previously deduced there is an oestrogen effect leading to an overall loss of mineral as a result of negative bone turnover. Furthermore, Seeman also demonstrated that bone toughness increases in the initial hyper-mineralisation phase, however this then leads to a negative balance when it exceeds a peak level [190]. It has also been shown that as a result of deranged remodelling with ageing, the crystals that are present are larger than those found in healthy young bone. Furthermore, these larger crystals act as a site of stress concentration and therefore more likely to be the initiation point for micro-cracking [191].

It has been argued that the effect of ageing on the collagen matrix underpins the negative effect on bone toughness [189]. Previous studies by Langdahl and Mann have shown that bone toughness can be independent of mineralisation level, this therefore implies an essential role in other structures such as the collagen matrix [192, 193]. Overall, the effect of collagen on ageing is not clearly understood. However, one potential method has been demonstrated in baboon bone. Wang et al expanded on work by Kovach et al [194] who had studied the effect of ageing cortical baboon bone on fracture toughness. In a separate study, he demonstrated that the specific mechanism of non-enzymatic glycation was thought to be a contributor to the reduced mechanical properties of the collagen network [195].

Perhaps the most proposed mechanism seems to be age related effects on the intramolecular collagen crosslinks without necessarily hindering the overall collagen concentration [196-199]. Exact mechanical testing on young, middle-aged and elderly bone has also been tested with the collagen network being shown to have a 35% decrease in mechanical strength, 30% reduction in elastic modulus and 50% reduction in ability to absorb energy between the young and elderly [177].

### 2.7.2 Macro-structural change

On a macro-structural level, bone mineral density describes bone mineral per unit volume of bone. Ageing shows changes leading to hyper-mineralisation in varying areas of bone, with overall loss of bone volume being the greatest contributor. This is contrary to the view that bone mineral density decreases with ageing. Reid et al analysed the ribs of human from varying ages from 8 weeks to 59 years of age. Scanning electron microscopy was used to assess bone density, by analysing the proportion of pixels falling in a uniform set of grey levels. This was then converted into a digital computerised image. Higher density bone was found in those in the older age ranges [200]. Zagba et al analysed the cadaveric femora of subjects aged 18-96 years old, both micro-radiographically and histologically. He noticed that from the age of 48, subperiosteal bone appeared to become more hyper-calcified, this is in addition to calcification of the periosteum itself [201].

Perhaps more importantly, is the effect of ageing on bone mineral units themselves. Ruff et al studied 119 human cadaveric cortical bone of femora and tibiae, aged 20 to 70 years old. Cross-sectional analysis utilising photon absorptiometry was undertaken on these specimens, with visible increased cross-sectional bone area consisting with expansion after the age of 35 years. However, there was also loss of overall bone density, as a result of loss of bone volume. It was deduced that the increase in cross-sectional area is part of the remodelling process to compensate for loss of mechanical strength through loss of bone volume [202]. Basle et al studied osteoporotic bone density in cadaveric iliac bones of the pelvis. Calcium and phosphorus element concentrations were evaluated in cortical and trabecular bones using energy dispersive x-ray. The results suggested that the decrease in bone density in osteoporosis is related to bone volume as opposed to changes in the elements within the bone mineral units [203].

The overall reduction in bone mineral units seems to be as a result of remodelling "uncoupling" meaning bone formation cannot keep up with bone resorption. There is no clear understanding of signal transduction disruption although a few mechanisms have been postulated. Previous mechanisms proposed include; 1) a change in calcium hormone secretion or metabolism being a factor [204-206], 2) a decrease supply of hormones via reduced bone perfusion [207, 208], 3) changes in crystalline properties of bone material [209] and 4) an age related decrease in metabolic activity of osteoblasts [210-212]. The resultant hyper mineralisation and reduction in bone volume leads to the accumulation of unchecked micro cracks which ultimately affects the macrostructure of bone thereby leading to fracture [164, 213-215].

### 2.7.3 Mechanical change

Between the ages of 35 and 70 years old, cortical bone strength in bending is diminished by around 20% and cancellous bone strength in compression is diminished by upto 50% [216]. It is known that there is a change in bony architecture with increasing age, and this is associated with an increased risk of fractures [7]. Both qualitative and quantitative changes occur in bone architecture resulting in a decrease in bone mass and strength. Whilst there is an extra-skeletal element to this increased incidence such as impaired reflexes, altered proprioception, reduced visual acuity and co-morbidities, there is also a skeletal element.

Zioupos et al obtained cylindrical cortical bone specimens from cadaver human males, aged 35-92 years without any underlying bone pathology. He was able to show a linear fall per decade of life in bone elastic modulus, strength, fracture toughness and work to fracture. Zioupos concluded that this was due to; a) reduced ability of ageing bone to absorb damage and b) reduced ability to resist the formation of a macrocrack [7]. Further work by Currey [5] and Zioupos supported these findings [217].

Previous evidence has also suggested that age related deterioration of bone quality may be due to the interaction between the mineral and collagen matrix as part of remodelling [218]. Bone remodelling is constant in healthy tissue and is a result of bone resorption through osteoclasts being balanced by bone formation through osteoblasts. This results in no net loss in bone tissue [219].

Various specific age related changes have been proposed. This includes failure of osteonal and endotrabecular remodelling to replace and repair fatigue damage. Remodelling also affects collagen fibre orientation, mineralisation and amount of unrepaired fatigue damage, which are determinants of bone stiffness and strength. Finally, changes in bone mechanical properties as a direct result of reduced regional collagen fibre variability and new cement line interfaces seem to weaken bone during monotonic tests. All of these deficiencies are considered crucial during the ageing process and seem to have a direct impact on mechanical properties [216, 220-222].

Ageing alters the force required to fracture, particularly in trabecular regions, causing the common variations in elderly fractures to occur here, such as the neck of femur, vertebral compression fractures and distal radius fractures [223]. Trabecular bone stiffness varies with variation in bone density. Carter and Hayes undertook compressive mechanical testing on trabecular bone in human and bovine femora, showing that the strength of bone was proportional to the square of the apparent density, and the elastic modulus was proportional to the cube of apparent density [224]. Russo et al, looked at both cortical and trabecular bone in the tibia in over 1000 patients aged from 20 - 102 years old. Bone density, mass and cross-section was analysed using quantitative computed tomography. Cortical bone density was seen to reduce linearly with age in both sexes, being significantly smaller in women aged over 60 years old despite. The theorised minimum moment of inertia was significantly lower in older women, whereas in men this remained stable. One reason for the sex difference was thought to be due to a more efficient change in cross-sectional area to density in men, compared to that in women [225]. This was further substantiated by Burstein et al, who machined cadaveric human femora/tibiae and tested these mechanically. There was a progressive decrease with age in ultimate strength, strain and elastic modulus [91].

### 2.7.4 Young sportsmen

Young active individuals are expected to have optimal mechanical properties. Exercise is known as a positive contributor to peak bone mass in young adulthood [226]. There is a general lack of understanding as to the mechanisms surrounding this process with conflict in the literature particularly with animal models. Judex et al studied the effect of high strain jumps on the metatarsals of growing roosters. In vivo strain gauges were used as roosters were dropped at force, at least 50 times a day for 3 weeks. There was a positive correlation between bone formation rate and those roosters that underwent high jumping compared to controls. On histochemical analysis, an increased osteogenic profile was noted on the endosteal surface of metatarsals [227]. The reasons for this were thought to be due to osteocyte mechanosensors leading to osteoblast and osteoclast de-coupling, to enhance bone formation, following the same principles of Wolff's law as explored above.

This is not supported by rat models which were conducted. Zernicke et al, conducted rat tibial testing following a 10 week exercise program against controls. The tibia were then sectioned and underwent mechanical and histological testing. The elastic modulus and yield points of the exercised tibiae were significantly less, although cross section and histology did not differ [228]. Forwood et al undertook a similar study, with rats undergoing treadmill testing, then conducted similar mechanical studies on femora and tibiae. A reduction in stiffness was noted in the exercised group. Furthermore, the bone formation seen in the study by Judex et al was not supported in the above rat models [229]. There are significant confounders between these studies which can explain the discrepancy however. Firstly the animal model and bones tested significantly different (rooster metatarsals versus rat tibia). Secondly the exercises and duration of exercise differed, with high impact loading for roosters, and cyclic treadmill testing for rats, which puts the rat bones at risk of fatigue damage and increased micro-crack formation. It is therefore difficult to reach any conclusion between the two models, however it does seem that there is a mechano-stimulatory effect on bone regardless of exercise.

In contrast, there is clear correlation between exercise and mechanical properties in humans, with a consensus in the literature. Bradney et al compared the adolescents of two schools (twenty patients) of similar socio-economic background, with one group undertaking an 8 month exercise program compared to the control. Dual x-ray absorptiometry scanning, with a significantly increased cortical bone thickness and bone density seen in the exercise group [230]. This finding was supported by Courteix et al, when looking at bone mineral density in pre-pubertal girls who underwent high loading activities such as gymnastics compared to controls [231]. Several longitudinal studies in adults have also been undertaken. Lloyd et al retrospectively analysed 81 caucasian female university students, using self-assessments of their exercise patterns from the ages of 12-18 years old. DEXA scanning was utilised to assess hip bone mineral density at time of study, finding a positive correlation between activity in early teenage years and bone density [232]. Nilsson et al compared the bone density of 184 healthy 24 year old male athletes, to 177 age matched controls. Quantitative-CT (bone cross-section) and DEXA (bone density) were used to assess the radius and tibiae of these patients. There was a higher mean in the athletes with higher cross-sectional area (16.4% increase) cortical thickness (5.4% increase) and bone density (14.5% increase) compared to the control group [233].

This correlation with increased bone density with exercise, directly correlated with a mechanically stronger construct. There are higher elastic moduli for bone with increased density, which increases the proportional limit and yield points. The resulting outcome would be one in which a higher energy would be required to achieve failure of bone. For example if one adult who does not exercise, is impacted by the same vector, as an age-matched adult who does exercise, the resulting mechanics of bone would be different. And it is more likely that the exercising adult would be able to resist more of this force before fracture [234]. This also has implications on orthopaedic practice, whereby the process of drilling and reaming of long bones is a more arduous task, generating greater thermal necrosis of bone, in younger healthier individuals [235].

### 2.7.5 Transitional change

**Paediatric to adult**

The age at which bone behaviour transitions from paediatric to adult type behaviour in humans is also a subject of debate. Little work has been done on paediatric bone, partly because of the difficulty in collecting this tissue. Mueller et al carried out work on trabecular iliac bone from newborn to elderly and found no significant change in the organic fraction with age [30]. Currey et al looked at the femora from 9 subjects ranging from 2-48 years old and observed a lower ash content in children. He also found that paediatric bone was weaker and less stiff, deflecting more and absorbing more energy before failure [5]. Ohman et al studied cortical bone (tibia) of children and adults, looking at compressive behaviour. It was found that due to the increased ash density in adult bone, there was higher young's modulus and yield point. The oldest cortical bone studied in the paediatric group was 15 years old [236]. The disadvantage of this study was that the paediatric bone studied was pathological, being harvested form patients who suffered from cancer. None of these studies were able to study a large enough number to delineate a transition point in behaviour from paediatric to adult.

Much remains unknown about the point at which bone transitions from paediatric to adult behaviour. Perhaps the best assessment is using markers of skeletal maturity. The "Tanner-Whitehouse (TW) protocol for Assessment of Skeletal Age" is the most widely recognised predictor [237]. The original version provided a maturity indicator based on 20 bones including radius, ulna, carpals, matacarpals and phalanges. The radius, ulna and carpals were later eliminated as these were thought to be too difficult to assess reliably. The latest TW3 version has been modified based on a longitudinal European/American study in which 1090 radiographs of 450 males and females were studied for maturity scores. Skeletal ages of maturity were agreed upon as a result of earliest maximum scores, with males at 16.5 (from 18.2 years) years and females at 15 years old (from 16.5 years) [238].

As a result of a lack of consensus in the literature, and to enable capture of as many skeletally immature patients as possible, the age limit in this study before progression to the adult group was <17 years old.

**Adult to Older**

On a nano-structure level relevant to this thesis, extensive work has been undertaken in animals, however, this has not translated accurately in clinical practice given the variability in mechanical properties and mineral content [239, 240]. In human bone, Zioupos et al assessed the effect of ageing on human cadaveric femora. Cortical specimens were prepared from the femora of humans ranging from 35 - 92 years of age, and these were subjected to rigorous three-point bend testing. The elastic modulus and toughness decreased by 2.3% and 3.7% respectively, per decade of femur tested [7]. Wang et al studied 30 human cadaveric femora, with ages ranging from 18-91 years old. These were divided into three groups, young (18-49), middle-aged (50-69) and older (>70), in an arbitrary fashion. Bone segments were created and were untampered. The bending properties of these groups were assessed, finding a significant difference in the toughness of bone between the older and middle-age groups [241].

On a macro-structural level Forman et al studied the effect of age on moment arm required to fracture a human cadaveric femoral shaft in the paediatric, adult and advanced age populations. Eighty-three femoral shafts were obtained through their national tissue donation program and tested under three point bending about the anteroposterior axis via a force applied in the medial direction. Forman concluded that femoral midshaft moment exhibited a rapid increase in the late teenage and early twenties and peaked and plateaued between the ages of 25-50 years old. What followed was a gradual decline after age 50. This was though to be primarily attributable due to an initial increase in cortical thickening and cross sectional area during growth, followed by increased porosity and reduced cross sectional area in later years [242]. Sai et al assessed the trabecular bone density of a Japanese population in 2380 volunteers from 26-85 years old. The distal radius density was assessed using peripheral quantitative computed tomography. Trabecular bone density fell significantly for both sexes commences at age 55 years and over [243]. Steiger et al analysed bone mineral density decrements in women aged over 65 years only. This was done using DXA scanning, and found a strong inverse relationship for a decrease in density with every year. This was upto 16% between the age of 65 and 85 [244].

Further clinical studies analysing post-traumatic mortality rates have also been conducted. Campbell-Furtick et al analysed 872,861 adult trauma patients, from their regional trauma database, over a 7 year period and showed three age spikes at 37, 60 and 80 years old correlating with an increased mortality. He suggested a data-driven elderly age of 60 years old [245]. This is also supported by a landmark study in the New England Journal of Medicine, by MacKenzie et al, who analysed mortality rates in 18 level 1 trauma centres versus 51 non-trauma centres across the United States. Propensity-score weighting was used to analyse over 5000 patients, finding a larger effect of treatment in level 1 trauma centres in the under 55 year olds compared to over 55 year olds, suggesting a physiological change at this age cut-off [246]. Smaller trauma observational studies of this nature have looked at mortality risk and defined the elderly population commencing at 55 years onwards [247, 248]. The age cut-off in these studies was based on the premise that a higher age would lead to “under-triaging” of patients who have similar risks of mortality but are not treated as seriously.

The National Institute of Clinical Excellence (NICE) in the United Kingdom, recommends fracture assessment as part of falls assessment for anyone over the age of 65 years in women, or 75 years in men, or anyone under these ages who display risk factors. This seems to be primarily based on the estimate of those over 65 years who sustain a fall. Almost a third of over 65 year olds sustain a fall at least once each year in the United Kingdom, with an estimated 500,000 fragility fractures.

There is also a financial element with this age-group that balances the health risk with the economic burden. Previous studies in the United States (Preventative Services Task Force) have shown that only 75 - 143 women would need to be fracture screened in age over 75, to prevent one vertebral or hip fragility fracture, compared to between 453 and 1856 in the 60 - 64 year age group [249]. This has obvious economic costs, with cost per quality adjusted life year in over 75 year old women being $5600, compared to $43,000 in 65 year old women [250]. Despite this knowledge however, there does not seem to be any evidence correlating an exact physiological age correlation to a transition point of bone to brittle behaviour.

Given these values, and to avoid the risk of “under-triaging” the elderly, an age cut-off of 55 years old was used.

## 2.8 Pathological change

It is important to explore pathological changes in bone, or conditions which weaken bone as they correspond with fragility fractures, that is, the susceptibility of fracture as a result of forces that would not ordinarily cause this [251]. A condition which affects the quality or quantity of bone will therefore have an effect on fracture risk, which is a significant epidemiological concern [252]. Understanding the processes behind a condition will enable more focussed prevention and treatment of fragility fractures. Furthermore, they are a source of economic burden with direct medical costs as a result of fragility in the United Kingdom estimated at £1.8bn in 2000, rising to £2.2bn in 2025 [253].

### 2.8.1 Osteoporosis

Osteoporosis is relevant to the primary aims of this thesis. Osteoporotic bone affects both the mineral and collagen components amongst others. However, there is a change in both elements in concert as opposed to being mutually exclusive. A change in collagen alone would reflect a condition similar to that of osteogenesis imperfect, with a change in mineral alone reflecting a condition similar to rickets/osteomalacia. Therefore the importance of designing a protocol for each element cannot be underestimated, as it could provide data for the cyclic loading of bone for the staged demineralisation and decollagenisation in order to replicate the nanostructure and mechanical behaviour of osteoporotic bone.

Over the years, various definitions have been proposed for this condition. The consensus definition recognised by the World Health Organisation states that osteoporosis is “a disease characterised by low bone mass and micro-architectural deterioration of bone tissue, leading to enhanced bone fragility and a consequent increase in fracture risk”.

Osteoporosis is now objectively defined by bone mass density (BMD) using dual energy x-ray absorptiometry (DEXA). The World Health Organisation uses the definition of osteoporosis as a DXA score of greater than 2.5 standard deviations below the young adult mean. This score is sex and race matched but not age-matched and is known as the “t-score”. A score of between -1 and -2.5 standard deviations is defined as osteopenia and puts the patient at higher risk of developing osteoporosis [254].

There remains debate as to how fracture risk should be measured with not all osteoporotic fractures such as vertebral fractures being explained by reduced bone mineral density in isolation [255]. Therefore, measurement of “bone quality” has been proposed as this encompasses parameters such as BMD, microarchitecture of trabecular bone, microcrack prevalence, bone geometry and bone matrix material properties [256].

The clinical significance of osteoporosis is primarily in its relation to fracture risk (most commonly of the hip , distal radius and vertebrae). Over the first three decades of life there is an increase in bone mineral density (BMD) and this can peak in different regions at different ages i.e. it can peak in the hip at 18 years of age and distal radius at an age closer to 30 [257, 258].

Once peak bone mass is reached this can plateau in women until the menopause when a change in female sex hormones leads to a reduction in bone density over the next decade [257, 259]. Primary involutional osteoporosis, relating to the ageing process, is the cause in 80% of women and 50% of men, however other causes may contribute and this is likely multifactorial including renal, endocrine, metabolic, gastrointestinal or haematological. In causes other than primary involutional osteoporosis such as those secondary causes named above, the male sex predominates and this is likely due to alcoholism, hypogonadism, malignancy and long term steroid treatment [260].

When discussing the increasing mechanical fracture risk associated with osteoporosis, it is important to refer to factors such as the degree of mineralisation, bone mineral density, effects on collagen network and altered remodelling, all of which alter bone strength. This has been explored extensively above (sections 2.5 and 2.6). However, other risk factors leading to an increased fracture risk include the significant falls risk. This risk is well recognised and many studies in the past have focussed on falls prevention in order to prevent osteoporotic fragility fractures [261]. The factors leading to falls can be attributed to both intrinsic and extrinsic factors, with modifiable risk factors including alcohol intake, smoking, caffeine intake and activity levels.

Loss of bone mineral density alone therefore, does not explain the increased fracture risk. Therein lies the main limitation of DEXA scanning. It is considered the gold standard and works by emitting two radiation energies, which is therefore able to differentiate degree of mineralised bone more clearly from the surrounding soft tissues. The reason DEXA scanning is considered gold standard lies in its ability to diagnose osteoporosis as per the WHO criteria [262, 263], assess fracture risk and response to treatment. There are currently no other economically viable imaging modalities that carry out these functions as efficiently. Furthermore, there is evidence to suggest that DEXA scanning is an effective predictor of a major fragility fracture, hip fractures [264-266].

Whilst bone mineral is an essential component in the stiffening process, DEXA scanning does not take into account significant factors that also correlate with mechanical behaviour, such as the increase in cross-sectional area, loss of structural water content, cross-link disruption and its effect on toughening mechanisms, the effect of advanced glycation products with ageing, or changes in collagen orientation.

Perhaps the most comprehensive solution, which takes into account the 3-dimensional nature, of bone, cross-section and elements, include quantitative computed tomography scanning which is used to input into a finite element analysis model [267]. There are however significant cost and precision indications particularly with unstandardised data input errors and the difficulty in adjusting for the soft tissue envelope. Furthermore, the main body of research revolves around vertebral fractures, and is not applicable to other fragility fractures such as the hip [268]. Given the advantages of this method in analysing the various elements and cross-section, this would perhaps offer the most accurate assessment of bone quality for this thesis, however, this would require significant research facilities and costs, which were not within the resources available in the study unit.

### 2.8.2 Osteogenesis imperfecta

The decollagenisation process of bone alone is perhaps most reflective of a condition effecting collagen quality or quantity alone. One such condition leading to fragility fractures is osteogenesis imperfecta.

Osteogenesis imperfecta (OI) is a rare condition affecting bone and connective tissue with many known subtypes. It is a genetic disorder characterised by bone fragility and low bone mass density with varying severity and manifestations, both skeletal and extra-skeletal [269]. It is a predominantly autosomal dominant disorder affecting approximately 1 in 10,000 and it results from genetic mutations in the most abundant protein in bone, collagen type 1 [270]. More specifically, the genetic mutations affect two genes of the alpha chains of collagen type 1, resulting in two types; COL1A1 and COL1A2 [271].

With regards to pathogenesis, the most typical mutation is a point mutation in COL1A1/2 which affects the glycine residue. This leads to a mix of both normal and abnormal collagen mutations, the degree of which is variable [272]. When the glycine residue is affected this has a deleterious effect on the triple helical structure rendering it less competent. The abnormalities in the organic compound also seems to have a compound effect on the inorganic mineral content. Bone becomes hyper-mineralised with smaller crystals that are abnormally aligned [273, 274]. In addition bone thickness is much reduced compared to age-matched controls as a result of sluggish periosteal bone formation. Trabeculae are thinner, and despite osteoblast formation being amplified within these trabeculae, this does not have a net gain effect in bone volume as seen in Figure 19 [275].

These effects on collagen and mineral impact bone biomechanics. Mouse models, described as osteogenesis imperfecta murine (OIM) have been studied by Misof et al. In his study, he showed that OIM have similar abnormally aligned collagen/crystal structure as seen in humans. Collagen of homozygous OIM in the form of tendon were studied and their mechanical testing showed values of ultimate tensile stress and strain that were almost half of that in control models. Misof concluded that brittleness of this bone was in part due to this dramatic reduction in collagen tensile properties [276].

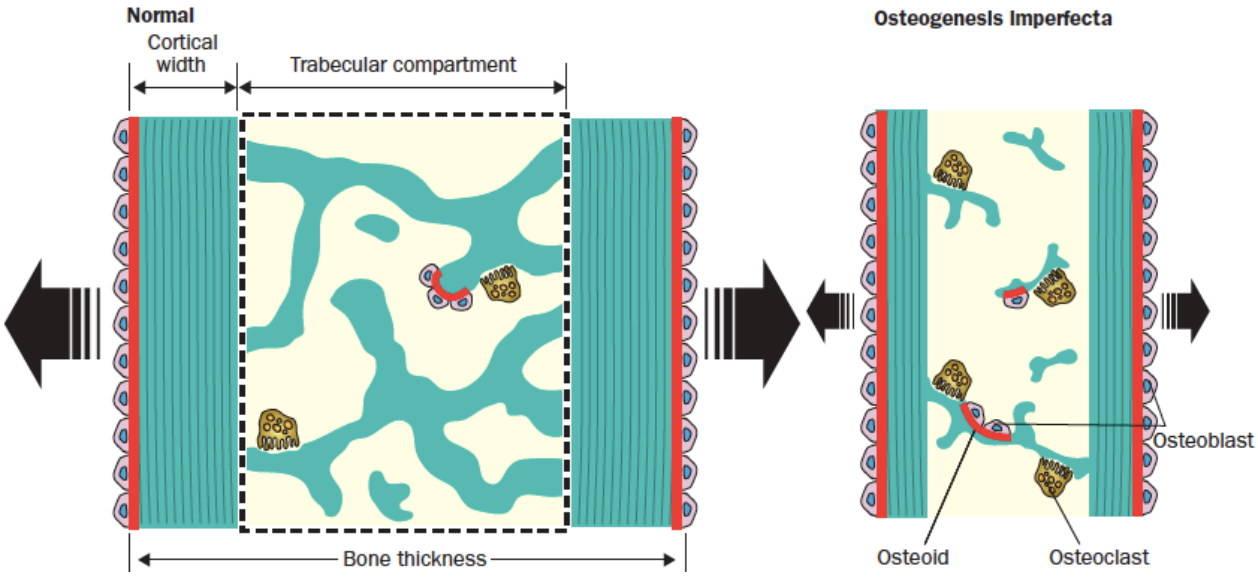


**Figure 19. Showing reduced bone thickness in control and OI bone. *Modified from Rauch et al***

Further mechanical testing of OIM by Camacho et al showed that stiffness in homozygous OIM femur was significantly reduced in torque compared to heterozygous OIM or control mice. Furthermore, the mean ash weight of mineral content was reduced in homozygous OIM reflecting the reduction in bone volume [274].

### 2.8.3 Hypomineralisation

Perhaps the best clinical examples of hypomineralisation affecting biomechanics of bone clinically is in rickets and osteomalacia. The underlying mechanism for both is a failure to mineralise osteoid, with rickets being the subadult and osteomalacia being the adult expression of this condition [277]. The extent to which reduced poor bone mineralisation diminishes bone strength in the early phase of infantile rickets remains unclear and is at best described in case reports [278]. This differs to the knowledge that reduced bone mineralisation leads to an increased fracture risk. Thacher et al conducted a radiographic analysis of 264 Nigerian children with nutritional rickets and found that there is a correlation with reduced bone mineral density but increased bone mineral area. This seemed to be more pronounced in diaphyseal as opposed to metaphysical regions [279].

Chapman et al also conducted a retrospective radiographic analysis of children under 2 years old who sustained fractures, and found that in those with radiographic evidence of rickets and were mobile, a significantly higher proportion had fractures. The study went further to suggest that the classic signs of multiple fractures associated with rickets were not supported by their study, and were more in keeping with non-accidental injury [278].

There is a paucity of evidence on the biomechanics of bone with poor mineralisation such as that seen in rickets/osteomalacia. It is thought that this bone has a lower yield point, however, manifests greater post-yield properties through greater ductility and ultimate displacement. As a result of the lower yield point, these bones exhibit reduced extrinsic stiffness and undergo fracture more easily. The understanding of fracture risk in these conditions seems to be understood when comparing immature paediatric to mature adult bone, with the working knowledge that paediatric bone has adequate collagen content but a relative deficiency in mineralisation. Subit et al tested bone coupons of various age groups under tensile load. He found that paediatric bone had lower Young's modulus than the adult or elderly bone [280]. This seems to concur with studies carried out on fresh paediatric long bone of autopsy subjects, and found that ultimate tensile stress was less than that obtained for dry embalmed adult bone. A combination of these biomechanical factors seems to result in the fragility fracture picture described for rickets and osteomalacia.

## 2.9 Previous protocol work

### 2.9.1 Demineralisation

Several studies in the past have looked at the effect of demineralisation and the biomechanical effects of this. Bowman was perhaps the first to describe how the demineralisation process on bone effects mechanical properties. Bovine humeral diaphysis were demineralised using disodium Ethylene diamine tetra-acetic acid (EDTA) over a period of two weeks with spectrophotometry used to scale this process. Following mechanical testing, the stress-strain curves produced showed similar tensile values to that of tendon and cartilage [281]. Shah was able to study this demineralisation process further in feline femurs using a similar decalcification process by the use of EDTA. Shah varied the demineralisation process, with up to 100% demineralisation compared to control bone and these specimens were then loaded to failure. The study concluded that calcium was integral to strength of osteopenic bone as bending strength exponentially decreased with increased decalcification [282].

More recent literature that has looked at the effect of demineralisation on ovine bone was by Wallace et al. Forty ovine femurs were demineralised at an enhanced rate by immersing these femurs in EDTA within an ultrasonic bath to enhance demineralisation rate. This process was staged to obtain bone with mineral levels seen in osteomalacia and osteoporosis, with mechanical testing taking place via three-point bending for both low and high strain rates. There was a significant difference in stress seen at high strain rate in the demineralised bone, highlighting the importance of mineral at traumatic loads. However, it was noted that at low strain rate, a toughness reduction of 25% could be seen in the control and demineralised bone, with a negligible difference seen at high strain rate (Figure 20 a) and b)). Wallace deduced that this indicated removal of mineral alone cannot account for this reduction in toughness, and that another factor was at play, potentially collagen removal or deficiency [64].

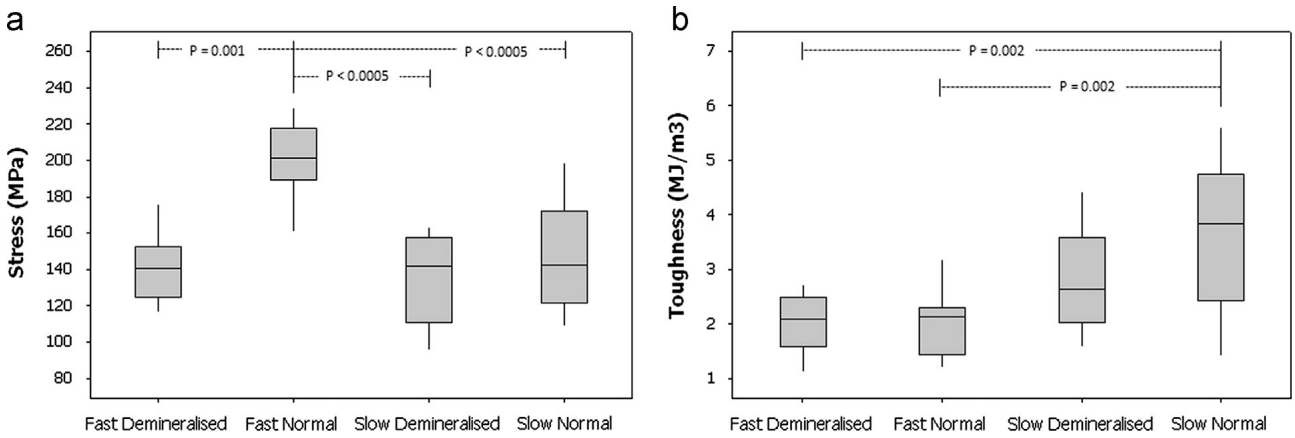


**Figure 20. Showing a) effect of loading rate on stress and b) effect of loading rate on toughness. *Taken from Wallace et al***

## 2.9.2 Decollagenisation

There is a relative paucity of evidence looking at selective collagen extraction form bone and its effect on bone mechanics in cortical bone with intact mineral. Wang et al has previously shown the effect of collagen disruption on bone toughness as discussed above. Hey et al in his biochemical studies showed that collagen ”swells” when immersed in highly alkaline solutions at room temperature or above [283]. This is advantageous as this “swelling” allows for easier extraction of collagen without disruption of the mineral compound. Amadasi et al assessed the effect exerted by acidic (sulfuric acid) and basic (sodium hydroxide) solution on porcine bone. Energy dispersive x-ray analysis, scanning electron microsopy and powder diffraction ash content was measured. He noted that only the acidic solution made a difference to the mineral content and was able to dissolve this completely [284]. The collagen can also be extracted as one unit by raising the temperature in this alkaline solution as opposed to leading to the formation of gelatin. This is based on work by Privalov et al looking at thermostability of collagen in relation to osteogenesis imperfecta, concluding that collagen is most stable at a temperature below body temperature and the unfolding of the triple helical structure occurs exponentially with temperatures over 37 degrees [285].

Yang et al used the above method and extracted collagen molecules form pigskin through chemical hydrolysis in a neutral solution such as saline [286]. Bi et al also studied the effect of an alkaline solution such as Sodium Hydroxide (NaOH) on the mineral content of bovine femur as part of looking at the effect of NaOH on prion transmission in bone graft. He used energy dispersive X-ray spectroscopy to identify if any difference was seen in NaOH treated and control bovine bone, noting no statistical difference between the two groups in mineral content. This was also confirmed on scanning electron microscopy before and after immersion in NaoH, showing structural damage, but no loss of mineral. Additionally, ultimate load and ultimate stress mechanics on NaOH treated bovine bone was noted to be much lower than that of controls using compression testing at low strain [287].

The effect of an alkaline solution on bone cells has been previously studied but the histology remains unclearly understood. Bone mineral itself is known to be an alkaline material which has an ability to buffer hydrogen ions for acid base balancing [288, 289]. An acidic environment is thought to invoke bone resorption via an osteoclastic response (require and perpetuate an acidic environment), with an alkaline solution creating an osteoblastic response, as a result of alkaline phosphatase (marker for osteoblastic function) [290, 291].

It is on this understanding of known physiology, as well as studies mentioned above, that the mineral is thought to remain undisturbed in experimental models utilising an alkaline solution. However to the author's knowledge, there are no known studies which have explained the process behind this relative preservation of the mineral content in animal models.

The use of higher temperatures to aid the decollagenisation process does not affect the mineral content, primarily due to the fact that the mineral melting point is well above 1000 degrees celsius [292].

Given this knowledge, in this thesis, a protocol was devised for the staged extraction of collagen from cortical bone without undue effect on the mineral content as will be explored in more details in the methods section. This forms a novel aspect of this thesis.

### 2.9.3 Animal models

The selection of animal models for orthopaedic research is multifactorial. Considerations to take into account include; a) genetic uniformity of animals; b) cost effectiveness; c) availability of said animal; d) ease of adaptability to experiments; e) ethical implications and f) ecological implications [293].

Ovine bone is a convenient, readily available and cost-effective model for orthopaedic research. Ovine bone is an accepted form of large animal that is readily used in orthopaedic research due to its size, weight, bone structure and bone remodelling processes. This in turn allows ovine bone to be a suitable model for biomechanical analysis as was recognised by Bergmann et al who identified sheep hip joint reaction forces and vectors as being similar to those in humans [294, 295]. Newman recognised the need to identify an animal model that was suitable for analysis of post-menopausal osteoporosis. In it he compared various animal models and identified advantages and disadvantages with each, however, he recognised that sheep are seen as most ideal due to them being docile, easy to house, inexpensive, readily available and spontaneously ovulate with hormone profiles similar to women [296]. Disadvantages have been noted in using sheep bone for osteoporosis studies, which mainly revolve around the lack of natural menopause in sheep as well as seasonal changes in bone metabolism [297].

The bovine animal model is another large animal model that has been used in orthopaedic research and was also considered to be potentially suitable for use in this study. Whilst bovine is suitable in terms of joint biomechanics, compared to dog, pig and sheep bone which have similar ash content to humans, bovine ash content differs significantly. Furthermore, the cortical to trabecular ash content within bovine bone also differs significantly [298].

Murine bone remains less expensive than others. They also have the advantage of being able to be purpose bred more readily in order to reduce biological variation. Their disadvantage lies in their size, meaning their bones and joints are proportionally small [299].

Finally, rodents mature at a slower rate than other animals, resulting in the growth plates remaining open for a prolonged period, which reduces the availability of suitable bone for the types of study in this thesis. [300]. For this study, due to the significantly varying gait pattern and biomechanical loading of joints, they have more limited potential for translational research in this subtopic of orthopaedic engineering [299, 301].

Given the above information, in this study, the balance of pros and cons favoured healthy, mature ovine femur for ex-vivo experimentation.

## 2.10 Epidemiology of femoral shaft fractures

Femoral shaft fractures are common and potentially devastating injuries at all age groups. The epidemiology of fractures have been studied since the 1800's. Bruns et al in 1882 noted the effects of age and gender on incidence and fracture types [302]. In an epidemiological study from Edinburgh by Court-Brown et al, utilising prospective data from the unit trauma database, all presenters with fractures over the age of 12 were analysed. With a known population of over 500,000, an estimated incidence of femoral shaft fractures of 10.3 per 100,000 person years was seen [223]. In the same year (2000), Salminen et al analysed the incidence and treatment methods of femoral shaft fractures in a Finnish population. The incidence was found to be very similar at 9.9 fractures per 100,000 per year [303]. More recently in 2009, and in the largest known study to date, Weiss et al in a further Scandanavian study, looked at the incidence stability of femoral shaft fractures over a 6 year period (1998 - 2004). Over this period, 6409 fractures were identified, with an annual incidence of 10 per 100,000 per year. This was found to have remained stable over this time period [304]. This stable incidence, particularly in Scandanavia, is also supported by the fact an incidence of 9.65 per 100,0000 annually was noted by Bengner et al in the 1950's [305].

However, some discrepancy in the literature does exist. Donaldson et al, in an English population (Leicester) in 1990, quoted an overall femoral shaft incidence of 3.1 per 100,000. They were cautious to draw conclusions from their study due to perceived underlying variations in demographic compared to other studies, the inaccuracy with the prevalence of osteoporosis in their study population, and their overall lack of certainty with regards to their accuracy [306].

There tends to be a bimodal distribution of these fractures in both age and gender, occurring in young males as a result of high energy trauma, and elderly females as a result of fall from a standing height [305, 307]. Weiss et al in the largest known study of femoral shaft fractures noted a bimodal distribution in the under 10 year olds and over 90 year olds [304]. Singer et al, in another Edinburgh epidemiological study, prospectively studied population incidence of all fractures involving over 15,000 patients between 1992 and 1993. Femoral shaft fractures were found to be more common than metaphyseal, but a bimodal distribution was only noted in males [308]. In young males, the main mechanism seems to be as a result of road traffic accidents accounting for almost 80% in a study conducted in an urban US city [309]. Pedestrian versus vehicle, fall from a significant height and gunshot injuries were found to be other causes of such an injury, however it is difficult to extrapolate these findings to a UK population given the differing demographic. Salminen et al found that a high energy mechanism accounted for almost 75% as a cause of injury [303].

The paediatric population seem to have a much higher fracture incidence than adults. Nafei et al analysed children under the age of 15 years old over a 9 year period in Denmark. Children under the age of 3 years old were found to have the highest incidence in the studied population. Overall incidence was found to be 28 fractures per 100,000 per year. The main modes of injury seemed to be as a result of road traffic accidents (43.1%) and falls (42.2%) [310]. The paediatric population seems to follow a similar bimodal spread to the overall population, with a double-peak in toddler years and early adolescence respectively [311, 312]. Femoral fractures in toddlers seem to be specifically as a result of low energy mechanisms such as non-accidental injury [313], with higher energy mechanisms being attributed as a cause of femoral fracture in adolescents [314]. Furthermore, in a Swedish study over an 18 year period examining the Swedish Discharge Registry, a seasonal cause of variation was also found, with spikes seen in March and August [315].

## 2.11 Fracture pattern

An understanding of long bone failure mechanisms and resultant fracture patterns is helpful in developing better systems and environments in order to minimise both incidence and severity. The key to preventing comminution lies in their worse reported functional outcomes, possibly as a result of the larger traumatic load that transfers through the soft tissues, which compromises the vascular envelope involved in bony healing [153]. An example of this includes the distal tibia, which has a reduced surface area compared to the proximal tibia, and its worse outcomes likely as a result of energy transfer through the articular surface [316]. However, despite the widely cited intuitive relationship between energy and comminution, there is a distinct lack of literature supporting this. A monotonic relationship would be expected between energy absorption and the number of fracture lines created given the varying areas of stress on a focal point in bone. Beardsley et al conducted an animal study on bovine femoral cortical bone segments. These were subject to loads ranging from 0.423 to 0.702J/g and the impacted surface areas which were freed were measured using computed tomography and translated into digital image analysis. The de novo surface area created was greatest in those that absorbed the highest energy. Kress et al tested 136 geriatric cadaveric femora under bending and axial loads. He concluded that high comminution was only observed under high strain rates (7.5m/s and above) [317]. Cheong et al looked at strain rate dependancy on fracture in ovine tibiae. Following four-point bending tests, he concluded that comminuted fractures only seemed to occur at higher strain rates [318]. The degree of comminution in relation to high strain rate has also been studied using micro-CT by Hibbeler et al. Three fracture patterns (oblique, tension wedge and transverse) were observed under low strain. However at higher strain rates, comminuted fractures were seen, as bone fails at multiple locations due to stress concentrations that exceed the material endurance limit of bone [319]. Further imaging studies assessing the correlation between energy, joint articular comminution and degree of post-traumatic arthritis have also been conducted, but these fall out-with the remit of that to be studied in this thesis [320].

To date however, and to the best of the author's knowledge, there have not been any studies directly addressing the correlation between mechanism of energy, degree of comminution and how this relates to age as a surrogate of bone quality. This forms a novel aspect of this thesis, and could potentially provide data on the transitional age at which bone behaviour is more likely to "switch" to a simpler pattern regardless of energy.

# 3. TESTING APPARATUS & METHODS

The following chapter will outline the means and modalities by which ovine bone was sourced, harvested, prepared and tested. Methods for the clinical study will also be stipulated

## 3.1 Bone harvest

Freshly euthanised mature ovine bone was obtained from the Bush Research Facility and AP Jess abattoir. Two-year old ovine bone was used. It has been previously demonstrated that one month of life in sheep is equivalent to one year of life in humans [240]. The choice of ovine bone which was two years old is on the basis that it is older than 18 months, which is the known age for skeletal maturity in this animal [321, 322]. Skeletally mature bone was required as this would provide a control group. Studies have also shown haversian remodelling of ovine bone occurs at 7 years of age onwards [296], therefore acquiring bone between 18 months and 7 years is optimal. As explored above, the joint reaction forces occurring across the hip joints of ovine femora are similar to that of the human. This is also coupled with the resources available for the study, whereby the ovine bone obtained from the abattoir was that which was of two years old. These reasons provided a sound basis on which to acquire the ovine bone chosen.

For the purposes of this study only the femora from the hindlimb were removed. These were then transported in labelled clinical waste heavy duty plastic sacks, to the University of Edinburgh Orthopaedic Engineering research laboratory.

All specimens introduced into the research laboratory were subject to the strict animal handling code to avoid contamination. Twelve femora were further de-bulked and skeletalised using size 10 blades, again taking care to avoid damage to the bone. The femora were stripped to the level of the periosteum. The periosteum was then hand stripped off the bone to leave only exposed femoral shaft, taking care to avoid injury to the bone in order to leave the cortex intact and minimise risk of inadvertent indentation or notching of the bone surface.

The periosteum was removed to avoid this layer conveying any mechanical strength, especially as the periosteal thickness of mature ovine femur was noted to be variable, which could skew the mechanical results.

The femora were kept in pH neutral 1M phosphate buffer solution (PBS) solution in order for them to remain in a moist condition. When ready for storage, the whole femur was placed into airtight labelled bags at -20 degrees celsius in a freezer before processing.

## 3.2 Bone preparation

It is not practical to prepare, test and analyse freshly harvested bone. These therefore required freezing and storage until ready for testing. Previous studies have demonstrated that freezing specimens is a means of protecting their mechanical properties [64, 323, 324]. For processing, the bones were thawed in PBS overnight for a period of 12 hours at room temperature.. The specimens were then blot dried using paper towel and left at room temperature for a further 6 hours.

The whole femur was placed into a vice and the bone was cut proximally and distally with a Bosch multi-cutter saw, leaving the diaphysis for processing only. The bone marrow was gently scalloped out using a small blunt curette. The use of a blunt curette was preferred to minimise risk of surface notching of the endosteal surface of the femur. The hollow cylindrical femoral shaft was then longitudinally cut in half, and each half was then sawn into six matchstick samples as show below in Figure 21.

This protocol for the preparation of cutting of samples has been previously used by Zioupos et al and Wang et al [7, 241].

A black dot was used to mark the proximal aspect of the end-steal surface of each sample. This allowed for standardisation of measurements for each sample, which was then input into a formatted database.


**Figure 21. Example of sample taken for processing and digital micrometer used.**

Each sample was measured using a digital calliper at 5 different points. The measurements were in millimetres to within 2 decimal places. This was to improve accuracy for mathematically calculating mechanical values, which are geometrically dependant. It was also to take into account the slight variations in size arising from the freehand cutting of bone segments.

The dimensions were recorded with respect to loading direction, with depth being collinear to direction of loading and width orthogonal to this. The width of each specimen was measure at the proximal, middle and distal portions. Mean and standard deviation for specimen length was 39.7mm (standard deviation 4.7mm), height 4.9mm (standard deviation 0.9mm) and depth 4.5mm (standard deviation 0.9mm). Bone specimens which differed significantly in measurements, and fell out-with the standard deviations above were discarded for greater homogeneity.

Bone segments were used as opposed to whole bone for several reasons: 1) bone segments enabled testing of multiple specimens, 2) the standardised specimen size was beneficial for laboratory handling and processing; 3) the multiple fragments from the whole bone was an excellent preliminary stage prior to scaling up to whole bone and 4) the standardised specimens were easier to store and to test mechanically using 4-point bending. This remained in line with the methods in the literature [7, 61, 241].

All bone segments were then grouped into 5 per trial set for further testing. Each set was placed into appropriately labelled sterile air-tight bags and frozen for later processing in solution.

Prior to processing, the bones were taken out of the freezer and thawed overnight for a period of 12 hours at room temperature immersed in luke warm water. The specimens were then blot dried using paper towel and left at room temperature for a further 6 hours.

## 3.3 Demineralisation process

In this study, the decision was made to use the solution EDTA based on evidence explored in section 2.9.1. This was at a concentration of 10% and pH of 6.38. This solution is water soluble and its mechanism of action is by binding to Calcium and Ferrous ions. As the mineral component of bone is rich in calcium, the result is removal of this component and thereby demineralisation of the bone. EDTA demineralises any surface of bone it comes into contact. This was initially conceived by Verdenius et al, and this method of bone demineralisation has since been expanded on and validated through replication of results in the literature [64, 282, 325]. More recently, Savi et al assessed various methods of decalcification models using rat mandibles. The same concentration of EDTA was used as in this study, and this was compared to nitric and formic acid at various concentrations and temperatures. It was concluded that using 10% EDTA at room temperature remained the recommended method of demineralisation as this led to the greatest morphological and structural preservation in bone tissue [326].

The bone segments were removed from the freezer and thawed. EDTA was accurately drawn up using an automated pipette gun. A Kerry Cuyson KC3 Ultrasonic bath was used, which was large enough to allow all trial bone segments to be placed inside it simultaneously. Thorpe et al has previously demonstrated in a study that the ultrasonic bath accelerates the demineralisation process without changing bone morphology [327]. Furthermore, Wallace et al has previously demonstrated on ovine tibia, that EDTA and ultrasonification of 14 hours can achieve demineralisation levels seen in 6 days of demineralisation in EDTA immersion alone [64].

Bone segments were processed similarly. Each bone segment was placed into a labelled sterile test tube, with each test tube containing exactly 10ml of EDTA, enough to immerse the segment fully and circumferentially. The test tubes were placed into a 50ml glass beaker after the beaker had been filled with PBS to the brim. The ultrasonic bath was then filled with PBS to a level indicator mark and the beaker was then inserted. This allowed the effects of the ultrasonic bath to be exerted onto the specimens whilst keeping the specimens stable in the bath. Control segments were placed into a test-tube containing PBS and underwent the same ultrasonification process. The experiments were performed at room temperature. To prevent build up of temperature, the ultrasonic baths remained uncovered. To correct for the natural evaporation process of PBS, the fluid level was constantly checked to make sure this did not drop below the indicator level of the bath. Overnight mean drop in fluid level in the ultrasonic bath was around 12mm, so the ultrasonic bath was carefully topped up regularly to avoid a significant drop that could influence the ultrasonic process.

Whole bone and bone segments were treated for control (0 hours PBS), 6, 12, 24 and 48 hours. There were 5 bone segment trials for each time interval. In total therefore, including the controls, there were 25 bone segment trials for EDTA processing. Each test tube was labelled by type of solution, time interval and trial number. An example of this process is shown in Figure 22.

The novel part of the above method related to the staged demineralisation at the time points chosen. The time periods chosen doubled the time period at each stage, to help best capture a correlation to mechanical values.This has not been described previously.This applies to both the demineralisation and decollagenisation processes.

**Figure 22. Showing a) Top left - extracting solution using pipette; b) Top right - segment labelling and c) Bottom - immersion in ultrasonic bath.**

## 3.4 Decollagenisation process

Bone segments were used and prepared in the same way as that for demineralisation. Whole bone samples were not used.

Sodium hydroxide of 10 Molar and 5 Molar concentrations were used in this study. Time intervals remained constant, with samples being immersed in PBS as controls. All preparation and handling of NaOH solution was done under a defumigator at every stage and as standard, eye protection and breathing masks were always used as the fumes of NaOH can be potentially harmful.

To prepare 10M NaOH solution the following method was used:

1. NaOH pellets were weighed and 399.9g were used.
2. Pellets placed into a dry sterile glass bottle and then bottle placed into an ice bath.
3. Distilled water 600ml poured into bottle.
4. The reaction then starts and wait until pellets dissolve.
5. As reaction is highly exothermic, top up of ice may be required in ice bath.
6. More water may be added to bottle but not exceeding a total of 1 litre.
7. Once reaction is over, top up of distilled water to 1 litre total.

This method was adjusted accordingly to prepare 5 molar solution. The reaction is temperature dependant and may either take a few hours or longer depending on the room temperature.

The bone was processed at time intervals of control (0 hours PBS), 6, 12, 24 and 48 hours for both 10M and 5M NaOH solution. Five trials were done for each time interval therefore 50 samples were processed. The test-tubes containing the samples (each with 10ml NaOH) were placed into an incubator at 44 degrees celsius to denature the collagen and it had an added effect of being a rotatory agitator to make sure all bone segments were constantly being immersed in the solution. An example of the process can be seen in Figure 23.

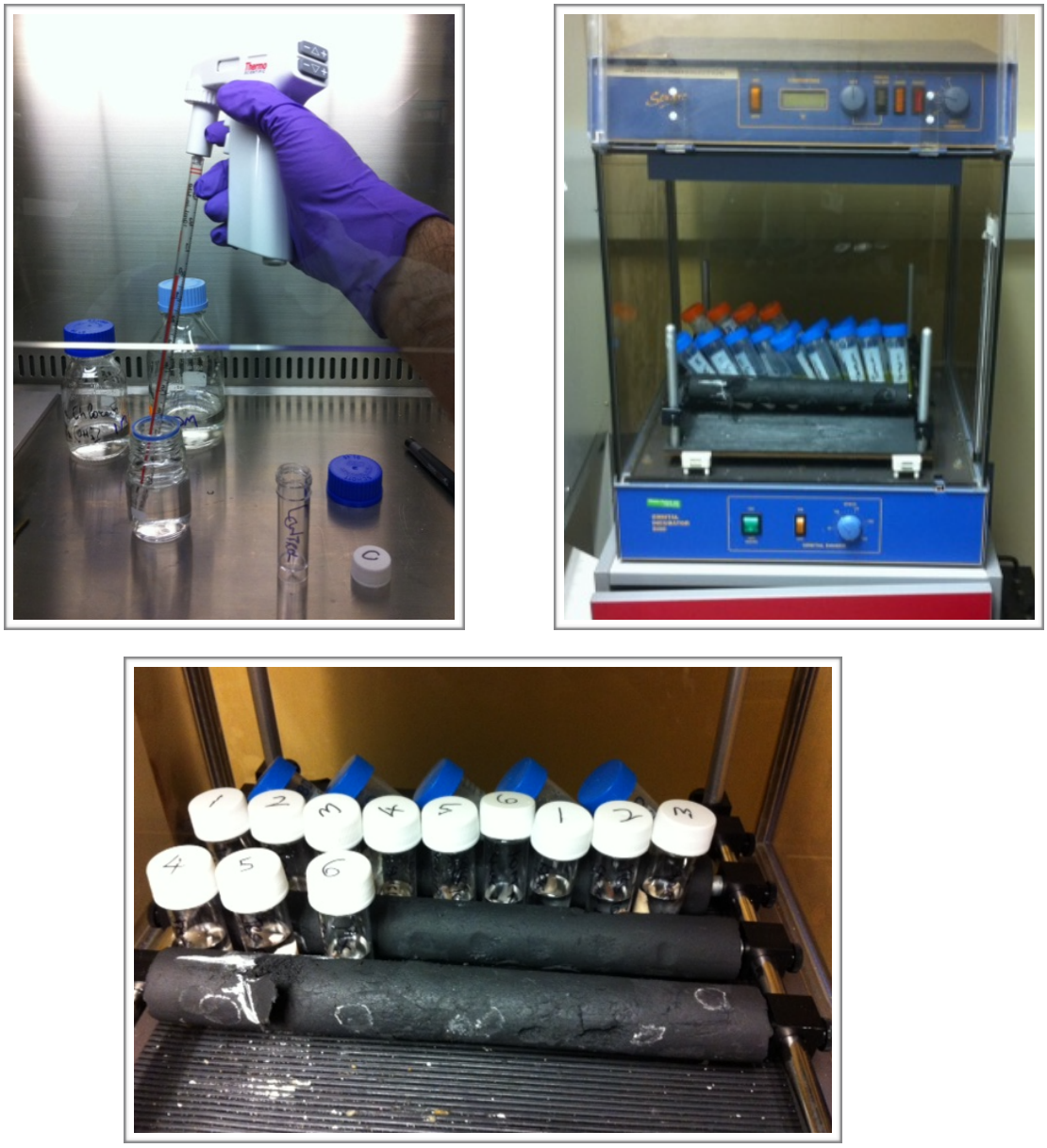

**Figure 23. Showing a) Top left - extracting solution using pipette under defumigator; b) Top right - Incubator/agitator c) Bottom - labelled samples in incubator.**

Control specimens were immersed in PBS independently and subject to the same conditions to the tested segments. For example, 5 control segments would be tested in their respective tubes (immersed in PBS) with the test segments immersed in NaOH. These would be placed into the agitator at 44 degrees celsius alongside the decollagenised samples. This is visible in the figure below where the blue topped tubes in Figure 23, are control samples in PBS subject to the same environmental conditions.

## 3.5 Assessment of demineralisation

The whole bone and bone segments were then imaged using x-ray to assess the degree of demineralisation. Bone was transferred to the animal imaging section of our laboratory in accordance with University of Edinburgh policy. This involved placing the samples into sealed and labelled bags and spraying the bags with virkon for infection control purposes.

The researcher wore personal protective equipment including coverage of hair and footwear. Gloves were used at all times and forceps to handle the bone specimens and to place them on the x-ray plate. The x-ray parameters of 63mV and 1.8mA were kept constant. The plates were analysed in the Royal Infirmary of Edinburgh radiology department and images stored on an encrypted USB.

The level of ultrasonic demineralisation was assessed using pixel value of each bone segment on the radiograph. The pixel value describes how “bright” a pixel is on an image. Radiographs were assessed using ImageJ as an 8-bit integer, giving a greyscale image pixel value for each pixel. These range from 0 (black) to 255 (white). A pixel value was assessed at the proximal, middle and distal poles of each bone segment and a mean derived. The single mean for each bone segment was recorded and a mean value for each trial set was calculated. The means were then compared for solutions PBS, EDTA, 5M NaOH and 10M NaOH at each time point. Analysis was carried out using Two-Way ANOVA testing with Sidak’s multiple comparison test for assessment of significance. A p-value of $<0.05$ was deemed significant. This provided an absolute degree of demineralisation and rate of de-mineralisation in all solutions. The null hypothesis was that immersion in EDTA and NaOH had no significant effect on pixel value and therefore mineral level at any time point.

Control specimens were statistically analysed using a one-way ANOVA test. This was done to ensure that biomechanical values were unaffected despite submersion in PBS for 48 hours. It was important to ascertain this prior to proceeding with statistical analysis of demineralised and decollagenised samples. P-values $>0.05$ denoted no statistical significance.

Two experimental variable factors were tested, namely bone 'quality' (control v demineralisation v decollagenisation) and time. Two-way ANOVA analysis was performed on combined data sets to investigate two experimental factors on mechanical outcomes. These outcomes comprised maximum force, maximum deflection, elastic modulus, ultimate stress, ultimate strain, yield stress, yield strain, post-yield behaviour and finally toughness. P-values $<0.05$ denoted statistical significance.

## 3.6 Mechanical testing

The timing of bone preparation, processing, imaging and mechanical testing was such that the bone was only kept frozen at one stage - after preparation in anticipation of processing. Processing in solution, imaging and mechanical testing was accurately timed to avoid having to re-freeze and store samples or allow samples to be left exposed for prolonged periods of time. This was to mitigate against destruction of certain samples which were more fragile following processing in solution for prolonged periods. All samples had to undergo the same method to reduce risk of method bias.

All of the specimens were tested to failure using a 4-point bend testing machine with the load carefully applied at the midpoint of specimens. This was all done at a low strain rate. It was recognised that four-point bending created an environment of pure bending with tensile and compressive forces, as opposed to three-point bending which also applied shear forces. Furthermore, four-point bending is tested on rectangular long and relatively thin (ideally with a ratio in excess of 20:1) beams most accurately, which is a further reason why rectangular beam segments were used for this study as opposed to whole bone.

A free body diagram (Figure 24) is shown below that outlines how the 4 point bender functions.

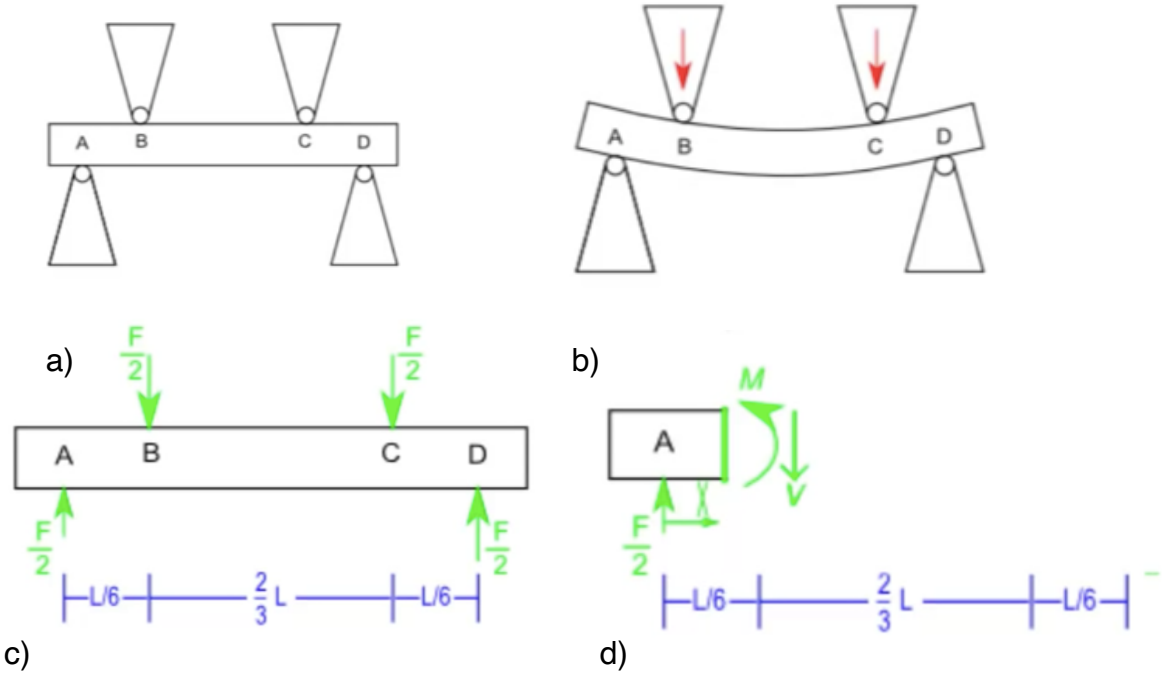


**Figure 24. Free body diagram of four point bender**

In Figure 24: a) demonstrates the applied load on a rectangular beam (bone segment). Care needs to be taken to place the beam symmetrically each time; b) the top loaders apply the load (F), this produces a compressive load on concave side and tensile load on convex side; c) shows the length of the beam and its proportion over the 4 point bender and the relative force applied by each roller. Finally d) shows more clearly the moment arm (M) and the shear force applied (X). The positive shear force is only applied between points A-B and a negative shear force C-D, therefore shear forces are cancelled out and in portion B-C an equal moment arm is maintained throughout this section.

Slow loading rate experiments were undertaken using the Zwick/Roell z005 (Zwick GmbH & Co, Ulm, Germany) testing machine. Data capture was provided by TestXpert V9.01 (Zwick GmbH & Co, Ulm, Germany). This is the proprietary software for the Zwick mechanical testing apparatus and as such acted as the control system for the experiments.

The initial mechanical tests were piloted on matchsticks in order to calibrate the loading rate. This created 4-point bending at a loading velocity of 1mm/s. The average strain rate in the bone specimens created was $6.25 \times 10^{-3}$ $s^{-1}$. This strain rate was grossly equivalent to that found for compressive strain rates, when walking on a level surface, by Burr et al [328].

During testing the bone was located on two bottom loaders measuring 2.5mm in thickness which were 10mm apart. The top loader had two equally sized rollers to apply the load and compressive force however their distance was 5mm apart as can be seen in Figure 25. The bottom loaders against which the load was applied were a distance of 20mm apart. Therefore the total length of segment tested was 20mm. There was no resistance to rotation applied as this was not considered necessary due to the low loading rate. The load was carefully applied symmetrically through the middle of the bone segment in all cases.

Deflection (or displacement) was measured directly from the crosshead travel distance on the four-point testing machine. As the beam (bone specimen) had variable stiffness following processing compared to the loader, the deflection output was taken to be that from the beam alone. This was captured and exported from mechanical into electronic data via the TestXpert system.

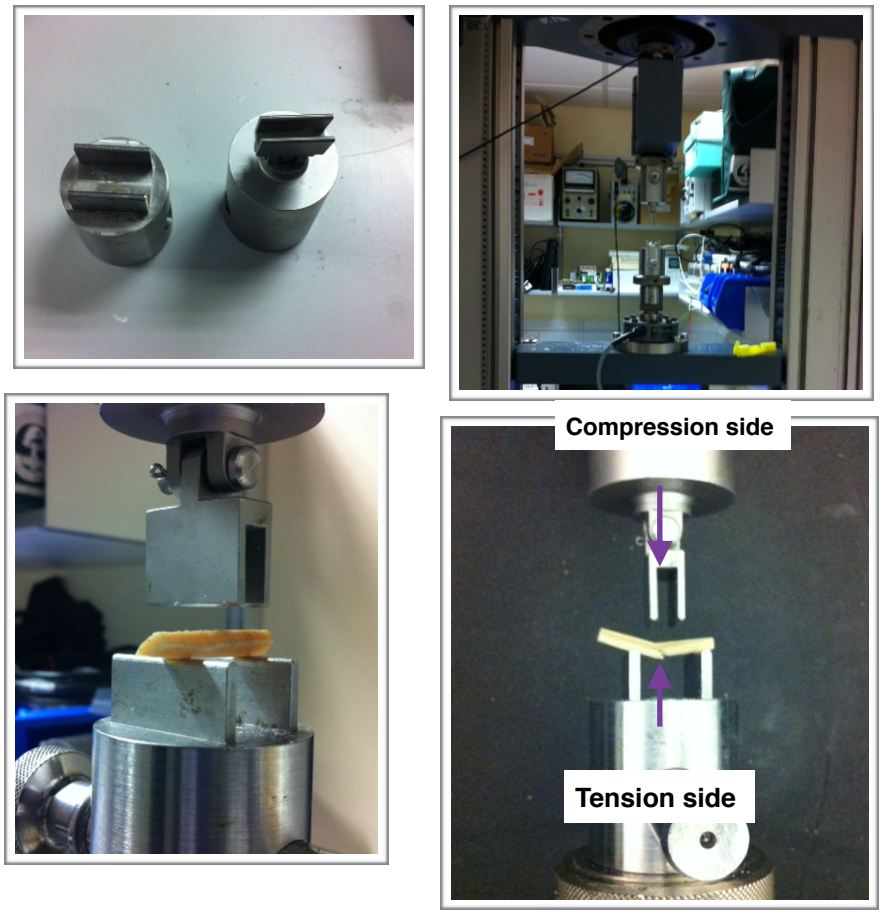


**Figure 25. Showing a) Top left - top and bottom loaders; b) Top right - Mechanical tester c) Bottom left - positioned bone specimen and d) Bottom right - Compression and tension loading with crack on tension side of EDTA sample**

## 3.7 Biomechanical analysis

A dynamic force sensor was used to capture force applied to the bone at discrete time intervals by the data acquisition system described above. This data was formed for each bone specimen mechanically processed and was translated into graph form of “Force v Deflection/Displacement” over time.

The force data was in the form of a smooth waveform due to the intrinsic stiffness found in bone specimens at the low strain rate used as opposed to whole bones. The values of force, displacement and time, allowed for the derivation of values such as “Stress” and “Strain”. Furthermore, the area under the subsequent “Stress v Strain” graph allowed for the derivation of bone toughness under strain. An example graph of “Force v Displacement” is shown below in Figure 26.

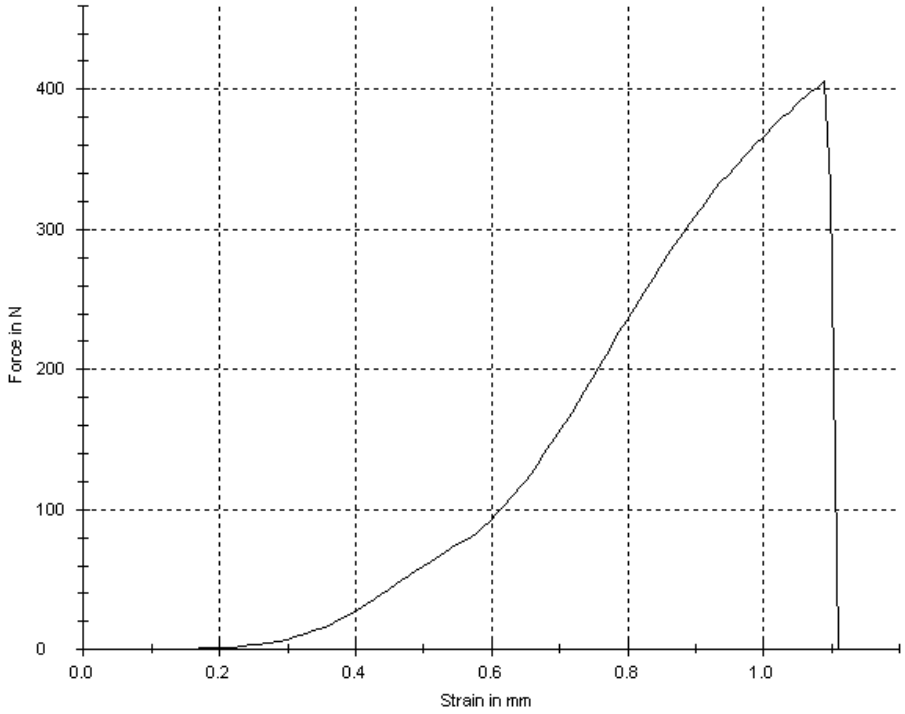


**Figure 26. Showing an example force versus displacement curve**

### 3.7.1 Moment

For this section it was necessary to utilise certain engineering definitions.

Moment of inertia: Also known as second moment of area. The capacity of a cross section to resist bending. Denoted by "***I***".

Bending moment: A reaction induced in a structural beam when an external bending force (moment) is applied. Denoted with an "***M***".

In order to calculate the stress and strain from force and deflection over time it was vital to know the moment of inertia. This is effectively the contribution of the bone segment (beam) towards stiffness or Young's modulus. It pertains to how the stress will be distributed across the segment.

To calculate the moment of inertia of a rectangular beam, known engineering equations were used, for a base of rectangular area with a breadth and width.

This equation is: Moment of inertia (Ix) = $bh^3/12$

To make further sense of this, the below Figure 27 explains the cross sectional area of a rectangular beam.

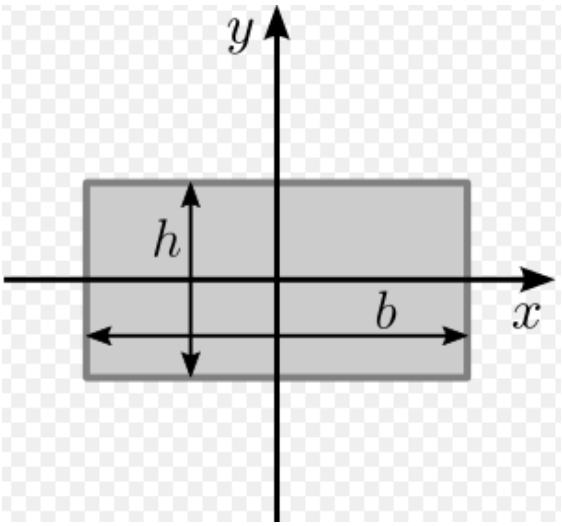


**Figure 27. Cross sectional area of rectangle.**

Figure 27 shows the cross sectional area looking directly at the beam from either end. In the same figure, h = height , b = base, and an X and Y axis are drawn. Moment of inertia will be about the X axis in four point bending.

In order to progress to calculating bending stress, it was also essential to know the maximum bending moment. To calculate moment of inertia, further engineering principles were deduced with the use of a free body diagram shown in Figure 28.

Figure 28 shows a) The positive and negative shear forces (V(x)) at either end of the beam. The midsection therefore has zero shear forces. In b) A plateau is observed in the midsection and a constant moment magnitude. The maximum bending moment (Mmax) which is the reaction force from the beam secondary to an externally applied bending force, is dependant on the initial spacing in the midsection of the beam between the two applied loads.

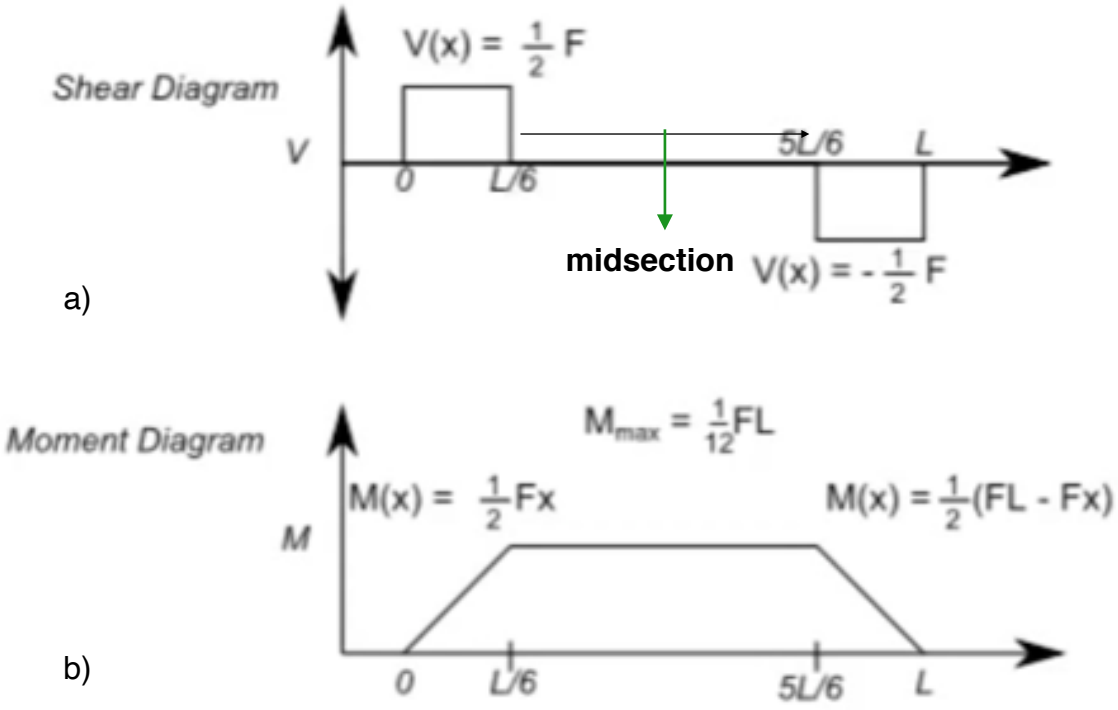


**Figure 28. Free body diagram of shear and bending moment.**

The formula for maximum bending moment therefore is: **Mmax = FL/12**

F = Force applied
L = Length of specimens

These formulas for the maximum bending moment (Mmax) and the moment of Inertia (Ix) were input into an excel spreadsheet and values for each specimen tested were calculated.

### 3.7.2 Bending Stress

The maximum load (P) during bending was used to derive the “ultimate stress” in the beam. The “P” value was taken from the TestXpert programme used to control the mechanical testing machine. The ultimate stress is defined as the maximum stress a beam can take in bending before failure. Ultimate stress will be made clear in this study and will be differentiated from other values such as “yield stress” to avoid confusion.

For all tests at the low strain rate, the top supports were set at a distance of 20mm. As the loading occurred at the midpoint of the beam, the maximum bending moment will occur at the point of loading, the equation of which has been described above.

In the ideal conditions, the ultimate stress due to bending can be found using the engineering equation below:

Ultimate Stress: $\sigma B = M_{max} * y / I_{NA}$

Where:

| | | |
|---|---|---|
| $\sigma B$ | = | ultimate stress due to bending |
| Mmax | = | Bending moment |
| $y$ | = | distance from the neutral axis to outermost point in the cross-section |
| $INA$ | = | Second moment of area |

Based on the elastic theory of bending, the maximum bending stress in the elastic range in a rectangular cross-section will be greatest when furthest from the neutral axis. It is important to note that the tensile and compressive loads will be re-distributed in the plastic phase. As the load on a beam gradually increases, the outermost fibres of the beam will progress to the plastic phase first after their yield point is reached. It is at this point that the beam will “recruit” the stiffer fibres, which are closer to the neutral axis, to take over the increased load until their yield point is reached. This continues until enough fibres have reached their yield point, the beam undergoes a considerable increase in strain and a deflection of the beam occurs.

### 3.7.3 Strain

As the force and deflection were calculated directly from mechanical testing using software, strain due to bending can be calculated from this indirectly in ideal conditions. Strain will be denoted by the symbol “$\in$” and the equation for this is the following:

Strain due to bending: $\in = 12 * d * y / L2$

Where: $d$ = deflection

$y$ = distance from the neutral axis to outermost point in the cross-section

**L** = Length of span

The bending stress versus strain graphs were then plotted for each mechanically tested bone segment. The strain is expressed as a percentage given that in effect it is a ratio formula.

### 3.7.4 Stiffness

In order to conduct the analysis of the effect of solutions on bone specimens, a single value was derived to describe the resistance of bone, as a single structure, in response to bending deformation. This was important given that bone is anisotropic, or behaves differently when loaded under a different direction-

To describe an accurate value for bending behaviour up to the elastic limit, The Young's Modulus ($E$) equation was used as follows:

Young's modulus: $E = P * L / 48 * d * I_{NA}$

The value for "$d$" is taken from the maximum deflection in the linear region of the elastic phase on the loading graphs.

### 3.7.5 Yield

The yield point, or elastic limit, is the point at which the elastic phase ends and plastic deformation occurs under bending load. In bending behaviour, the stress at which a material exhibits change from elastic to plastic behaviour is not easily detected. For this reason, an "offset yield point" is defined.

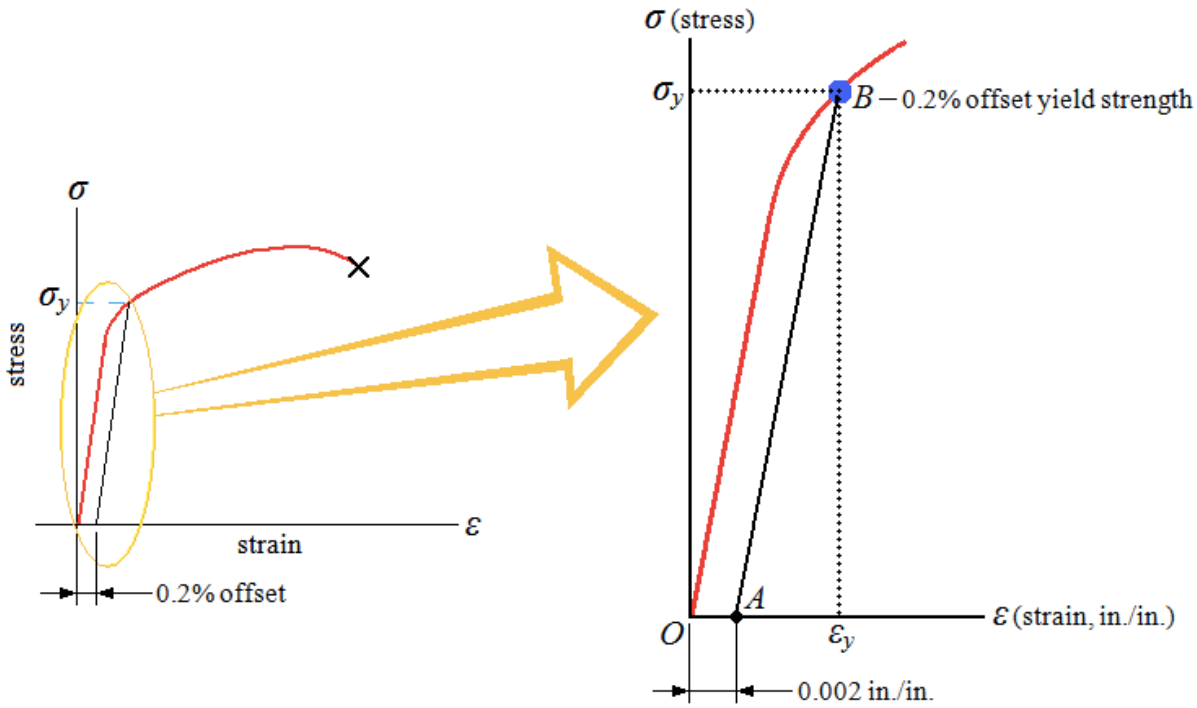


**Figure 29 - Defining the yield stress using 0.2% strain.**
**Taken from www.engineeringarchives.com**

This is otherwise known as “proof stress” and is applied to a structure that does not have a defined yield point due to the nature of it’s structure [329].

A standard strain value is taken at 0.2%, and the yield stress is defined by drawing a line of equal gradient to the elastic gradient, and measuring where this intersects the stress v strain curve on the x axis (Figure 29). This yield point is otherwise known as the “Proportional limit” and follows the principles of Hooke’s law.

This is defined as strain being proportional to stress up to a limit, above which it becomes disproportionate.

As can be seen in Figure 30, a line of equal gradient to that of the bending stress in the elastic phase is used with 0.2% strain as a starting point on the x axis.

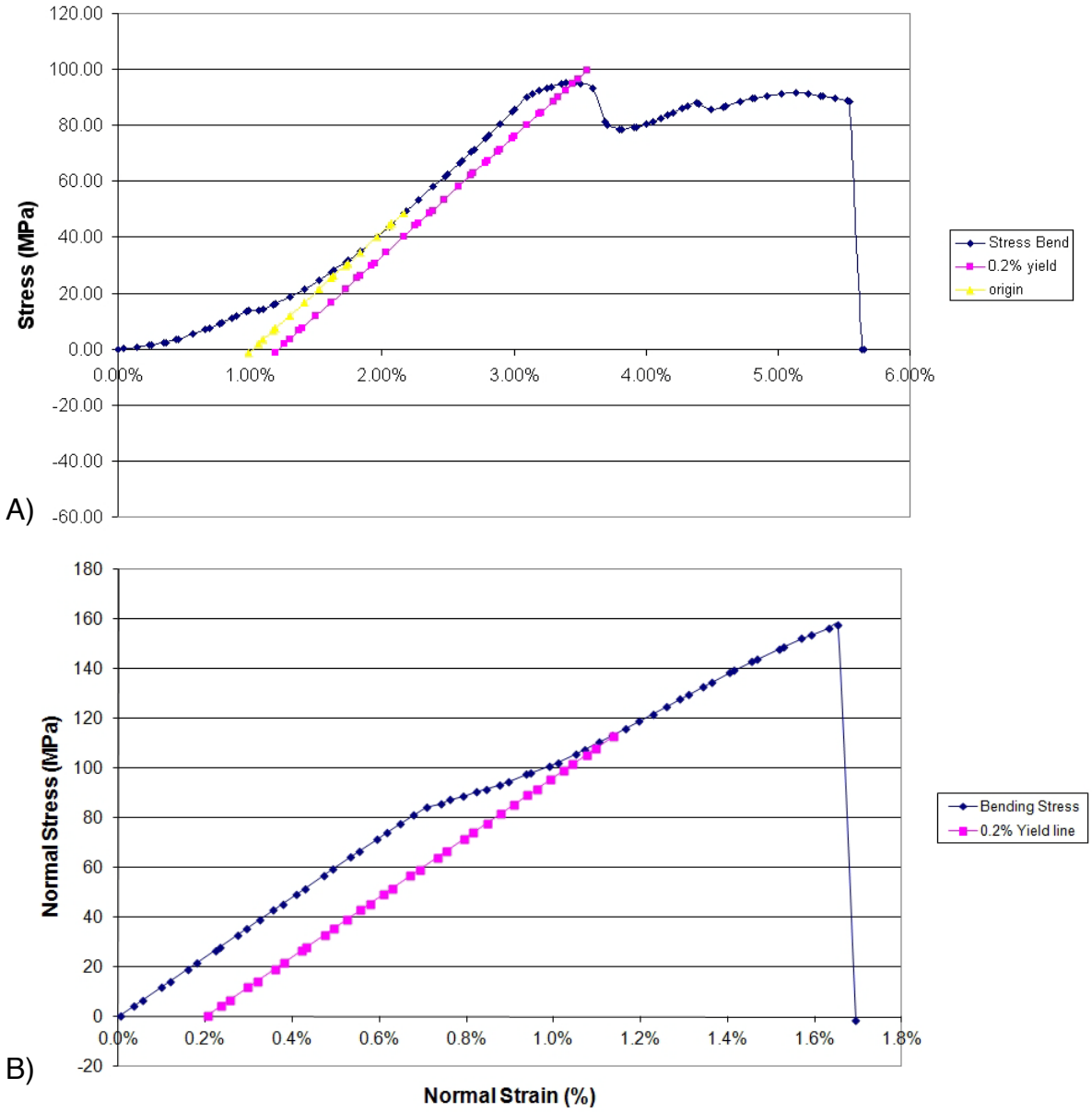


**Figure 30 - Showing A) Interpolation of the origin by negating the "toe in" region and B) Revised graph with the "toe in" region excluded.**
**Taken from Wallace et al**

The point at which this offset line intersects the stress v strain curve is the yield point. It is important to note that the gradient was taken from a point above the "toe in region" (initial erratic gradient) of the stress v strain graph, as stress due to bending is not of an equal gradient from "0" on both x and y axis. The gradient after the "toe in region" would then be interpolated back to the x axis from the stress strain curve to find a representative origin for loading, thus negating the "toe in" effect.

This is important when deriving toughness or strain at yield and failure. The plastic strain could be derived by subtracting yield strain from ultimate strain at failure.

This process is demonstrated in figure 30 above, and was done for each individual graph derived from each bone specimen, which including control values, is 100 specimens in total.

### 3.7.6 Bending toughness

Toughness can be defined as the energy required to deform one cubic unit of area. It is therefore express in the units Joules per cubed unit eg $J/mm^3$ . For a given material to be considered “tough”, it must be able to withstand both high stress and high strain i.e. both strong and ductile. Therefore, a brittle material such as osteoporotic bone, is not considered tough due to it being able to withstand a degree of stress, but inability to exhibit ductile behaviour.

Toughness in this case will be derived from the area under the stress-strain curve. This represents the toughness of bone in bending. It will therefore include a combination of parameters such as specimen acumen, geometry, material stiffness, boundary conditions and loading type.

To measure this area, it was important to distinguish between the area under the curve in the elastic range, and the area in the plastic range. The area under the stress strain curve up to the elastic limit is otherwise known as the “modulus of resilience”, given that if the load was removed the bending effects would reset. An example of how this was derived is shown in figure 31.

Toughness = Area in elastic phase + Area in plastic phase.

The software “Graphpad Prism” was used to import graph data of each specimen and the area derived. An average toughness was used for each trial and the means compared for later significance analysis as described above.

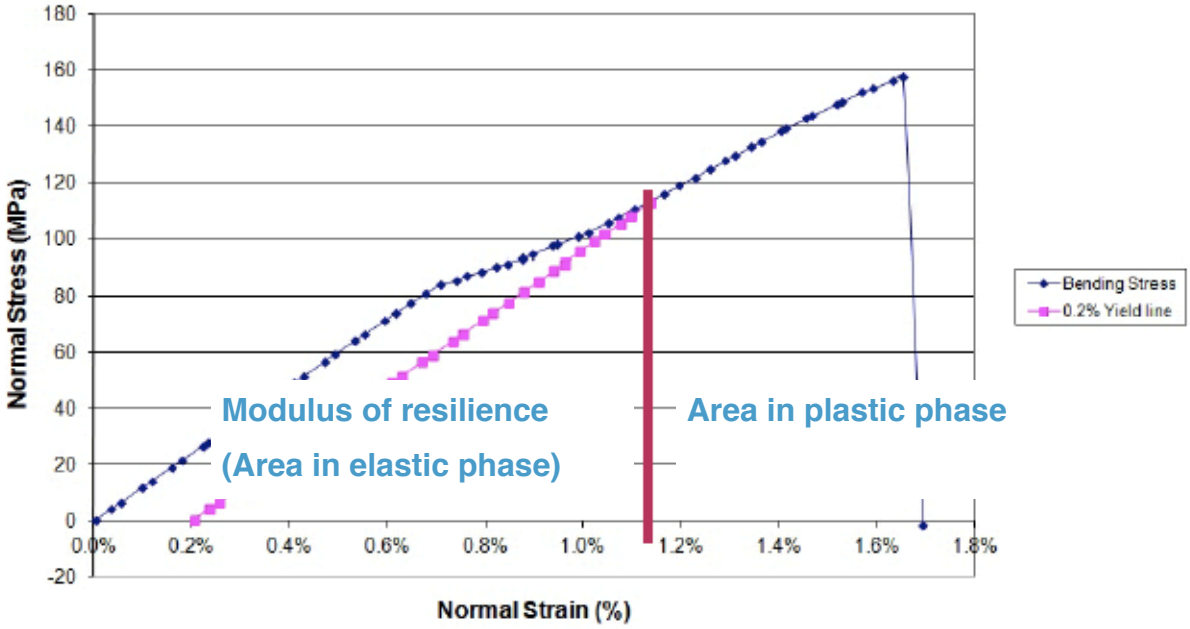


**Figure 31 - Showing exemplar graph of how area was derived.**

## 3.8 Clinical data

Over a 2 year period, between February 2015 - February 2017, a cross-sectional analysis of all femoral diaphyseal fractures that presented to a Trauma and Orthopaedic unit was conducted. All orthopaedic trauma patients in the area attend the unit for diagnosis, management and follow up. Follow up occurs in outpatient fracture clinics which are supervised by an orthopaedic consultant surgeon. Paediatric fractures attend the tertiary paediatric referral centre and these are managed and followed up utilising standardised protocols. This allowed capture of a spectrum of ages ranging from the neonate onwards.

In compliance with ethical standards, this component of the thesis was considered an audit of practice against “Australian Femoral Shaft Fracture Guidelines” (for paediatric fractures) and “National Institute of Clinical Excellent” limb and joint fracture guidelines (for adult fractures) [330, 331]. Additionally, according to the Health Research Authority, this component was not considered research. This was in accordance with their research tool outcome as 1) No randomisation occurred; 2) No change of service was required and 3) the study was not considered generalisable to all fractures or populations.

The trauma unit picture archiving communication system (PACS Carestream) was used to search for all radiographs taken of the pelvis, femora and knee in order to capture as many injuries as possible. The criteria “XR FEMUR” was also used an additional cross-reference search on the PACS system over a study range of “2 years”. This search process identified all femoral diaphyseal fractures over the time period specified, which presented to the unit. The search generated a total of 2298 patient x-ray “packs". When applying more than one plane of view ie antero-posterior and lateral views, this generated a total of 4130 x-rays required for initial analysis.

A simple fracture was defined as a fracture with one fracture line and two fragments. A comminuted fracture was one in which more than two fragments were present, and/or greater than one fracture line.

Care was taken to obtain an accurate mechanism of injury through electronic documented notes on the hospital system. Mechanisms were grouped into high and low energy injury. Mechanism energy was categorised into a binary “low” or “high” based on Landin’s trauma level system, for paediatric patients [332]. High energy in adults was deemed any mechanism that resulted after a mechanism other than simple fall based on World Health Organisation criteria [251]. Fracture pattern was coded as binary, with either “simple” or “comminuted”.

For the strict purpose of analysing inter-observer variability in radiographic measurement of fracture pattern, medical student recruitment was required. This was due to the sheer volume of radiographs which required analysis. Furthermore, validity of categorisation into either fracture pattern required more than one observer, and this was considered essential in reducing data collection/input bias. The medical student role was limited to only this process and not involved in any other aspect of this thesis. Training was provided by the author of this thesis on observation of fracture type and fracture pattern. There was consensus agreement on all fractures included in the study.

### 3.8.1 Exclusion criteria and grouping

The diaphyseal segment was defined as an AO-42 classified injury, or the anatomical area between the lesser trochanter and the supracondylar distal femur. Any patient sustaining an injury out-with the diaphyseal segment of the femur was excluded. Any fracture extending into the articular surface, or involving the hip or knee was excluded. Patients who had a previous prosthesis or sustained a peri-prosthetic fracture were also excluded. All pathological fractures were also excluded from the final cohort.

A total of 206 femoral shaft fractures were identified with 43 excluded as per the exclusion criteria above. Twenty-eight (n=28) patients had a peri-prosthetic injury and fifteen (n=15) patients sustained pathological fractures. Of the excluded patients other than the older age group, one (n=1) patient had a peri-prosthetic fracture in the adult group and three (n=3) patients had a pathological fracture in the paediatric group. This left a total of 163 patient eligible for final analysis.

Three age groups were identified and fractures subdivided into these groups. These were as follows:

1. Paediatric group: Any patient equal to or under 16 years of age,
2. Young Adult group: Any patient ranging from 17-54 years old
3. Older Adult group: Any patient who was 55 year and older.

The concept of transitional change of bone behaviour has been reviewed in the section 2.7.5. However, it is important to note that these “cut-off” values were a best estimate of when transitional change occurs based on the available literature. There is no consensus in the literature on this matter, and this is largely non-evidence based. The results of any data provided in this thesis for age and transitional change of bone behaviour based on clinical fracture pattern should be considered a novel aspect of this thesis.

### 3.8.2 Statistical Analysis

All data was stored on secure national health service computers to protect patient confidentiality. Statistical analysis was undertaken with IBM “SPSS” Statistics version 23 (IBM Corp. Released 2015. IBM SPSS Statistics for Windows, Version 22.0. Armonk, NY: IBM Corp). Descriptive statistics were used for categorical data and Shapiro-Wilkes testing for normality for any continuous data. Parametric data was expressed as mean and standard deviation, with non-parametric data as median and interquartile range (IQR). Collinearity testing via data tolerance and variance inflation factors (VIF) for independent variables was carried out. No correlation was found between variables.

The primary outcome variable was fracture pattern, namely simple or comminuted. The independant variables included sex, age, significant co-morbidities, whether on bone strengthening/modifying medications, risk factors for osteoporosis, mechanism of energy, low/high energy, fracture type and open/closed soft tissue injury.

Binary logistic regression was undertaken for the primary outcome variable of fracture pattern. Two-tailed binomial testing was carried out when comparing a group versus an outcome variable. A chi-squared test was used when comparing two categorical variables within an age group. This would provide an idea of expected results.

An age histogram was used to show distribution in energy and fracture pattern categories. An independent samples t-test was used to compare mean ages when patients were split according to mechanism energy or fracture pattern.

A receiver operating characteristic curve was used with age as a risk model to identify the age at which bone appears to transition from paediatric to adult behaviour, and from adult to older age group behaviour. Using age as a continuous risk model has previously been described by Grunkemeier et al [333].

Inter-observer reliability of fracture pattern (simple/comminuted) measurement was assessed using Cohen's Kappa coefficient. Interpretation of agreement was undertaken using the Landis and Koch reference values [334]. Kappa value of < 0 indicates no agreement, 0 - 0.20 as slight agreement, 0.21 - 0.40 as fair agreement, 0.41 - 0.60 as moderate agreement, 0.61 - 0.80 as substantial agreement and 0.81 - 1 as almost perfect agreement.

We assumed *a priori* that p values of less than 0.05 were significant.

The incidence of a population was derived through the following equation:

$$\frac{\text{new cases}}{\text{total population}}$$

The total population should take into account the number of deaths for that year. The total live population of the area studied, for the period studied, according to the Office of National Statistics was 545,390.

# 4. RESULTS MECHANICAL TESTING

The results for mechanical testing in all groups were collated for analysis and for standardisation and presented in the following order:

1. Force - quality compared. The units is newtons.
2. Deflection - quality compared. The unit is millimetres.
3. Ultimate stress - quality compared. The unit is $N/mm^{2.}$
4. Ultimate strain - quality compared. The unit is percent change (%).
5. Yield stress - quality compared. The unit is $N/mm^{2.}$
6. Yield strain - quality compared. The unit is percent change (%).
7. Elastic modulus - quality compared. The unit is gigapascal (GPa).
8. Post-yield - behaviour quality compared.
9. Ductility - quality compared. The unit is percent change (%).
10. Toughness - quality compared. The units for toughness is $J/mm^3$
11. Pixel intensity

The results were also considered in subsections; pre-yield, yield and post-yield.

Force deflection graphs for all samples will be shown in Appendix A.

Values for mechanical testing for all samples will be shown in Appendix B.

Mechanical testing box and whisker plots will be shown an Appendix C.

## 4.1 Mechanical testing controls

None of the control results showed any significant difference between samples regardless of time immersed in PBS. Furthermore, ultimate stress, yield stress and elastic modulus values in controls were similar to that found in human femora as shown in a study by Agrawal et al [195]. This vindicated the use of PBS as a solution for control samples, and ovine bone specimens as a surrogate for human femora. Based on these findings, an appropriate control data set was used for comparison with de-mineralised and decollagenised specimens.

The force and deflection values, presented are crude values and not geometrically adjusted to reflect dimensions of each bone specimen. For this reason, a greater variation in values between trials was seen. This small variation was not significant compared to the control values.

## 4.2 Demineralisation (EDTA) results

This subsection will focus on de-mineralised specimen results. Results are presented by showing a mean, mean difference value, p-value and whether this was significant. Mean values express the mean of all five values achieved in each trial or time point. Mean difference value is the difference in mean value between the EDTA sample and the control specimen. The results presented here are **"Control mean value minus NaOH mean value"**.

Graph representation of these values are in appendix A.

### 4.2.1 Force

**Table 4.2.1 - Force values of EDTA immersion over time**

| | 0 hours | 6 hours | 12 hours | 24 hours | 48 hours |
|---|---|---|---|---|---|
| **Mean** | 404 | 390 | 357 | 321 | 219 |
| **Mean difference** | 8 (-1.9%) | 81 (-17.2%) | 55 (-13.4%) | 144 (-31.0%) | 241 (-52.4%) |
| **P-Value** | >1 | 0.884 | 0.976 | 0.412 | 0.038 |
| **Significant** | No | No | No | No | Yes |

Table 4.2.1 shows at 48 hours, immersion in EDTA had a significant effect on force applied across bone segment, with a gradual decrease in force across all time points compared to control samples.

### 4.2.2 Deflection

**Table 4.2.2 - Deflection values of EDTA immersion over time**

| | 0 hours | 6 hours | 12 hours | 24 hours | 48 hours |
|---|---|---|---|---|---|
| **Mean** | 1.32 | 1.276 | 1.296 | 1.63 | 1.88 |
| **Mean difference** | 0.05 (-3.6%) | -0.246 (+19.3%) | -0.084 (+6.5%) | -0.48 (+29.5%) | -0.628 (+33.5% |
| **P-Value** | 0.999 | 0.822 | 0.998 | 0.199 | 0.046 |
| **Significant** | No | No | No | No | Yes |

Table 4.2.2 shows at 48 hours, immersion in EDTA had a significant effect on deflection across bone segment, with a gradual increase in deflection across all time points compared to control samples.

### 4.2.3 Ultimate Stress

| Table 4.2.3 - Ultimate Stress values of EDTA immersion over time | | | | | |
|---|---|---|---|---|---|
| | **0 hours** | **6 hours** | **12 hours** | **24 hours** | **48 hours** |
| **Mean** | 175.4 | 169.8 | 150.7 | 124.9 | 91.1 |
| **Mean difference** | 3.2 (-1.8%) | 36.4 (-17.7%) | 48.5 (-24.3%) | 74.9 (-37.5%) | 105.1 (-53.6%) |
| **P-Value** | 0.963 | 0.803 | 0.555 | 0.136 | 0.014 |
| **Significant** | No | No | No | No | Yes |

Table 4.2.3 shows at 48 hours, immersion in EDTA had a significant effect on ultimate stress across bone segment, with a gradual decrease in ultimate stress across all time points compared to control samples.

### 4.2.4 Ultimate Strain

| Table 4.2.4 - Ultimate Strain values of EDTA immersion over time | | | | | |
|---|---|---|---|---|---|
| | **0 hours** | **6 hours** | **12 hours** | **24 hours** | **48 hours** |
| **Mean** | 2.476 | 2.848 | 2.824 | 2.782 | 2.922 |
| **Mean difference** | -0.16 (+6.5%) | -0.604 (+21.3%) | -0.462 (+16.4%) | -0.554 (+19.9%) | -0.728 (+24.9%) |
| **P-Value** | 0.983 | 0.145 | 0.392 | 0.213 | 0.049 |
| **Significant** | No | No | No | No | Yes |

Table 4.2.4 shows at 48 hours, immersion in EDTA had a weak significant effect on ultimate strain across bone segment, with a minimal increase in ultimate strain across all time points compared to control samples.

### 4.2.5 Yield Stress

| Table 4.2.5 - Yield Stress values of EDTA immersion over time | | | | | |
|---|---|---|---|---|---|
| | **0 hours** | **6 hours** | **12 hours** | **24 hours** | **48 hours** |
| **Mean** | 157.6 | 148.2 | 131.8 | 106 | 71 |
| **Mean difference** | 6.4 (-3.9%) | 45.6 (-23.5%) | 55.6 (-29.7%) | 81.2 (-43.4%) | 112 (-61.2% |
| **P-Value** | 0.923 | 0.616 | 0.408 | 0.088 | 0.008 |
| **Significant** | No | No | No | No | Yes |

Table 4.2.5 shows at 48 hours, immersion in EDTA had a strong significant effect on yield stress across bone segment, with a progressive decrease in yield stress across all time points compared to control samples.

### 4.2.6 Yield Strain

| Table 4.2.6 - Yield Strain values of EDTA immersion over time | | | | | |
|---|---|---|---|---|---|
| | **0 hours** | **6 hours** | **12 hours** | **24 hours** | **48 hours** |
| **Mean** | 1.97 | 2.304 | 2.278 | 2.28 | 2.594 |
| **Mean difference** | 0.01 (-0.5%) | -0.384 (+16.7%) | -0.236 (+10.4%) | -0.392 (+17.2%) | -0.716 (+27.6% |
| **P-Value** | 0.999 | 0.395 | 0.833 | 0.373 | 0.014 |
| **Significant** | No | No | No | No | Yes |

Table 4.2.6 shows at 48 hours, immersion in EDTA had a strong significant effect on yield strain across bone segment, with a progressive increase in yield strain across all time points compared to control samples.

### 4.2.7 Elastic Modulus

| Table 4.2.7 - Elastic modulus values of EDTA immersion over time | | | | | |
|---|---|---|---|---|---|
| | **0 hours** | **6 hours** | **12 hours** | **24 hours** | **48 hours** |
| **Mean** | 11.2 | 8.9 | 7.3 | 7.5 | 6.6 |
| **Mean difference** | -0.39 (-3.4%) | -1.7 (-15.9%) | -3.6 (-33.0%) | -3.8 (-33.8%) | -5.3 (-44.4%) |
| **P-Value** | 0.999 | 0.797 | 0.109 | 0.081 | 0.006 |
| **Significant** | No | No | No | No | Yes |

Table 4.2.7 shows at 48 hours, immersion in EDTA had a strong significant effect on elastic modulus of bone segment. with a progressive decrease in elastic modulus across all time points compared to control samples.

### 4.2.8 Post-yield stress

| Table 4.2.8 - Post-yield stress values of EDTA immersion over time | | | | | |
|---|---|---|---|---|---|
| | **0 hours** | **6 hours** | **12 hours** | **24 hours** | **48 hours** |
| **Mean** | 17.8 | 19.2 | 18.86 | 18.9 | 20.1 |
| **Mean difference** | -0.2 (+1.1%) | -6.8 (+35.5%) | -7.06 (+37.4%) | -6.3 (+33.4%) | -6.9 (+34.4%) |
| **P-Value** | 0.846 | 0.524 | 0.484 | 0.602 | 0.508 |
| **Significant** | No | No | No | No | No |

Table 4.2.8 shows at 48 hours, immersion in EDTA had no significant effect on post-yield stress across bone segment, with a steady state in post-yield stress across all time points compared to control samples.

### 4.2.9 Post-yield strain

| Table 4.2.9 - Post-yield strain values of EDTA immersion over time | | | | | |
|---|---|---|---|---|---|
| | **0 hours** | **6 hours** | **12 hours** | **24 hours** | **48 hours** |
| **Mean** | 0.506 | 0.544 | 0.546 | 0.502 | 0.328 |
| **Mean difference** | -0.016 (+3.2%) | -0.22 (+41.5%) | -0.226 (+41.4%) | -0.162 (+32.3%) | 0.056 (+17.1%) |
| **P-Value** | 0.886 | 0.674 | 0.654 | 0.881 | 0.992 |
| **Significant** | No | No | No | No | No |

Table 4.2.9 shows at 48 hours, immersion in EDTA had no significant effect on post-yield strain across bone segment.

### 4.2.10 Ductility

| Table 4.2.10 - Ductility values of EDTA immersion over time | | | | | |
|---|---|---|---|---|---|
| | **0 hours** | **6 hours** | **12 hours** | **24 hours** | **48 hours** |
| **Mean** | 0.99 | 1.45 | 1.74 | 1.92 | 2.17 |
| **Mean difference** | 0.064 (-6.3%) | -0.46 (+31.7%) | -0.65 (+37.4) | -0.98 (+51.1) | -1.26 (+58.1%) |
| **P-Value** | 0.998 | 0.537 | 0.183 | 0.014 | 0.001 |
| **Significant** | No | No | No | Yes | Yes |

Table 4.2.10 shows at 24 and 48 hours, immersion in EDTA had a strong significant effect on ductility of bone segment, with a significant increase in ductility at 24 hours onwards.

### 4.2.11 Toughness

| Table 4.2.11 - Toughness values of EDTA immersion over time | | | | | |
|---|---|---|---|---|---|
| | **0 hours** | **6 hours** | **12 hours** | **24 hours** | **48 hours** |
| **Mean** | 148.5 | 163.5 | 184 | 201.4 | 223.8 |
| **Mean difference** | 0.01 (-0.7%) | -13.36 (+8.2%) | -42.26 (+23.0%) | -69.96 (+34.7) | -78.95 (+34.2%) |
| **P-Value** | 0.999 | 0.994 | 0.543 | 0.088 | 0.041 |
| **Significant** | No | No | No | No | Yes |

Table 4.2.11 shows at 48 hours, immersion in EDTA had a significant effect on toughness of bone. This is further demonstrated in graph 5.2.11 which shows a significant increase in toughness at 48 hours.

## 4.3 Decollagenisation (5M NaOH) results

This subsection will focus on de-collagenised specimen results. Results are presented by showing a mean, mean difference value, p-value and whether this was significant. Mean values express the mean of all five values achieved in each trial or time point. Mean difference value is the difference in mean value between the EDTA sample and the control specimen. The results presented here are **“Control mean value minus NaOH mean value”**.

Graphical representation of these values is presented as a bar-plot, with whiskers being maximum value are in appendix C.

The results for de-collagenisation in 5M NaOH are presented first followed by 10M NaOH in section 4.4.

### 4.3.1 Force

| Table 4.3.1 - Force values of 5M NaOH immersion over time | | | | | |
|---|---|---|---|---|---|
| | **0 hours** | **6 hours** | **12 hours** | **24 hours** | **48 hours** |
| **Mean** | 454 | 418 | 328 | 108 | 97.4 |
| **Mean difference** | -42 (+9.3%) | 53 (-11.3%) | 84 (-20.4%) | 357 (-76.7%) | 362.6 (-78.7%) |
| **P-Value** | 0.994 | 0.983 | 0.888 | 0.0014 | 0.0012 |
| **Significant** | No | No | No | Yes | Yes |

Table 4.3.1 shows at 24 and 48 hours, immersion in 5M NaOH had a significant effect on force applied across bone segment, with a gradual decrease in force across all time points compared to control samples.

### 4.3.2 Deflection

| Table 4.3.2 - Deflection values of 5M NaOH immersion over time | | | | | |
|---|---|---|---|---|---|
| | **0 hours** | **6 hours** | **12 hours** | **24 hours** | **48 hours** |
| **Mean** | 1.3 | 1.23 | 1.17 | 1.14 | 0.672 |
| **Mean difference** | 0.07 (-5.1%) | -0.2 (+1.4%) | 0.042 (-3.5%) | 0.01 (-0.9%) | 0.58 (-46.3%) |
| **P-Value** | 0.999 | 0.921 | 0.999 | 0.999 | 0.085 |
| **Significant** | No | No | No | No | No |

Table 4.3.2 shows after immersion in 5M NaOH at 48 hours, there was no significant effect on deflection across bone segments, with a steady state in deflection across all time points compared to control samples. Note at 48 hours, a decrease was seen, however this was not deemed significant.

### 4.3.3 Ultimate Stress

| Table 4.3.3 - Ultimate Stress values of 5M NaOH immersion over time | | | | | |
|---|---|---|---|---|---|
| | **0 hours** | **6 hours** | **12 hours** | **24 hours** | **48 hours** |
| **Mean** | 193.6 | 187.7 | 137.8 | 58.4 | 39.0 |
| **Mean difference** | -5.4 (+2.8%) | 18.52 (-8.9%) | 61.4 (-30.8%) | 141.4 (-70.7%) | 157.2 (-80.1%) |
| **P-Value** | 0.999 | 0.988 | 0.323 | 0.0007 | 0.0002 |
| **Significant** | No | No | No | Yes | Yes |

Table 4.3.3 shows at 24 and 48 hours, immersion in 5M NaOH had a strongly significant effect on ultimate stress across bone segment, with a significant decrease, particularly at 24 hours onwards, in ultimate stress across all time points compared to control samples.

### 4.3.4 Ultimate Strain

| Table 4.3.4 - Ultimate Strain values of 5M NaOH immersion over time | | | | | |
|---|---|---|---|---|---|
| | **0 hours** | **6 hours** | **12 hours** | **24 hours** | **48 hours** |
| **Mean** | 2.18 | 2.124 | 1.78 | 1.19 | 0.586 |
| **Mean difference** | 0.136 (-5.9%) | 0.12 (-5.3%) | 0.582 (-24.6%) | 1.03 (-46.6%) | 1.608 (-73.3%) |
| **P-Value** | 0.984 | 0.991 | 0.083 | 0.0004 | <0.0001 |
| **Significant** | No | No | No | Yes | Yes |

Table 4.3.4 shows at 48 hours, immersion in 5M NaOH had a strongly significant effect on ultimate strain across bone segment, with a significant decrease, particularly at 24 hours onwards, in ultimate strain across all time points compared to control samples.

### 4.3.5 Yield Stress

**Table 4.3.5 - Yield stress values of 5M NaOH immersion over time**

| | 0 hours | 6 hours | 12 hours | 24 hours | 48 hours |
|---|---|---|---|---|---|
| **Mean** | 174.4 | 169.2 | 123.4 | 54.8 | 38.4 |
| **Mean difference** | -10.4 (+6.0%) | 24.6 (-12.7%) | 64 (-34.2%) | 132.4 (-70.7%) | 144.6 (-79.0%) |
| **P-Value** | 0.999 | 0.957 | 0.281 | 0.002 | 0.0005 |
| **Significant** | No | No | No | Yes | Yes |

Table 4.3.5 shows at 24 and 48 hours, immersion in 5M NaOH had a strong significant effect on yield stress across bone segment, with a progressive decrease in yield stress across all time points compared to control samples.

### 4.3.6 Yield Strain

**Table 4.3.6 - Yield Strain values of 5M NaOH immersion over time**

| | 0 hours | 6 hours | 12 hours | 24 hours | 48 hours |
|---|---|---|---|---|---|
| **Mean** | 1.852 | 1.908 | 1.666 | 1.12 | 0.572 |
| **Mean difference** | 0.118 (-5.9%) | 0.012 (-0.6%) | 0.376 (-18.4%) | 0.768 (-40.7%) | 1.306 (-69.5%) |
| **P-Value** | 0.987 | 0.999 | 0.352 | 0.004 | <0.0001 |
| **Significant** | No | No | No | Yes | Yes |

Table 4.3.6 shows at 24 and 48 hours, immersion in 5M NaOH had a strong significant effect on yield strain across bone segment, with a progressive decrease in yield strain, particularly at 24 hours onwards, across all time points compared to control samples.

### 4.3.7 Elastic Modulus

| Table 4.3.7 - Elastic modulus values of 5M NaOH immersion over time | | | | | |
|---|---|---|---|---|---|
| | **0 hours** | **6 hours** | **12 hours** | **24 hours** | **48 hours** |
| **Mean** | 11.2 | 14.9 | 6.6 | 1.8 | 1.7 |
| **Mean difference** | 0.34 (-2.9%) | -4.3 (+28.8%) | 4.4 (-40.0%) | 9.5 (-83.9%) | 10.2 (-85.7%) |
| **P-Value** | 0.9996 | 0.029 | 0.024 | <0.0001 | <0.0001 |
| **Significant** | No | Yes | Yes | Yes | Yes |

Table 4.3.7 shows at 6 hours, there was a strong significant increase in elastic modulus after immersion in 5M NaOH. At 12 hours, elastic modulus had dropped to a significant decrease again and this significance was maintained at 24 and 48 hours.

### 4.3.8 Post-yield stress

| Table 4.3.8 - Post-yield stress values of 5M NaOH immersion over time | | | | | |
|---|---|---|---|---|---|
| | **0 hours** | **6 hours** | **12 hours** | **24 hours** | **48 hours** |
| **Mean** | 19.2 | 11.88 | 9.6 | 3.6 | 0.6 |
| **Mean difference** | 0.2 (-1.5%) | 0.52 (-4.2%) | 2.2 (-18.6%) | 9 (-71.4%) | 12.6 (-95.5%) |
| **P-Value** | 0.665 | 0.652 | 0.986 | 0.008 | 0.001 |
| **Significant** | No | No | No | Yes | Yes |

Table 4.3.8 shows at 48 hours, immersion in 5M NaOH had a strongly significant effect on post-yield stress across bone segment, with a progressive decrease in post-yield stress across all time points compared to control samples. Note at 48 hours, the mean value is almost 0.

### 4.3.9 Post-yield strain

| Table 4.3.9 - Post-yield strain values of 5M NaOH immersion over time | | | | | |
|---|---|---|---|---|---|
| | **0 hours** | **6 hours** | **12 hours** | **24 hours** | **48 hours** |
| **Mean** | 0.328 | 0.216 | 0.114 | 0.058 | 0.014 |
| **Mean difference** | 0.018 (-5.2%) | 0.108 (-33.3%) | 0.206 (-64.4%) | 0.282 (-82.9%) | 0.3485 (-96.1) |
| **P-Value** | 0.999 | 0.905 | 0.394 | 0.116 | 0.031 |
| **Significant** | No | No | No | No | Yes |

Table 4.3.9 shows at 48 hours, immersion in 5M NaOH had a strong significant effect on post-yield strain across bone segment, with was a drop in strain at 48 hours, to almost 0.

### 4.3.10 Ductility

| Table 4.3.10 - Ductility values of 5M NaOH immersion over time | | | | | |
|---|---|---|---|---|---|
| | **0 hours** | **6 hours** | **12 hours** | **24 hours** | **48 hours** |
| **Mean** | 1.104 | 1.286 | 1.17 | 0.538 | 0.502 |
| **Mean difference** | -0.09 (+8.2%) | 0.004 (-0.4%) | 0.038 (-3.5%) | 0.406 (-43.0%) | 0.402 (-44.5%) |
| **P-Value** | 0.932 | 0.999 | 0.999 | 0.005 | 0.006 |
| **Significant** | No | No | No | Yes | Yes |

Table 4.3.10 shows at 24 and 48 hours, immersion in 5M NaOH had a strong significant effect on ductility of bone segment, with a significant increase in ductility at 24 hours onwards.

### 4.3.11 Toughness

| Table 4.3.11 - Toughness values of 5M NaOH immersion over time | | | | | |
|---|---|---|---|---|---|
| | **0 hours** | **6 hours** | **12 hours** | **24 hours** | **48 hours** |
| **Mean** | 166.3 | 149.3 | 135.1 | 68.21 | 38.63 |
| **Mean difference** | -9.8 (+6.2%) | 0.89 (-0.6%) | 6.68 (-4.7%) | 63.19 (-48.1%) | 106.2 (-73.3%) |
| **P-Value** | 0.919 | 0.999 | 0.999 | 0.012 | <0.0001 |
| **Significant** | No | No | No | Yes | Yes |

Table 4.3.11 shows at 24 and 48 hours, immersion in 5M NaOH had a strong significant effect on toughness of bone, with a significant decrease in toughness at 24 hours onwards.

## 4.4 Decollagenisation (10M NaOH) results

### 4.4.1 Force

**Table 4.4.1 - Force values of 10M NaOH immersion over time**

| | 0 hours | 6 hours | 12 hours | 24 hours | 48 hours |
|---|---|---|---|---|---|
| **Mean** | 414 | 356 | 76 | 50.4 | 8.2 |
| **Mean difference** | -2 (+0.5%) | 115 (-24.4%) | 336 (-81.6%) | 414 (-89.2%) | 452 (-98.3%) |
| **P-Value** | 0.999 | 0.576 | 0.0007 | <0.0001 | <0.0001 |
| **Significant** | No | No | Yes | Yes | Yes |

Table 4.4.1 shows at 12, 24 and 48 hours, immersion in 10M NaOH had a strongly significant effect on force applied across bone segment, with a significant decrease in force across all time points compared to control samples.

### 4.4.2 Deflection

**Table 4.4.2 - Deflection values of 10M NaOH immersion over time**

| | 0 hours | 6 hours | 12 hours | 24 hours | 48 hours |
|---|---|---|---|---|---|
| **Mean** | 1.4 | 1.3 | 1.12 | 0.872 | 0.58 |
| **Mean difference** | -0.03 (+2.1%) | -0.27 (+21.0%) | 0.096 (-7.9%) | 0.278 (-24.2%) | 0.672 (-53.7%) |
| **P-Value** | 0.999 | 0.791 | 0.997 | 0.770 | 0.039 |
| **Significant** | No | No | No | No | Yes |

Table 4.4.2 shows after immersion in 10M NaOH at 48 hours, there was a significant effect on deflection across bone segments, with a steady decrease in deflection across all time points compared to control samples.

### 4.4.3 Ultimate Stress

| Table 4.4.3 - Ultimate Stress values of 10M NaOH immersion over time | | | | | |
|---|---|---|---|---|---|
| | **0 hours** | **6 hours** | **12 hours** | **24 hours** | **48 hours** |
| **Mean** | 185.2 | 176 | 38 | 24 | 4.4 |
| **Mean difference** | -6.6 (+3.6%) | 30.2 (-14.6%) | 161.2 (-80.9%) | 175.8 (-87.9%) | 191.8 (-97.8%) |
| **P-Value** | 0.996 | 0.882 | <0.0001 | <0.0001 | <0.0001 |
| **Significant** | No | No | Yes | Yes | Yes |

Table 4.4.3 shows at 12, 24 and 48 hours, immersion in 10M NaOH had a strongly significant effect on ultimate stress across bone segment, with a significant decrease, particularly at 12 hours onwards, in ultimate stress across all time points compared to control samples.

### 4.4.4 Ultimate Strain

| Table 4.4.4 - Ultimate Strain values of 10M NaOH immersion over time | | | | | |
|---|---|---|---|---|---|
| | **0 hours** | **6 hours** | **12 hours** | **24 hours** | **48 hours** |
| **Mean** | 2.224 | 1.804 | 1.464 | 0.938 | 0.512 |
| **Mean difference** | 0.092 (-3.9%) | 0.44 (-19.6%) | 0.898 (-38.0%) | 1.29 (-57.9%) | 1.682 (-76.7%) |
| **P-Value** | 0.997 | 0.254 | 0.0013 | <0.0001 | <0.0001 |
| **Significant** | No | No | Yes | Yes | Yes |

Table 4.4.4 shows at 12, 24 and 48 hours, immersion in 10M NaOH had a strongly significant effect on ultimate strain across bone segment., with a significant decrease, particularly at 12 hours onwards in ultimate strain across all time points compared to control samples.

### 4.4.5 Yield Stress

**Table 4.4.5 - Yield stress values of 10M NaOH immersion over time**

| | 0 hours | 6 hours | 12 hours | 24 hours | 48 hours |
|---|---|---|---|---|---|
| **Mean** | 167.2 | 162 | 34.2 | 21.5 | 3.61 |
| **Mean difference** | -3.2 (+2.0%) | 31.8 (-16.4%) | 153.2 (-81.8%) | 165.7 (-88.5%) | 179.4 (-98.0%) |
| **P-Value** | 0.985 | 0.861 | 0.0001 | <0.0001 | <0.0001 |
| **Significant** | No | No | Yes | Yes | Yes |

Table 4.4.5 shows at 12, 24 and 48 hours, immersion in 10M NaOH had a strong significant effect on yield stress across bone segment, with a significant decrease in yield stress particularly at 12 hours onwards, compared to control samples.

### 4.4.6 Yield Strain

**Table 4.4.6 - Yield Strain values of 10M NaOH immersion over time**

| | 0 hours | 6 hours | 12 hours | 24 hours | 48 hours |
|---|---|---|---|---|---|
| **Mean** | 1.928 | 1.646 | 1.366 | 0.902 | 0.506 |
| **Mean difference** | 0.042 (-2.1%) | 0.274 (-14.3% | 0.676 (-31.6%) | 0.986 (-52.2%) | 1.372 (-73.1%) |
| **P-Value** | 0.999 | 0.619 | 0.008 | <0.0001 | <0.0001 |
| **Significant** | No | No | Yes | Yes | Yes |

Table 4.4.6 shows at 12, 24 and 48 hours, immersion in 10M NaOH had a strong significant effect on yield strain across bone segment, with a progressive decrease in yield strain, particularly at 12 hours onwards, across all time points compared to control samples.

### 4.4.7 Elastic Modulus

**Table 4.4.7 - Elastic modulus values of 10M NaOH immersion over time**

| | 0 hours | 6 hours | 12 hours | 24 hours | 48 hours |
|---|---|---|---|---|---|
| **Mean** | 10.6 | 15.1 | 2.9 | 1.4 | 0.1 |
| **Mean difference** | 1.0 (-8.8%) | -4.4 (+29.5%) | 8.1 (-73.9%) | 9.9 (-87.6%) | 11.8 (-99.1%) |
| **P-Value** | 0.924 | 0.003 | <0.0001 | <0.0001 | <0.0001 |
| **Significant** | No | Yes | Yes | Yes | Yes |

Table 4.4.7 shows at 6 hours, there was a strong significant increase in elastic modulus after immersion in 10M NaOH. At 12 hours, elastic modulus had dropped to a significant decrease again and this significance was maintained at 24 and 48 hours.

### 4.4.8 Post-yield stress

**Table 4.4.8 - Post-yield stress values of 10M NaOH immersion over time**

| | 0 hours | 6 hours | 12 hours | 24 hours | 48 hours |
|---|---|---|---|---|---|
| **Mean** | 12.4 | 14 | 3.8 | 2.5 | 0.19 |
| **Mean difference** | 0.8 (-6.0%) | -1.6 (+11.4%) | 8 (-67.8%) | 10.1 (-80.2%) | 13.01 (-98.6%) |
| **P-Value** | 0.991 | 0.993 | 0.095 | 0.019 | 0.002 |
| **Significant** | No | No | No | Yes | Yes |

Table 4.4.8 shows at 24 and 48 hours, immersion in 10M NaOH had a strongly significant effect on post-yield stress across bone segment, with a progressive decrease in post-yield stress across all time points compared to control samples. Note at 48 hours, the mean value is almost 0.

### 4.4.9 Post-yield strain

| Table 4.4.9 - Post-yield strain values of 10M NaOH immersion over time | | | | | |
|---|---|---|---|---|---|
| | **0 hours** | **6 hours** | **12 hours** | **24 hours** | **48 hours** |
| **Mean** | 0.296 | 0.158 | 0.098 | 0.036 | 0.006 |
| **Mean difference** | 0.02 (-6.3%) | 0.166 (-51.2%) | 0.222 (-69.4%) | 0.304 (-89.0%) | 0.356 (-98.3%) |
| **P-Value** | 0.999 | 0.609 | 0.304 | 0.071 | 0.024 |
| **Significant** | No | No | No | Yes | Yes |

Table 4.4.9 shows at 24 and 48 hours, immersion in 10M NaOH had a strong significant effect on post-yield strain across bone segment. Note there was a drop in strain at 24 and 48 hours, to almost 0.

### 4.4.10 Ductility

| Table 4.4.10 - Ductility values of 10M NaOH immersion over time | | | | | |
|---|---|---|---|---|---|
| | **0 hours** | **6 hours** | **12 hours** | **24 hours** | **48 hours** |
| **Mean** | 1.072 | 1.246 | 0.884 | 0.548 | 0.414 |
| **Mean difference** | -0.058 (+5.4%) | 0.024 (-2.4%) | 0.204 (-18.8%) | 0.396 (-41.9%) | 0.49 (-54.2%) |
| **P-Value** | 0.986 | 0.998 | 0.301 | 0.041 | 0.003 |
| **Significant** | No | No | No | Yes | Yes |

Table 4.4.10 shows at 24 and 48 hours, immersion in 10M NaOH had a strong significant effect on ductility of bone segment, with a significant increase in ductility at 24 hours onwards.

### 4.4.11 Toughness

| Table 4.4.11 - Toughness values of 10M NaOH immersion over time | | | | | |
|---|---|---|---|---|---|
| | **0 hours** | **6 hours** | **12 hours** | **24 hours** | **48 hours** |
| **Mean** | 170.3 | 179.8 | 26.83 | 21.01 | 9.31 |
| **Mean difference** | 2.5 (-1.7%) | 4.56 (-3.0%) | 114.9 (-81.1%) | 110.4 (-90.9%) | 135.5 (-93.6%) |
| **P-Value** | 0.999 | 0.999 | <0.0001 | <0.0001 | <0.0001 |
| **Significant** | No | No | Yes | Yes | Yes |

Table 4.4.11 shows at 12, 24 and 48 hours, immersion in 10M NaOH had a strong significant effect on toughness of bone, with a significant decrease in toughness at 12 hours onwards.

## 4.5 Bone density measurement

This section provides results of mean pixel values of the specimens from all of the solutions.

The Control group (Con), Demineralisation group (EDTA), decollagenisation group at 5M NaOH (5NaOH) and decollagenisation at 10M NaOH (10NaOH) were compared.

Two experimental factors were tested, namely bone quality (control v demineralisation v decollagenisation) and time, and with greater than three time group variables, a Two-way ANOVA analysis was performed on combined data sets to investigate the two experimental factors on mechanical outcomes. For this section, these outcomes comprised pixel values for each group over times 0, 6hours, 12hours, 24hours and 48 hours. P-values $<0.05$ denotes statistical significance.

The results for pixel values in all groups were collated for analysis and for standardisation of presentation they will be presented in the following order:

1. EDTA specimens
2. 5M NaOH specimens
3. 10M NaOH specimens

Control values will be presented in Appendix B and C. None of the control results showed any significant difference between samples regardless of time immersed in PBS. Based on these findings, an appropriate control data set was used for comparison with de-mineralised and de-collagenised specimens.

### 4.5.1 Demineralised (EDTA) specimens

**Table 4.5.1 - Pixel values of EDTA immersion over time**

| | 0 hours | 6 hours | 12 hours | 24 hours | 48 hours |
|---|---|---|---|---|---|
| **Mean** | 188 | 162.4 | 154 | 144.6 | 130.4 |
| **Mean difference** | -0.2 (+0.3%) | 19.2 (-10.6%) | 26.8 (-14.8%) | 39.4 (-21.4%) | 54 (-29.3%) |
| **P-Value** | 0.999 | <0.0001 | <0.0001 | <0.0001 | <0.0001 |
| **Significant** | No | Yes | Yes | Yes | Yes |

Table 4.5.1 shows at 6, 12, 24 and 48 hours, immersion in EDTA had a strong significant effect on pixel value of bone specimens, with a significant decrease in values at 6 hours onwards.

### 4.5.2 Decollagenised (5M NaOH) specimens

**Table 4.5.2 - Pixel values of 5M NaOH immersion over time**

| | 0 hours | 6 hours | 12 hours | 24 hours | 48 hours |
|---|---|---|---|---|---|
| **Mean** | 187 | 185.2 | 186.1 | 188.4 | 188 |
| **Mean difference** | 0.4 (-0.2%) | -3.6 (+1.8%) | -5.4 (+2.9%) | -4.2 (+2.3%) | -3.6 (+2.0%) |
| **P-Value** | 0.999 | 0.765 | 0.371 | 0.634 | 0.765 |
| **Significant** | No | No | No | No | No |

Table 4.5.2 shows at all time points, immersion in 5M NaOH had no significant effect on pixel value of bone specimens, with a a relatively unchanged pixel value over time.

### 4.5.3 Decollagenised (10M NaOH) specimens

**Table 4.5.3 - Pixel values of 10M NaOH immersion over time**

| | 0 hours | 6 hours | 12 hours | 24 hours | 48 hours |
|---|---|---|---|---|---|
| **Mean** | 188 | 181.2 | 180.8 | 183 | 185.4 |
| **Mean difference** | 0.6 (-0.3%) | 0.4 (-0.2%) | 0.1 (0%) | 1 (0%) | -1 (0%) |
| **P-Value** | 0.999 | 0.999 | 0.999 | 0.994 | 0.994 |
| **Significant** | No | No | No | No | No |

Table 4.5.3 shows at all time points, immersion in 10M NaOH had no significant effect on pixel value of bone specimens. with a relatively unchanged pixel value over time

## 4.6 Compression failure

This finding should be considered additional but has been included as it was considered significant. During mechanical testing, it was noted that there was an abnormality in the failure mechanism compared to control segments. To this effect, slow cut videographic evidence of a bending load being applied to the decollagenised samples at 48 hours were taken. These showed that there was sequential failure at the compression surface of bone before any tensile failure. This would account for the significant reduction in elastic modulus.

Figure 32 shows the sequence of events leading to compressive failure prior to tensile failure under load in decollagenised bone. At the moment of impact of the loader onto compression surface, an unzipping process occurs across the bone beam, with the appearance a delamination process. The applied load is most visible on the outer surface of the bone specimen with the greatest gap, however this resulted from the central load.

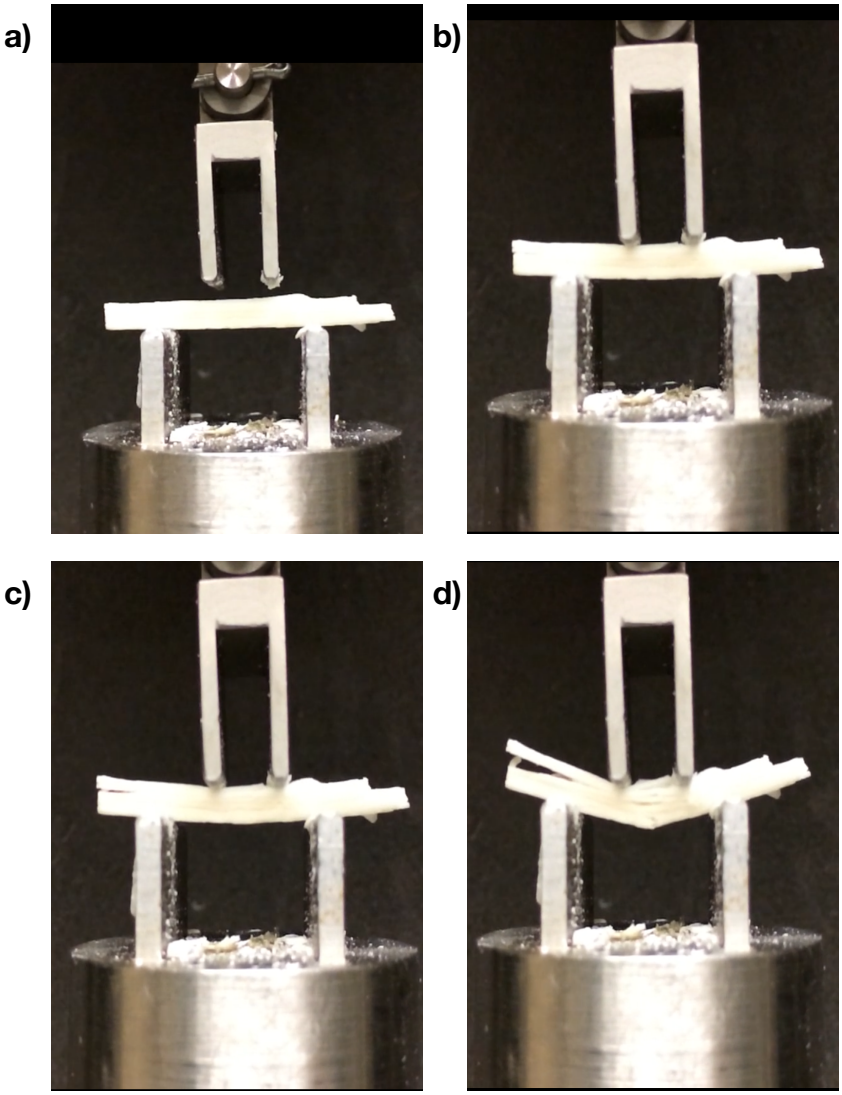


**Figure 32. Showing a) Initial position of loader and bone specimen; b) Indentation of compression surface under load; c) Failure of compression surface; d) Failure of tension surface**

# 5. RESULTS CLINICAL STUDY

In this section results for the clinical study of this thesis will be presented. In order to deduce the probability of results being significant, the observed (post-hoc) statistical power was calculated based on the estimated effect size.

Chi-Squared tables for each age group showing energy versus fracture pattern/type and gender versus fracture pattern in the all age groups are shown in appendix D.

## 5.1 Descriptive statistics

A partial eta value of 0.341 indicates a large effect size, signifying that age group has a large effect on the significance of the above result.

The total live population of the area studied, for the period studied, according to the Office of National Statistics was 545,390. For the paediatric population, incidence of femoral shaft fractures was 3.5 per 100,000 per year. For the adult population, this was higher at 11.5 per 100,000 per year. Total population incidence was 14.9 per 100,000 person years.

A total of 163 patients were eligible for final analysis. The final numbers of patients analysed are shown in table 5.1.1.

**Table 5.1.1 - Patient breakdown**

| Group | Initial number | Excluded | Final number |
|---|---|---|---|
| **Paediatric (<16)** | 41 | 3 | 38 |
| **Adult (16-54)** | 38 | 1 | 37 |
| **Old-age (>55)** | 127 | 39 | 88 |

Of the 163 eligible for analysis, mean age was 50.8 (SD 32.8, range 0-101) with a male to female ratio of 1:1.2. This is shown in table 5.1.2 with a subgroup breakdown.

**Table 5.1.2 - Mean age and standard deviation**

| Group | Mean age | SD |
|---|---|---|
| Overall | 50.8 | 32.8 |
| Paediatric (<16) | 3.8 | 4.04 |
| Adult (16-54) | 35.3 | 11.7 |
| Old-age (>55) | 77.8 | 12.1 |

Overall male to female distribution was similar. A breakdown per age group is shown in table 5.1.3.

**Table 5.1.3 - Gender distribution per group**

| Group | Male | Female | Total |
|---|---|---|---|
| Overall | 78 (47.9%) | 85 (52.1%) | 163 |
| Paediatric (<16) | 30 (78.9%) | 8 (21.1%) | 38 |
| Adult (16-54) | 27 (72.9%) | 10 (27.1%) | 37 |
| Old-age (>55) | 21 (23.9%) | 67 (76.1%) | 88 |

There was a bimodal distribution in age for those who sustained a femoral shaft fracture, with peaks in the paediatric and elderly age groups. This is shown in Figure 33.

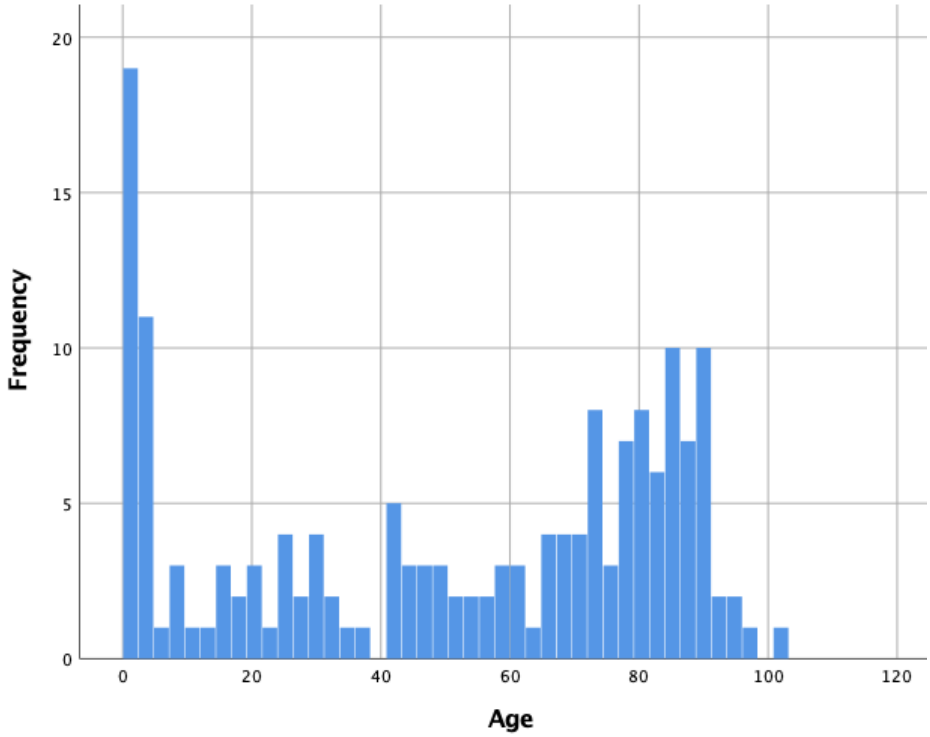


**Figure 33. Showing bimodal distribution of all fractures.**

Furthermore, With regards to gender, this study also showed a bimodal distribution when looking at all fractures, with a second peak evident in the elderly female population. This is shown in figure 34, with “1” being male and “2” being female.

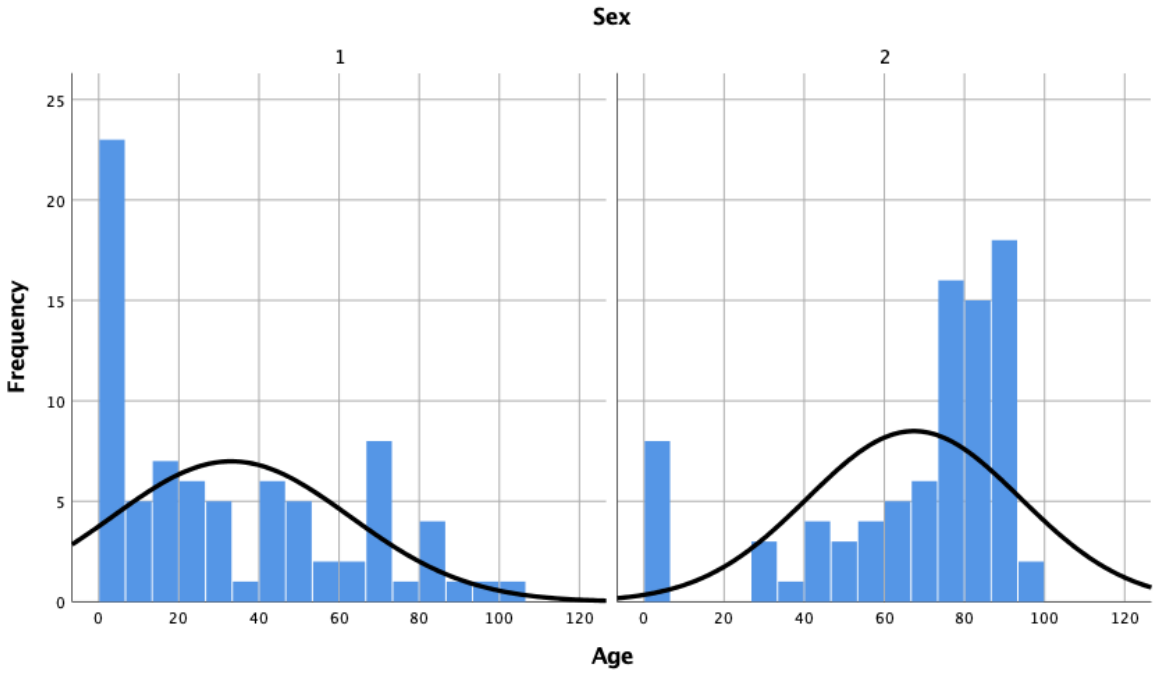


**Figure 34. Showing unimodal distribution of sex in all fractures.**

Most fractures were oblique with the least transverse. A final breakdown according to group is shown in table 5.1.4.

**Table 5.1.4 - Fracture type per group**

| Group | Transverse | Oblique | Spiral | Total |
|---|---|---|---|---|
| Paediatric (<16) | 5 (13.2%) | 15 (39.5%) | 18 (47.3%) | **38** |
| Adult (16-54) | 5 (13.5%) | 27 (73.0%) | 5 (13.5%) | **37** |
| Old-age (>55) | 11 (12.5%) | 46 (52.3%) | 31 (32.2%) | **88** |
| **Total** | **21 (12.9%)** | **88 (54.0%)** | **54 (33.1%)** | **163** |

The vast majority of fractures were closed with only 3 open fractures occurring in the adult group. Furthermore, the vast majority of fractures were simple two part fractures in both the paediatric and old age groups. The majority of injuries in the adult group were comminuted. A breakdown of these results is shown in table 5.1.5.

**Table 5.1.5 - Fracture pattern per group**

| Group | Simple | Comminuted | Total |
|---|---|---|---|
| Paediatric (<16) | 35 (92.1%) | 3 (7.9%) | **38** |
| Adult (16-54) | 5 (13.5%) | 32 (86.5%) | **37** |
| Old-age (>55) | 62 (70.5%) | 26 (29.5%) | **88** |
| **Total** | **102 (62.6%)** | **61 (37.4%)** | **163** |

A low energy fall, owing to the old age group, was the most common mechanism of injury. A high energy mechanism as a result of a road traffic accident was the most common cause in the adult population, with a split between low and high energy falls being the most common mechanism in the paediatric group. A full breakdown of these numbers is shown in table 5.1.6.

Inter-observer reliability for fracture pattern was 0.77, indicating a substantial agreement.

| Table 5.1.6 - Energy of mechanism per group | | | | |
|---|---|---|---|---|
| **Mechanism** | **Paediatric** | **Adult** | **Old Age** | **Total** |
| Fall (High energy) | 17 (48.6%) | 6 (17.1%) | 12 (34.3%) | **35 (21.5%)** |
| RTA (High energy) | 1 (4.2%) | 23 (9.6%) | 0 | **24 (14.7%)** |
| Sports (Low energy) | 2 (50%) | 0 | 2 (50%) | **4 (2.5%)** |
| Sports (High energy) | 6 (66.7%) | 2 (22.2%) | 1 (11.1%) | **9 (5.5%)** |
| **Total** | | | | **163** |

There were 3 open injuries in the adult group as a result of high energy mechanism.

### 5.1.1 Group descriptive analysis

The following section will provide a subgroup analysis of the old age group. This group was simulated in the laboratory studies. Furthermore, this population were those on bone affecting medication as well as having most comorbidities.

Most in this age group did not have any documented co-morbidities at the time of injury. However of the rest there was a range from one medical condition up to six co-morbidities at time of injury. These included cardiorespiratory, thyroid, hypertension, arrhythmias and hypercholesterolaemia. This breakdown is shown further in table 5.1.7.

| Table 5.1.7 - Number of comorbidities | |
|---|---|
| **Comorbidities** | **Number** |
| 1 | 7 (8.4%) |
| 2 | 10 (12.0%) |
| 3 | 16 (19.4%) |
| 4 | 7 (8.4%) |
| 5 | 3 (3.6%) |
| 6 | 1 (1.2%) |
| **Total** | **83** |

Additionally, it was important to note which patients were on bone affecting medications. This was divided into three groups, namely bone supplements, bisphosphonates and steroid based. Bone supplements included calcitriol, cholecalciferol, Adcal and theca D3. Bisphosphonates included alendronate and zolendronate. Steroid based substances were prednisolone and dexamethasone. A breakdown is shown in table 5.1.8.

| Table 5.1.8 - Bone affecting medications | |
|---|---|
| **Medication** | **Number** |
| Bone supplement | 18 (56.2%) |
| Bisphosphonates | 10 (31.3%) |
| Steroid | 4 (12.5%) |
| **Total** | **32** |

## 5.2 Paediatric age group

This section will present results of statistical analysis. Results will be presented in table format with observed totals, expected totals and chi-squared value. The expected total is the value that one would expect to observe if there was no association between the two categorical variables being assessed. A cramer's V value for effect size will also be presented.

### 5.2.1 Age group and fracture pattern

Table 5.2.1 presents two-tailed binomial testing performed to test null hypothesis test proportion of 0.5.

**Table 5.2.1 - Age group versus fracture pattern**

| | Number | Observed proportion | Significant |
|---|---|---|---|
| **Simple** | 35 | 92% | Yes |
| **Comminuted** | 3 | 8% | Yes |

P value for this test was <0.0001. The above result shows simple fracture occurring in the paediatric age-group was strongly significant. The null hypothesis has therefore been rejected.

### 5.2.2 Age group and mechanism energy

Table 5.2.2 presents two-tailed binomial testing performed to test null hypothesis test proportion of 0.5.

**Table 5.2.2 - Age group versus mechanism energy**

| | Number | Observed proportion | Significant |
|---|---|---|---|
| **Low** | 14 | 37% | No |
| **High** | 24 | 63% | No |

P value for this test was 0.143. The above result shows mechanism energy occurring in the paediatric age-group was not significant. The null hypothesis has therefore not been rejected.

### 5.2.3 Fracture pattern

Cramer's V value was 0.224. Chi-Squared was 1.900. Binary logistic regression did not show a significant association between outcome and predictor variable. In the paediatric group, three patients (3/38) had comminuted injuries. Logistic regression did not show any association between predictor variables and outcome.

**Table 5.2.3 - Logistic regression for fracture pattern**

| PREDICTOR VARIABLE | Significance ($p < 0.05$) |
|---|---|
| **Age** | No |
| **Gender** | No |
| **Energy** | No |
| **Specific mechanism** | No |
| **Fracture type** | No |
| **Open v closed** | No |

## 5.3 Adult age group

This section will present results of the adult age group (17-54 years old).

### 5.3.1 Age group and fracture pattern

Table 5.3.1 presents two-tailed binomial testing performed to test null hypothesis test proportion of 0.5.

**Table 5.3.1 - Age group versus fracture pattern**

| | Number | Observed proportion | Significant |
|---|---|---|---|
| **Simple** | 5 | 86% | Yes |
| **Comminuted** | 32 | 14% | Yes |

P value for this test was <0.0001. The above result shows simple fracture occurring in the adult age-group was strongly significant. The null hypothesis has therefore been rejected.

### 5.3.2 Age group and mechanism energy

Table 5.3.2 presents two-tailed binomial testing performed to test null hypothesis test proportion of 0.5.

**Table 5.3.2 - Age group versus mechanism energy**

| | Number | Observed proportion | Significant |
|---|---|---|---|
| **Low** | 6 | 16% | Yes |
| **High** | 31 | 84% | Yes |

P value for this test was <0.0001. The above result shows energy occurring in the adult age-group was strongly significant. The null hypothesis has therefore been rejected.

### 5.3.3 Fracture pattern

In the adult group, thirty-two patients (32/37) had comminuted injuries. Cramer's V value was 0.684. Chi-Squared was 17.311. Logistic regression showed an association between predictor variable and outcome ie a high energy injury being associated with bone comminution. A Cramer's V value of 0.684 indicates a large effect size (table 5.3.3).

**Table 5.3.3 - Logistic regression for fracture pattern**

| PREDICTOR VARIABLE | Significance ($p < 0.05$) |
|---|---|
| **Age** | No |
| **Gender** | No |
| **Energy** | Yes |
| **Specific mechanism** | Yes ($p = 0.036$) |
| **Fracture type** | No |
| **Open v closed** | No |

Additionally binary logistic regression showed an association with specific fracture mechanism. Subanalysis showed this was for a road traffic accident.

## 5.4 Older age group

This section will present results of the older age group (55 years and over).

### 5.4.1 Age group and fracture pattern

Table 5.4.1 presents two-tailed binomial testing performed to test null hypothesis test proportion of 0.5.

**Table 5.4.1 - Age group versus fracture pattern**

| | Number | Observed proportion | Significant |
|---|---|---|---|
| **Simple** | 62 | 70% | Yes |
| **Comminuted** | 26 | 30% | Yes |

P value for this test was <0.0001. The above result shows simple fracture occurring in the older age-group was strongly significant. The null hypothesis has therefore been rejected.

### 5.4.2 Age group and mechanism energy

Table 5.4.2 presents two-tailed binomial testing performed to test null hypothesis test proportion of 0.5.

**Table 5.4.2 - Age group versus mechanism energy**

| | Number | Observed proportion | Significant |
|---|---|---|---|
| **Low** | 75 | 85% | Yes |
| **High** | 13 | 15% | Yes |

P value for this test was <0.0001. The above result shows mechanism energy occurring in the older age-group was strongly significant. The null hypothesis has therefore been rejected.

### 5.4.3 Fracture pattern

Cramer's V value was 0.222. Chi-Squared was 4.327. Logistic regression showed an association between predictor variables and outcome, with low energy mechanism being associated with a simple fracture. A Cramer's V value of 0.222 indicates a moderate effect size (table 5.4.3).

**Table 5.4.3 - Logistic regression for fracture pattern**

| PREDICTOR VARIABLE | Significance (p < 0.05) |
|---|---|
| **Age** | Yes (p = 0.001) |
| **Gender** | No |
| **Energy** | Yes |
| **Specific mechanism** | Yes (p = 0.001) |
| **Fracture type** | No |
| **Open v closed** | No |

Further logistic regression showed an association between fracture pattern and age, with every one year increase in age leading to a 2% decrease in risk of comminution. Additionally, sub analysis showed a low energy fall was significantly associated with a simple fracture.

## 5.5 Age and fracture pattern

To explore the distribution of age with fracture pattern further, an age histogram was created as a visual representation. Figures 35 displays overall age distribution and age distribution of simple versus comminuted fractures respectively.

For those who sustained a simple fracture (shown in the histogram on the left), there was a bimodal distribution of age correlating with paediatric and older age groups. There was a dip in frequency correlating with the adult age group. With regards to the comminuted fractures (shown in the histogram on the right), there seemed to be a central spike in frequency correlating with the adult age group.

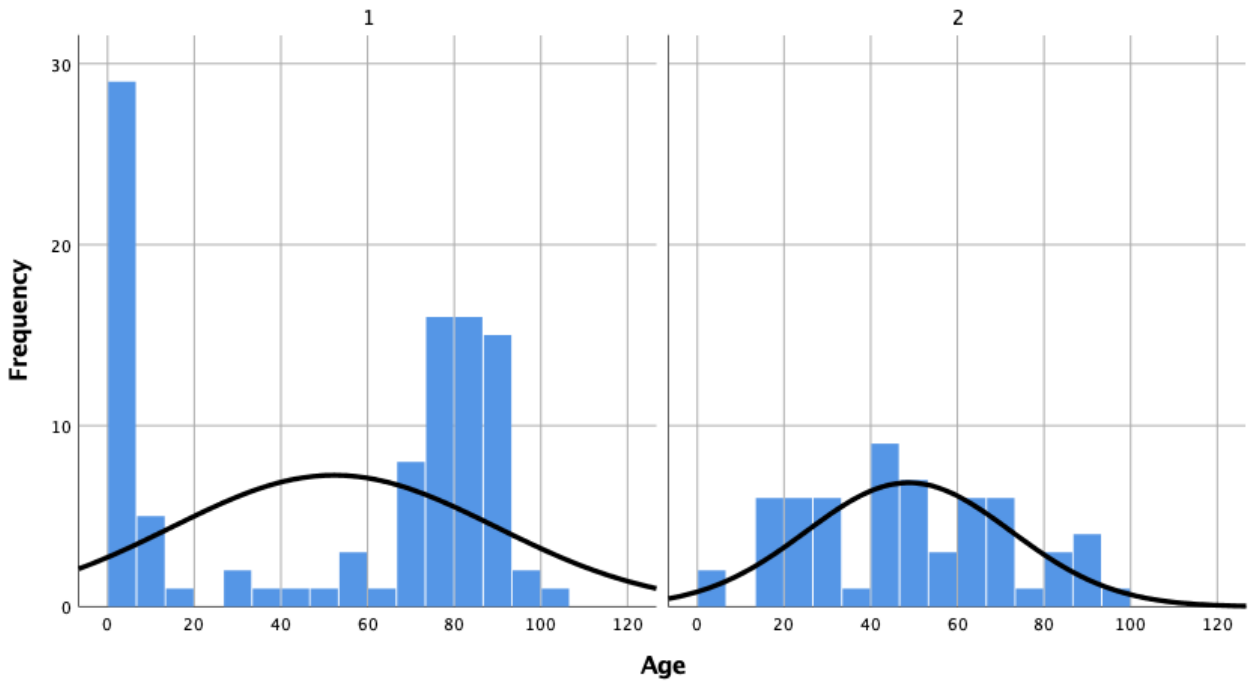


**Figure 35. Showing bimodal distribution of fracture pattern for simple fractures (Simple = 1, Comminuted = 2).**

### 5.5.1 Assessment of age and mechanism energy

To explore the distribution of age with mechanism energy further, an age histogram was created as a visual representation. Figure 36 displays the age distribution of low versus high energy fractures (1 = low energy fracture, 2 = high energy).

For those who sustained a low energy fracture, there seems to be a bimodal distribution of age correlating with paediatric and older age groups. There is a dip in frequency correlating with the adult age group. With regards to the high energy mechanism fractures, this seems to be more prevalent in the paediatric age group, particularly in the <2 year olds. This distribution peaks between the ages of 40-50 and tails off thereafter.

The above results can be further demonstrated by breakdown of energy and fracture pattern based on age as shown in Figure 37. This shows that low energy simple fractures occurred in a bimodal distribution in the paediatric and elderly populations. However comminuted fractures peaked in the adult age group, particularly under high energy.

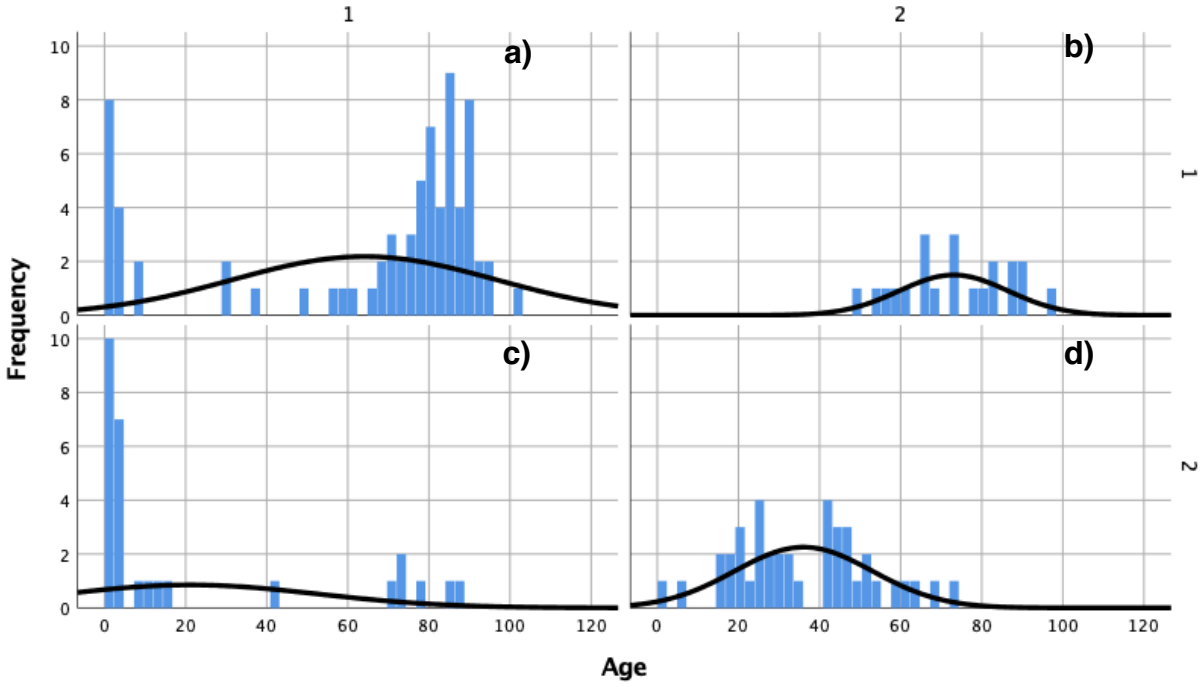


**Figure 37. Age histogram according to a) Low energy, simple fractures, b) Low energy, comminuted fractures, c) High energy, simple fractures and d) High energy, comminuted fractures.**

## 5.6 Analysis of transitional age

Given the above findings, the association of age with fracture pattern was explored in greater detail. In this section, an assumption will be made that the adult age group, are acting as a surrogate for peak bone density.

### 5.6.1 Adult v older age group comparison

Mean age for simple fracture group was 77.6 (SD 14.5) and mean age for comminuted group was 50.9 (SD 22.2). The higher mean age for simple fracture and lower mean age for comminuted fracture proved to be significant ($p<0.0001$). This shows there is an association with age and fracture pattern.

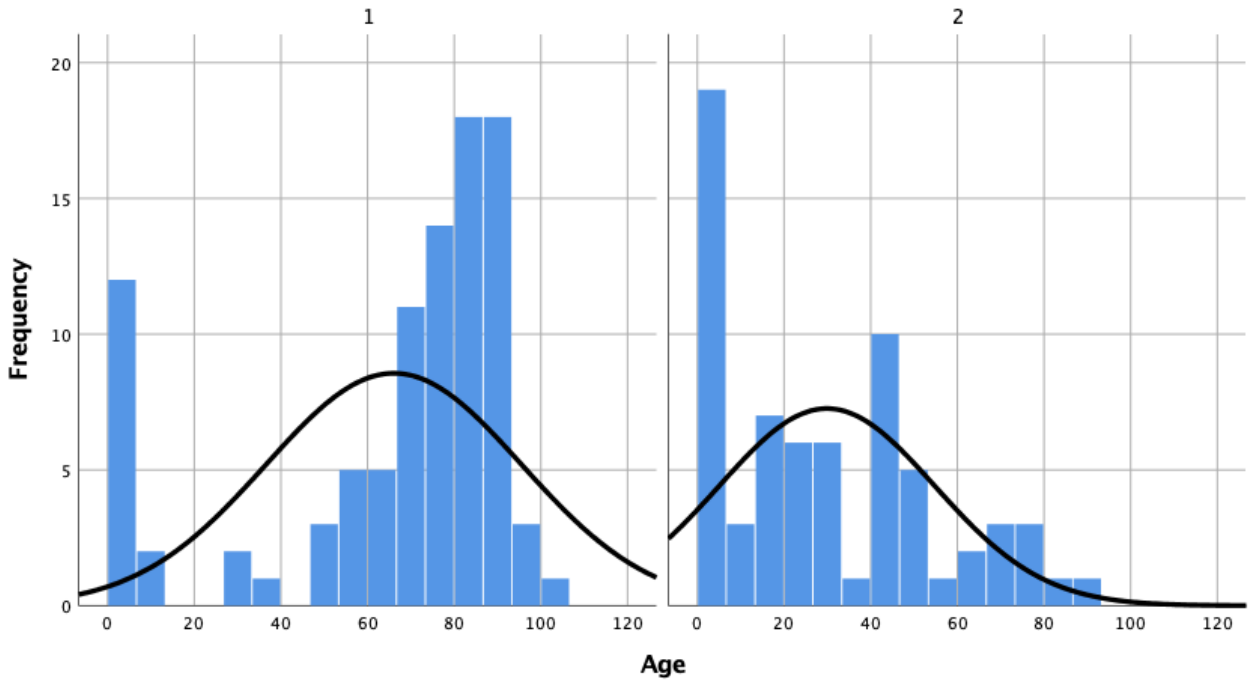


**Figure 36. Showing histogram of age versus mechanism energy (Low = 1, High = 2)**

The regression model showed age was a significant predictor for fracture pattern ($p<0.0001$). The odds of a comminuted fracture being 0.866 ie less than one. To test the variation in fracture pattern explained by this age model, Cox and Snell R-squared is used. This value was shown to be 0.328, meaning that 32.8% or one third of variation in fracture pattern is explained by age alone.

Finally, a receiver operating characteristic (ROC) curve was applied with age as the risk model for the pattern of fracture switched from comminuted to simple. For the purposes of the test, a “positive” outcome was deemed to be a simple fracture. The ROC curve is shown in Figure 38.

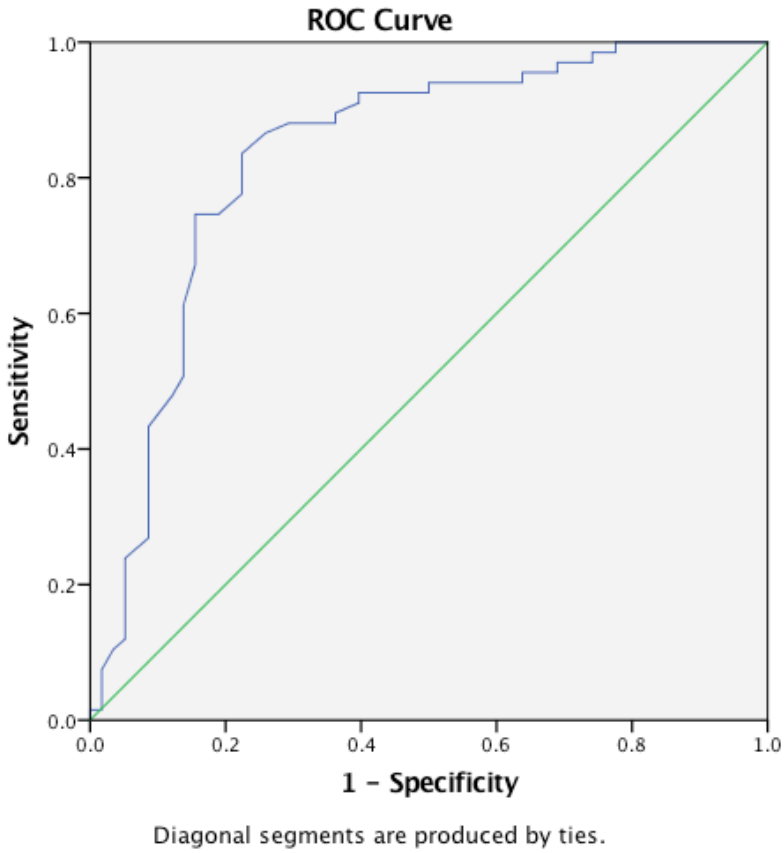


**Figure 38. ROC curve for age (adult and older groups only)**

The ROC curve is situated in the top left hand corner of the graph, which indicates age is likely to be a good marker for fracture pattern. The area under the curve (AUC), is 0.839, $p<0.0001$. An AUC value of >0.8 indicates good sensitivity and specificity characteristics for age.

To achieve an excellent sensitivity, a value of over 0.9 was desired. Analysing the coordinates for the ROC curve, the most accurate age is 56.5, with a sensitivity of 0.925 and "1 - specificity" or false positive rate of 0.397 which identified the best balance out of all ages. This justifies the age cut off for the adult to older age groups. This result suggests at the age of 56.5 years, bone seems to behave more in an older adult pattern.

To conclude, in the older and adult age groups, if using age as the only marker for predicting a comminuted fracture, then the number is 56.5 years of age, after which a simple fracture is more likely to occur.

### 5.6.2 Adult v paediatric age group comparison

Mean age for simple fracture group was 5.81 (SD 9.77) and mean age for comminuted group was 31.2 (SD 14.5). The lower mean age for simple fracture and higher mean age for comminuted fracture proved to be significant ($p<0.0001$). This shows there is a relationship with age and fracture pattern.

To explore this relationship further, a linear logistic regression model was fitted. The regression model showed the age was a significant predictor for fracture pattern ($p<0.0001$). The odds of a an individual in both groups sustaining a comminuted fracture would be 1.139. To test the variation in fracture pattern explained by this age model, Cox and Snell R-squared is used. This value was shown to be 0.444, meaning that 44.4% of variation in fracture pattern is explained by paediatric age alone.

Finally, a receiver operating characteristic (ROC) curve was applied with age as the risk model for the pattern of fracture switched from simple to comminuted. For the purposes of the test, a "positive" outcome was deemed to be a comminuted fracture. The ROC curve is shown in Figure 39.

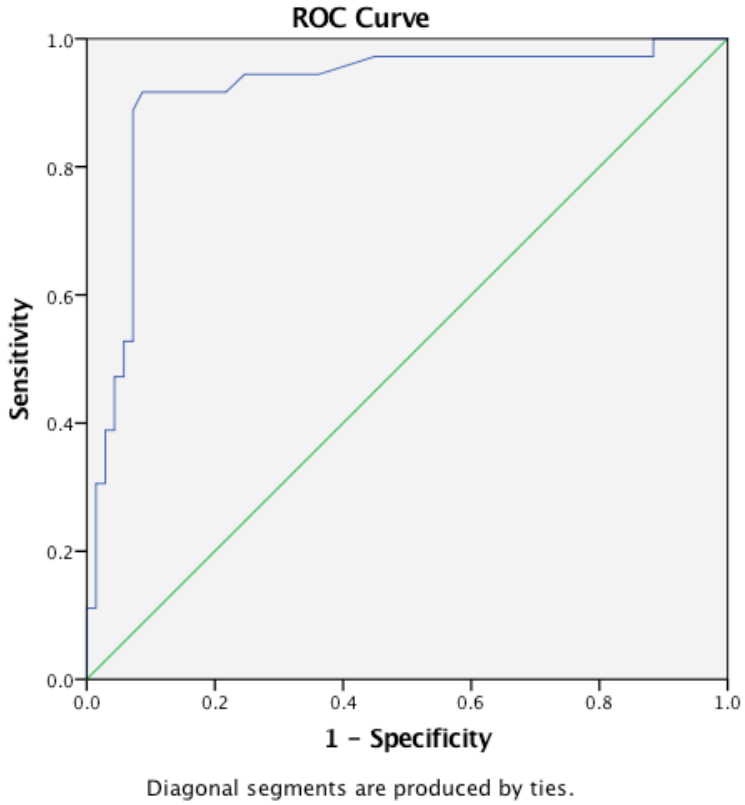


**Figure 39. ROC curve for age (adult and paediatric groups only)**

The ROC curve is situated in the top left hand corner of the graph, which indicates age is likely to be a good marker for fracture pattern. To determine this more accurately the exact coordinates of the ROC curve are ascertained. The area under the curve (AUC), is 0.917, $p<0.0001$. An AUC value of >0.9 indicates excellent sensitivity and specificity characteristics for age.

Analysing the coordinates for the ROC curve, the most accurate age is 14.0, with a sensitivity of 0.917 and "1 - specificity" or false positive rate of 0.087 which identified the best balance out of all ages. This seems to suggest at the age of 14 years old, bone begins to behave more in an adult pattern.

To conclude, in the paediatric and adult age groups, if using age as the only marker for predicting a comminuted fracture, then the age at which bone behaviour seems to change is 14, after which a comminuted fracture is more likely to occur.

# 7. DISCUSSION

This thesis has explored the biomechanical implications of demineralisation and decollagenisation of ovine cortical bone segments, that were mechanically tested at a low strain rate. The research shows mechanical effects on pre-yield, yield and post-yield properties of these segments following both demineralisation and decollagenisation. In demineralised samples, there was a reduction in ultimate stress, however, post-yield strain increased, indicating a more ductile material. In decollagenised samples, there was an initial increase in elastic modulus under bending, followed by a marked decrease. There was also a reduction in yield and post-yield properties, indicating a material that is less tough. There was compression sided failure noted in the extreme decollagenised samples.

For the clinical aspect of this thesis, an incidence of 11.5 per 100,000 per year was seen in adult femoral shaft fractures. The paediatric population were more likely to sustain a simple fracture regardless of energy. The adult population representing peak bone age were more likely to sustain high energy comminuted fractures, with the older population more likely to sustain a simple fracture regardless of energy. The transitional age noted for clinical fracture behaviour was 14 years old and 56.5 years old.

## 7.1 Staged demineralisation

### 7.1.1 Bone strength

Ultimate stress is a surrogate marker for bone strength. The demineralised segments showed a progressive reduction in pre-yield and yield values. At 48 hours, There was a 53% reduction in strength (ultimate stress) and 44.4% elastic modulus, which implies a greater resistance to bending behaviour. This implies that the intrinsic properties were affected following demineralisation. This process of loss of strength and elastic modulus also occurred in stages at the time points outlined in this study, and therefore this staging process if possible.

This has implications on the wider scope of orthopaedic clinical practice. Burstein et al, in 1974, analysed cadaveric femoral cortical bone of various ages (21 - 86 years old). These were segmented and underwent controlled bend testing. It was found that 70 year old human femoral cortical bone correlated with a 10% reduction in strength and 10-20% reduction in elastic modulus compartment to peak bone age [90]. Yamada et al conducted a similar study, showing a 20% reduction in elastic modulus compared to in a 70 year old femur compared to a peak 35 year old femur [216, 335]. These values correlate with 6 hours immersion in EDTA in this research. The staged artificial recreation of the mechanical values of 70 year old human bone in the laboratory has immense implications. It is a novel finding that can be built on and fine tuned to achieve the required manipulation of bone, which can then be used in fracture modelling. To date, fracture models have been mainly confined for use in vertebral fractures [336], with a significant paucity of evidence in long bone studies. As was evidences in chapter 2, there is copious evidence to suggest that the ageing process significantly impacts on cortical as well as cancellous bone, and therefore long bone fractures are also susceptible to failure due to the accumulation of micro-cracks [337].

Shah et al looked at staging this process but in whole bone in feline femora. Progressively higher concentrations of EDTA were used in order to achieve the desired outcome. It was found that at 20% decalcification, this led to 35% loss in bending strength and 60% decalcification caused 75% loss of strength [282]. This is in comparison to results of this study, whereby with a crude decalcification of 29%, a 54% reduction in ultimate stress was found. The difference in these two results can be primarily explained by the nature of bone tested, ie ovine versus feline. Additionally the use of progressively higher concentrations of EDTA are known to exert their effect primarily on the parosteal surface of bone, as opposed to any effect on the endosteal surface, potentially skewing the results. Furthermore, Shah et al used whole bone, therefore testing extrinsic bone strength as opposed to this clinical study which looked at intrinsic properties, which provides a more accurate understanding of the nano-structure.

Additionally, Burstein et al looked at the idea of bone being a two-phase model ie mineral and matrix. Bone was tested following progressive surface decalcification with hydrochloric acid of increasing contraptions in order to stage the process. This resulted in a reduction in ultimate stress. However, the use of hydrochloric acid also affects the collagen content of bone and therefore it is difficult to correlate these findings with reduction in mineral content alone [164].

Vose et al, in 1959, tested ultimate bending strength using a hydraulic testing device in 25 embalmed human femurs, with ash content measured via x-ray transmission from each femur under load. An exponential relationship was concluded, showing ultimate stress increased with increased ash content of femur. Vose also found that an increase in ash content from 63% to 70% led to a three-fold increase in breaking stress [338]. This was hypothesised to be as a result of appatite “needles” surrounding the collagen fibres, thereby providing a stiffening mechanism preventing collagen from taking much of the load. This relationship can be applied to findings in this study, where a decalcification of 10% over the first 6 hours, led to a 17% change (decrease) in ultimate stress, thereby agreeing with this exponential relationship. This association was significant at the 48 hour stage.

Todoh et al studied the effect of gradual demineralisation on the mechanical properties of bovine cortical segments. This was conducted through immersion of these segments in 10% EDTA, over specific time periods of 12, 24, 48, 72 hours and 14 days. These were dried in a vacuum oven in order to achieve the dry weight. Radiographic measurement of x-ray diffraction was used to assess degree of demineralisation, and were mechanically tested under tension using an Insteon 4411 machine which introduces significant shear. There was a significant reduction (88%) in ultimate stress at 14 days, correlating with a reduced mineral content [339]. This study did not reach such significant demineralisation levels, primarily due the significant differences in methods. The specimens varied in both cross-section (bovine vs ovine), and preparation (no oven drying in this study). A smaller beam with a smaller cross-section, such as that in this study, is inherently stiffer than a longer beam with a larger cross-section. This is due to the concept of second moment of area as described earlier. Furthermore, the oven drying of a specimen removes the structural water mechanical properties. Finally, the method for bending used by Todoh et al introduces a significant shear effect. These concepts lead to the reduced primary ultimate stress and elastic modulus values seen in the control samples compared to this study.

### 7.1.2 Elastic Modulus

Deriving elastic modulus via bending tests is more difficult to assess in comparison to linear tensile or compressive tests. This is partly due to the fact it is intrinsic properties that are being tested as opposed to structural extrinsic properties. That being said, many fractures evident in clinical practice are seen following a bending load, therefore tests performed in this format have a very significant clinical relevance.

This study found mean values of elastic modulus for control specimens of ovine bone to be 11GPa. The values of this study correlate with the values of whole bone human femora and bovine tibia provided by Currey et al of 16.7GPa and 19.7GPa respectively [340], and those provided by Reilly et al in bovine bone of 10.1GPa [51]. The variation in values could be as a result of the methods by which elastic modulus was derived, with specimens in this study being loaded in bending, as opposed to tensile or compression testing as seen in other studies. Load in bending leads to reduced value as loading in a femur is designed to be in the longitudinal plane. Furthermore, the strain rate at which samples are loaded in bending has a significant effect on elastic modulus, with higher strain rates leading to a higher elastic modulus [64, 94].

It was noted in demineralised bone specimens, that with a reduction in pixel intensity of 29%, there was a decrease in elastic modulus of 44% (11Gpa to 6.6GPa). Currey et al has previously shown an association between mineral content in bone and elastic modulus. In a study looking at compact bone of mammal, bird and reptile, Currey was able to show a linear relationship between mineral content and elastic modulus [341]. It is reasonable to apply these findings to this study, however, care should be taken not to apply Currey's conclusions too robustly, given the variation in bone used and the variation in mineral content of each species' bone. Schaffler et al also reported similar conclusions when looking at compact bone in cattle. It was shown that elastic modulus is proportional to the apparent density of bone to a power of 7.4 [342].

Studies conducted on the demineralisation of bone and its effect on elastic modulus and yield are abundant in the literature. However there is a paucity of studies which stage this process. Todoh et al is perhaps the closest to this thesis, however significant discrepancies between this research and Todoh's work exist. Segment size differed in the two studies. A smaller beam with a smaller cross-section, such as that in this study, is inherently stiffer than a longer beam with a larger cross-section due to its smaller second moment of area. Additionally, Todoh oven dried segments, as opposed to thawing at room temperature in this study. Therefore there will be a discrepancy in the structural water content. Finally, the method for three-point bending used by Todoh introduced a significant shear effect.

Previous research has identified the role of the mineral phase and its relationship to elastic modulus accurately, however, no standardised protocol of demineralisation has been created. Studies have also focussed on the extrinsic properties [64], involving different animal models, or have looked at demineralisation through cadaveric bone of varying ages [90, 91]. In essence, studies have often looked at bone at the extremes of the spectrum with extrapolation of data in between [241]. Whilst this work can be extrapolated to fracture modelling, it does not provide a reproducible method to delineate properties of specific bone segments to accurately base a model around.

### 7.1.3 Yield and post-yield

The difference between the yield and ultimate stress of bone are generally relatively small, to the point where it is difficult to distinguish easily on a graph. This applied for both demineralised and decollagenised specimens. The demineralised samples showed a 61% decrease in yield stress at 48 hours.

The values for demineralisation correlate with the findings by Currey et al, who was able to show that strain increased as mineral volume fraction decreased, and that yield stress decreased as apparent density decreased [343]. It is important to note that due to the difficulties in distinguishing a yield point, this was taken as the point at which the stress-strain curve had deviated by a strain of 0.002 from the straight line describing the initial part of the curve.

What is perhaps more interesting is the effect of demineralisation on post-yield values. Currey et al also looked at the effect of demineralisation on post-yield values. Firstly, post-yield stress and strain were shown to follow the same trend in bone, ie if post-yield stress increased, so did the post-yield strain. Secondly, as bone mineral density increased, post-yield values showed a marked reduction, with the opposite trend being shown in decreased density given that this was a negative correlation [343]. It is important to interpret Currey's results with some caution, given that in his studies bone from multiple with a spectrum of bone densities were analysed. Conversely however, Les et al studied the post-yield values in the third metacarpal bone of ten horses. Post-yield stress and strain values were shown to be affected by ash content, with lower values shown with increased ash content [344].

The laboratory biomechanics studies reported in this thesis are in line with Currey's findings, showing a similar pattern, with an increase in post-yield values with increased demineralisation however this was not shown to be significant.

## 7.2 Staged decollagenisation

### 7.2.1 Bone strength

The vast majority of the literature which looks at decollagenisation involves ionising/ thermal denaturation of the organic phase [7, 147, 177, 345], collagen content in aged bone [5, 194, 241], or animal models with collagen disruption [178, 179]. These studies have been explored in chapter 2. The issue with these studies is that they have a defined start and end point, with no continuum of measurements. This makes extrapolation of results significantly inaccurate. It also cannot lend itself to the development of an accurate protocol in orthopaedic fracture modelling or preventative/treatment strategies.

The main way of analysing collagen disruption or deficiency is by looking at the ratio of mineral to collagen, which influences its biomechanical properties. Decollagenisation effectively increases the mineral to collagen ratio. Currey et al built on the work of Vose et al and offered evidence of increased ash content leading to a decrease in ultimate stress. Metatarsals of skeletally immature wild rabbits were impact tested via three point loading.

The findings of Vose were confirmed, showing a rapid rise in ultimate stress with an initial rise in ash content, however perhaps more interestingly, there was a sharp fall in stress at higher values of ash content [158]. This finding can be used to explain the brittle behaviour found in decollagenised specimens with an increased mineral to organic ratio in this clinical study.

Gupta et al also described a model of strain sharing based on the collagen versus mineral and fibril versus extra fibril nanostructures in bone. Gupta was able to show, that in bovine bone, there is a bone hierarchical decoupling that occurs when either entity is compromised. This leads to a tensile load transfer in bone matrix from mineral to collagen. Ordinarily when this composition is healthy, the mineral is design to “damage shield” the collagen by preventing gross deformation through the stiffer mineral construct [346]. It is important to note, that much of this study revolved around principles described by Gao et al, who showed that tissue, fibril and mineral take up successively decreased levels of strain respectively, at a ratio of 12:5:2 [347]. This contradicts an earlier parallel model which suggested that there was equal strain uptake in mineral and collagen phases [348]. Furthermore, Currey was also able to show in multiple bone species, that a decreased mineral volume fraction led to an increase in ultimate strain, hypothesising that this may be as a result of greater load distribution throughout the whole structure as opposed to only near the fracture line [343].

Gao and Gupta’s models therefore, are able to explain the reduction in strain in decollagenised bone specimens. In this study, it was significantly shown that at 5M NaOH there was an absolute reduction in strain to 0.59% (73% decrease compared to control) and at 10M NaOH an absolute reduction in strain to 0.50% (77% decrease compared to control). It can be stated therefore, that in these specimens, as the collagen phase is compromised, there is an increased loading of the stiffer mineral phase which is known to take less strain than collagen. This can also be used to explain the predisposition of fracture in certain bone diseases such as osteogenesis imperfecta, in which the organic content is compromised [166].

With regards to stress, decollagenised bone specimens showed a significant decrease in ultimate stress at both concentrations of 5M and 10M NaOH, being more pronounced in the stronger concentration group. Values were over 70% decrease in stress at 24 hours for 5M NaOH and almost 90% at 24 hours for the 10M NaOH specimens, with a significant decrease in ultimate stress evident at 12 hours onwards for both NaOH concentrations. Given that NaOH is not considered to affect the mineral or ash content, the results presented in this thesis suggest that the two-phase inorganic to organic content ratio was affected. This leads to a proportionally higher mineral to collagen ratio which leads to an "over-stiffening" effect on bone.

Another explanation for the significant decrease in ultimate stress seen in the decollagenised groups is the disruption of collagen cross-links. Knott et al have previously studied the role of collagen on ultimate stress in avian cortical bone. Their detailed biomchemical analysis showed that osteoporosis in avian bone was not simply a loss of apatite and collagen, but rather a decrease in mechanical stress was also due to post-translational modifications such as the intermolecular collagen cross-link profile [349]. Oxlund et al further backed these findings in an animal study of female rat bone, by inhibiting the enzymatic formation of pyridinoline cross-links. They found that a 45% decrease in these cross-links led to a 26% decrease in bending stress. This study also showed a concurrent decrease in both deflection and stiffness in bone [174]. It is possible therefore that changes in the collagen cross-links, could to some extent, account for the stress results reported in this thesis.

Clinical correlation of these results is closest to the effect found in those on long-term bisphosphonates, as both the decollagenisation and bisphosphonate drug treatment processes increase the mineral to collagen ratio. Mashiba et al studied pathogenesis of bisphosphonate induced atypical fractures on dog ribs, and found that the altered tissue repair process as a result of continued suppression of bone turnover rate led to micro-damage accumulation [350]. Ettinger et al explored and found that long term suppression of bone turnover rate led to brittle bone that was susceptible to crack progression and therefore atypical femoral fractures (AFF) [351].

Taken together, these findings suggest that in decollagenised bone, when a load is applied, micro-crack formation occurs at a lower stress, and crack-propagation is more pronounced leading to the significant effect on ultimate stress seen. It is important to note however, that AFF are not as a result of microarchitecture of bone alone. Extrinsic properties of femora are also responsible. Previous studies have shown that whilst bowing of the femur is intended to direct tensile forces to the shaft, over-bowing of the femur may be an accusative factor as has been postulated by Sasaki et al [352]. This was further supported by a study which used finite element analysis to evaluate bowing of femurs in AFF. It found that those who incurred an AFF had excessive tensile stress on the anterolateral surface of the femoral shaft, making these patients high risk for an AFF. The study named this high risk stage as a “Stress fracture of the bowed femoral shaft” (SBF) [353].

### 7.2.2 Elastic modulus

The decrease in elastic modulus of decollagenised specimens differed. At 6 hours in both concentrations of NaOH, there was a significant increase in elastic modulus that was significant. This correlated to a 30% increase at 6 hours in both 5M and 10M NaOH. It can be hypothesised, that the decollagenisation led to a relative hyper-mineralisation of bone specimens at 6 hours. This relative and apparent density increase led to an exponential rise in elastic modulus. Furthermore, the increase in stiffness seen at 6 hours, may arise secondary to the load sharing or “recruitment” of the mineral phase, which has a lower strain and higher stiffness, a vital difference between both phases. Evaluating the literature, this seems to be a novel finding, this finding is supported by Les et al, who suggested a higher elastic modulus is associated with more brittle properties [344].

Traditionally, it is known that mineral content contributes to the stiffness of bone in the elastic phase [354, 355]. However, Burstein et al has also previously shown that plastic deformation of bone is via a mechanism that combines both the elastic-perfectly-plastic behaviour of mineral, and the purely elastic behaviour of collagen [164]. It was hypothesised that the sum of both components would have an effect on the elastic properties of bone, with a deficiency in one leading to a difference in mechanical properties. At time points of 12, 24 and 48 hours in the decollagenised specimens, a significant decrease in elastic modulus was found, more so than that found in demineralised specimens. This was an over 90% decrease at 48 hours in the 10M NaOH concentration.

These findings are backed by several studies. Jonas et al looked at copper deficiency as a cause of impaired collagen cross-links in rat femora. Under torsional testing, he showed a decrease in mechanical properties including elastic modulus [178]. Lees et al studied the cortical tibia and femora of New Zealand white rabbits after feeding them a weight determined dose of B-aminopropionitrile (BAPN), showing an increased collagen equatorial diffraction which correlated with a decreased elastic modulus [179]. Oxlund et al found similar in rat cancellous bone, after daily injection of BAPN [174].

This does however contradict findings by Wang, who attempted to denature collagen in human cadaveric bone, and whilst there was a decrease in elastic properties, this was not as significant, with a less than 10% variation with incomplete denaturation of all collagen [177].

One could also surmise that the affected mineral to collagen ratio seen in decollagenised specimens could act as a surrogate for osteopetrosis. Pathological bone disease such as osteopetrosis is characterised by an overproduction of calcified collagen and failure of bone to remodel during growth. The entire cross-section of bone is composed with poorly organised mineralised bone, which tends to lead to transverse brittle type fracture [356] . Ashman et al studied measured the elastic properties of an osteopetrotic Angus calf. The long bone were segmented and compared to control normal bone segments from another angus calf. Ultrasonic testing was conducted to test the elastic properties, finding that the osteopetrotic bone was less stiff than its normal counter-part [357].

There are few other studies which look at the effects of this bone disease in such detail given the rarity of this condition, and it is difficult to ascertain whether this thesis could support the findings by Ashman et al given the difference in hierarchical level studied. However, the macro-structural mechanical changes that occurred with Ashman et al, give baseline values on which the results of this thesis can be correlated with.

### 7.2.3 Yield and post-yield properties

Yield stress of the decollagenised samples was significantly reduced (71% and 82%) at 24 hours for 5M NaOH processed specimens and 12 hours for 10M NaOH specimens respectively. For yield strain, there was a significant increase of 28% at 48 hours for demineralised samples, and a more pronounced significant decrease at 24 and 12 hours for both 5M and 10M NaOH. This was expected given the values for ultimate stress.

The values shown for decollagenised bone specimens varied substantially to that seen in demineralised bone. Post-yield values for these specimens were close to zero at the 48 hour stage, with a 96% reduction at 48 hours in 5M NaOH and a similar value even earlier in the 10M NaOH samples (24 hours). Wang et al, in his study, denatured human femoral cadaveric bone through thermal means. The post-yield values were shown to reduce significantly at greater temperatures with values close to zero at 200 degrees celsius [177]. Zioupos et al also studied human cadaveric bone and the ageing effect on post-yield values. There were also found to be decreased. Zioupos hypothesised that “pre-failure” post-yield mechanisms were related to bone toughness which have traditionally been attributed to collagen [7]. However factors such as micro-crack formation and crack-bridging (which are affected by collagen) also need to be considered.

Decollagenisation seemed to have a greater effect on post-yield values than in demineralised samples. Toughening mechanisms are likely crucial in this pre-failure stage.

## 7.3 Ductile to brittle transition

A material that shows increased post-yield strain following is thought of as ductile, with the opposite being true of brittle behaviour.

In demineralised specimens, ductile behaviour was demonstrated, with a significant increase of 51% ductility at 24 hours. In decollagenised specimens, the opposite behaviour was observed, with over 40% reduction in ductility significant at 24 hours onwards. In effect, this study has shown a tendency for demineralised bone to exert increased ductile behaviour, with increased brittle behaviour in decollagenised bone. This ties in with the literature showing hyper-mineralised bone being associated with brittle properties.[5, 64] [358]. Currey et al observed the tympanic highly mineralised bulla of the fin whale (Balaonoptera physalus) compared to ones from other species with mineralisation of varying degrees. It was observed that there is a critical level at which bone with increased mineralisation begins to behave differently, specifically in a more brittle manner as observed in this thesis. This is in contrast to peer antler which has a relatively low mineralisation, having a very high work to fracture. It forms a “U” shape but does not fracture under high stress. In humans, the best example would be the ossicles of the ear, which are highly mineralised and exhibit brittle failure, however this is less likely given their intracranial position with less load transfer.[359] This becomes relevant in fracture prevention strategies, particularly with the use of bisphosphonates. Allen et al showed beneficial effects of these on fracture risk for 2-5 years, after which the relative hypermineralisation may make bone more susceptible to brittle fracture [360]. Additionally, there seems to be a confounding factor of lack of remodelling as a result of this medication.[361]

Zioupos et al studied bone segments of cortical mid-diaphysral bone in ageing human femora, and under three-point bending extrapolated ages at which ductile to brittle transition seemed to occur. This was found to be at age 55 years old in females and 70 years old in males [147].

The transition from ductile to brittle behaviour was associated with a 45% reduction in the deformation seen in bone prior to failure, with a reduced or absent plastic phase in the brittle bone. This 45% reduction in ductility in Zioupos' study, correlates with the results of this study, where a similar reduction in ductility correlated to 24 hours immersion in both 5M (43% reduction) and 10M NaOH (42% reduction).

## 7.4 Toughness

This study has demonstrated that toughness in demineralised specimens increased significantly by 35% at 24 hours. Previous work by Currey et al has shown that mineral does have a relationship with fracture toughness, with low mineral deer antler bone showing a higher toughness, as opposed to the highly mineralised ear ossicle bone, which are more brittle [362]. Further work by Zioupos in 1996 assessing ash content on bone mechanical properties showed that there was a negative relationship between ash content and bone toughness [5]. Additional work to support these findings in polar bears was carried out by Brear et al [363], and Currey et al, who both showed that in bone of various species, highly mineralised segments showed increased elastic modulus but decreased strain to failure [337]. This is however in contrast to work by Wang et al, who analysed crack propagation, a marker of bone toughness in baboon femora of varying ages. He noted despite no significant changes in bone mineral density in the older bone, fracture toughness and micro-hardness both decreased, concluding that the mineral phase alone is not responsible and other factors at play [6]. This was also supported by Wallace et al, who demineralised ovine who whole femora, and mechanically tested, finding that at a slow strain rate, there was minimal change in strength, but that fracture toughness was more reduced in the demineralised samples [64]. Wallace deduced that other processes were likely affected, particularly collagen.

In the decollagenised bone specimens, there was a uniform reduction of bone toughness over time, with 5M NaOH samples showing a significant 48% decrease at 24 hours and a more pronounced reduction the 10M NaOH, with an 80% decrease at 12 hours.

Currey studied the effect of collagen on bone toughness. By looking at irradiated human bone used for allografting, a marked reduction in toughness was seen in the highly irradiated bone. Irradiation has been reported to affect the collagen network but to have little effect on the mineral [345]. Other work on the effect of collagen on bone toughness has been performed by Wang et al, with thermal denaturation of human cadaveric femoral cortical segments which underwent mechanical testing [177].

Clinical this has significant translational implications. Burstein et al, in 1974, analysed cadaveric femoral cortical bone of various ages (21 - 86 years old). This bone was machined into segments and following mechanical tesing, it was found that 70 year old human femoral cortical bone correlated with a 40-50% reduction in toughness [90]. In this study, this would require processing in EDTA for >48 hours, or 24 hours in 5M NaOH. 10M NaOH would not be suitable given the significant loss of toughness achieved between 6 and 12 hours (3% to 81%). This again has significant positive implications for translational research, as this thesis has shown a protocol where a percentage reduction in staged fashion could be achieved.

However it remains important to note that collagen alone, whilst providing a toughening mechanism in itself, is one part of a group of mechanisms. such as micro cracks and crack-bridging for which collagen cross links are required. This is in addition to the toughening mechanisms provided by enzymatic and non-enzymatic cross-linking as explored in the literature review.

## 7.5 Clinical findings

### 7.5.1 Epidemiology

The incidence of paediatric femoral shaft fractures was found to be 3.5 per 100,000 person years, and in adults 11.5 per 100,000 person years. Total population incidence stands at 14.9 per 100,000 person years. There was a bimodal distribution of simple fracture pattern in paediatric and older adult age groups, with a unimodal distribution of comminuted fractures in adults. There was a similar bimodal distribution of low energy fractures simple in paediatric and elderly ages, with a unimodal comminuted high energy mechanism in adults. Elderly females were a specific high risk group, with the majority sustaining low energy simple fractures. Conversely, adult males were more likely to sustain a high energy comminuted fracture.

The incidence of femoral shaft fracture found in this study is within the ranges in the literature (9.65 - 21 per 100,000 person years) [223, 303, 304, 307, 364, 365]. The main studies in the literature have a similar demographic and therefore the incidence is more closely related to those studies. However, Enninghorst et al, in a prospective study in an Australian trauma centre, identified 136 femoral shaft fracture in one year, giving an incidence of 21 per 100,000 person years [365]. There is obviously a significant discrepancy between Enninghorst's work and this thesis. Enninghorst's work included the paediatric population, as opposed to just adult in previous studies. Furthermore, there is a significantly larger population within their catchment area compared to that studied here (850,000 vs 545,000). There is also support for Enninghorst's work in another study from Rochester, where an incidence of 19 per 100,000 person years was shown [307].

A bimodal distribution of femoral shaft fractures was also seen, particularly in the very young (<2 years old) paediatric population and the elderly population. This can be seen in Figure 34. This is contrary to that seen by Benger et al, who showed peaks for high energy young males and low energy elderly females [305]. This was also supported by Enninghorst et al, who showed bimodal peaks for 21-30 year olds and 81-90 year olds [365].

There was no overall gender discrepancy. When analysing the sub-groups however, the majority in the paediatric (30 males v 8 females) and young adult population (27 males vs 10 females) were male. This is in contrast to the older population, of who the majority were females (67 females vs 21 males). This is supported by Salminen et al in an adult Scandanavian population study where the highest age and gender specific incidence were seen in males of 15-24 years old and females over 75 years old [303]. However, this was contrary to work by Enninghorst et al, who found that 65% of males sustained a femoral shaft fracture in a total population [365]. Therefore, it is likely that epidemiological incidences in Western Europe such as Scandanivia and the United Kingdom, differ significantly to those in Australia and the United States, where the rates are not comparable.

### 7.5.2 Clinical implications of biomechanical study

If age is considered to be a surrogate for bone quality, the results of the mechanical tests in this study may explain the findings of the clinical study. The premise for the interpretation of the results lies in the assumption that demineralised bone samples represent paediatric bone, control bone samples represent peak adult bone age, and decollagenised specimens represent older osteoporotic bone.

It has been established that peak bone mass is reached around the third decade of life, which forms the basis of the working assumption of an adult group as a surrogate for peak bone density [366]. Furthermore, it is likely peak bone-age has double the bone mineral density to that following the age of 50 years old [367]. This is as a result of optimised mineral to collagen ratio, with increased mineral resulting from both an increase in mineral content in bone mineral units, as well as an increase in bone volume as a result of elongation of long bones through endochondral ossification [368]. Results of this study showed that the adult group suffered more high energy comminuted fractures and this was significant. This is directly associated to the control values in this study, which are uniformly higher than those in demineralised and decollagenised samples. Ultimate stress (surrogate of strength) values were between 170 - 190 MPa in control values, whereas these are as low as 90MPa (48 hours EDTA), 39MPa (48 hours 5M NaOH) and 4MPa (48 hours 10M NaOH).

Yield stress values followed the same trajectory as ultimate stress values above. This is important as this means that the energy required to achieve yield is lower in demineralised and decollagenised bone.

This is particularly relevant in the older age population, the majority of whom sustained a low energy mechanism fracture. The mineral and collagen phases are both affected in ageing bone. The yield point is therefore achieved at a lower energy (low strain model), and therefore plastic deformation occurs at a lower energy. If this bone is less tough, then it is easy to see how elderly osteoporotic bone would fail at a lower energy.

It has previously been explored by Wallace et al, at a low strain rate, that demineralised bone has a reduced toughness to normal bone [64]. This study has shown that the decollagenised specimens had a significantly reduced toughness, almost to 100% in the 10M NaOH specimens. This can explain the discrepancy found in previous demineralisation studies, particularly at low strain rate. This thesis has also demonstrated that in both demineralised and decollagenised bone, the elastic phase, young's modulus and yield stress are reduced as a result of these processes. In the decollagenised specimens, post-yield properties are almost zero - implying a more brittle type failure, whereas in the demineralised specimens, there was an increase in post-yield properties, implying a ductile mechanism of failure. This can be directly used to explain results seen in the clinical section, whereby the adult bone age is more likely to be ductile, and has a much higher ductile to brittle transition threshold. Therefore the main way to reach this threshold is through a high energy mechanism, which is more likely to lead to a comminuted fracture as evidenced in the results. Conversely, elderly bone has a much lower ductile to brittle transition threshold, with a lower energy required, and when that energy is reached, a brittle simple fracture occurs.

This is also relevant to fragility fractures, as can occur in elderly or osteoporotic bone. Fragility fractures are different to pathological or stress fractures as they occur after a load is applied onto bone with an abnormal elastic phase [369]. Furthermore, traditionally the approach to fragility fracture theories has been through approaching it via an energy or a stress mechanism. It remains incompletely understood primarily due to the difficulty in interpreting energy changes during a compression type fracture, which occur as a result of reduced bone toughness, as seen in the decollagenised segments [370]. Compression fractures result not along the lines of maximal stress as in tension fractures, but rather once a crack is initiated, it may propagate obliquely along osteons [370, 371]. Clinical examples of such fractures include vertebral bodies, sacral and pubic rami fractures. On occasion, axial loading of long bones may produce a compression type fracture such as that seen in a buckle in the paediatric population as explored above. Both types of mechanical failure occur on the compression surface and can be thought of as age related compression fractures [372, 373]. Elderly osteoporotic bone is likely to behave in such a way as a result of reduced organic content, which markedly reduces the toughness [5]. The decollagenised samples correlate more with a clinical picture of insufficiency brittle fracture seen in clinical practice in osteoporotic bone or can be as a result of ageing as described by Zioupos et al [7]. In both demineralised and decollagenised segments, the strength and yield stress of bone is markedly reduced. As both processes are disrupted in osteoporotic bone, this is likely to have an additive effect compared to paediatric bone.

### 7.5.3 Paediatric bone failure

The paediatric population displayed a predominance of simple fracture, which was a surprisingly similar finding to that in the elderly population. This was despite an even distribution in mechanism energy. This is perhaps a surprising findings which implies that bone behaviour is altered to allow this to happen. Demineralised segments were used as a surrogate for paediatric bone, where bone has not reached adequate mineralisation compared to peak bone age. Furthermore, it is known that between the ages of 2 and 20 years old, bone mineral density shows a direct linear relationship each increased year of age [374]. It is important to note that the majority of paediatric fractures occurred in those under 2 years of age, and there was a predominance for low energy simple fractures in this sub-group. The collagen phase is therefore proportionally higher in this age group.

The demineralised samples showed a reduced yield point and strength but increased ductility and toughness. This is helpful in explaining why in a fracture such as a greenstick fracture, the tension side fails but the compression side plastically deforms. The mechanical interpretation of this would be an increase in the plastic phase, with higher plastic energy dissipation during fracture [375]. This is part of the reason why in paediatric bone, plastic deformation in a forearm can occur, which is not usually seen in the adult or elderly populations. It also helps to explain greenstick fractures, where the convex tension side fails with plastic deformation of the concave compression side.

However this does not fully explain why the compression side does not fail entirely, or why a buckle compression fracture occurs. This is unlikely linked to demineralisation or decollagenisation in isolation and the findings of this thesis fails to explain these fractures entirely. Rather, such fracture patterns are thought to occur as a result of the immature/ mature cross link ration in paediatric bone. Berteau et al looked at this ratio in paediatric fibular fractures. Seven cadaveric paediatric fibulae were compared to three elderly fibulae. There were mechanically tested using three-point bending as well as biochemically analysed for quantification of cross-links. A greater degree of plastic deformation was seen, and this was thought to occur as a result of greater ratio of immature cross-links compared to adult bone. Bone with a greater ratio of immature cross-links was shown to be able to plastically deform to greater degrees under stress [376]. This correlates with the compression surface, which is under less stress than a tension surface, being able to withstand greater deformation.

In a buckle fracture, the compression surface fails. This is likely to do with bone location, being a metaphysical injury, as well as type of load applied (axial). Trabecular bone can withstand much greater strains than cortical bone, exhibiting greater viscoelasticity [36, 94]. The aim of this thesis was not to study compression failure, however given this finding in the results, it has formed an important discussion point around an area which shows a distinct lack of biomechanical research in clinical practice. The process is likely multifactorial and as of yet not clearly understood.

### 7.5.4 Transitional change

Perhaps one of the most interesting findings is the quantification of how much age contributed to fracture pattern in this study. Adult bone was used as the clinical “control”, with the assumption that this correlated to peak bone density.

When comparing fracture patterns in paediatric versus adult age groups, it was found that age alone accounted for 44.4% of this variation. Similarly, age was found to account for 33% of variation in fracture pattern between the older and adult age groups. These were both significant findings as there is a distinct lack of clinical correlation of physiological age with bone behaviour in femoral shaft fractures in the literature. The higher contribution of age in the paediatric age group compared to the older group is possibly as a result of higher number of comorbidities in the elderly population, leading to greater number of confounding factors. This is in comparison to a healthier paediatric population with less comorbidities and therefore a “purer” age contribution.

By applying receiver operating characteristic curves, ages at which bone behaviour seemed to change were identified and this could predict likelihood of certain fractures in each age category. The paediatric age of 14 years justified the arbitrary cut off of 16 in this study. Similarly, the older age of 56.5 years justified the arbitrary cut off of 55 in this study. It is however important to note that the cut off values were based on a balance between high sensitivity and low false positive rate. This interpretation can be operator dependant, with other interpreters possibly valuing a lower false positive rate in return for the sacrifice of a reduced sensitivity.

When analysing the literature for correlation to these findings, there is a discernible lack of evidence. There are epidemiological studies which have looked at the distribution of femoral fractures in various populations as discussed in the literature review, however, the study of physiological age, energy and fracture pattern in the format laid out in this study is not known, and this is considered a novel finding in the literature.

## 7.6 Limitations

It is likely that load orientation played a significant role in stress results seen. It is known that the femur resists vertical compressive loads better than it does horizontal bending. In four-point bending, bone is loaded at at right angles to the longitudinal direction encountered in most activities of daily living and this may account for the low ultimate stress values seen in this study. This is particularly evident in the 10M NaOH group, where a final mean ultimate stress value of $4N/mm^2$ was seen, almost a 100% decrease at 48 hours. Furthermore, bone can fail in a multitude of ways, which includes shear, torsion, or a combination of these loads in tandem. The results of this thesis should be utilised for bending loads only, and are not generalisable for all failure mechanisms.

Much of the previous literature has validated the use of EDTA and patterns observed with regards to effect on density and mechanical properties, however it is not definitively clear with regards to NaOH. As explored in the literature review, it is not likely the mineral phase is affected in such a solution, and this was crudely measured using pixel intensity as a measure of density/mineralisation. However, further validation of the method is required with histological sampling of these bone specimens. This would provide the scientific community with further qualitative/quantitative effects of NaOH on both the mineral, collagen, collagen cross-link and water contents. Histology would be more reflective of the ultra-structure of bone. Any change to the structural water content would have effects on the viscoelasticity. This would ordinarily require histology to visualise accurately. The use of confocal laser microscopy has become more common to reconstruct 3-dimensional images akin to histology (which is 2-dimensional). This is an optical imaging technique by means of a pin-hole, which blocks out other light, increasing the optical resolution and micrograph of a section. Multiple images at different depths are possible and these can be reformatted into a 3-dimensional image.

The free-hand cutting of bone segments using the methods outlined could have potentially led to notching or micro-crack formation on cortical bone surface. This could also have occurred with periosteal stripping, however this is less likely given this was done via a peeling mechanism and no sharp instrumentation used. Any notching on the surface could have a significant effect on the mechanical properties, particularly in the decollagenised

segments, in which reduced limitation of crack-propagation occurs and therefore reduced toughness. Any notch would therefore have a confounding effect.

A further limitation of this study, and in particular mechanical testing, is the assumption that mechanical properties of decollagenised and demineralised samples is due to the bony response alone. It was out-with the remit of this thesis to study the effects of soft tissues on the mechanical results seen. It is well known that the soft tissues surrounding bone has an influence on both the magnitude and direction of force. This is particularly applicable to the periosteum, Previous ovine studies have shown the femoral periosteum contributes positively to both the elastic modulus and anisotropic effect of the femora shaft [377]. This effect is likely to be amplified in paediatric patients who have a thicker periosteum, and is uncalcified unlike those in the osteoporotic population [378]. The effect of the periosteum in paediatric bone should not be understated, as this thicker structure must fail along with the more ductile bone in order for the bone to fail. Additionally, this is an important structure for fracture reduction and stability. This is particularly true to fracture of the forearm in children [379]. The periosteum, for the purposes of this thesis was therefore removed in order to standardise the cortical bone segments, and therefore the results should be interpreted with this in mind.

Finally, it is inaccurate to simply use physiological age as a surrogate for bone quality. There is no clear consensus in the literature to suggest this is the case. However, the use of ROC curves to delineate changes in bone behaviour did yield results which justified the age cut-offs used in this study.

## 7.7 Future work

It would be helpful to analyse more specifically the effect of sodium hydroxide on the micro-structure of bone and its effect on both the collagen content and its effect on collagen fibril orientation. Light-based imaging techniques such as confocal laser scanning microscopy can give information on the water, cross-links, collagen and mineral phases in 3-dimensions within the bone specimens being tested.[380] Orientation-based techniques such as polarised light microscopy are useful to study the effect of sodium hydroxide on the orientation of collagen fibrils.[381] These techniques can also be utilised to measure any effect, if any, the sodium hydroxide has on the mineral crystals which may have confounded the findings of the study. This is in addition to the histology which is suggested in the limitations.

Future studies should apply the laboratory methods of this study onto whole ovine femoral bone via cyclic loading of bone in varying solutions to achieve the required fracture model to be studied. Bone segments will behave differently to whole bone as intrinsic properties of bone segments are amplified. It would be essential to measure the extrinsic properties of bone to see if the results of this thesis translate to a macro-structure. Furthermore, once cortical bone testing has been exhausted, attention should be switched to the effects of demineralisation and decollagenisation on trabecular bone, particularly the neck of femur, given the frequency of this injury in the elderly.

Another area of future work would be to assess the degree of compression versus tension failure in decollagenised specimens. In this study, slow video was taken to assess which surface failed first under slow loading. A potential solution to this would be micro-computed tomography. This would allow the measurement of stepwise rather than continuous measurement of compression. A micro-compression device can be used to image the loaded specimen directly in the micro-CT scanner. Successive increased loads can be applied to allow dynamic failure assessment of bone at a low strain rate.

Given the anisotropic and load-dependant failure variation in bone, one final area that should be studied is the effect of high strain rate on decollagenised specimens. Toughness is rate dependant, and this would allow quantification of the effects of a higher strain rate on bone mechanical properties.

## 7.8 Conclusion

Decollagenised cortical bone behaves as a brittle material at low strain rate, with reduced mechanical properties at all stages, including toughness. However, with increased decollagenisation there is a two-phase stiffening process, whereby there is an initial compensatory increase in stiffness followed by a progressive decrease. Post-yield properties are almost zero with greater rates of decollagenisation, directly relating the role of collagen to this pre-failure stage. Failure at the compression surface was noted at the extremes of decollagenisation under a low strain bending load. Demineralised bone was found to have reduced pre-yield and yield properties, however behaved as a more ductile material with increased toughness.

Femoral shaft fractures in this British population show a bimodal distribution with low incidence, and a double peak in the very young (under 2 years of age) and elderly age groups, with elderly females being most at risk of this injury. Until age 14, a simple fracture is more likely to occur. Between the ages of 14 to 56.5, a comminuted fracture is more likely to occur. After age 56.5, a simple fracture is more likely to occur.

# 8. APPENDIX

## 8.1 Appendix A - Force deflection graphs

### 8.1.1 EDTA Control trials 1 - 5

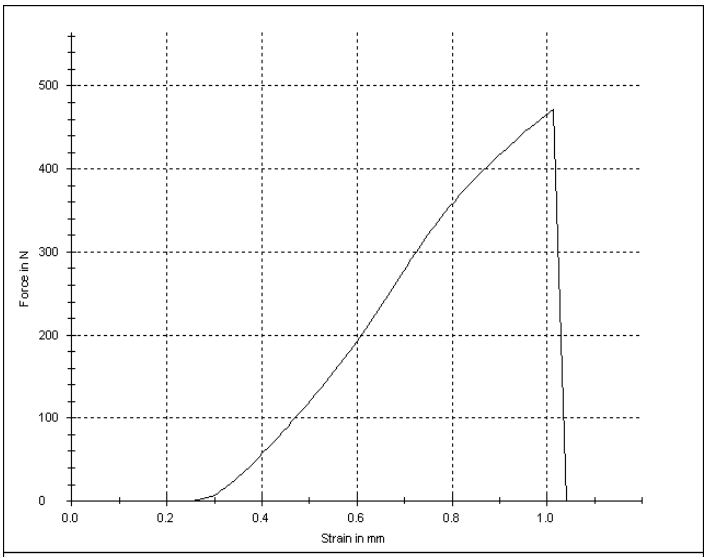


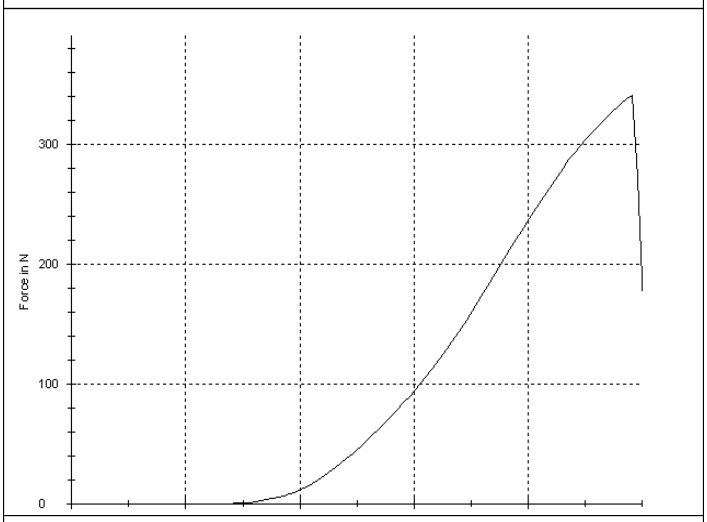


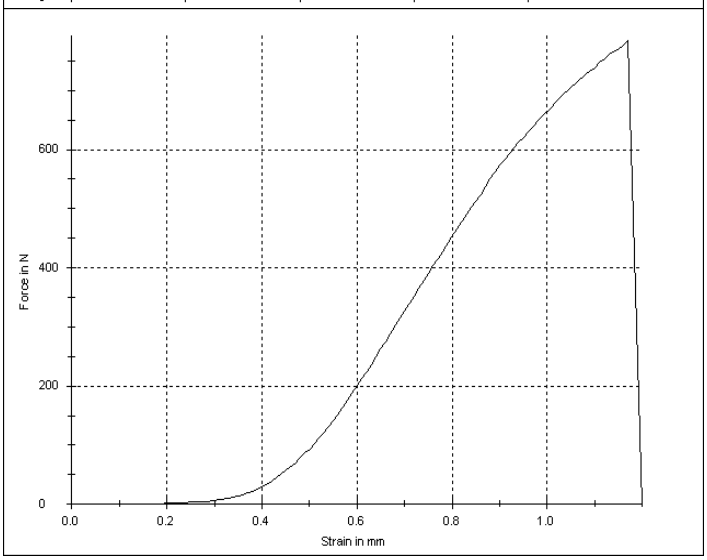

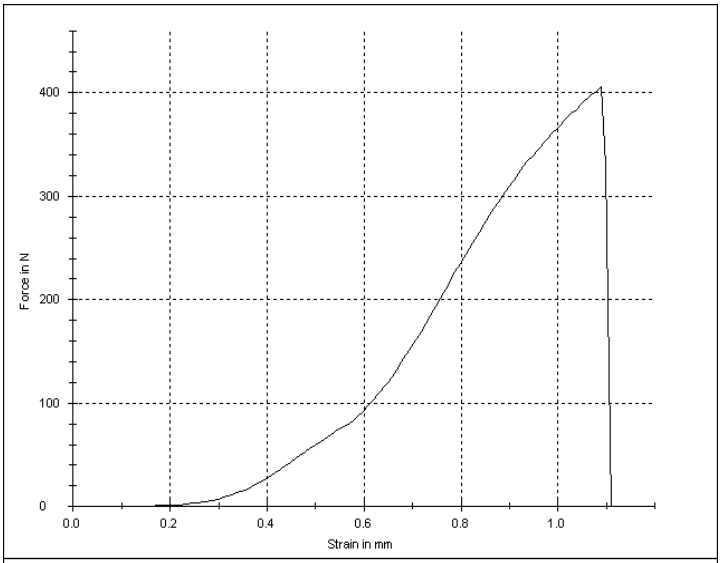
Force in N
400
300
200
100
0
0.0
0.2
0.4
0.6
0.8
1.0
Strain in mm

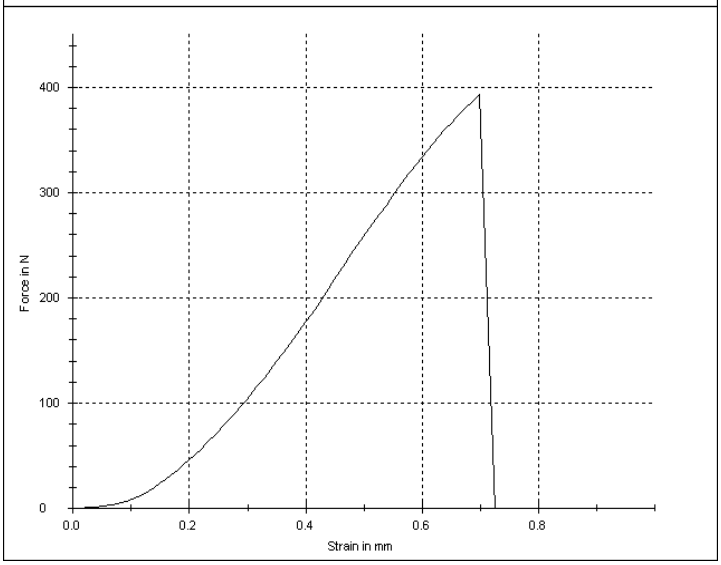
Force in N
400
300
200
100
0
0.0
0.2
0.4
0.6
0.8
Strain in mm

## 8.1.2 EDTA 6 hours trials 1 - 5

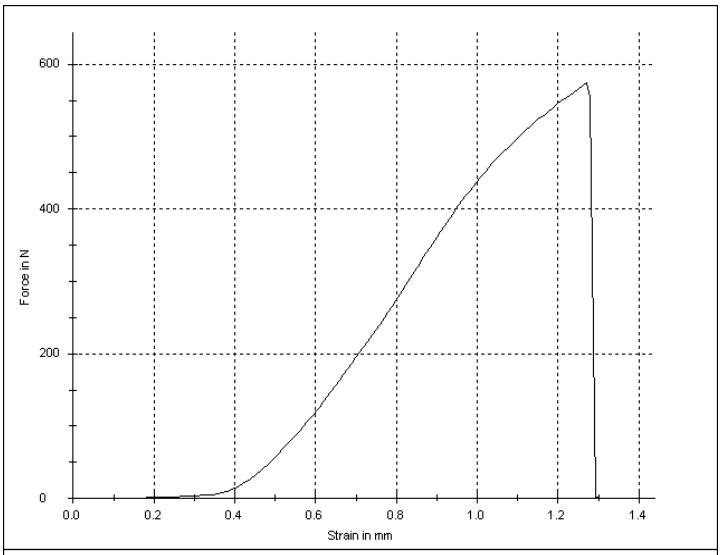


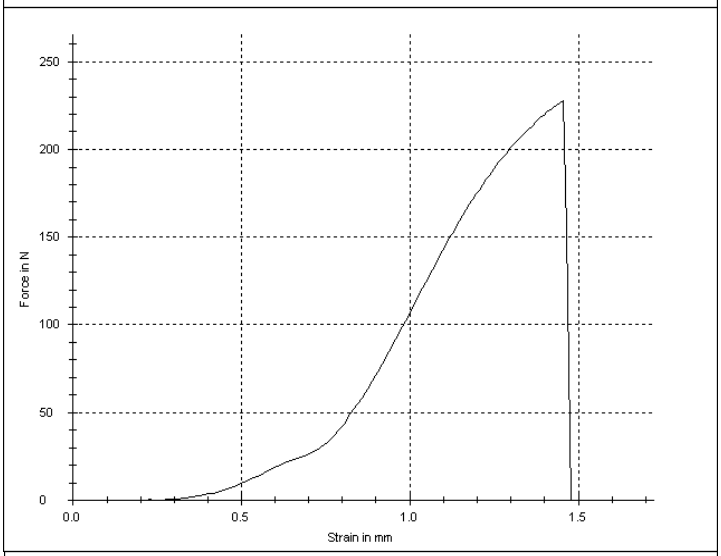


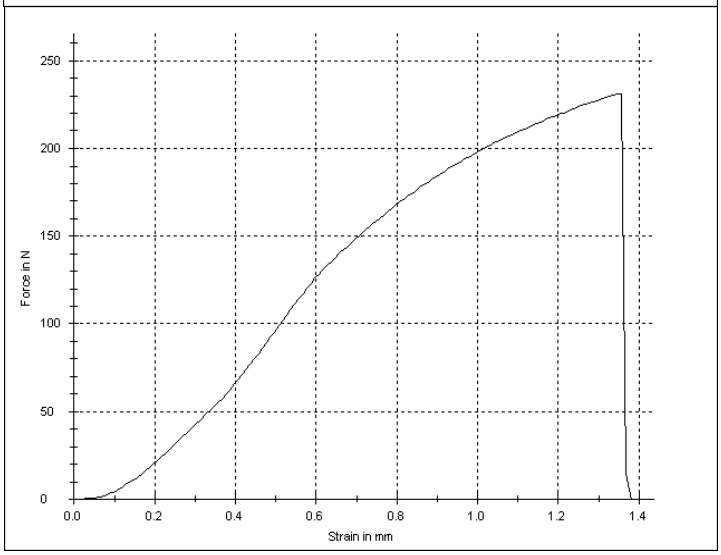

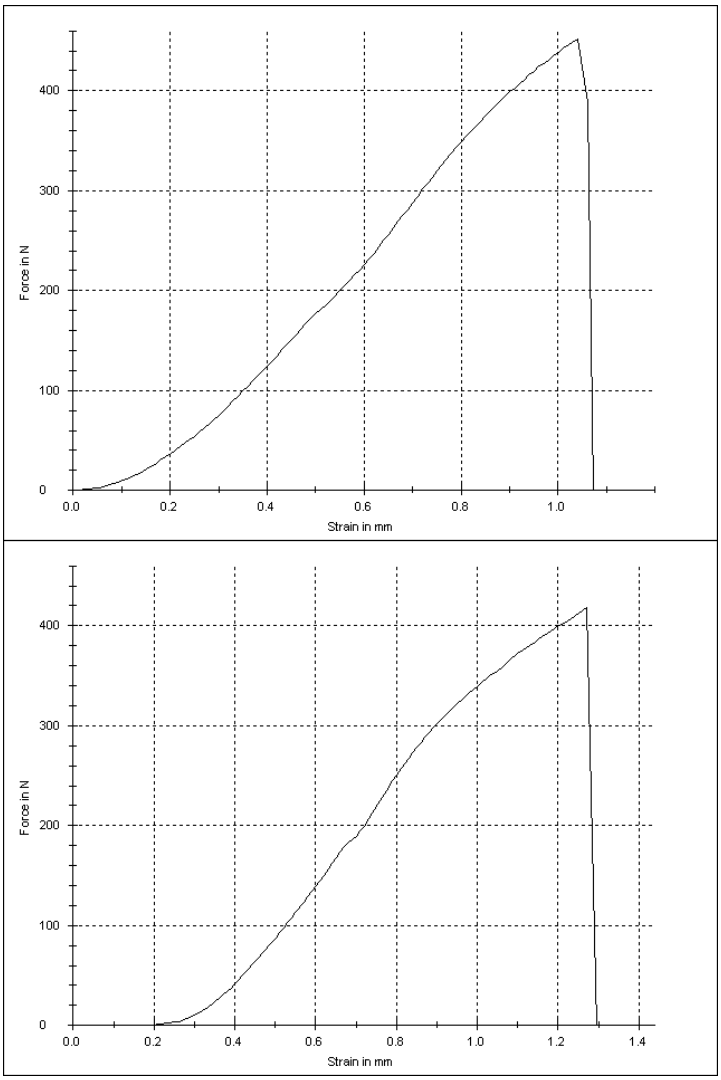
Force in N
0
100
200
300
400
0.0
0.2
0.4
0.6
0.8
1.0
Strain in mm
Force in N
0
100
200
300
400
0.0
0.2
0.4
0.6
0.8
1.0
1.2
1.4
Strain in mm

## 8.1.3 EDTA 12 hours trials 1 - 5

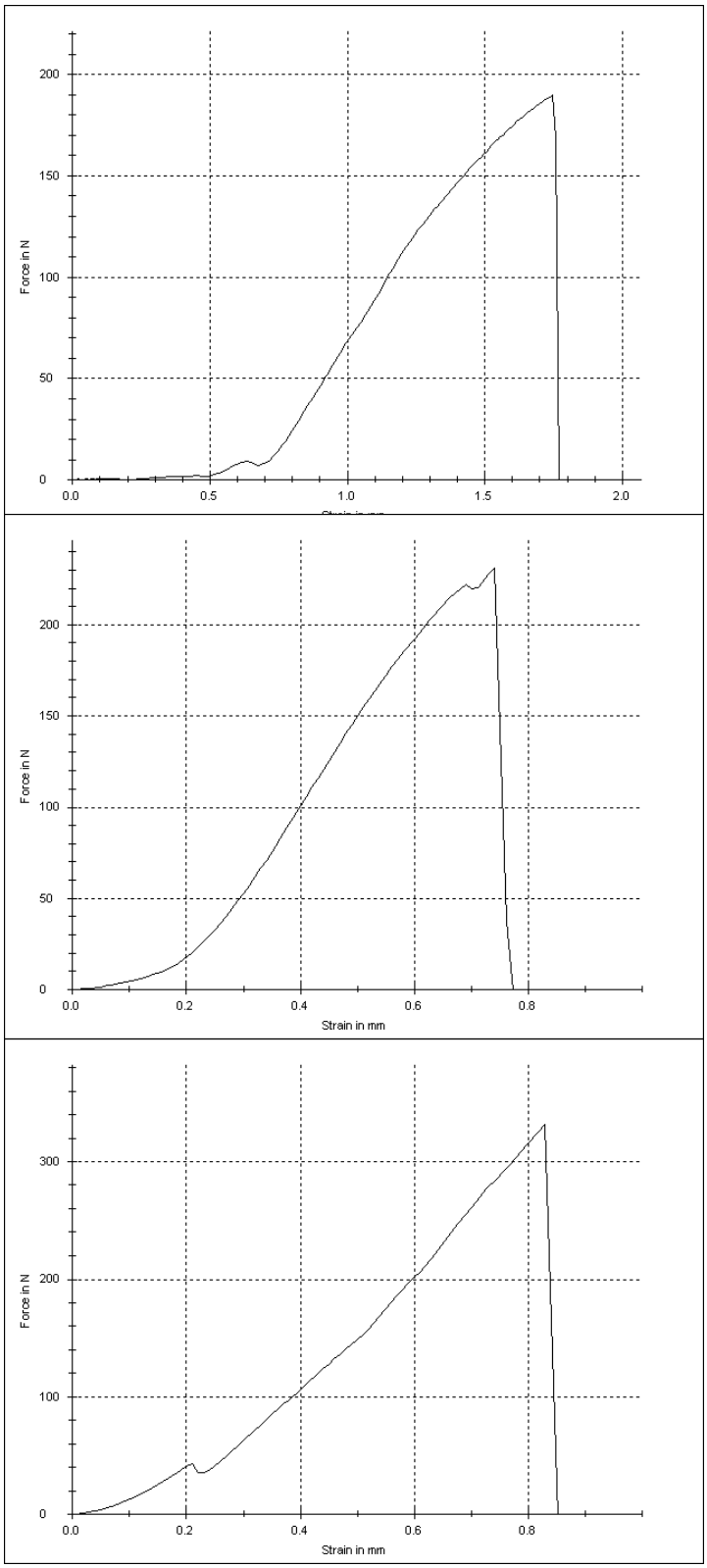

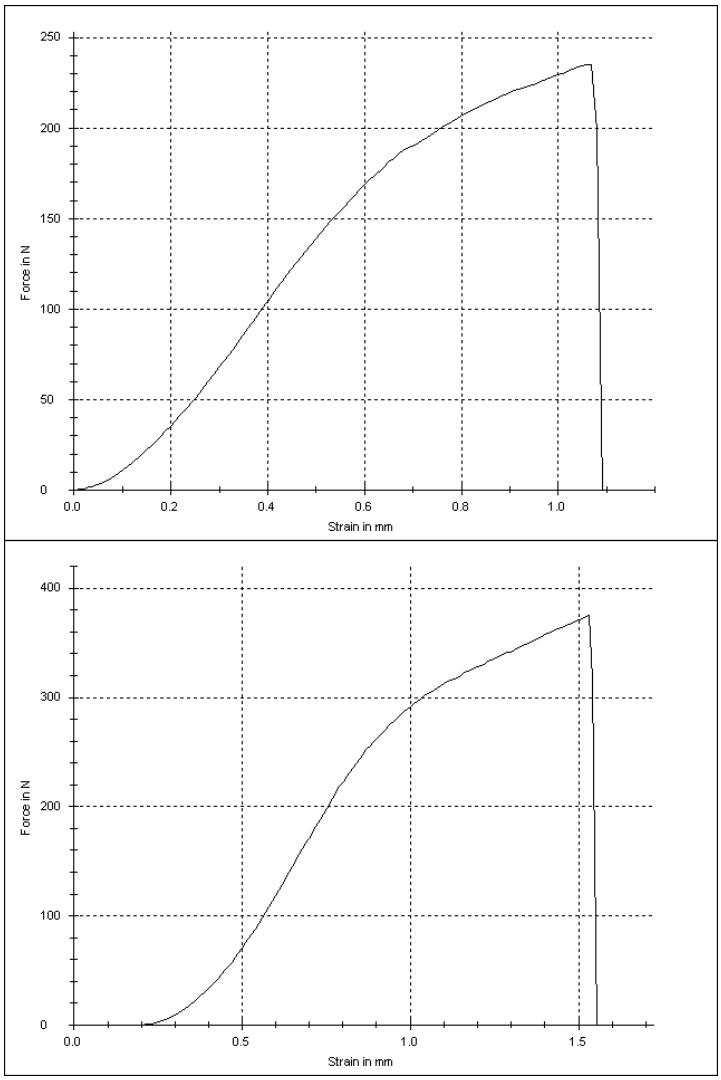
250
200
150
100
50
0
Force in N
0.0
0.2
0.4
0.6
0.8
1.0
Strain in mm
400
300
200
100
0
Force in N
0.0
0.5
1.0
1.5
Strain in mm

## 8.1.4 EDTA 24 hours trials 1 - 5

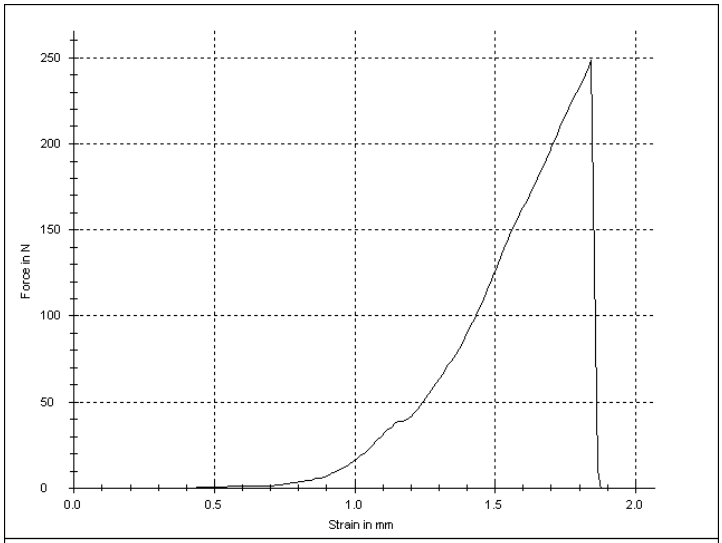


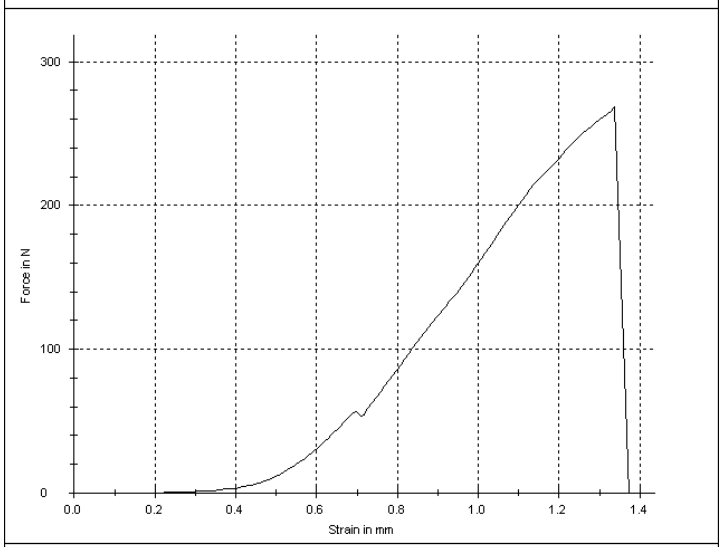


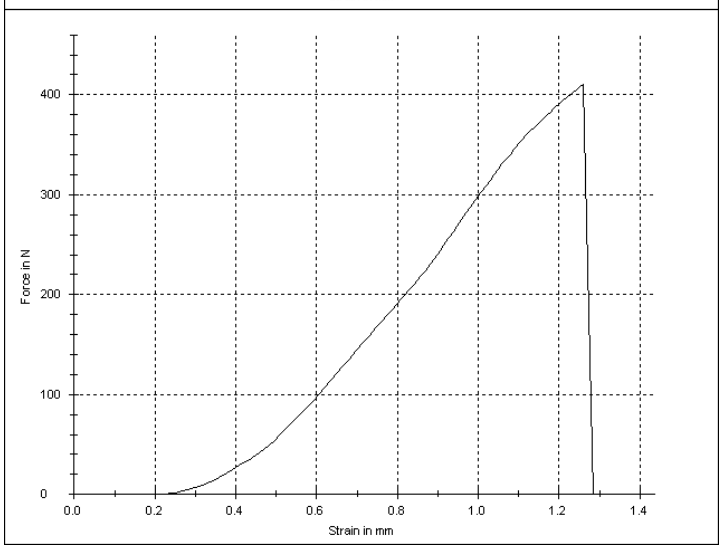

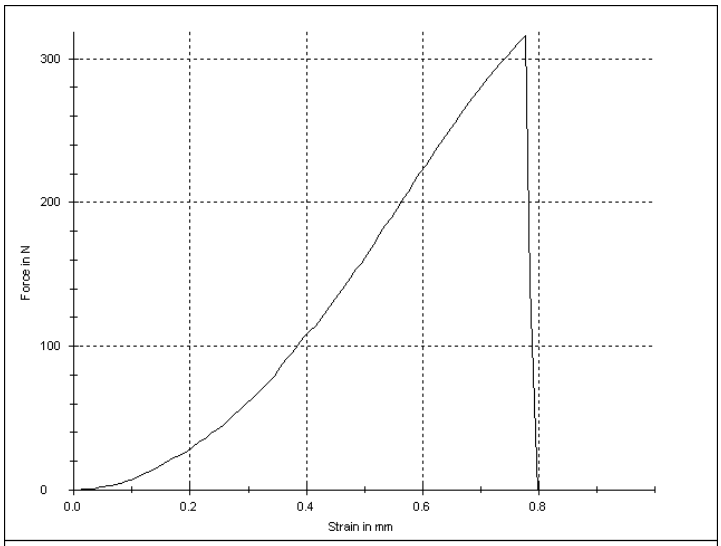
300
200
100
0
Force in N
0.0
0.2
0.4
0.6
0.8
Strain in mm

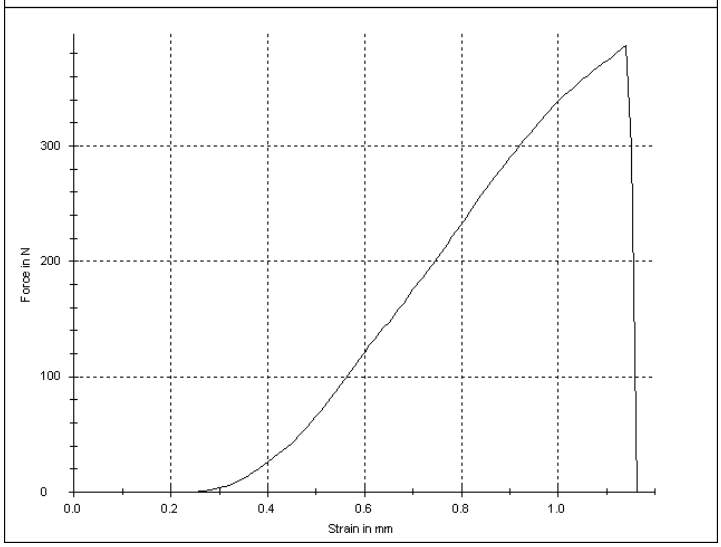
300
200
100
0
Force in N
0.0
0.2
0.4
0.6
0.8
1.0
Strain in mm

## 8.1.5 EDTA 48 hours trials 1 - 5

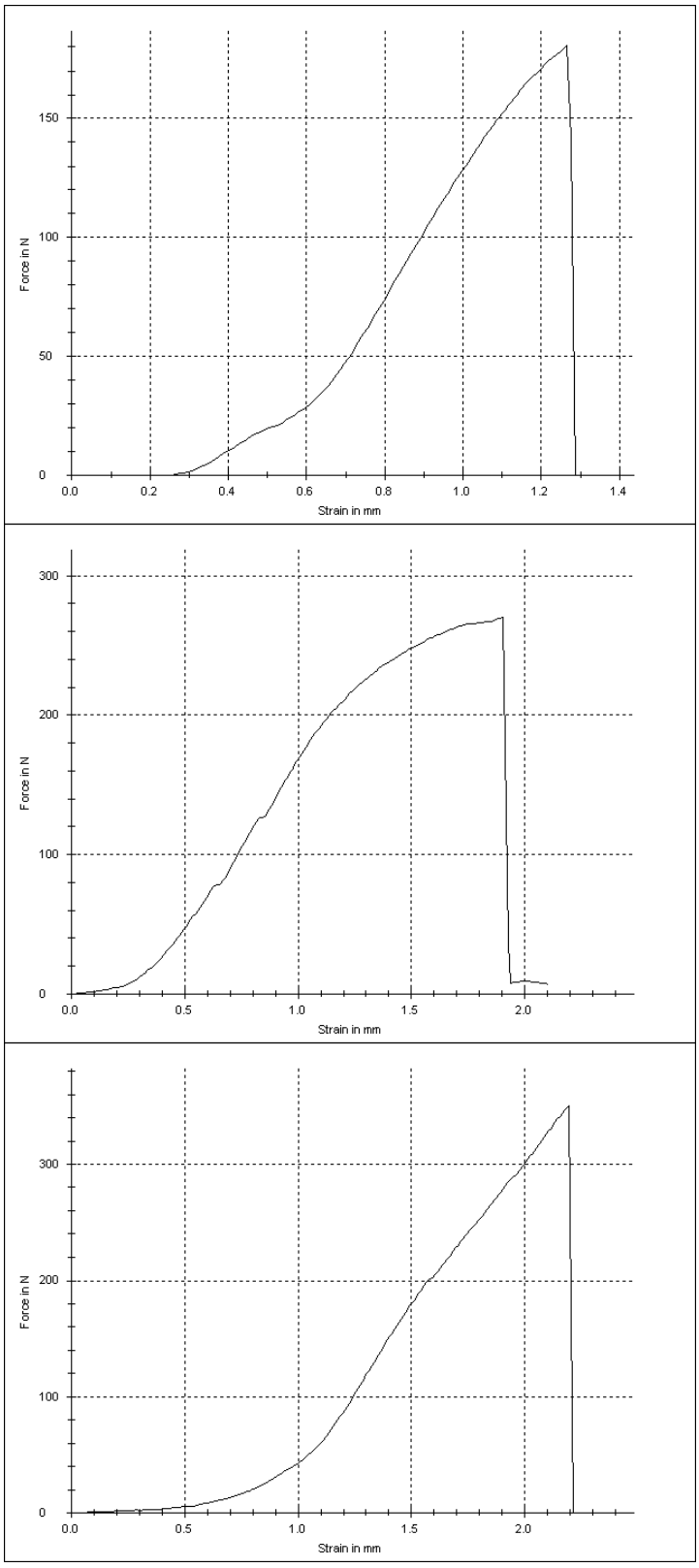

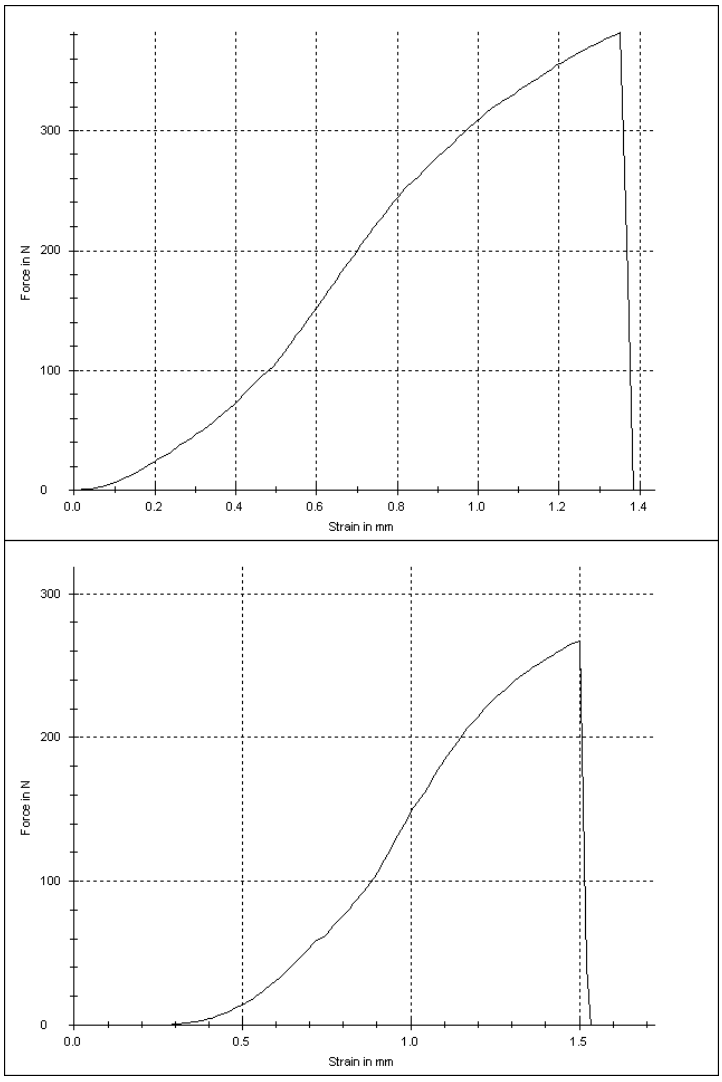
300
200
100
0
Force in N
0.0
0.2
0.4
0.6
0.8
1.0
1.2
1.4
Strain in mm
300
200
100
0
Force in N
0.0
0.5
1.0
1.5
Strain in mm

## 8.1.6 5M NaOH Control trials 1 - 5

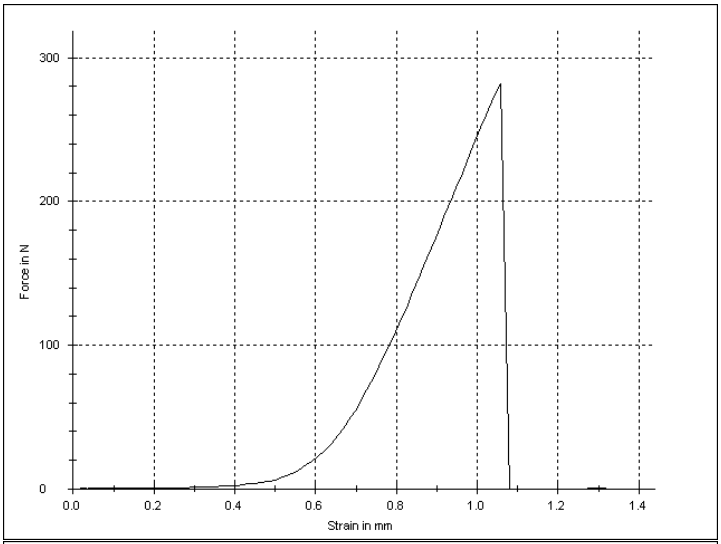


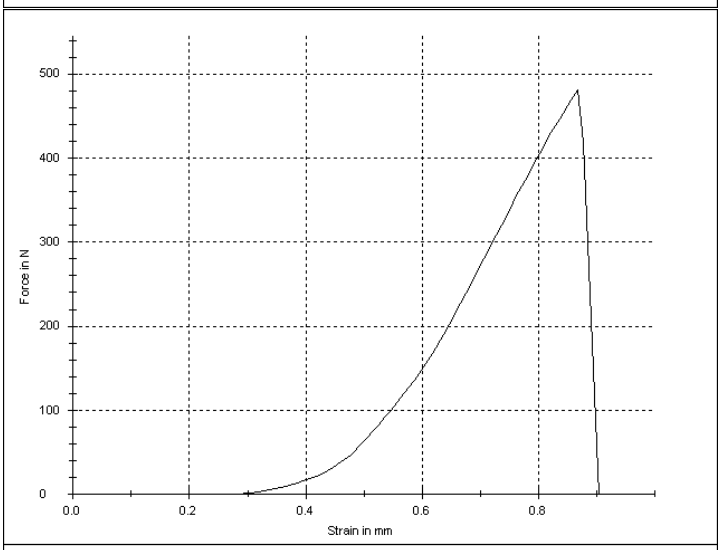


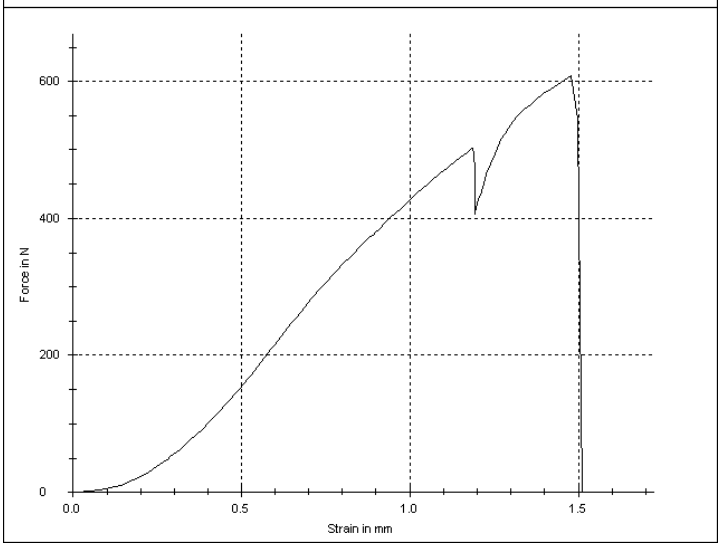

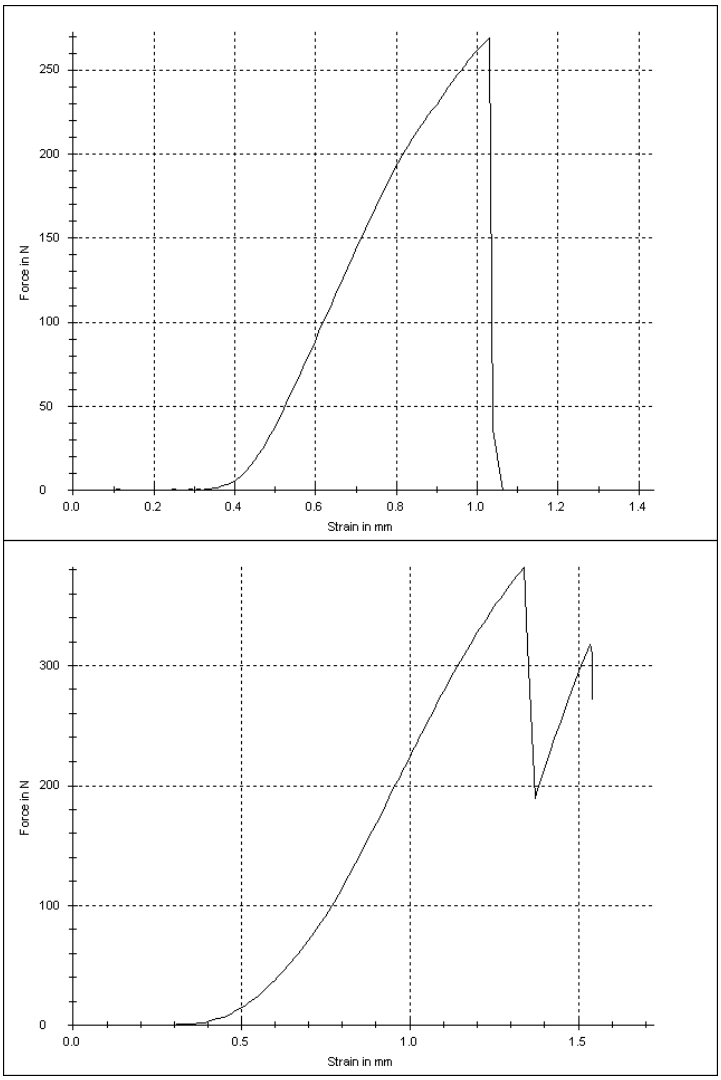
Force in N
250
200
150
100
50
0
0.0
0.2
0.4
0.6
0.8
1.0
1.2
1.4
Strain in mm
Force in N
300
200
100
0
0.0
0.5
1.0
1.5
Strain in mm

## 8.1.7 5M NaOH 6 hours trials 1 - 5

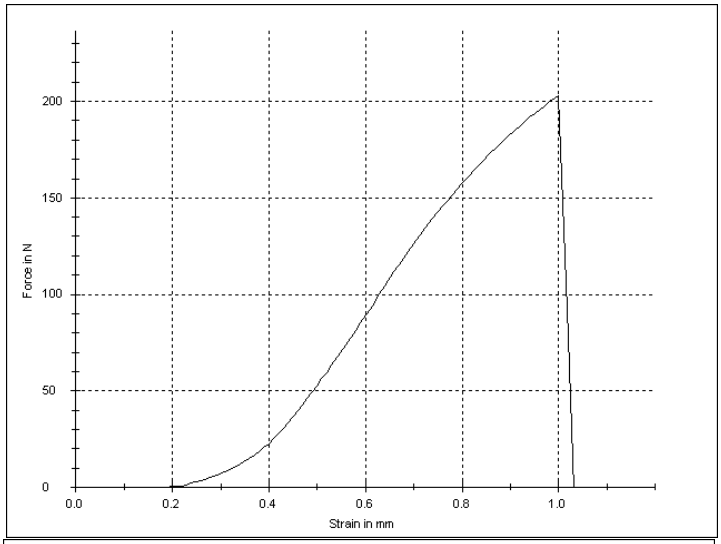


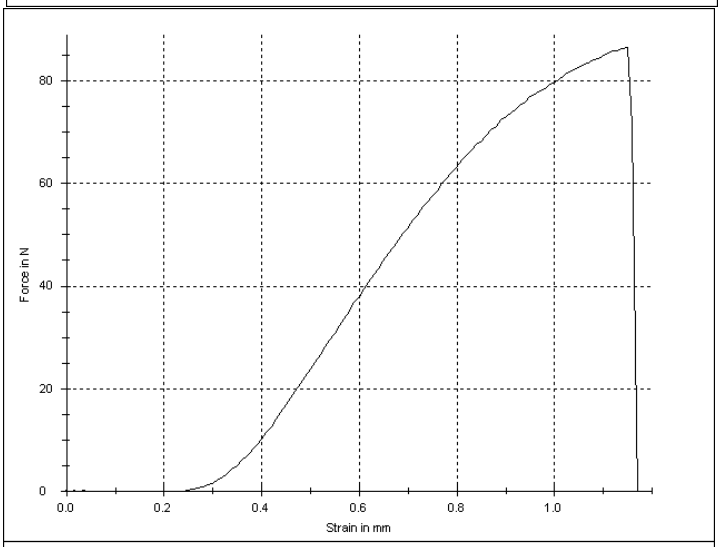


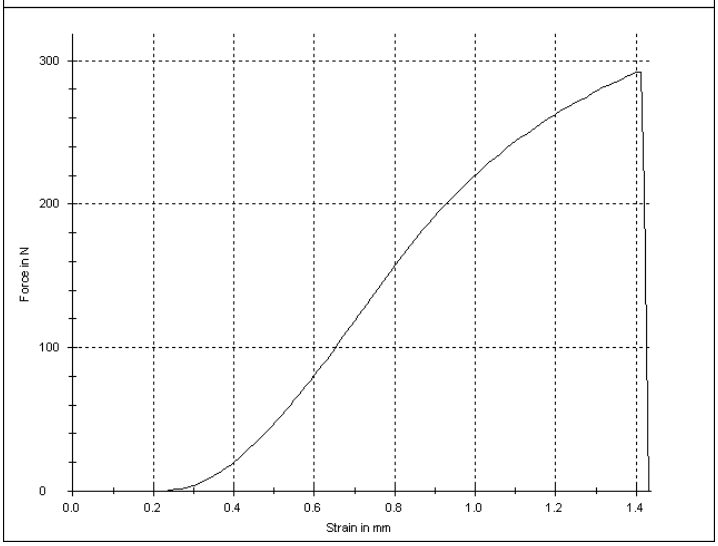

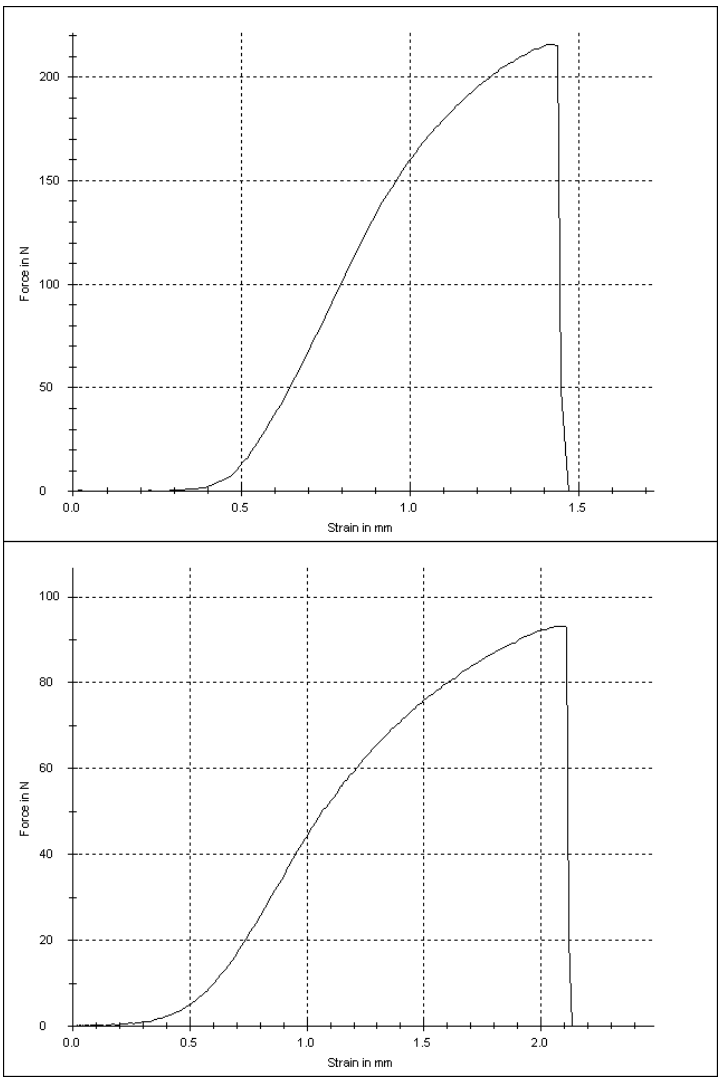
Force in N
200
150
100
50
0
0.0
0.5
1.0
1.5
Strain in mm
Force in N
100
80
60
40
20
0
0.0
0.5
1.0
1.5
2.0
Strain in mm

## 8.1.9 5M NaOH 12 hours trials 1 - 5

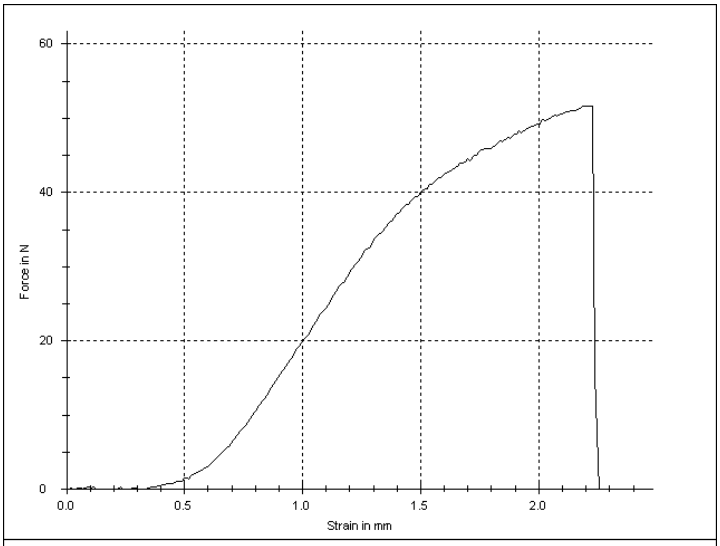


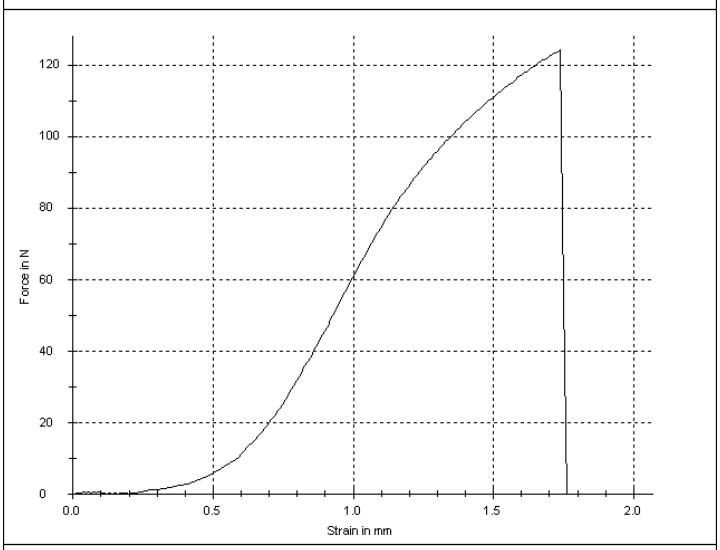


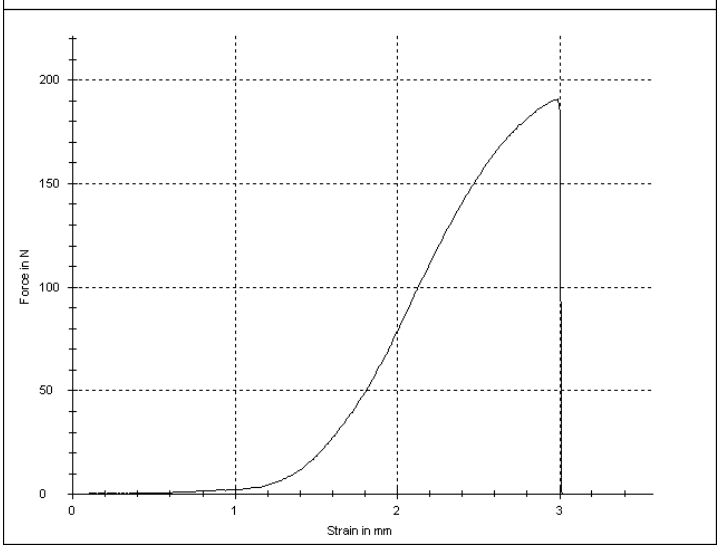

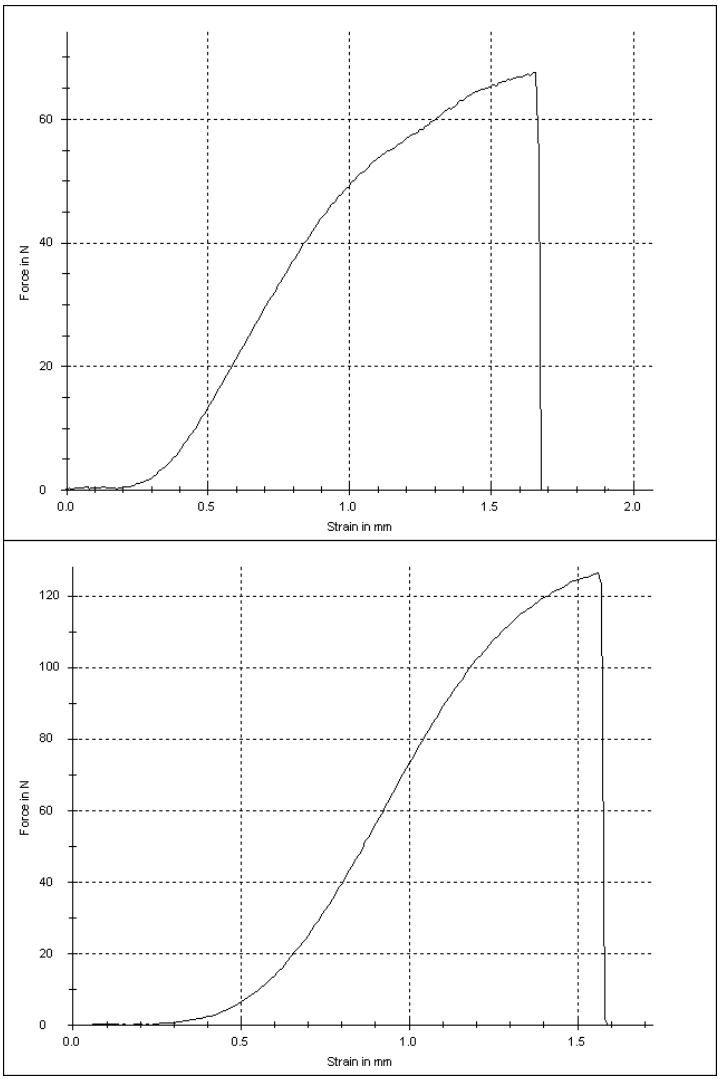
Force in N
0
20
40
60
0.0
0.5
1.0
1.5
2.0
Strain in mm
Force in N
0
20
40
60
80
100
120
0.0
0.5
1.0
1.5
Strain in mm

## 8.1.10 5M NaOH 24 hours trials 1 - 5

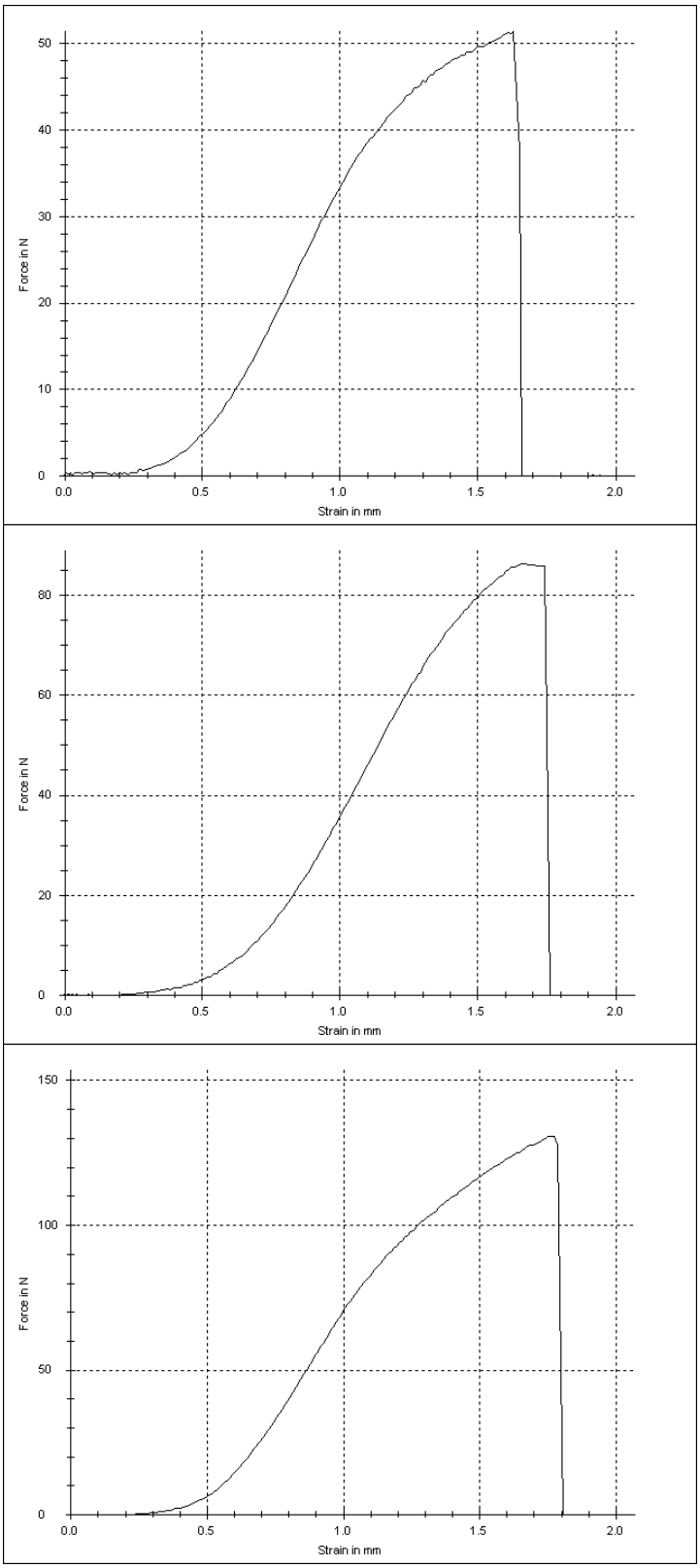

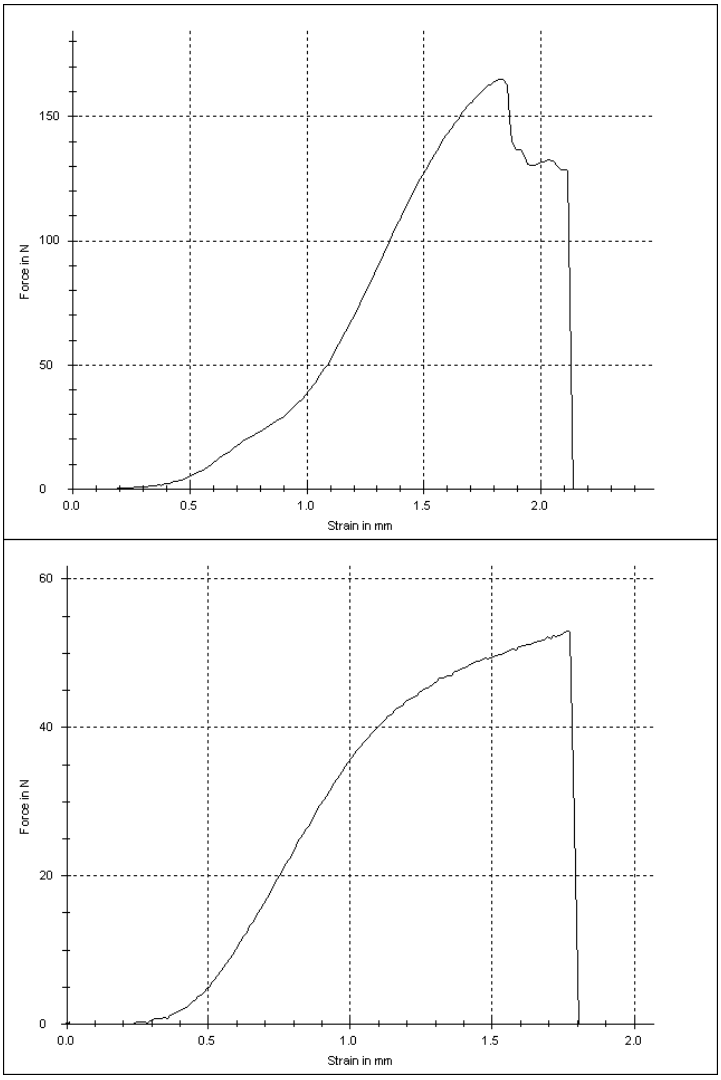
150
100
50
0
Force in N
0.0
0.5
1.0
1.5
2.0
Strain in mm
60
40
20
0
Force in N
0.0
0.5
1.0
1.5
2.0
Strain in mm

## 8.1.11 5M NaOH 48 hours trials 1 - 5

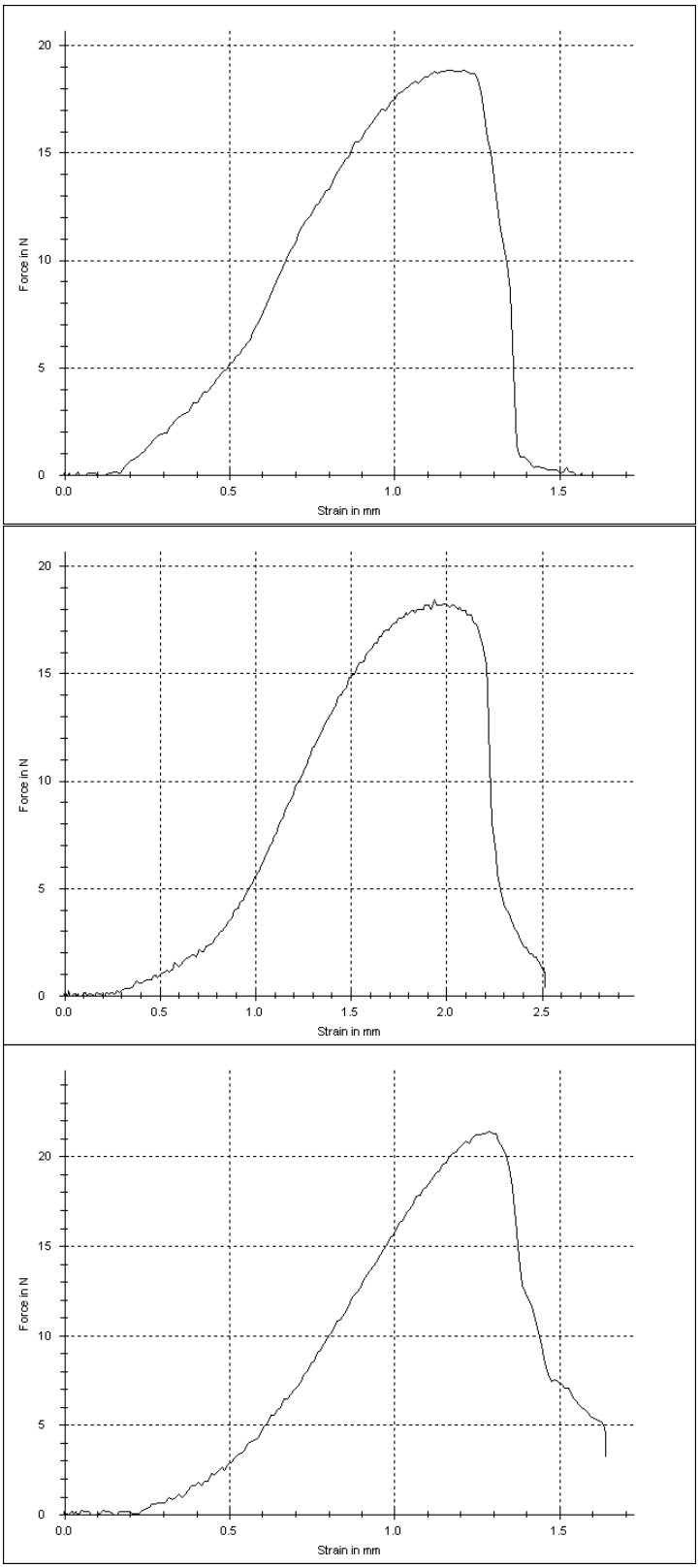

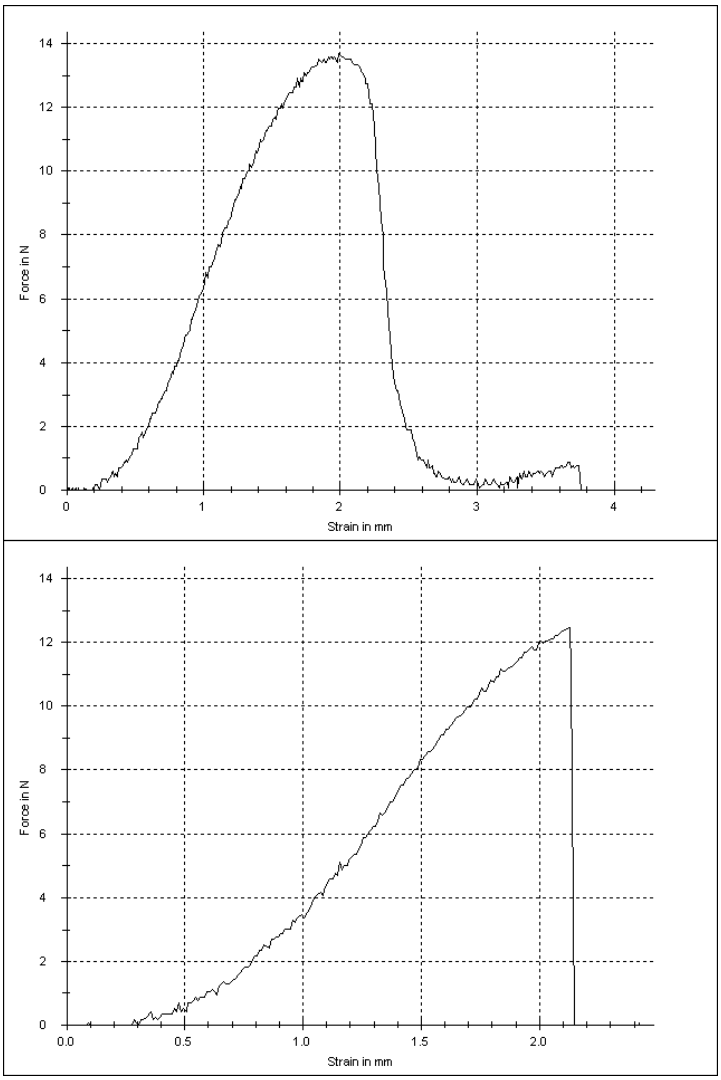
Force in N
Strain in mm
0
2
4
6
8
10
12
14
0
1
2
3
4
Force in N
Strain in mm
0
2
4
6
8
10
12
14
0.0
0.5
1.0
1.5
2.0

## 8.1.12 10M NaOH Control trials 1 - 5

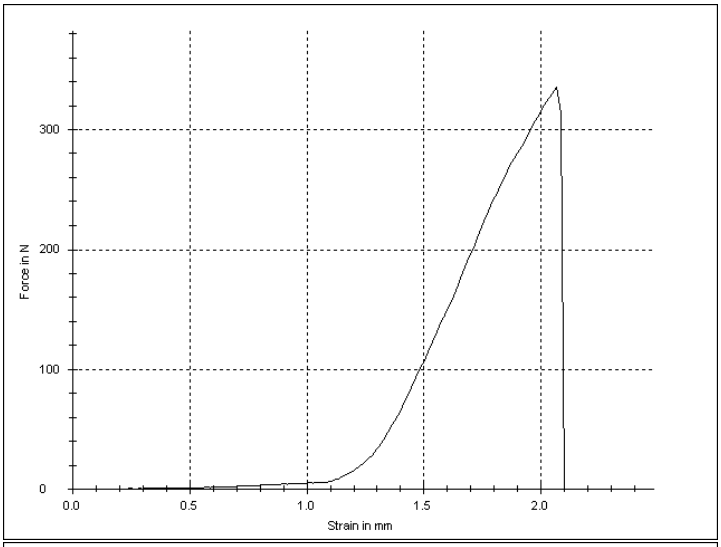


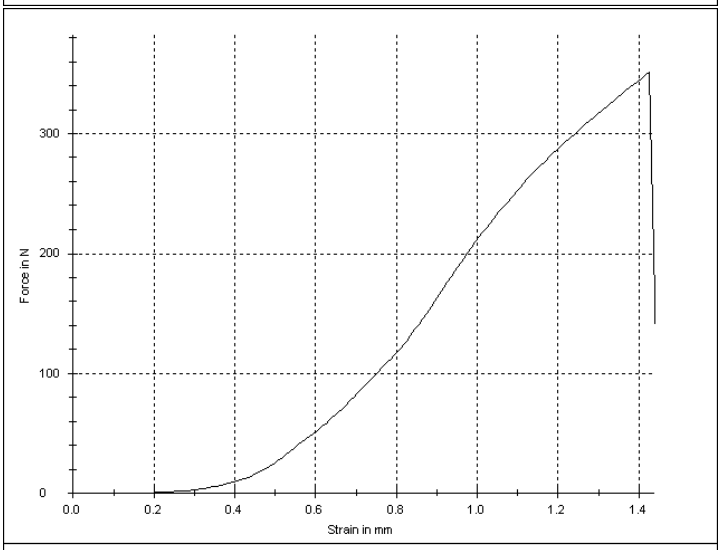


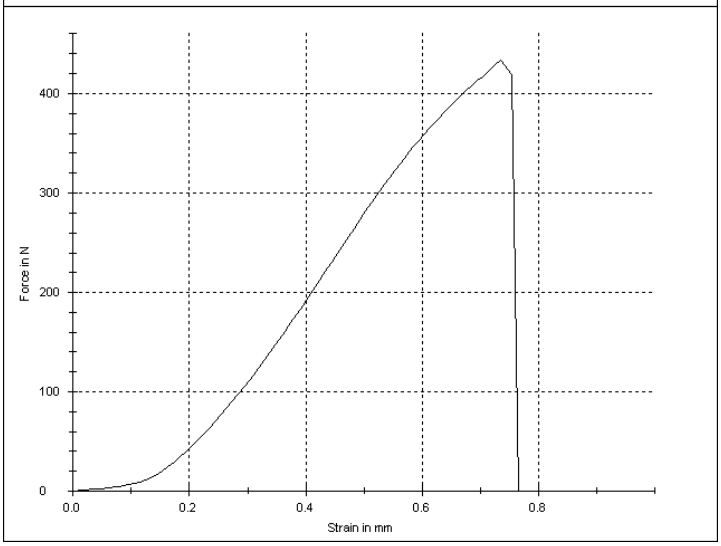

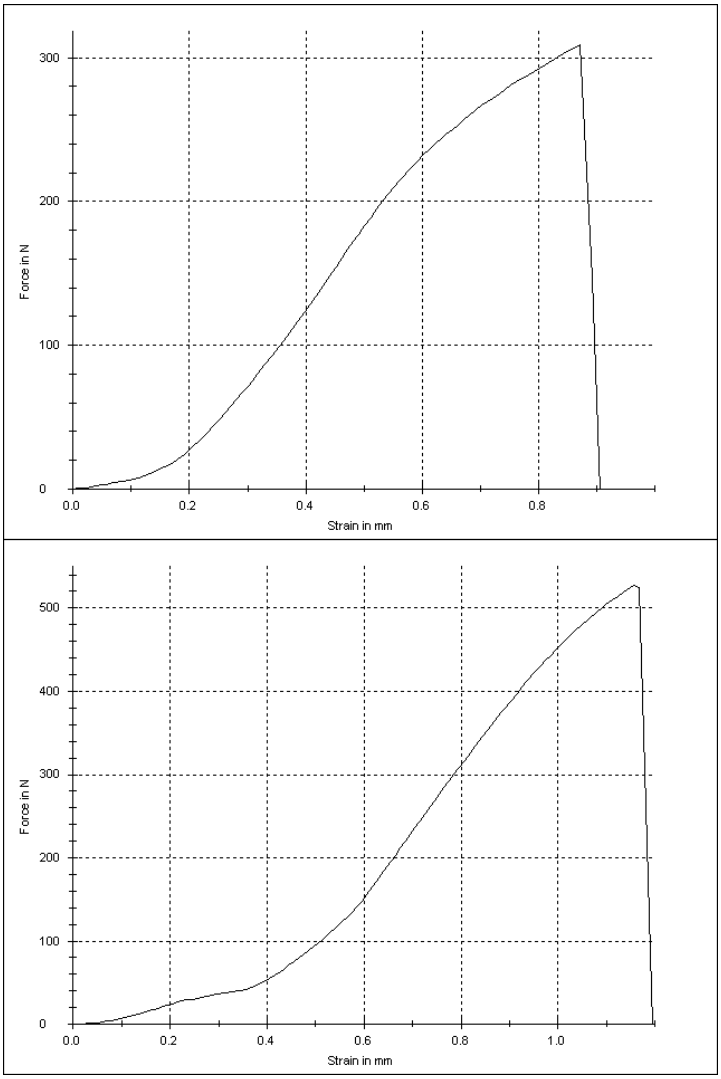
300
200
100
0
Force in N
0.0
0.2
0.4
0.6
0.8
Strain in mm
500
400
300
200
100
0
Force in N
0.0
0.2
0.4
0.6
0.8
1.0
Strain in mm

## 8.1.13 10M NaOH 6 hours trials 1 - 5

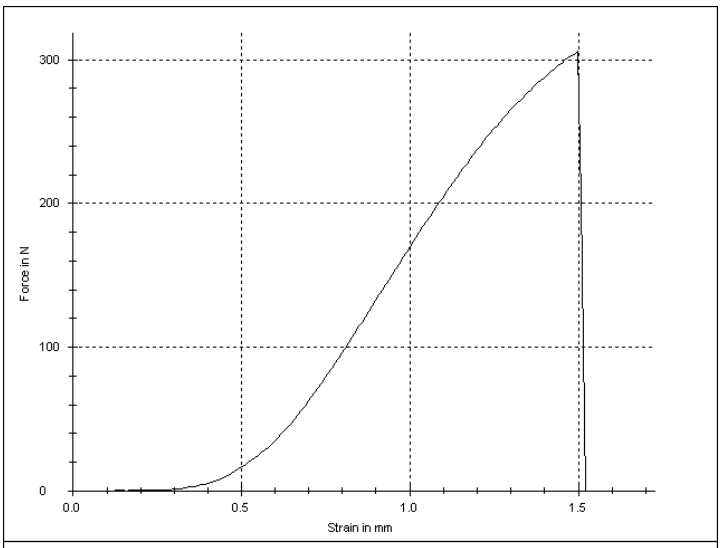


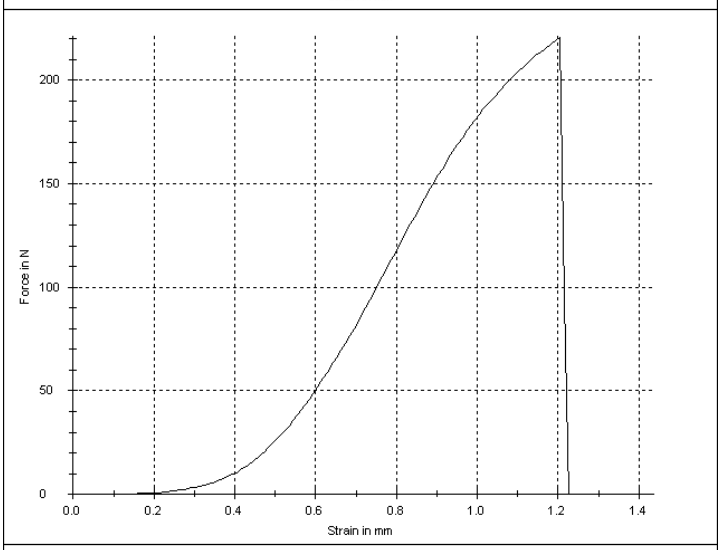


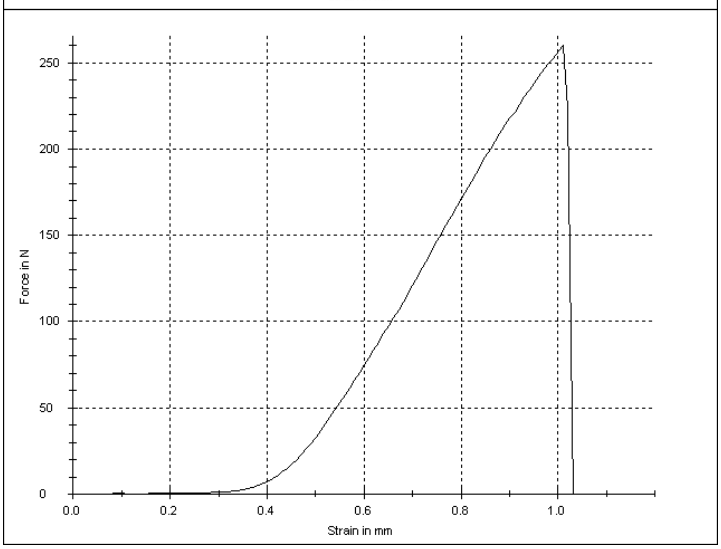

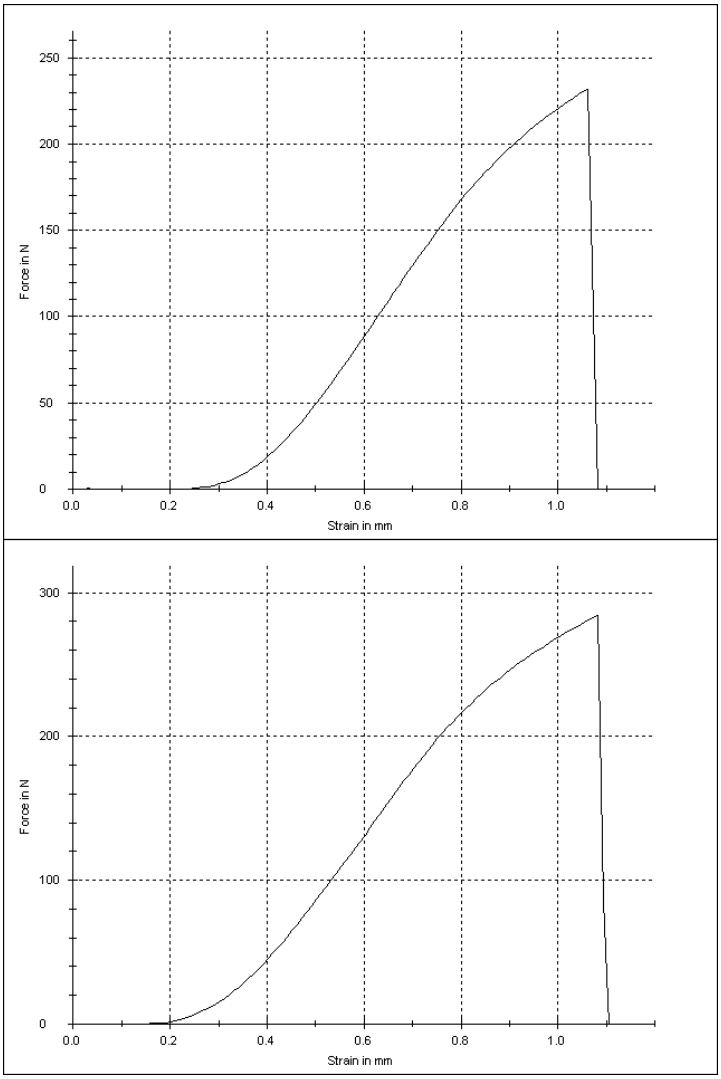
250
200
150
100
50
0
Force in N
0.0
0.2
0.4
0.6
0.8
1.0
Strain in mm
300
200
100
0
Force in N
0.0
0.2
0.4
0.6
0.8
1.0
Strain in mm

## 8.1.14 10M NaOH 12 hours trials 1 - 5

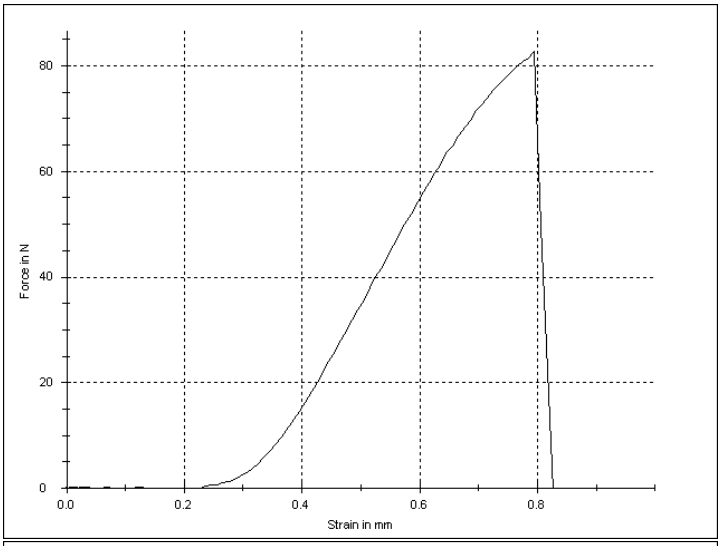


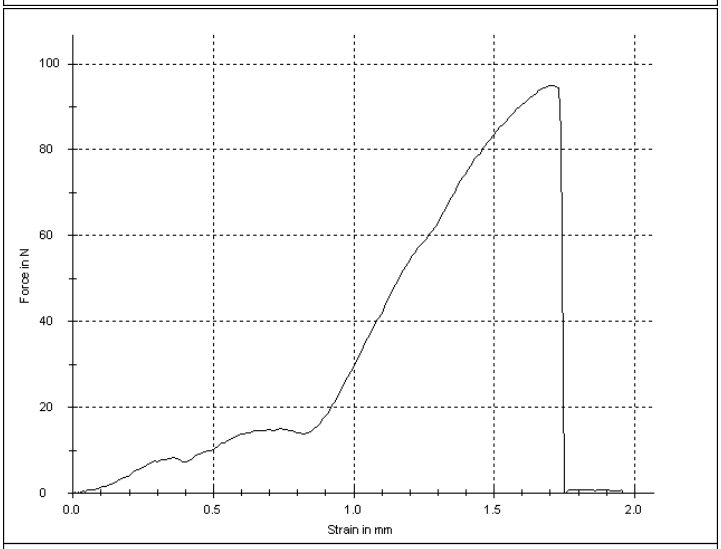


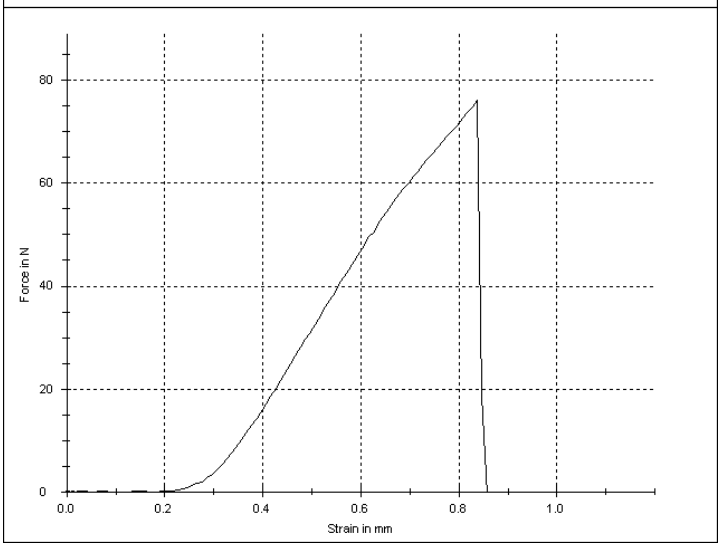

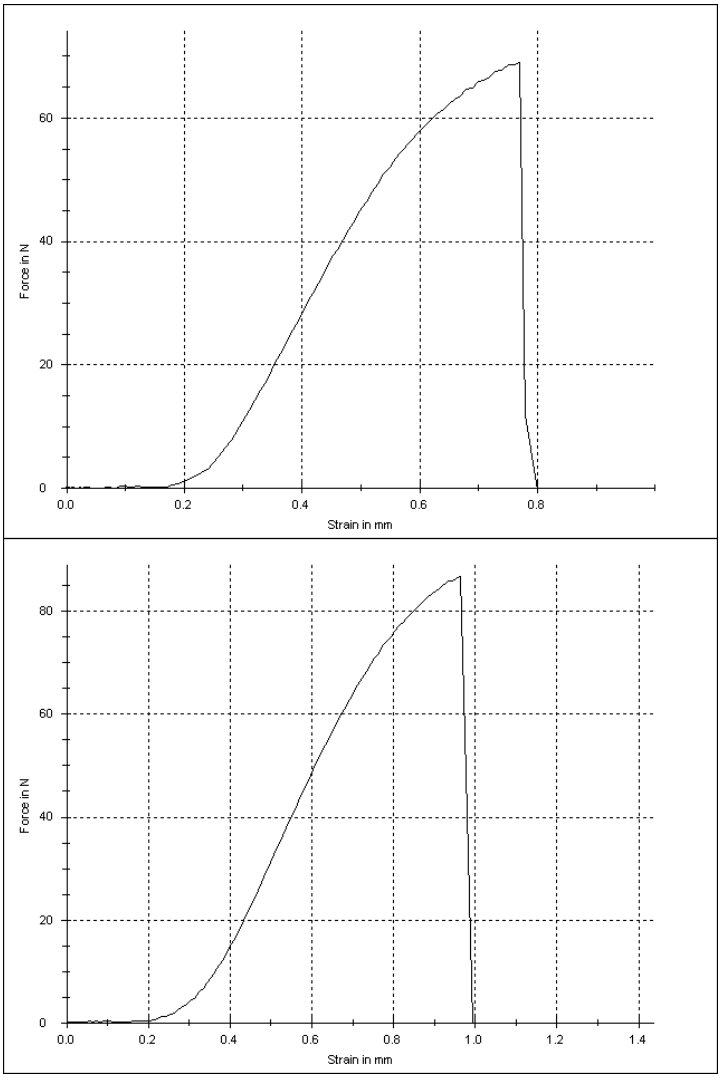
Force in N
0
20
40
60
0.0
0.2
0.4
0.6
0.8
Strain in mm
Force in N
0
20
40
60
80
0.0
0.2
0.4
0.6
0.8
1.0
1.2
1.4
Strain in mm

## 8.1.15 10M NaOH 24 hours trials 1 - 5

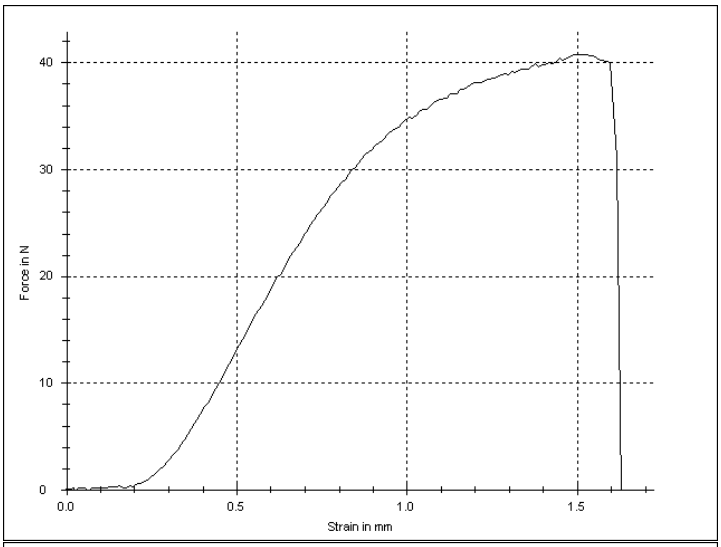


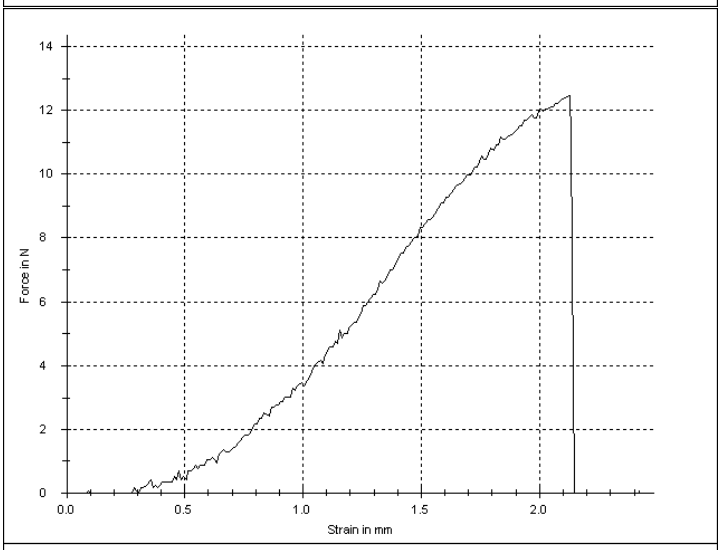


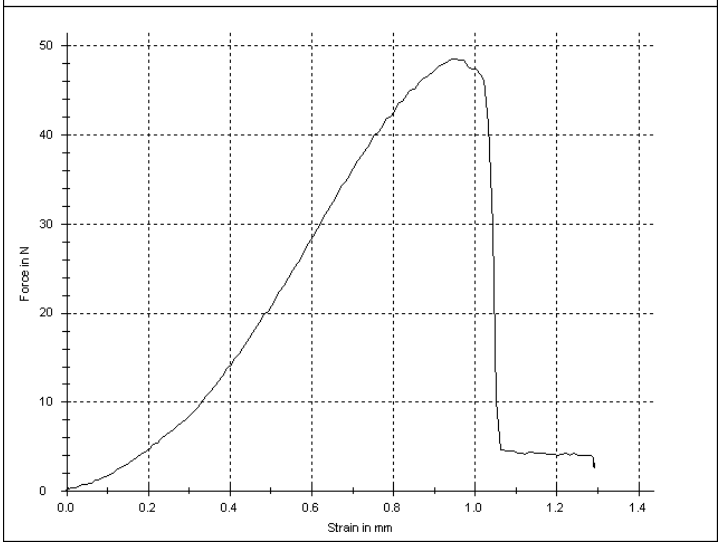

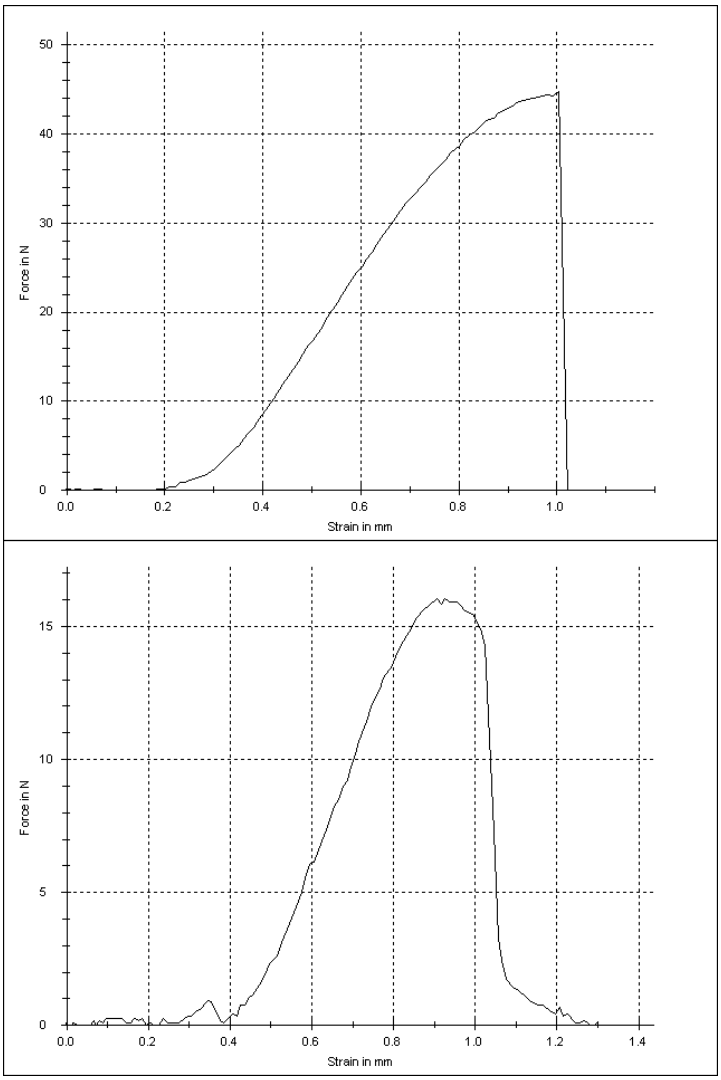
50
40
30
20
10
0
Force in N
0.0
0.2
0.4
0.6
0.8
1.0
Strain in mm
15
10
5
0
Force in N
0.0
0.2
0.4
0.6
0.8
1.0
1.2
1.4
Strain in mm

## 8.1.16 10M NaOH 48 hours trials 1 - 5

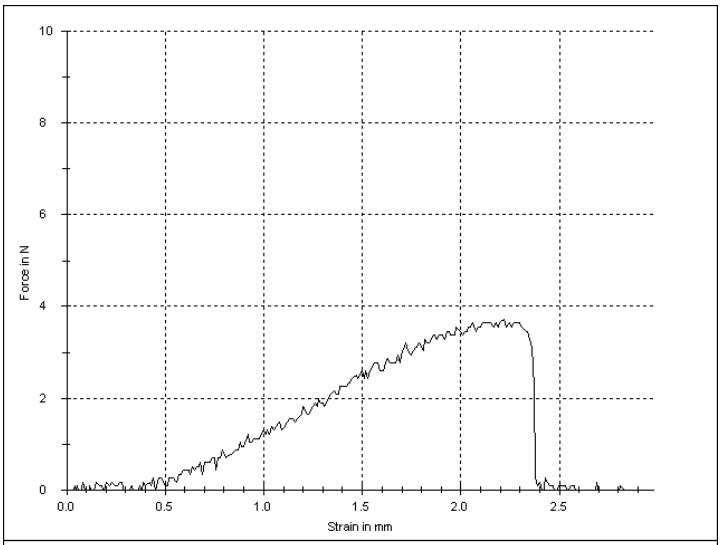


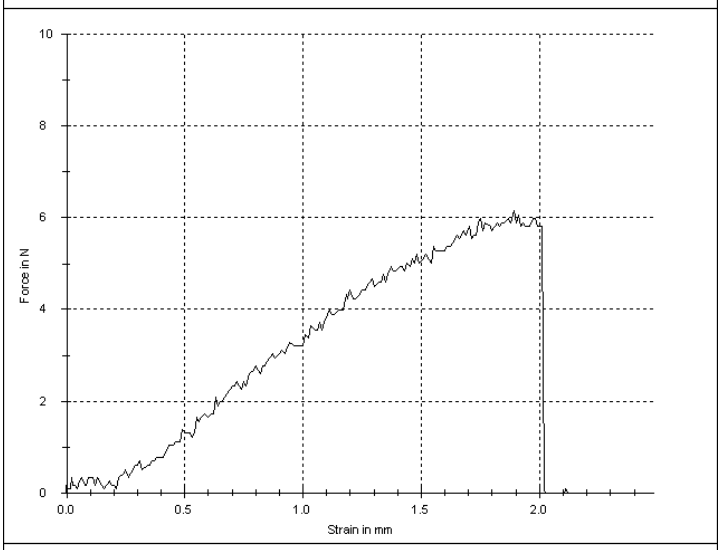


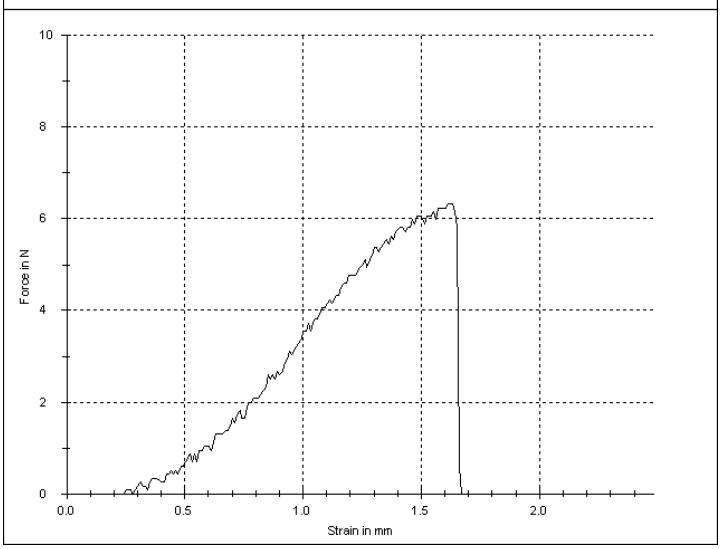

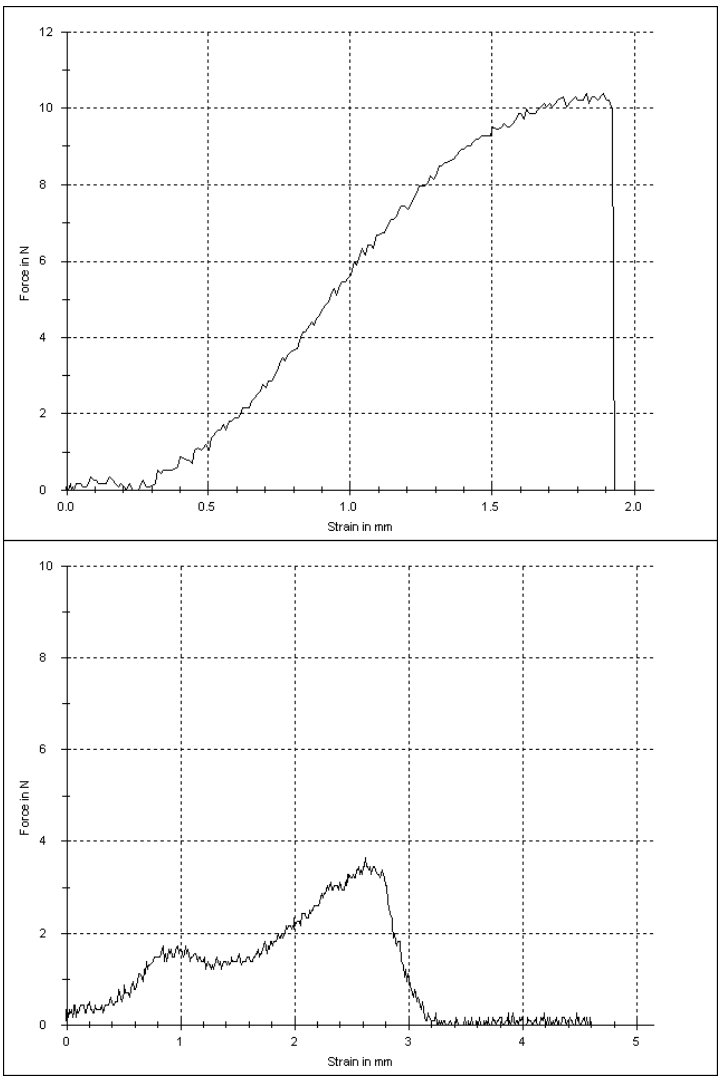
Force in N
Strain in mm
0
2
4
6
8
10
12
0.0
0.5
1.0
1.5
2.0
Force in N
Strain in mm
0
2
4
6
8
10
0
1
2
3
4
5

## 8.2 Appendix B - tables mechanical values

### 8.2.1 Control values

| FORCE | | | | | |
|---|---|---|---|---|---|
| | **0 hours** | **6 hours** | **12 hours** | **24 hours** | **48 hours** |
| **Trial 1** | 360 | 480 | 360 | 310 | 360 |
| **Trial 2** | 240 | 330 | 340 | 510 | 240 |
| **Trial 3** | 910 | 750 | 600 | 1010 | 910 |
| **Trial 4** | 380 | 405 | 440 | 405 | 380 |
| **Trial 5** | 410 | 390 | 320 | 390 | 410 |

| DEFLECTION | | | | | |
|---|---|---|---|---|---|
| | **0 hours** | **6 hours** | **12 hours** | **24 hours** | **48 hours** |
| **Trial 1** | 1.4 | 1.1 | 2.1 | 1.75 | 2.1 |
| **Trial 2** | 0.9 | 1 | 1.45 | 1.05 | 1.4 |
| **Trial 3** | 2.4 | 1.2 | 0.85 | 1.1 | 1.1 |
| **Trial 4** | 1.05 | 1.1 | 0.76 | 1.1 | 0.8 |
| **Trial 5** | 1.1 | 0.75 | 0.9 | 0.75 | 0.86 |

| ULTIMATE STRESS | | | | | |
|---|---|---|---|---|---|
| | **0 hours** | **6 hours** | **12 hours** | **24 hours** | **48 hours** |
| **Trial 1** | 120 | 225 | 164.4 | 140 | 164 |
| **Trial 2** | 152 | 195 | 181 | 235 | 119 |
| **Trial 3** | 160 | 304 | 300 | 280 | 319 |
| **Trial 4** | 235 | 128 | 212 | 140 | 193 |
| **Trial 5** | 310 | 115 | 153 | 176 | 212 |

| ULTIMATE STRAIN | | | | | |
|---|---|---|---|---|---|
| | 0 hours | 6 hours | 12 hours | 24 hours | 48 hours |
| Trial 1 | 1.98 | 2.9 | 3.1 | 1.93 | 3.16 |
| Trial 2 | 2.08 | 1.82 | 2.15 | 2.66 | 1.93 |
| Trial 3 | 3.19 | 2.45 | 2.13 | 2.22 | 2.22 |
| Trial 4 | 2.76 | 2.33 | 1.78 | 2.11 | 1.73 |
| Trial 5 | 2.32 | 1.83 | 2.24 | 1.78 | 2.5 |

| YIELD STRESS | | | | | |
|---|---|---|---|---|---|
| | 0 hours | 6 hours | 12 hours | 24 hours | 48 hours |
| Trial 1 | 109 | 210 | 150 | 139 | 142 |
| Trial 2 | 150 | 160 | 162 | 232 | 105 |
| Trial 3 | 140 | 294 | 285 | 265 | 299 |
| Trial 4 | 229 | 130 | 205 | 129 | 165 |
| Trial 5 | 300 | 180 | 135 | 171 | 204 |

| YIELD STRAIN | | | | | |
|---|---|---|---|---|---|
| | 0 hours | 6 hours | 12 hours | 24 hours | 48 hours |
| Trial 1 | 1.66 | 1.76 | 2 | 1.86 | 2.89 |
| Trial 2 | 1.96 | 1.65 | 2.82 | 2.1 | 1.65 |
| Trial 3 | 2.45 | 2.29 | 1.85 | 1.9 | 1.78 |
| Trial 4 | 1.83 | 2.2 | 1.7 | 1.94 | 1.59 |
| Trial 5 | 1.95 | 1.7 | 1.84 | 1.64 | 1.48 |

| ELASTIC MODULUS | | | | | |
|---|---|---|---|---|---|
| | 0 hours | 6 hours | 12 hours | 24 hours | 48 hours |
| **Trial 1** | 10337 | 15227 | 8172 | 10049 | 8153 |
| **Trial 2** | 9218.59 | 12113 | 8129 | 12094 | 8064 |
| **Trial 3** | 9509 | 15021 | 13412 | 12640 | 15460 |
| **Trial 4** | 13553 | 10901 | 14819 | 9342 | 12773 |
| **Trial 5** | 13392 | 13802 | 10170 | 12294 | 15096 |

| POST-YIELD STRESS | | | | | |
|---|---|---|---|---|---|
| | 0 hours | 6 hours | 12 hours | 24 hours | 48 hours |
| **Trial 1** | 7.3 | 20.3 | 7 | 8 | 17 |
| **Trial 2** | 8 | 10 | 14 | 20 | 9 |
| **Trial 3** | 18 | 14 | 21 | 19 | 15 |
| **Trial 4** | 15 | 7 | 11 | 7 | 10 |
| **Trial 5** | 17 | 13 | 18 | 13 | 18 |

| POST-YIELD STRAIN | | | | | |
|---|---|---|---|---|---|
| | 0 hours | 6 hours | 12 hours | 24 hours | 48 hours |
| **Trial 1** | 0.32 | 0.19 | 0.11 | 0.69 | 0.27 |
| **Trial 2** | 0.12 | 0.17 | 0.33 | 0.56 | 0.28 |
| **Trial 3** | 0.3 | 0.55 | 0.28 | 0.32 | 0.44 |
| **Trial 4** | 0.6 | 0.25 | 0.5 | 0.17 | 0.14 |
| **Trial 5** | 0.37 | 0.13 | 0.4 | 0.13 | 0.23 |

| DUCTILITY | | | | | |
|---|---|---|---|---|---|
| | 0 hours | 6 hours | 12 hours | 24 hours | 48 hours |
| **Trial 1** | 1.17 | 1.02 | 1.13 | 0.81 | 1.23 |
| **Trial 2** | 0.88 | 0.88 | 1.24 | 1.26 | 0.92 |
| **Trial 3** | 1 | 1.39 | 0.98 | 0.67 | 0.67 |
| **Trial 4** | 1.28 | 0.94 | 0.7 | 1.01 | 0.97 |
| **Trial 5** | 1.2 | 0.72 | 1.39 | 0.97 | 0.73 |

| TOUGHNESS | | | | | |
|---|---|---|---|---|---|
| | **0 hours** | **6 hours** | **12 hours** | **24 hours** | **48 hours** |
| **Trial 1** | 120 | 180.2 | 156.7 | 99 | 156 |
| **Trial 2** | 98.5 | 91.7 | 185 | 130 | 106 |
| **Trial 3** | 178 | 201 | 90 | 198 | 198 |
| **Trial 4** | 201 | 160 | 145 | 112 | 118 |
| **Trial 5** | 145 | 118 | 132 | 118 | 146 |

| PIXEL INTENSITY | | | | | |
|---|---|---|---|---|---|
| | **TRIAL 1** | **TRIAL 2** | **TRIAL 3** | **TRIAL 4** | **TRIAL 5** |
| **0 HOURS** | 193 | 192 | 184 | 184 | 190 |
| **6 HOURS** | 177 | 180 | 179 | 188 | 184 |
| **12 HOURS** | 180 | 182 | 183 | 180 | 179 |
| **24 HOURS** | 193 | 180 | 190 | 182 | 175 |
| **48 HOURS** | 176 | 190 | 181 | 183 | 192 |

### 8.2.2 EDTA values

| FORCE | | | | | |
|---|---|---|---|---|---|
| | **TRIAL 1** | **TRIAL 2** | **TRIAL 3** | **TRIAL 4** | **TRIAL 5** |
| **0 HOURS** | 360 | 340 | 560 | 440 | 320 |
| **6 HOURS** | 580 | 230 | 240 | 460 | 440 |
| **12 HOURS** | 325 | 450 | 410 | 270 | 330 |
| **24 HOURS** | 340 | 310 | 320 | 320 | 315 |
| **48 HOURS** | 180 | 210 | 270 | 205 | 230 |

| DEFLECTION | | | | | |
|---|---|---|---|---|---|
| | **TRIAL 1** | **TRIAL 2** | **TRIAL 3** | **TRIAL 4** | **TRIAL 5** |
| **0 HOURS** | 1.3 | 1.5 | 1.4 | 1.1 | 1.3 |
| **6 HOURS** | 1.35 | 1.1 | 1.3 | 1.85 | 0.78 |
| **12 HOURS** | 1.28 | 1.35 | 1.25 | 1.4 | 1.2 |
| **24 HOURS** | 1.75 | 1.55 | 1.5 | 1.6 | 1.75 |
| **48 HOURS** | 1.8 | 1.85 | 1.95 | 1.9 | 1.9 |

| ULTIMATE STRESS | | | | | |
|---|---|---|---|---|---|
| | **TRIAL 1** | **TRIAL 2** | **TRIAL 3** | **TRIAL 4** | **TRIAL 5** |
| **0 HOURS** | 180 | 152 | 210 | 135 | 200 |
| **6 HOURS** | 235 | 122 | 160 | 154 | 178 |
| **12 HOURS** | 187.3 | 113 | 112 | 174 | 167 |
| **24 HOURS** | 111.5 | 135 | 148 | 103 | 127 |
| **48 HOURS** | 87.3 | 96 | 83.1 | 94 | 95.1 |

| ULTIMATE STRAIN | | | | | |
|---|---|---|---|---|---|
| | TRIAL 1 | TRIAL 2 | TRIAL 3 | TRIAL 4 | TRIAL 5 |
| 0 HOURS | 1.98 | 2.08 | 3.19 | 2.81 | 2.32 |
| 6 HOURS | 2.74 | 2.79 | 3.04 | 2.77 | 2.9 |
| 12 HOURS | 3.01 | 2.65 | 2.73 | 3.52 | 2.21 |
| 24 HOURS | 2.99 | 2.74 | 3.01 | 3.21 | 1.96 |
| 48 HOURS | 2.71 | 2.98 | 2.9 | 3.17 | 2.85 |

| YIELD STRESS | | | | | |
|---|---|---|---|---|---|
| | TRIAL 1 | TRIAL 2 | TRIAL 3 | TRIAL 4 | TRIAL 5 |
| 0 HOURS | 150 | 140 | 188 | 130 | 180 |
| 6 HOURS | 220 | 128 | 96 | 135 | 162 |
| 12 HOURS | 168 | 101 | 92 | 140 | 158 |
| 24 HOURS | 91 | 120 | 132 | 89 | 98 |
| 48 HOURS | 60 | 72 | 55 | 78 | 90 |

| YIELD STRAIN | | | | | |
|---|---|---|---|---|---|
| | TRIAL 1 | TRIAL 2 | TRIAL 3 | TRIAL 4 | TRIAL 5 |
| 0 HOURS | 1.66 | 1.96 | 2.45 | 1.83 | 1.95 |
| 6 HOURS | 2.35 | 1.8 | 2.18 | 2.29 | 2.9 |
| 12 HOURS | 2.6 | 1.94 | 2.12 | 2.75 | 1.98 |
| 24 HOURS | 2.4 | 2.29 | 2.35 | 2.66 | 1.7 |
| 48 HOURS | 2.6 | 2.77 | 2.4 | 2.5 | 2.7 |

| ELASTIC MODULUS | | | | | |
|---|---|---|---|---|---|
| | **TRIAL 1** | **TRIAL 2** | **TRIAL 3** | **TRIAL 4** | **TRIAL 5** |
| **0 HOURS** | 10337 | 9218.59 | 9509 | 13553 | 13392 |
| **6 HOURS** | 13901 | 5649 | 5293 | 9104 | 10628 |
| **12 HOURS** | 8338 | 6066 | 9434 | 6343 | 6467 |
| **24 HOURS** | 7721 | 7956 | 10185 | 5847 | 5650 |
| **48 HOURS** | 5737.07 | 9232 | 4311 | 4254 | 9566 |

| POST-YIELD STRESS | | | | | |
|---|---|---|---|---|---|
| | TRIAL 1 | TRIAL 2 | TRIAL 3 | TRIAL 4 | TRIAL 5 |
| 0 HOURS | 16 | 12 | 14 | 5 | 20 |
| 6 HOURS | 15 | 14 | 32 | 19 | 16 |
| 12 HOURS | 19.3 | 12 | 20 | 34 | 9 |
| 24 HOURS | 20.5 | 15 | 16 | 14 | 29 |
| 48 HOURS | 27.3 | 24 | 28.1 | 16 | 5.1 |

| POST-YIELD STRAIN | | | | | |
|---|---|---|---|---|---|
| | TRIAL 1 | TRIAL 2 | TRIAL 3 | TRIAL 4 | TRIAL 5 |
| 0 HOURS | 0.32 | 0.12 | 0.74 | 0.98 | 0.37 |
| 6 HOURS | 0.39 | 0.99 | 0.86 | 0.48 | 0 |
| 12 HOURS | 0.41 | 0.71 | 0.61 | 0.77 | 0.23 |
| 24 HOURS | 0.59 | 0.45 | 0.66 | 0.55 | 0.26 |
| 48 HOURS | 0.11 | 0.21 | 0.5 | 0.41 | 0.15 |

| DUCTILITY | | | | | |
|---|---|---|---|---|---|
| | TRIAL 1 | TRIAL 2 | TRIAL 3 | TRIAL 4 | TRIAL 5 |
| 0 HOURS | 1.02 | 0.88 | 1.19 | 0.94 | 0.72 |
| 6 HOURS | 1.56 | 1.55 | 1.21 | 1.83 | 1.1 |
| 12 HOURS | 1.73 | 1.62 | 2.27 | 1.4 | 1.69 |
| 24 HOURS | 1.75 | 1.11 | 1.52 | 1.52 | 3.71 |
| 48 HOURS | 1.51 | 1.33 | 3.32 | 2.93 | 1.75 |

| TOUGHNESS | | | | | |
|---|---|---|---|---|---|
| | **TRIAL 1** | **TRIAL 2** | **TRIAL 3** | **TRIAL 4** | **TRIAL 5** |
| **0 HOURS** | 120 | 98.5 | 178 | 201 | 145 |
| **6 HOURS** | 191.8 | 101.7 | 164.5 | 137.9 | 221.8 |
| **12 HOURS** | 174.9 | 222.4 | 228.8 | 119.3 | 174.55 |
| **24 HOURS** | 273.4 | 105.8 | 174.5 | 222.2 | 230.9 |
| **48 HOURS** | 178.87 | 165.7 | 282.1 | 254.2 | 237.9 |

| PIXEL INTENSITY | | | | | |
|---|---|---|---|---|---|
| | **TRIAL 1** | **TRIAL 2** | **TRIAL 3** | **TRIAL 4** | **TRIAL 5** |
| **0 HOURS** | 185 | 186 | 190 | 191 | 188 |
| **6 HOURS** | 165 | 155 | 167 | 163 | 162 |
| **12 HOURS** | 154 | 157 | 159 | 151 | 149 |
| **24 HOURS** | 149 | 142 | 152 | 141 | 139 |
| **48 HOURS** | 133 | 125 | 139 | 128 | 127 |

### 8.2.3 5M NaOH values

| FORCE | | | | | |
|---|---|---|---|---|---|
| | **TRIAL 1** | **TRIAL 2** | **TRIAL 3** | **TRIAL 4** | **TRIAL 5** |
| **0 HOURS** | 290 | 480 | 600 | 530 | 370 |
| **6 HOURS** | 360 | 390 | 520 | 440 | 380 |
| **12 HOURS** | 620 | 380 | 230 | 200 | 210 |
| **24 HOURS** | 95 | 55 | 130 | 190 | 70 |
| **48 HOURS** | 55 | 160 | 130 | 90 | 52 |

| DEFLECTION | | | | | |
|---|---|---|---|---|---|
| | **TRIAL 1** | **TRIAL 2** | **TRIAL 3** | **TRIAL 4** | **TRIAL 5** |
| **0 HOURS** | 1.75 | 1.35 | 1.25 | 1.2 | 0.95 |
| **6 HOURS** | 1.15 | 1.4 | 1.1 | 1.05 | 1.45 |
| **12 HOURS** | 1.1 | 0.9 | 1.5 | 1.25 | 1.1 |
| **24 HOURS** | 0.85 | 1.05 | 1.4 | 0.95 | 1.45 |
| **48 HOURS** | 0.58 | 0.75 | 0.7 | 0.68 | 0.65 |

| ULTIMATE STRESS | | | | | |
|---|---|---|---|---|---|
| | **TRIAL 1** | **TRIAL 2** | **TRIAL 3** | **TRIAL 4** | **TRIAL 5** |
| **0 HOURS** | 156 | 186 | 215 | 202 | 161 |
| **6 HOURS** | 134.4 | 176 | 240 | 235 | 153 |
| **12 HOURS** | 150 | 192 | 126 | 101 | 120 |
| **24 HOURS** | 37 | 54 | 58 | 90 | 53 |
| **48 HOURS** | 21.5 | 46 | 61 | 43.5 | 23 |

| ULTIMATE STRAIN | | | | | |
|---|---|---|---|---|---|
| | TRIAL 1 | TRIAL 2 | TRIAL 3 | TRIAL 4 | TRIAL 5 |
| 0 HOURS | 2.15 | 1.85 | 2.53 | 2.13 | 2.24 |
| 6 HOURS | 2.32 | 2.06 | 2.32 | 1.88 | 2.04 |
| 12 HOURS | 1.65 | 1.53 | 1.91 | 1.56 | 2.25 |
| 24 HOURS | 1.46 | 0.83 | 0.98 | 1.51 | 1.21 |
| 48 HOURS | 0.38 | 0.89 | 0.58 | 0.35 | 0.73 |

| YIELD STRESS | | | | | |
|---|---|---|---|---|---|
| | TRIAL 1 | TRIAL 2 | TRIAL 3 | TRIAL 4 | TRIAL 5 |
| 0 HOURS | 150 | 162 | 200 | 210 | 150 |
| 6 HOURS | 126 | 150 | 230 | 220 | 120 |
| 12 HOURS | 140 | 180 | 106 | 95 | 96 |
| 24 HOURS | 35 | 51 | 55 | 85 | 48 |
| 48 HOURS | 21 | 45 | 60 | 43 | 23 |

| YIELD STRAIN | | | | | |
|---|---|---|---|---|---|
| | TRIAL 1 | TRIAL 2 | TRIAL 3 | TRIAL 4 | TRIAL 5 |
| 0 HOURS | 1.85 | 1.38 | 2.3 | 1.9 | 1.83 |
| 6 HOURS | 2.01 | 1.86 | 2.13 | 1.7 | 1.84 |
| 12 HOURS | 1.52 | 1.49 | 1.76 | 1.44 | 2.12 |
| 24 HOURS | 1.44 | 0.68 | 0.95 | 1.48 | 1.05 |
| 48 HOURS | 0.35 | 0.88 | 0.56 | 0.35 | 0.72 |

| ELASTIC MODULUS | | | | | |
|---|---|---|---|---|---|
| | TRIAL 1 | TRIAL 2 | TRIAL 3 | TRIAL 4 | TRIAL 5 |
| 0 HOURS | 10337 | 9218.59 | 9808 | 13553 | 13392 |
| 6 HOURS | 11414.79 | 16819 | 12729 | 21817 | 11664 |
| 12 HOURS | 6489 | 6653 | 7144 | 6877 | 5666 |
| 24 HOURS | 1618 | 1097 | 2374 | 2544 | 1423 |
| 48 HOURS | 1185 | 2075 | 2654 | 1591 | 1011 |

| POST-YIELD STRESS | | | | | |
|---|---|---|---|---|---|
| | TRIAL 1 | TRIAL 2 | TRIAL 3 | TRIAL 4 | TRIAL 5 |
| 0 HOURS | 6 | 13 | 15 | 20 | 11 |
| 6 HOURS | 8.4 | 11 | 10 | 15 | 15 |
| 12 HOURS | 10 | 12 | 9 | 6 | 11 |
| 24 HOURS | 2 | 3 | 3 | 5 | 5 |
| 48 HOURS | 0.5 | 1 | 1 | 0.5 | 0 |

| POST-YIELD STRAIN | | | | | |
|---|---|---|---|---|---|
| | TRIAL 1 | TRIAL 2 | TRIAL 3 | TRIAL 4 | TRIAL 5 |
| 0 HOURS | 0.3 | 0.47 | 0.23 | 0.23 | 0.41 |
| 6 HOURS | 0.31 | 0.2 | 0.19 | 0.18 | 0.2 |
| 12 HOURS | 0.13 | 0.04 | 0.15 | 0.12 | 0.13 |
| 24 HOURS | 0.02 | 0.05 | 0.03 | 0.03 | 0.16 |
| 48 HOURS | 0.03 | 0.01 | 0.02 | 0 | 0.01 |

| DUCTILITY | | | | | |
|---|---|---|---|---|---|
| | TRIAL 1 | TRIAL 2 | TRIAL 3 | TRIAL 4 | TRIAL 5 |
| 0 HOURS | 0.93 | 1.08 | 1.12 | 1 | 1.39 |
| 6 HOURS | 1.05 | 1.1 | 0.94 | 0.97 | 0.87 |
| 12 HOURS | 1.23 | 0.92 | 1.04 | 0.93 | 1.13 |
| 24 HOURS | 0.51 | 0.64 | 0.46 | 0.47 | 0.61 |
| 48 HOURS | 0.47 | 0.53 | 0.37 | 0.55 | 0.59 |

| TOUGHNESS | | | | | |
|---|---|---|---|---|---|
| | **TRIAL 1** | **TRIAL 2** | **TRIAL 3** | **TRIAL 4** | **TRIAL 5** |
| **0 HOURS** | 156.7 | 145.5 | 215.9 | 140.8 | 132.6 |
| **6 HOURS** | 169.39 | 149.8 | 141.1 | 161.8 | 124.36 |
| **12 HOURS** | 125.21 | 126.6 | 122.74 | 158.17 | 142.6 |
| **24 HOURS** | 77.58 | 55.41 | 61.94 | 76.9 | 69.2 |
| **48 HOURS** | 47.79 | 39.5 | 33.2 | 33.35 | 39.31 |

| PIXEL INTENSITY | | | | | |
|---|---|---|---|---|---|
| | **TRIAL 1** | **TRIAL 2** | **TRIAL 3** | **TRIAL 4** | **TRIAL 5** |
| **0 HOURS** | 189 | 182 | 193 | 181 | 190 |
| **6 HOURS** | 191 | 187 | 183 | 180 | 185 |
| **12 HOURS** | 190 | 189 | 188 | 185 | 179 |
| **24 HOURS** | 185 | 193 | 192 | 190 | 181 |
| **48 HOURS** | 185 | 190 | 187 | 184 | 194 |

### 8.2.4 10M NaOH values

| FORCE | | | | | |
|---|---|---|---|---|---|
| | **TRIAL 1** | **TRIAL 2** | **TRIAL 3** | **TRIAL 4** | **TRIAL 5** |
| **0 HOURS** | 360 | 350 | 600 | 440 | 320 |
| **6 HOURS** | 345 | 320 | 340 | 400 | 375 |
| **12 HOURS** | 80 | 75 | 70 | 85 | 70 |
| **24 HOURS** | 26 | 82 | 44 | 40 | 60 |
| **48 HOURS** | 13 | 4 | 11 | 7 | 6 |

| DEFLECTION | | | | | |
|---|---|---|---|---|---|
| | **TRIAL 1** | **TRIAL 2** | **TRIAL 3** | **TRIAL 4** | **TRIAL 5** |
| **0 HOURS** | 1.2 | 1.65 | 2.05 | 1.2 | 0.9 |
| **6 HOURS** | 1.75 | 1.35 | 1.25 | 1.2 | 0.95 |
| **12 HOURS** | 1.05 | 0.95 | 1.05 | 1.33 | 1.2 |
| **24 HOURS** | 0.91 | 0.9 | 0.8 | 0.85 | 0.9 |
| **48 HOURS** | 0.57 | 0.6 | 0.7 | 0.48 | 0.55 |

| ULTIMATE STRESS | | | | | |
|---|---|---|---|---|---|
| | **TRIAL 1** | **TRIAL 2** | **TRIAL 3** | **TRIAL 4** | **TRIAL 5** |
| **0 HOURS** | 172 | 162 | 210 | 212 | 170 |
| **6 HOURS** | 120 | 164 | 176 | 190 | 230 |
| **12 HOURS** | 39 | 37 | 34 | 42 | 38 |
| **24 HOURS** | 13 | 40 | 22 | 20 | 25 |
| **48 HOURS** | 6 | 2 | 5 | 6 | 3 |

| ULTIMATE STRAIN | | | | | |
|---|---|---|---|---|---|
| | TRIAL 1 | TRIAL 2 | TRIAL 3 | TRIAL 4 | TRIAL 5 |
| 0 HOURS | 2.42 | 2.15 | 2.33 | 1.98 | 2.24 |
| 6 HOURS | 1.94 | 2.11 | 2 | 1.41 | 1.56 |
| 12 HOURS | 1.45 | 1.61 | 1.6 | 1.3 | 1.36 |
| 24 HOURS | 0.96 | 0.77 | 0.8 | 1.15 | 1.01 |
| 48 HOURS | 0.36 | 0.81 | 0.69 | 0.3 | 0.4 |

| YIELD STRESS | | | | | |
|---|---|---|---|---|---|
| | TRIAL 1 | TRIAL 2 | TRIAL 3 | TRIAL 4 | TRIAL 5 |
| 0 HOURS | 150 | 150 | 200 | 201 | 135 |
| 6 HOURS | 104 | 144 | 162 | 180 | 220 |
| 12 HOURS | 32 | 35 | 32 | 40 | 32 |
| 24 HOURS | 11.5 | 38 | 20 | 17 | 21 |
| 48 HOURS | 5.5 | 1.9 | 4.9 | 2.9 | 2.85 |

| YIELD STRAIN | | | | | |
|---|---|---|---|---|---|
| | TRIAL 1 | TRIAL 2 | TRIAL 3 | TRIAL 4 | TRIAL 5 |
| 0 HOURS | 2.15 | 1.82 | 2.13 | 1.7 | 1.84 |
| 6 HOURS | 1.82 | 1.96 | 1.9 | 1.17 | 1.38 |
| 12 HOURS | 1.41 | 1.48 | 1.43 | 1.26 | 1.25 |
| 24 HOURS | 0.92 | 0.71 | 0.76 | 1.12 | 1 |
| 48 HOURS | 0.35 | 0.8 | 0.68 | 0.3 | 0.4 |

| ELASTIC MODULUS | | | | | |
|---|---|---|---|---|---|
| | TRIAL 1 | TRIAL 2 | TRIAL 3 | TRIAL 4 | TRIAL 5 |
| 0 HOURS | 10337 | 9218.59 | 9509 | 11553 | 12303 |
| 6 HOURS | 13158 | 13239 | 15149 | 14866 | 18819 |
| 12 HOURS | 3558 | 2775 | 2895 | 2446 | 2593 |
| 24 HOURS | 1149 | 2585 | 1509 | 904 | 836 |
| 48 HOURS | 168 | 30 | 164 | 82 | 74 |

| POST-YIELD STRESS | | | | | |
|---|---|---|---|---|---|
| | TRIAL 1 | TRIAL 2 | TRIAL 3 | TRIAL 4 | TRIAL 5 |
| 0 HOURS | 12 | 13 | 10 | 16 | 11 |
| 6 HOURS | 16 | 20 | 14 | 10 | 10 |
| 12 HOURS | 7 | 2 | 2 | 2 | 6 |
| 24 HOURS | 1.5 | 2 | 2 | 3 | 4 |
| 48 HOURS | 0.5 | 0.1 | 0.1 | 0.1 | 0.15 |

| POST-YIELD STRAIN | | | | | |
|---|---|---|---|---|---|
| | TRIAL 1 | TRIAL 2 | TRIAL 3 | TRIAL 4 | TRIAL 5 |
| 0 HOURS | 0.27 | 0.33 | 0.3 | 0.32 | 0.4 |
| 6 HOURS | 0.12 | 0.15 | 0.1 | 0.24 | 0.18 |
| 12 HOURS | 0.04 | 0.13 | 0.17 | 0.04 | 0.11 |
| 24 HOURS | 0.04 | 0.06 | 0.04 | 0.03 | 0.01 |
| 48 HOURS | 0.01 | 0.01 | 0.01 | 0 | 0 |

| DUCTILITY | | | | | |
|---|---|---|---|---|---|
| | TRIAL 1 | TRIAL 2 | TRIAL 3 | TRIAL 4 | TRIAL 5 |
| 0 HOURS | 0.93 | 1.12 | 1.22 | 1 | 1.09 |
| 6 HOURS | 0.87 | 0.98 | 1 | 1.1 | 0.88 |
| 12 HOURS | 1.03 | 0.71 | 0.93 | 1 | 0.75 |
| 24 HOURS | 0.43 | 0.59 | 0.53 | 0.61 | 0.58 |
| 48 HOURS | 0.33 | 0.34 | 0.48 | 0.52 | 0.4 |

| TOUGHNESS | | | | | |
|---|---|---|---|---|---|
| | **TRIAL 1** | **TRIAL 2** | **TRIAL 3** | **TRIAL 4** | **TRIAL 5** |
| **0 HOURS** | 156.7 | 145 | 135 | 140.8 | 152.6 |
| **6 HOURS** | 145.3 | 122 | 152.1 | 149 | 159.7 |
| **12 HOURS** | 29.93 | 22.97 | 23.11 | 35.17 | 22.95 |
| **24 HOURS** | 18.79 | 12.9 | 19.79 | 28.18 | 25.37 |
| **48 HOURS** | 10.83 | 8.93 | 9.92 | 10.32 | 6.55 |

| PIXEL INTENSITY | | | | | |
|---|---|---|---|---|---|
| | **TRIAL 1** | **TRIAL 2** | **TRIAL 3** | **TRIAL 4** | **TRIAL 5** |
| **0 HOURS** | 189 | 182 | 198 | 181 | 190 |
| **6 HOURS** | 175 | 183 | 183 | 178 | 187 |
| **12 HOURS** | 180 | 182 | 183 | 180 | 179 |
| **24 HOURS** | 193 | 175 | 190 | 182 | 175 |
| **48 HOURS** | 176 | 190 | 186 | 183 | 192 |

## 8.3 Appendix C - mechanical values box plots

### 8.3.1 Control vs EDTA - mechanical values box plots

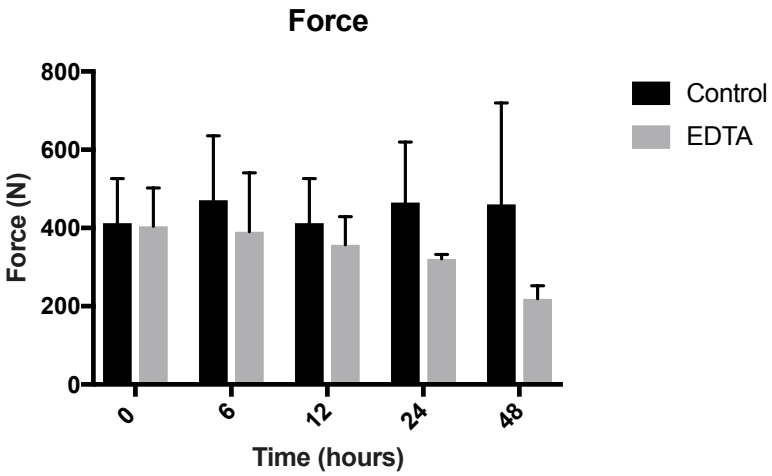


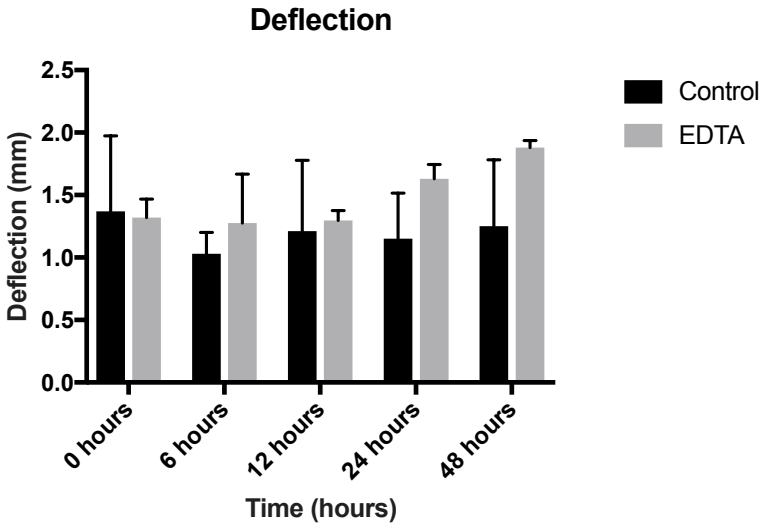


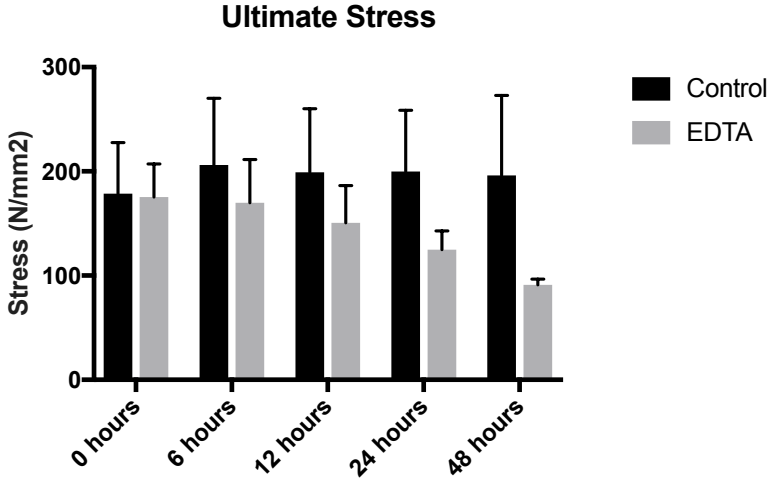

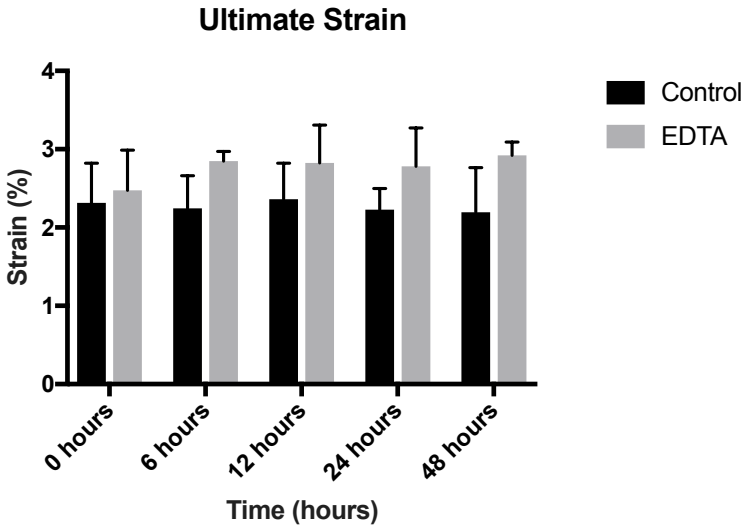
Ultimate Strain
Strain (%)
4
3
2
1
0
0 hours
6 hours
12 hours
24 hours
48 hours
Time (hours)
Control
EDTA

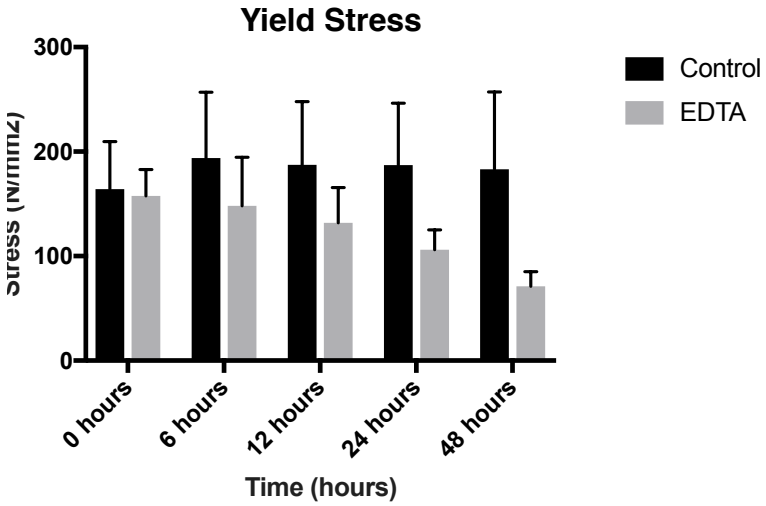
Yield Stress
300
200
100
0
0 hours
6 hours
12 hours
24 hours
48 hours
Time (hours)
Control
EDTA

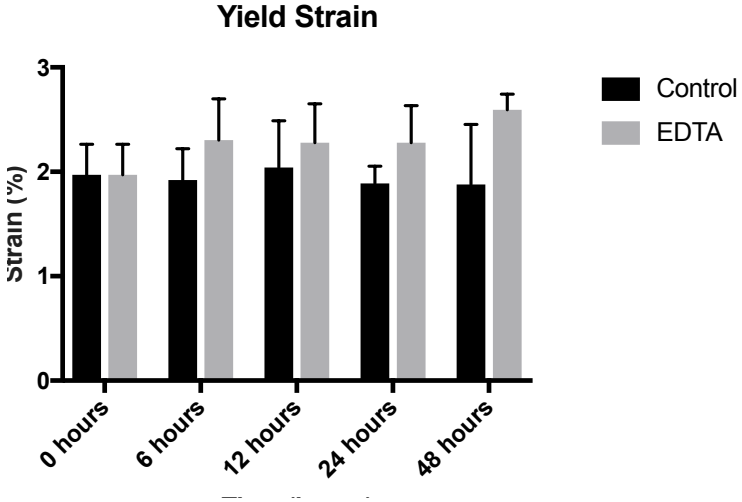
Yield Strain
Strain (%)
3
2
1
0
0 hours
6 hours
12 hours
24 hours
48 hours
Control
EDTA

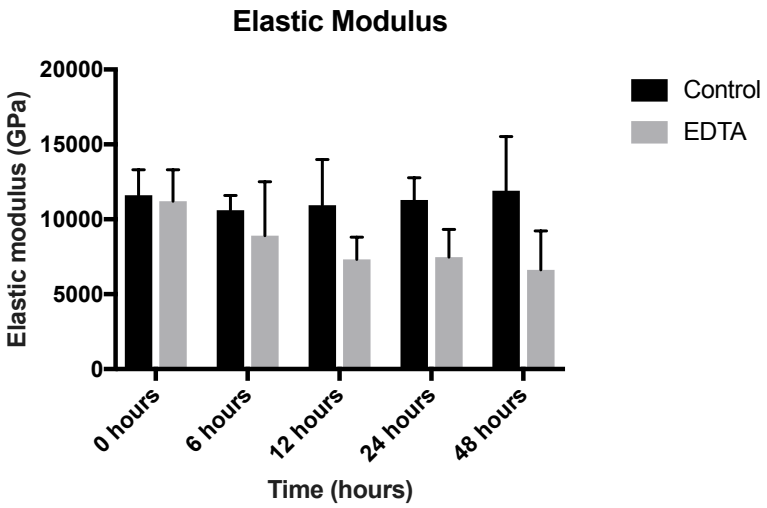
Elastic Modulus
Elastic modulus (GPa)
20000
15000
10000
5000
0
0 hours
6 hours
12 hours
24 hours
48 hours
Time (hours)
Control
EDTA

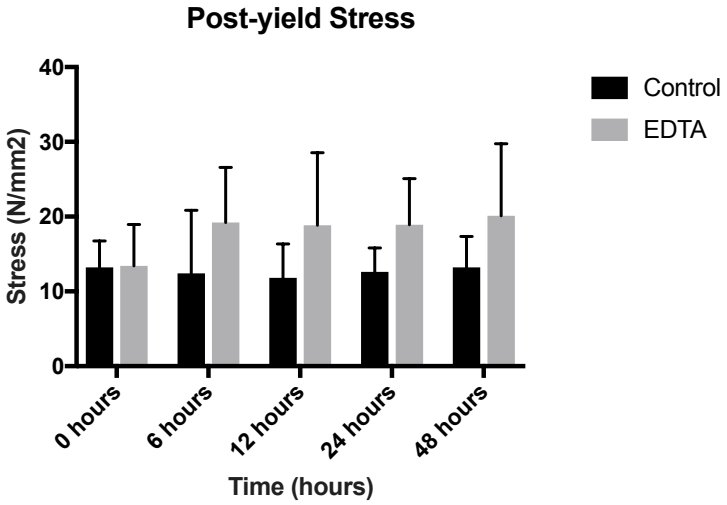
Post-yield Stress
Stress (N/mm2)
40
30
20
10
0
0 hours
6 hours
12 hours
24 hours
48 hours
Time (hours)
Control
EDTA

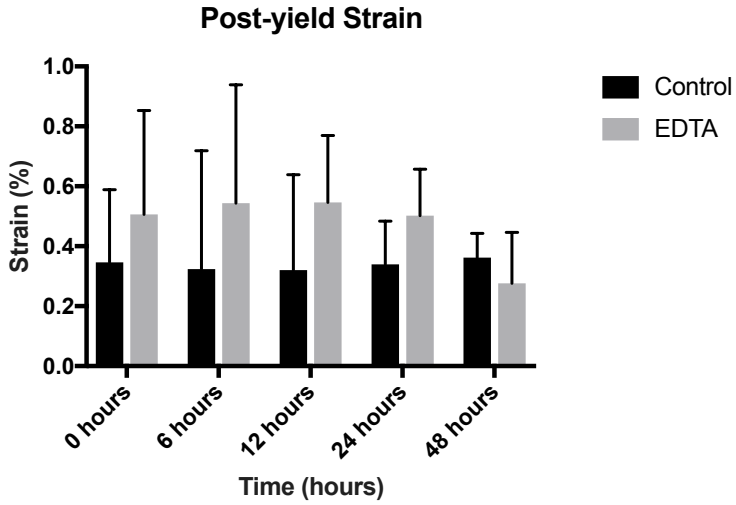
Post-yield Strain
Strain (%)
1.0
0.8
0.6
0.4
0.2
0.0
0 hours
6 hours
12 hours
24 hours
48 hours
Time (hours)
Control
EDTA

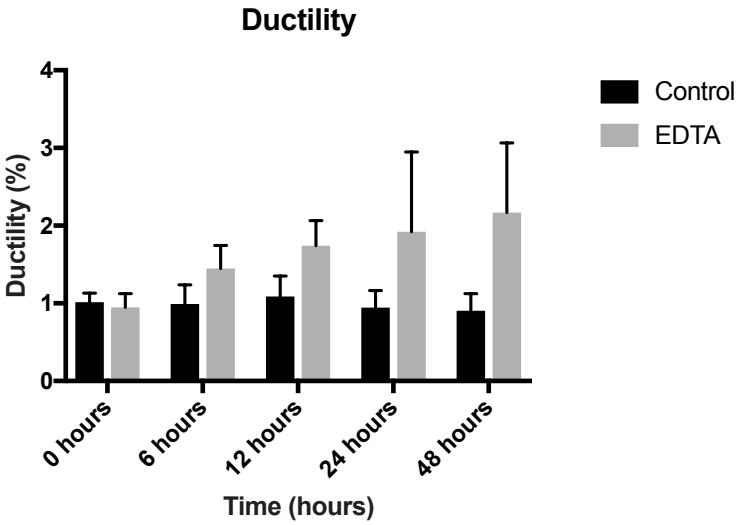
Ductility
Ductility (%)
4
3
2
1
0
0 hours
6 hours
12 hours
24 hours
48 hours
Time (hours)
Control
EDTA

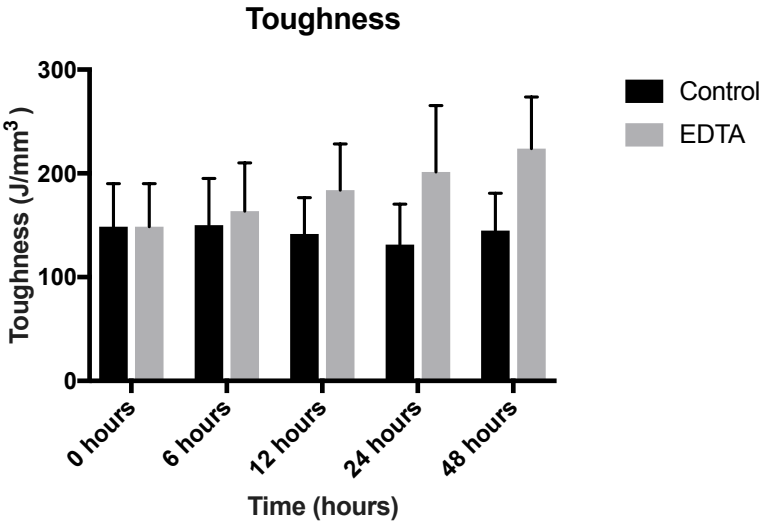
Toughness
Toughness (J/mm3)
300
200
100
0
0 hours
6 hours
12 hours
24 hours
48 hours
Time (hours)
Control
EDTA

## 8.3.2 Control vs 5M NaOH - mechanical values box plots

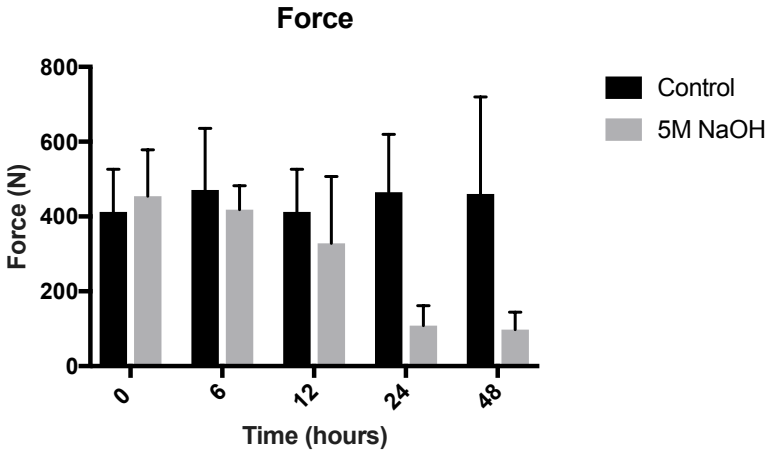


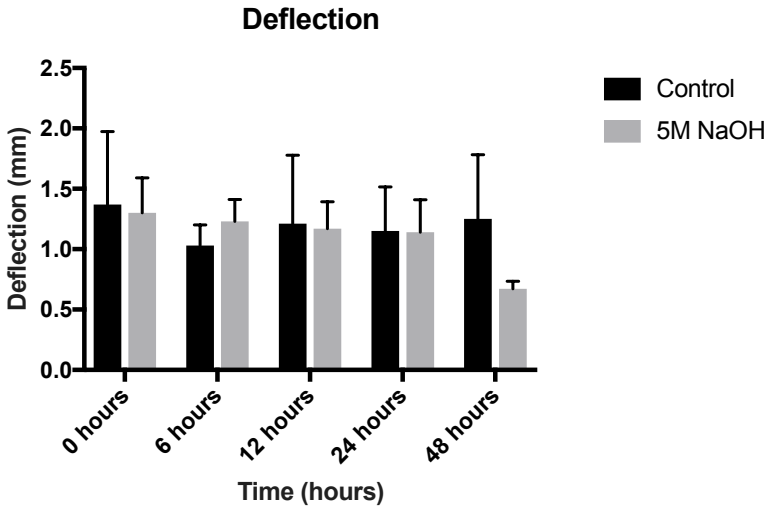


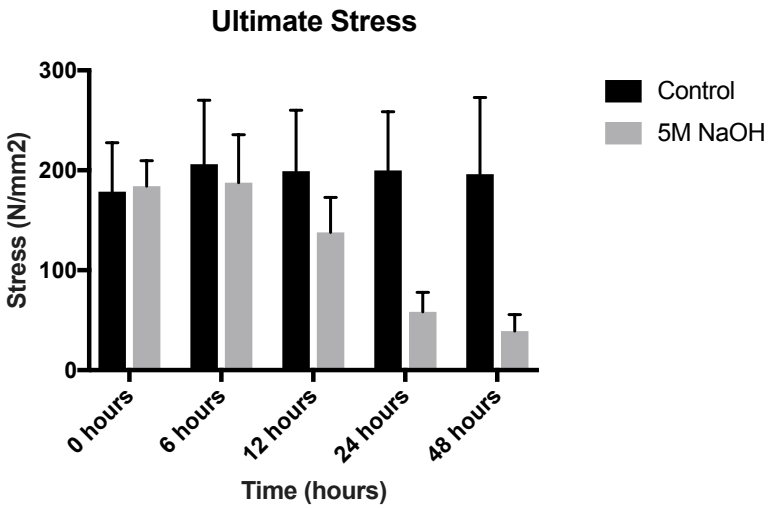

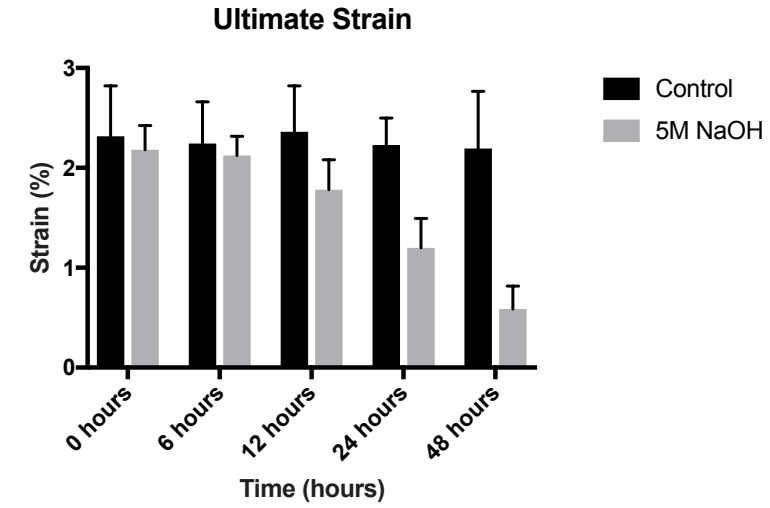
Ultimate Strain
Strain (%)
3
2
1
0
0 hours
6 hours
12 hours
24 hours
48 hours
Time (hours)
Control
5M NaOH

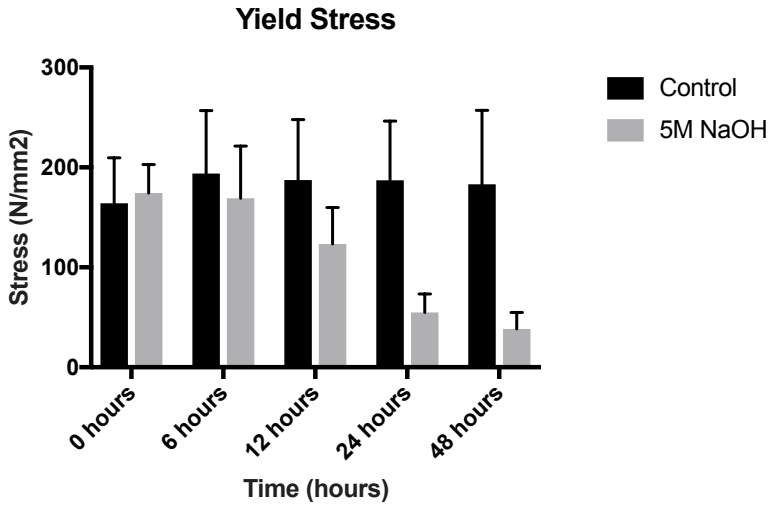
Yield Stress
Stress (N/mm2)
300
200
100
0
0 hours
6 hours
12 hours
24 hours
48 hours
Time (hours)
Control
5M NaOH

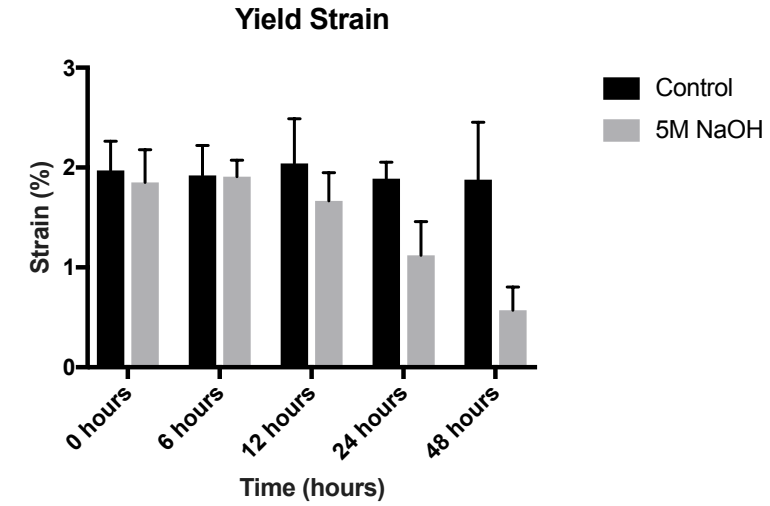
Yield Strain
Strain (%)
3
2
1
0
0 hours
6 hours
12 hours
24 hours
48 hours
Time (hours)
Control
5M NaOH

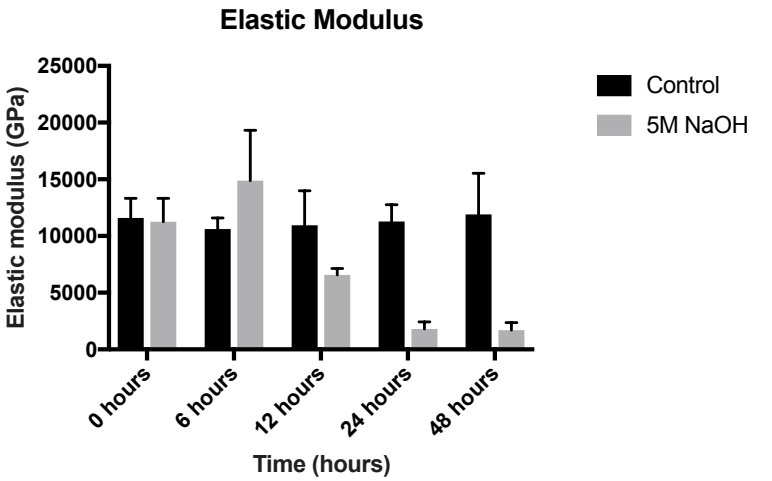
Elastic Modulus
Elastic modulus (GPa)
25000
20000
15000
10000
5000
0
0 hours
6 hours
12 hours
24 hours
48 hours
Time (hours)
Control
5M NaOH

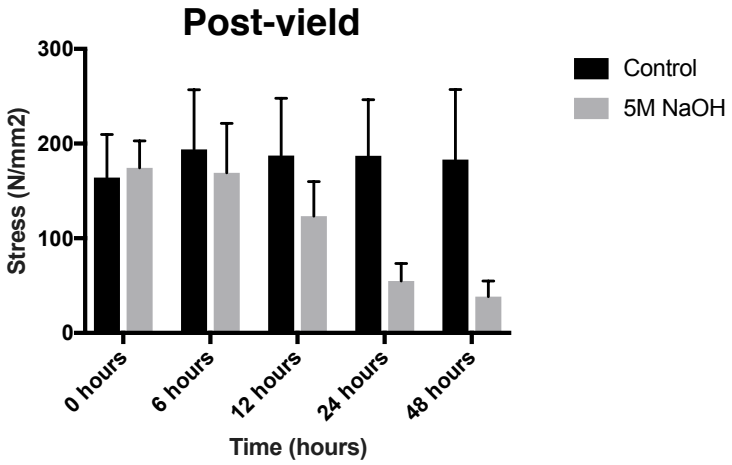
Post-yield
Stress (N/mm2)
300
200
100
0
0 hours
6 hours
12 hours
24 hours
48 hours
Time (hours)
Control
5M NaOH

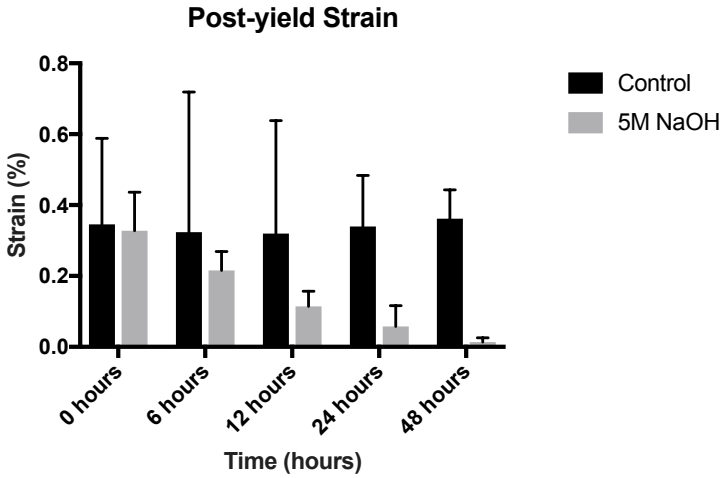
Post-yield Strain
Strain (%)
0.8
0.6
0.4
0.2
0.0
0 hours
6 hours
12 hours
24 hours
48 hours
Time (hours)
Control
5M NaOH

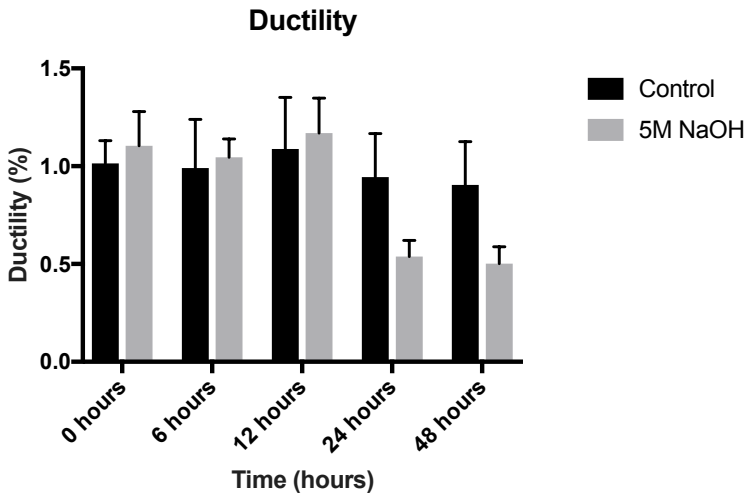
Ductility
1.5
1.0
0.5
0.0
Ductility (%)
0 hours
6 hours
12 hours
24 hours
48 hours
Time (hours)
Control
5M NaOH

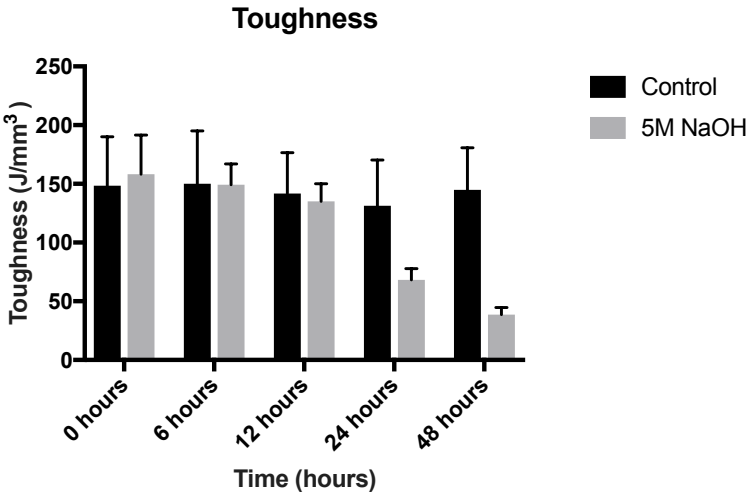
Toughness
250
200
150
100
50
0
Toughness (J/mm3)
0 hours
6 hours
12 hours
24 hours
48 hours
Time (hours)
Control
5M NaOH

### 8.3.3 Control vs 10M NaOH - mechanical values box plots

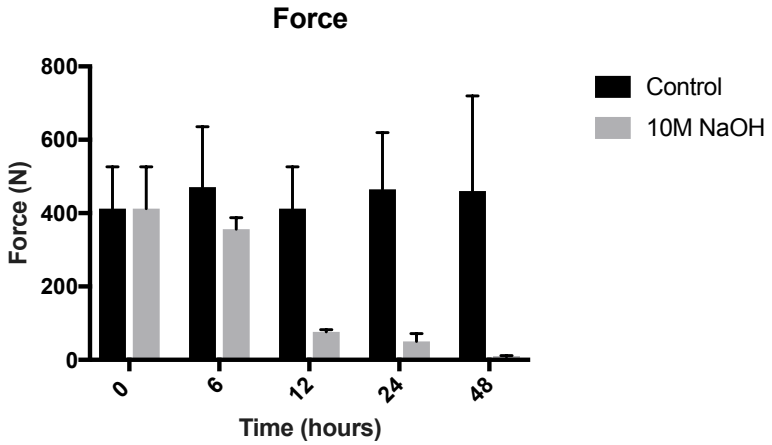


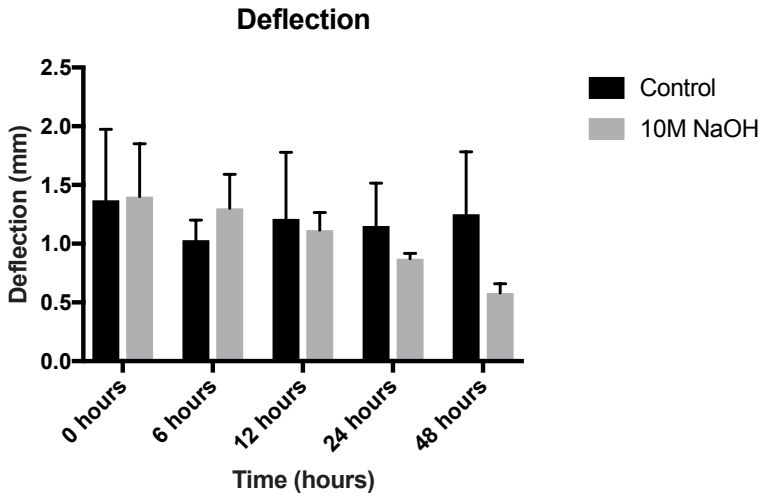


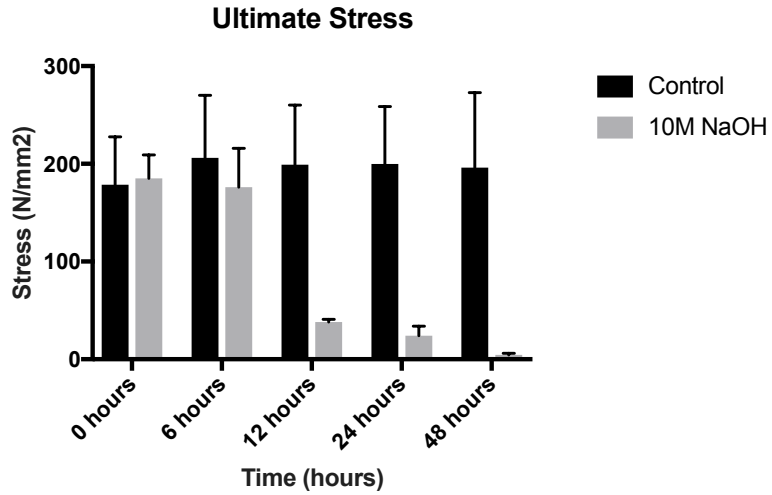

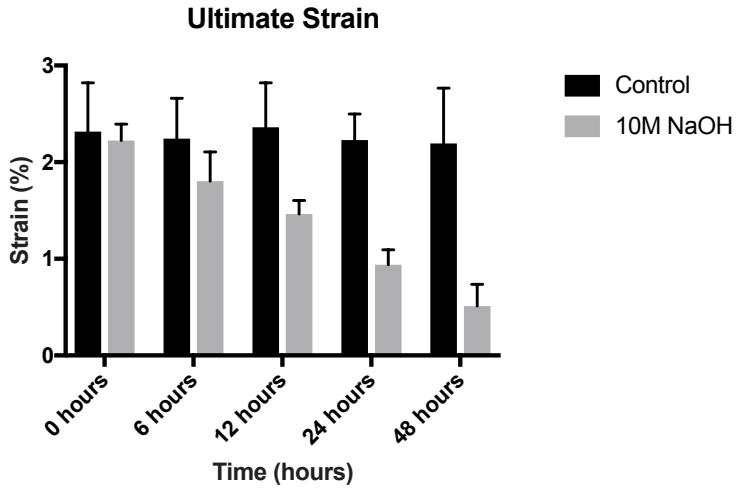
Ultimate Strain
Strain (%)
3
2
1
0
0 hours
6 hours
12 hours
24 hours
48 hours
Time (hours)
Control
10M NaOH

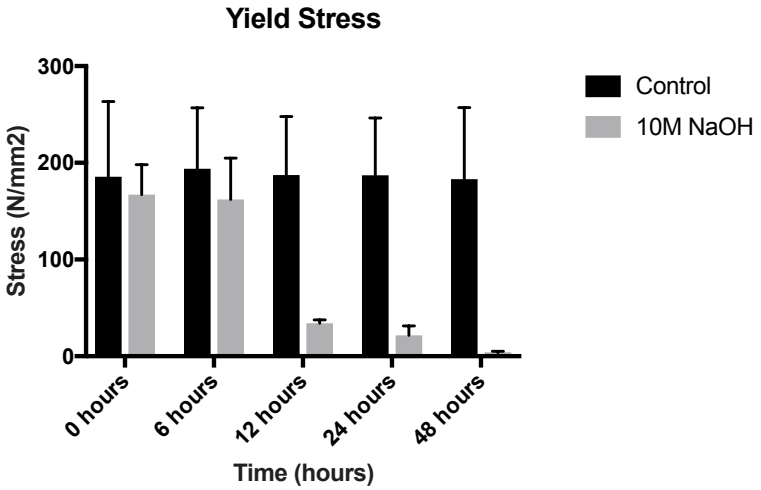
Yield Stress
Stress (N/mm2)
300
200
100
0
0 hours
6 hours
12 hours
24 hours
48 hours
Time (hours)
Control
10M NaOH

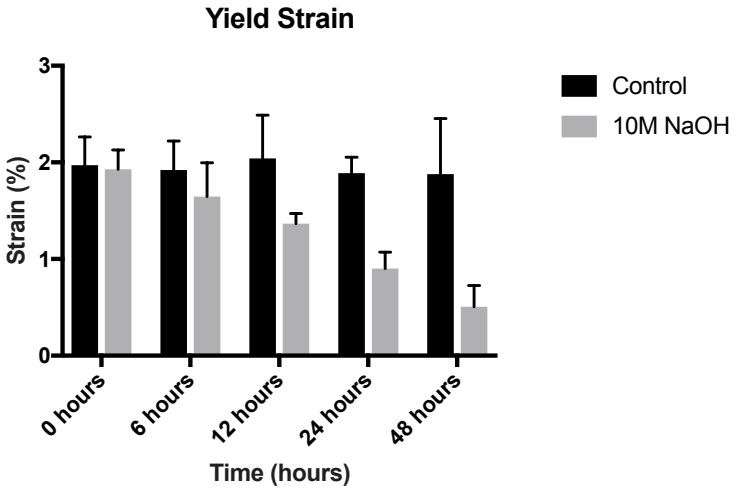
Yield Strain
Strain (%)
3
2
1
0
0 hours
6 hours
12 hours
24 hours
48 hours
Time (hours)
Control
10M NaOH

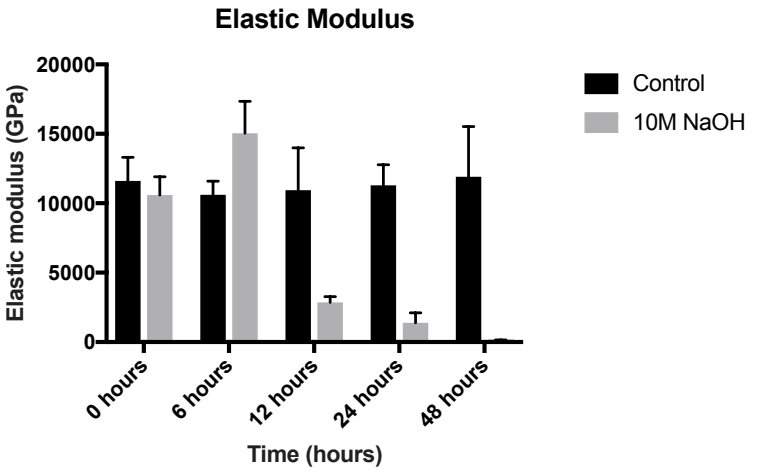
Elastic Modulus
Elastic modulus (GPa)
20000
15000
10000
5000
0
0 hours
6 hours
12 hours
24 hours
48 hours
Time (hours)
Control
10M NaOH

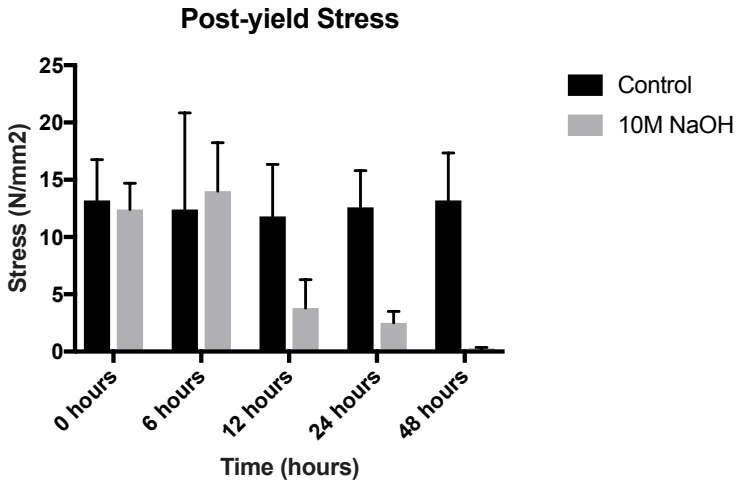
Post-yield Stress
Stress (N/mm2)
25
20
15
10
5
0
0 hours
6 hours
12 hours
24 hours
48 hours
Time (hours)
Control
10M NaOH

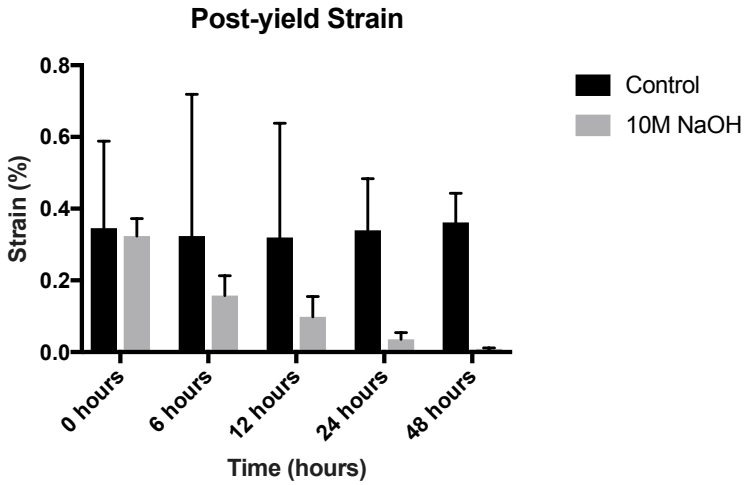
Post-yield Strain
Strain (%)
0.8
0.6
0.4
0.2
0.0
0 hours
6 hours
12 hours
24 hours
48 hours
Time (hours)
Control
10M NaOH

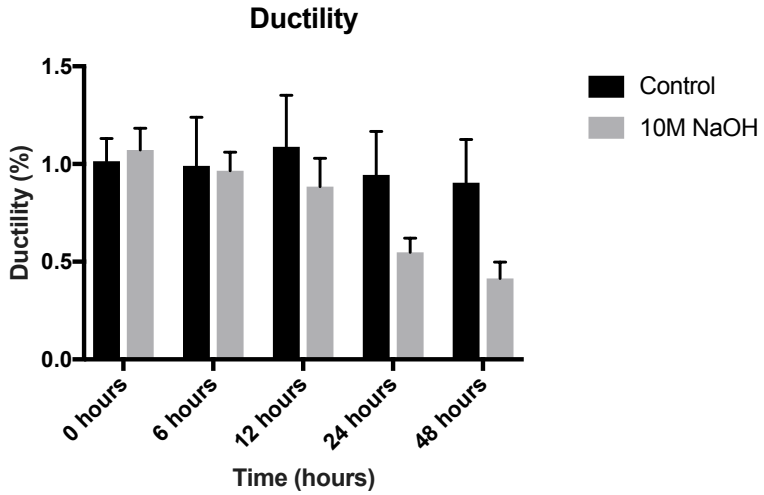
Ductility
1.5
1.0
0.5
0.0
Ductility (%)
0 hours
6 hours
12 hours
24 hours
48 hours
Time (hours)
Control
10M NaOH

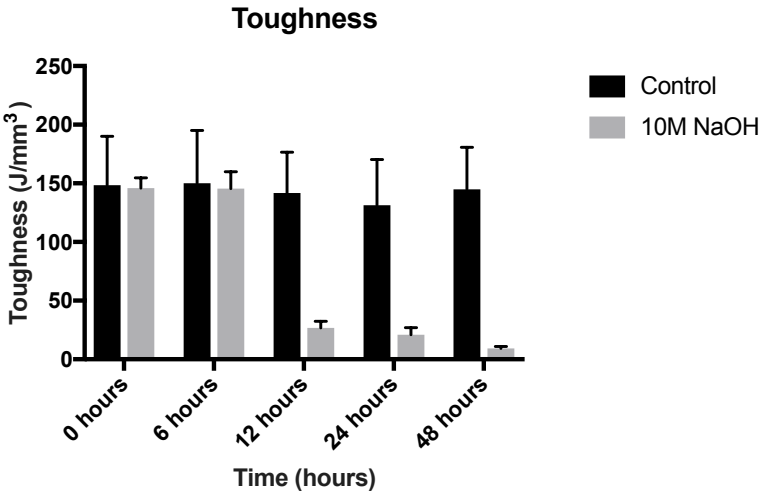
Toughness
250
200
150
100
50
0
Toughness (J/mm3)
0 hours
6 hours
12 hours
24 hours
48 hours
Time (hours)
Control
10M NaOH

### 8.3.4 Control vs solution pixel intensity

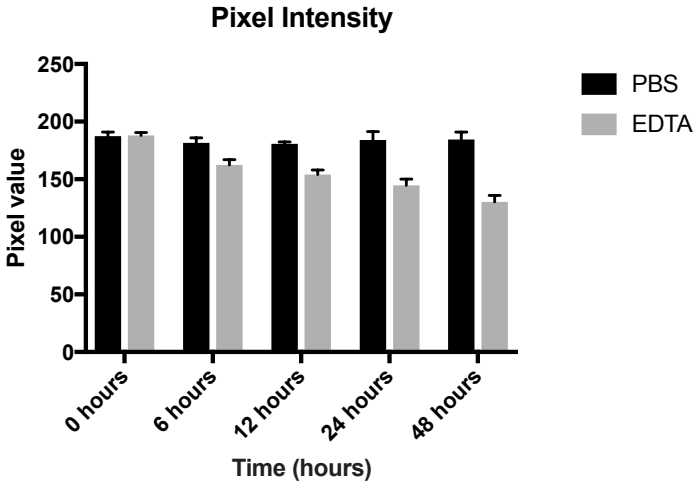


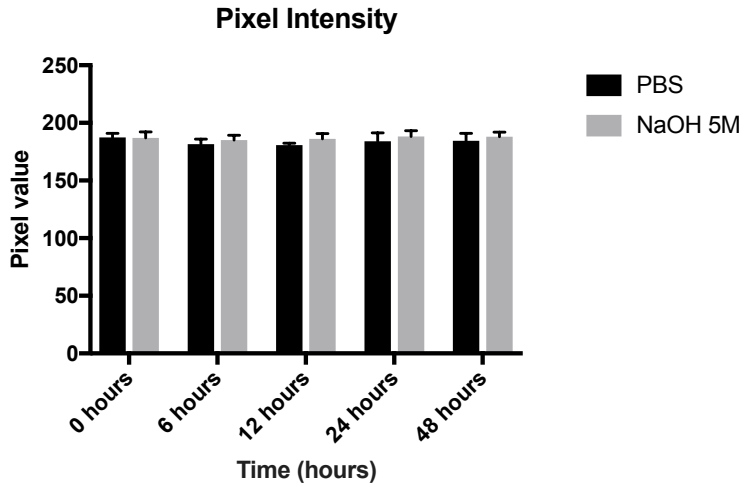


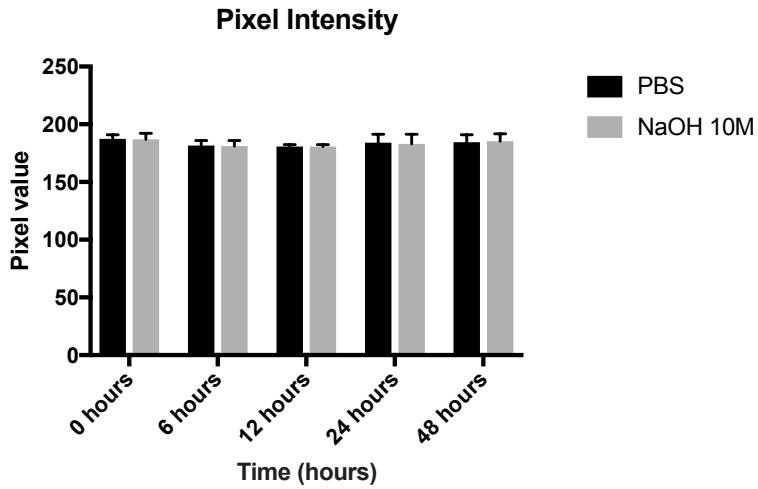

## 8.4 Appendix D - Contingency tables energy/gender vs fracture

### 8.4.1 Paediatric age group

| Paediatric group energy v fracture pattern | | | | |
|---|---|---|---|---|
| | | Simple | Comminuted | Total |
| Low energy | Observed | 14 | 0 | 14 |
| | Expected | 12.9 | 1.1 | 30 |
| High energy | Observed | 21 | 3 | 24 |
| | Expected | 22.2 | 1.9 | 38 |
| Total | Observed | 35 | 3 | 38 |
| | Expected | 35 | 3 | 38 |

| Paediatric energy v fracture type | | | | | |
|---|---|---|---|---|---|
| | | Transverse | Oblique | Spiral | Total |
| Low energy | Observed | 1 | 10 | 3 | 14 |
| | Expected | 1.8 | 5.5 | 6.6 | 14 |
| High energy | Observed | 4 | 5 | 15 | 24 |
| | Expected | 3.2 | 9.5 | 11.4 | 24 |
| Total | Observed | 5 | 15 | 18 | 38 |
| | Expected | 6 | 14 | 18 | 38 |

| Paediatric gender v fracture pattern | | | | |
|---|---|---|---|---|
| | | Simple | Comminuted | Total |
| Female | Observed | 7 | 1 | 8 |
| | Expected | 7.4 | 0.6 | 8 |
| Male | Observed | 28 | 2 | 30 |
| | Expected | 27.6 | 2.4 | 30 |
| Total | Observed | 35 | 3 | 38 |
| | Expected | 35 | 3 | 38 |

### 8.4.2 Adult age group

| Adult group energy v fracture pattern | | | | |
|---|---|---|---|---|
| | | Simple | Comminuted | Total |
| Low energy | Observed | 4 | 2 | 6 |
| | Expected | 0.8 | 5.2 | 6 |
| High energy | Observed | 1 | 30 | 31 |
| | Expected | 4.2 | 26.8 | 31 |
| Total | Observed | 5 | 32 | 37 |
| | Expected | 5 | 32 | 37 |

| Adult energy v fracture type | | | | | |
|---|---|---|---|---|---|
| | | Transverse | Oblique | Spiral | Total |
| Low energy | Observed | 0 | 5 | 1 | 6 |
| | Expected | 0.8 | 4.2 | 1.0 | 6 |
| High energy | Observed | 5 | 21 | 5 | 31 |
| | Expected | 4.2 | 21.8 | 5.0 | 31 |
| Total | Observed | 5 | 26 | 6 | 37 |
| | Expected | 5 | 26 | 6 | 37 |

| Adult gender v fracture pattern | | | | |
|---|---|---|---|---|
| | | Simple | Comminuted | Total |
| Female | Observed | 2 | 8 | 10 |
| | Expected | 1.4 | 8.6 | 10 |
| Male | Observed | 3 | 24 | 27 |
| | Expected | 3.6 | 23.4 | 27 |
| Total | Observed | 5 | 32 | 37 |
| | Expected | 5 | 32 | 37 |

### 8.4.3 Older age group

| Older group energy v fracture pattern | | | | |
|---|---|---|---|---|
| | | Simple | Comminuted | Total |
| Low energy | Observed | 56 | 19 | 75 |
| | Expected | 52.8 | 22.2 | 75 |
| High energy | Observed | 6 | 7 | 13 |
| | Expected | 9.2 | 3.8 | 13 |
| Total | Observed | 62 | 26 | 88 |
| | Expected | 62 | 26 | 88 |

| Older energy v fracture type | | | | | |
|---|---|---|---|---|---|
| | | Transverse | Oblique | Spiral | Total |
| Low energy | Observed | 9 | 37 | 29 | 75 |
| | Expected | 9.4 | 37.5 | 28.1 | 75 |
| High energy | Observed | 2 | 7 | 4 | 13 |
| | Expected | 1.6 | 6.5 | 4.9 | 13 |
| Total | Observed | 11 | 44 | 33 | 88 |
| | Expected | 11 | 44 | 33 | 88 |

| Older gender v fracture pattern | | | | |
|---|---|---|---|---|
| | | Simple | Comminuted | Total |
| Female | Observed | 49 | 18 | 67 |
| | Expected | 47.2 | 19.8 | 67 |
| Male | Observed | 13 | 8 | 21 |
| | Expected | 14.8 | 6.2 | 21 |
| Total | Observed | 62 | 26 | 88 |
| | Expected | 62 | 26 | 88 |

## 8.5 Appendix E - Conference papers

### European Orthopaedic Research Society, Galway, Ireland, 2018.

**"FEMORAL SHAFT FRACTURES: BONE BEHAVIOUR UNDER HIGH AND LOW ENERGY TRAUMA IN THE PAEDIATRIC, ADULT AND OLDER POPULATIONS"**

**Al-Hourani K, Wallace R, Simpson H**

**Orthopaedic Engineering Collaboration, University of Edinburgh, UK.**

**Background**

To improve understanding of fracture biomechanics in humans, bone architecture in animal models have been extensively investigated. Clinical correlation is vital in demonstrating the validity of these studies in clinical practice. This study aims to evaluate bone behaviour under high and low energy trauma in paediatric, adult and older patients.

**Methods**

Single-centre retrospective study identifying diaphyseal femoral fractures between Feb 2014 – 2017. Peri-prosthetic and pathological fractures were excluded. Patient demographics, injury mechanisms and fracture patterns were included. Patients were subdivided into groups 1 (<16yo), 2 (16-55yo) and 3 (>55yo) to reflect immature, peak bone age and osteoporotic bone respectively. Binary logistic analysis was used to assess significance of bone age with respect to fracture energy, degree of comminution and fracture pattern (p-value <0.05 was significant).

**Results**

Two hundred and six femoral shaft fractures were identified. Forty-three were excluded with 163 included in final analysis. Groups 1, 2 and 3 included 38, 37 and 88 patients respectively. One hundred and two (102) fractures were simple and 61 comminuted. Groups 1 and 3 included majority simple fractures (35/38 and 62/88 respectively); Group 2, comminuted injuries (32/37). Bone age to degree of comminution proved significant ($p<0.05$). In group 2, high energy injury was associated with comminution ($p<0.05$). Fracture pattern was not significantly associated with any group regardless of energy.

**Conclusion**

Our study demonstrates an association between degree of fracture comminution and bone age. Femoral shaft fractures showed a bimodal age distribution in paediatric and older patients with simple fractures being significantly associated with immature and osteoporotic bone. High energy mechanism trauma was directly related to fracture comminution at peak bone age.

# "THE EFFECT OF CORTICAL BONE DEMINERALISATION AND DECOLLAGENISATION ON FRACTURE BIOMECHANICS AT LOW STRAIN RATE"

**Al-Hourani K, Wallace R, Simpson H**

**Orthopaedic Engineering Collaboration, University of Edinburgh, UK.**

## Introduction

The ability of bone to resist failure is directly dependant on the material properties of bone matrix. Traditionally, inorganic content has been associated with stiffness of bone, whereas organic content has been associate with toughening mechanisms. We aimed to replicate the biomechanics of human osteoporotic cortical bone after staged demineralisation and decollagenisation of ovine cortical bone.

## Methods

Ovine femoral cortical bone specimens were demineralised in 10M EDTA under ultrasonic assistance. Decollagenisation was achieved using 5M and 10M NaOH solution. Bone mineral density was assessed by analysing radiographs of processed bone. Bone processing was undertaken at time points 0, 6, 12, 24 and 48 hours. Phosphate buffer solution was used for controls. Mechanical properties were ascertained after bone specimens underwent four-point bend testing (Zwick machine) at low strain rate. Pre-yield, yield and post-yield properties were delineated after data was captured and exported form mechanical into electronic data using TestXpert. IBM SPSS was used to input data. ANOVA testing was undertaken to compare groups with $p<0.05$ significant.

## Results

Control samples showed no difference in biomechanical properties at all time points. Demineralised bone specimens showed a gradual loss of density with a maximum loss of 29% at 48 hours ($p<0.05$). Decollagenised bone did not show a change in mineral content at 48 hours. Demineralised bone demonstrated a reduction of ultimate strength and strain at 48 hours ($p<0.05$). Decollagenised bone showed a reduction at 12 hours (10M NaOH, $p<0.05$) and 24 hours (5M NaOH, $p<0.05$). Demineralised bone showed a decrease of yield and elastic modulus at 48 hours ($p<0.05$). Decollagenised bone showed a decrease in yield properties at 12 hours and an increase in elastic modulus at 6 hours after immersion in both solution ($p<0.05$). Demineralisation had no post-yield effect. Decollagenised samples showed a significant post-yield reduction at 24 hours. Demineralised samples demonstrated an increased toughness at 48 hours ($p<0.05$) and over 90% decrease in decollagenised samples ($p<0.05$).

## Conclusion

The demineralisation of cortical bone in effect transfers load onto its organic matrix, thereby increasing its ductile behaviour. Whilst yield and ultimate stress properties decrease, demineralised bone develops an increased ability to deform under bending with an increase in yield and ultimate strain. Similarly this makes it tougher. In contrast, decollagenised cortical bone behaves as a brittle material. There is a progressive decrease in yield and ultimate properties of stress and strain with increased decollagenisation. However, there is a two-phase stiffening process, whereby there is an initial compensatory increase in stiffness, followed by a progressive decrease. Post-yield properties are almost zero with greater rates of decollagenisation, directly relating the role of collagen to this pre-failure stage.

# 9. BIBLIOGRAPHY

[1] Schlesinger PH, Blair HC, Beer Stolz D, Riazanski V, Ray EC, Tourkova IL, et al. Cellular and extracellular matrix of bone, with principles of synthesis and dependency of mineral deposition on cell membrane transport. Am J Physiol Cell Physiol. 2020;318:C111-C24.

[2] Nyman JS, Roy A, Shen X, Acuna RL, Tyler JH, Wang X. The influence of water removal on the strength and toughness of cortical bone. J Biomech. 2006;39:931-8.

[3] Ascenzi A, Bonucci E. The compressive properties of single osteons. Anat Rec. 1968;161:377-91.

[4] Ascenzi A, Bonucci E. The compressive properties of single osteons as a problem of molecular biology. Calcif Tissue Res. 1968:Suppl:44-a.

[5] Currey JD, Brear K, Zioupos P. The effects of ageing and changes in mineral content in degrading the toughness of human femora. J Biomech. 1996;29:257-60.

[6] Wang XD, Masilamani NS, Mabrey JD, Alder ME, Agrawal CM. Changes in the fracture toughness of bone may not be reflected in its mineral density, porosity, and tensile properties. Bone. 1998;23:67-72.

[7] Zioupos P, Currey JD. Changes in the stiffness, strength, and toughness of human cortical bone with age. Bone. 1998;22:57-66.

[8] Robinson RA. An electron-microscopic study of the crystalline inorganic component of bone and its relationship to the organic matrix. J Bone Joint Surg Am. 1952;34-A:389-435; passim.

[9] Robinson RA, Watson ML. Collagen-crystal relationships in bone as seen in the electron microscope. Anat Rec. 1952;114:383-409.

[10] Weiner S, Traub W. Organization of hydroxyapatite crystals within collagen fibrils. FEBS Lett. 1986;206:262-6.

[11] Traub W, Arad T, Weiner S. Growth of mineral crystals in turkey tendon collagen fibers. Connect Tissue Res. 1992;28:99-111.

[12] Weiner S, Traub W. Bone structure: from angstroms to microns. FASEB J. 1992;6:879-85.

[13] Landis WJ, Song MJ, Leith A, McEwen L, McEwen BF. Mineral and organic matrix interaction in normally calcifying tendon visualized in three dimensions by high-voltage electron microscopic tomography and graphic image reconstruction. J Struct Biol. 1993;110:39-54.

[14] Baselt DR, Revel JP, Baldeschwieler JD. Subfibrillar structure of type I collagen observed by atomic force microscopy. Biophys J. 1993;65:2644-55.
[15] Tzaphlidou M. The role of collagen in bone structure: an image processing approach. Micron. 2005;36:593-601.
[16] Viguet-Carrin S, Garnero P, Delmas PD. The role of collagen in bone strength. Osteoporos Int. 2006;17:319-36.
[17] Kuznetsova N, Leikin S. Does the triple helical domain of type I collagen encode molecular recognition and fiber assembly while telopeptides serve as catalytic domains? Effect of proteolytic cleavage on fibrillogenesis and on collagen-collagen interaction in fibers. J Biol Chem. 1999;274:36083-8.
[18] Robins SP, Bailey AJ. The chemistry of the collagen cross-links. Characterization of the products of reduction of skin, tendon and bone with sodium cyanoborohydride. Biochem J. 1977;163:339-46.
[19] Engel J, Prockop DJ. The zipper-like folding of collagen triple helices and the effects of mutations that disrupt the zipper. Annu Rev Biophys Biophys Chem. 1991;20:137-52.
[20] Saito M, Marumo K, Fujii K, Ishioka N. Single-column high-performance liquid chromatographic-fluorescence detection of immature, mature, and senescent cross-links of collagen. Anal Biochem. 1997;253:26-32.
[21] Uzawa K, Grzesik WJ, Nishiura T, Kuznetsov SA, Robey PG, Brenner DA, et al. Differential expression of human lysyl hydroxylase genes, lysine hydroxylation, and cross-linking of type I collagen during osteoblastic differentiation in vitro. J Bone Miner Res. 1999;14:1272-80.
[22] Saito M, Fujii K, Marumo K. Degree of mineralization-related collagen crosslinking in the femoral neck cancellous bone in cases of hip fracture and controls. Calcif Tissue Int. 2006;79:160-8.
[23] Saito M, Fujii K, Soshi S, Tanaka T. Reductions in degree of mineralization and enzymatic collagen cross-links and increases in glycation-induced pentosidine in the femoral neck cortex in cases of femoral neck fracture. Osteoporos Int. 2006;17:986-95.
[24] Shiraki M, Kuroda T, Tanaka S, Saito M, Fukunaga M, Nakamura T. Nonenzymatic collagen cross-links induced by glycoxidation (pentosidine) predicts vertebral fractures. J Bone Miner Metab. 2008;26:93-100.
[25] Saito M, Marumo K. Collagen cross-links as a determinant of bone quality: a possible explanation for bone fragility in aging, osteoporosis, and diabetes mellitus. Osteoporos Int. 2010;21:195-214.

[26] Niyibizi C, Eyre DR. Bone type V collagen: chain composition and location of a trypsin cleavage site. Connect Tissue Res. 1989;20:247-50.
[27] Niyibizi C, Chan R, Wu JJ, Eyre D. A 92 kDa gelatinase (MMP-9) cleavage site in native type V collagen. Biochem Biophys Res Commun. 1994;202:328-33.
[28] Niyibizi C, Eyre DR. Structural characteristics of cross-linking sites in type V collagen of bone. Chain specificities and heterotypic links to type I collagen. Eur J Biochem. 1994;224:943-50.
[29] Fujii K, Kuboki Y, Sasaki S. Aging of human bone and articular cartilage collagen: changes in the reducible cross-links and their precursors. Gerontology. 1976;22:363-70.
[30] Mueller KH, Trias A, Ray RD. Bone density and compostiton. Age-related and pathological changes in water and mineral content. J Bone Joint Surg Am. 1966;48:140-8.
[31] Dong P, Haupert S, Hesse B, Langer M, Gouttenoire PJ, Bousson V, et al. 3D osteocyte lacunar morphometric properties and distributions in human femoral cortical bone using synchrotron radiation micro-CT images. Bone. 2014;60:172-85.
[32] Robinson RA. Physiocochemical structure of bone. Clin Orthop Relat Res. 1975:263-315.
[33] Rho JY, Kuhn-Spearing L, Zioupos P. Mechanical properties and the hierarchical structure of bone. Med Eng Phys. 1998;20:92-102.
[34] Hodge A, J P. Recent studies with the electron microscope on ordered aggregates of the tropocollagen molecule. Aspect of Protein Structure. 1963:289-300.
[35] Katz JL. Anisotropy of Young's modulus of bone. Nature. 1980;283:106-7.
[36] Keaveny TM, Morgan EF, Niebur GL, Yeh OC. Biomechanics of trabecular bone. Annu Rev Biomed Eng. 2001;3:307-33.
[37] Bonfield W, Grynpas MD, Young RJ. Anisotropy of the Young’s modulus of bone. Nature. 1977;270:453-54.
[38] Dempster WT, Coleman RF. Tensile strength of bone along and across the grain. J App Physiol. 1960;16:355-60.
[39] J W. Uber die innere Architektur der Knochen und ihre Bedeutung fur die Frage vom Knochenwachstum. Archiv fur pathologische Anato/nie und Physiologie und fur klinische Medizin,. 1870;50:389-453.
[40] J W. The Law of Bone Remodelling. Springer-Verlag. 1986;Translated by P Maquet and R Furlong.
[41] Friedenberg ZB, Brighton CT. Bioelectric potentials in bone. J Bone Joint Surg Am. 1966;48:915-23.
[42] Fukada E, I Y. On the piezoeletric effect of bone. J Phys Soc Japan. 1957;12:1158-62.

[43] Pienkowski D, Pollack SR. The origin of stress-generated potentials in fluid-saturated bone. J Orthop Res. 1983;1:30-41.
[44] Bourrin S, Palle S, Pupier R, Vico L, Alexandre C. Effect of physical training on bone adaptation in three zones of the rat tibia. J Bone Miner Res. 1995;10:1745-52.
[45] Forwood MR, Turner CH. Skeletal adaptations to mechanical usage: results from tibial loading studies in rats. Bone. 1995;17:197S-205S.
[46] Hillam RA, Skerry TM. Inhibition of bone resorption and stimulation of formation by mechanical loading of the modeling rat ulna in vivo. J Bone Miner Res. 1995;10:683-9.
[47] Salter DM, Robb JE, Wright MO. Electrophysiological responses of human bone cells to mechanical stimulation: evidence for specific integrin function in mechanotransduction. J Bone Miner Res. 1997;12:1133-41.
[48] Qin YX, Lin W, Rubin C. The pathway of bone fluid flow as defined by in vivo intramedullary pressure and streaming potential measurements. Ann Biomed Eng. 2002;30:693-702.
[49] Butcher MT, Espinoza NR, Cirilo SR, Blob RW. In vivo strains in the femur of river cooter turtles (Pseudemys concinna) during terrestrial locomotion: tests of force-platform models of loading mechanics. J Exp Biol. 2008;211:2397-407.
[50] Scott A, Khan KM, Duronio V, Hart DA. Mechanotransduction in human bone: in vitro cellular physiology that underpins bone changes with exercise. Sports Med. 2008;38:139-60.
[51] Reilly DT, Burstein AH. The elastic and ultimate properties of compact bone tissue. J Biomech. 1975;8:393-405.
[52] Tornetta P, Ricci W, McQueen M. Rockwood and Green's fractures in adults. 2019;9th Edition. Chapter 1,:3-10.
[53] Z H. Elastic moduli of heterogeneous materials. J Appl Mech. 1962;29:143-50.
[54] Bucholz R, Court Brown C, ., Heckman J, Tornetta P. Rockwood and Green's Fractures in Adults. Seventh Edition ed2009.
[55] HB C. Thermodynamics and an Introduction to Thermostatistics. Second Ed John Wiley & Sons. 1985.
[56] Cowin SC. The mechanical and stress adaptive properties of bone. Ann Biomed Eng. 1983;11:263-95.
[57] Cowin SC. Bone stress adaptation models. J Biomech Eng. 1993;115:528-33.
[58] Lakes RS, Katz JL. Interrelationships among the viscoelastic functions for anisotropic solids: application to calcified tissues and related systems. J Biomech. 1974;7:259-70.

[59] Carter DR, Hayes WC. Compact bone fatigue damage--I. Residual strength and stiffness. J Biomech. 1977;10:325-37.
[60] Shepherd TN, Zhang J, Ovaert TC, Roeder RK, Niebur GL. Direct comparison of nanoindentation and macroscopic measurements of bone viscoelasticity. J Mech Behav Biomed Mater. 2011;4:2055-62.
[61] Crowninshield RD, Pope H. The response of compact bone in tension at various strain rates. Annals of Biomedical Engineering. 1974;2:217-25.
[62] Wright TM, Hayes WC. Tensile testing of bone over a wide range of strain rates: effects of strain rate, microstructure and density. Medical and biological engineering. 1976;14.
[63] Panjabi MM, White AA, 3rd, Southwick WO. Mechanical properties of bone as a function of rate of deformation. J Bone Joint Surg Am. 1973;55:322-30.
[64] Wallace RJ, Pankaj P, Simpson AH. The effect of strain rate on the failure stress and toughness of bone of different mineral densities. J Biomech. 2013;46:2283-7.
[65] Launey ME, Beuhler MJ, Ritchie RO. On the Mechanistic Origins of Toughness in Bone. Annu Rev Mater Res. 2010;40:25.
[66] Ritchie RO. Mechanisms of fatigue crack-propagation in metals, ceramics and composites: role of crack tip shielding. Mater Sci Eng. 1988;103:15-28.
[67] Ritchie RO. Mechanisms of fatigue-crack propagation in ductile and brittle solids. Int J Fract. 1999;100:55-83.
[68] ME L, RO R. On the fracture toughness of advanced materials. Adv Mater. 2009;21:2103-10.
[69] Ritchie RO, Koester KJ, Ionova S, Yao W, Lane NE, Iii AJ. Measurement of the toughness of bone: a tutorial with special reference to small animal studies. Bone. 2008;5:798-812.
[70] E-1820 AS. Standard test method for measurement of fracture toughness. West Conshohocken, PA: American Society for Testing and Materials. 2006.
[71] Ural A, Vashishth D. Effects of intracortical porosity on fracture toughness in aging human bone: a microCT-based cohesive finite element study. J Biomech Eng. 2007;129:625-31.
[72] Davies E, Muller KH, Wong WC, Pickard CJ, Reid DG, Skepper JN, et al. Citrate bridges between mineral platelets in bone. Proc Natl Acad Sci U S A. 2014;11:1354-63.
[73] Wess TJ, Orgel JP. Changes in collagen structure: drying, dehydrothermal treatment and relation to long term deterioration. Thermochimica Acta. 2000;1:119-28.

[74] Smith JW, Walmsley R. Factors affecting the elasticity of bone. Journal of Anatomy. 1959;4:503.
[75] Faingold A, Cohen SR, Shahar R, Weiner S, Rapoport L, HD. W. The effect of hydration on mechanical anisotropy, topography and fibril organization of the osteonal lamellae. J Biomech. J Biomech. 2014;47:367-72.
[76] Wenger MP, Laurent B, Michael AH, Patrick M. Mechanical properties of collagen fibrils. Biophysical journa. 2007;93:1255-63.
[77] Broz JJ, Simske SJ, Greenberg AR, Luttges MW. Effects of rehydration state on the flexural properties of whole mouse long bones. J Biomech Eng. 1993;115:447-9.
[78] Nyman JS, Anuradha R, Xinmei S, Rae LA, Jerrod HT, Xiaodu W. The influence of water removal on the strength and toughness of cortical bone. Journal of biomechanics. 2006;39:931-38.
[79] Nyman JS, Lacey E, Gorochow R, Horch A, Uppuganti S, Zein-Sabatto A, et al. Partial removal of pore and loosely bound water by low-energy drying decreases cortical bone toughness in young and old donors. Journal of the mechanical behavior of biomedical materials. 2013;22:136-45.
[80] Yan J, Amit D, Rajendra K, JJ. M. Fracture toughness and work of fracture of hydrated, dehydrated, and ashed bovine bone. Journal of biomechanics. 2008;41:1929-36.
[81] JW. M, Evans FG. Crack propagation in bone. Biomechanics Symposium ASME. 1973:87-8.
[82] Rho JY, Ashman RB, Turner CH. Young's modulus of trabecular and cortical bone material: ultrasonic and microtensile measurements. J Biomech. 1993;26:111-9.
[83] Bayraktar HH, Morgan EF, Niebur GL, Morris GE, Wong EK, Keaveny TM. Comparison of the elastic and yield properties of human femoral trabecular and cortical bone tissue. J Biomech. 2004;37:27-35.
[84] Choi K, Kuhn JL, Ciarelli MJ, Goldstein SA. The elastic moduli of human subchondral, trabecular, and cortical bone tissue and the size-dependency of cortical bone modulus. J Biomech. 1990;23:1103-13.
[85] Kuhn JL, Goldstein SA, Choi K, London M, Feldkamp LA, Matthews LS. Comparison of the trabecular and cortical tissue moduli from human iliac crests. J Orthop Res. 1989;7:876-84.
[86] Ryan SD, Williams JL. Tensile testing of rodlike trabeculae excised from bovine femoral bone. J Biomech. 1989;22:351-5.
[87] Mujika F. On the effect of shear and local deformation in three-point bending tests. Polymer Testing. 2007;26:869-77.

[88] Perren SM. Physical and biological aspects of fracture healing with special reference to internal fixation. Clin Orthop Relat Res. 1979:175-96.
[89] Fung Y. Biomechanics: Mechanical properties of living tissues. Springer New York. 1993.
[90] Reilly DT, Burstein AH, Frankel VH. The elastic modulus for bone. J Biomech. 1974;7:271-5.
[91] Burstein AH, Reilly DT, Martens M. Aging of bone tissue: mechanical properties. J Bone Joint Surg Am. 1976;58:82-6.
[92] Keller TS, Mao Z, Spengler DM. Young's modulus, bending strength, and tissue physical properties of human compact bone. J Orthop Res. 1990;8:592-603.
[93] Carter DR, Hayes WC. Compact bone fatigue damage: a microscopic examination. Clin Orthop Relat Res. 1977:265-74.
[94] Carter DR, Hayes WC. The compressive behavior of bone as a two-phase porous structure. J Bone Joint Surg Am. 1977;59:954-62.
[95] Carter DR, Caler WE, Spengler DM, Frankel VH. Fatigue behavior of adult cortical bone: the influence of mean strain and strain range. Acta Orthop Scand. 1981;52:481-90.
[96] McElhaney J, Fogle J, Byars E, Weaver G. Effect of Embalming on the Mechanical Properties of Beef Bone. J Appl Physiol. 1964;19:1234-6.
[97] McElhaney JH. Dynamic response of bone and muscle tissue. J Appl Physiol. 1966;21:1231-6.
[98] Crowninshield RD PM. The response of compact bone in tension at various strain rates. Annals of Biomedical Engineering. 1974;2:217-25.
[99] Currey JD. The effects of strain rate, reconstruction and mineral content on some mechanical properties of bovine bone. J Biomech. 1975;8:81-6.
[100] Carter DR, Hayes WC. Bone compressive strength: the influence of density and strain rate. Science. 1976;194:1174-6.
[101] Saha S, Hayes WC. Tensile impact properties of human compact bone. J Biomech. 1976;9:243-51.
[102] Wright TM, Hayes WC. Tensile testing of bone over a wide range of strain rates: effects of strain rate, microstructure and density. Med Biol Eng. 1976;14:671-80.
[103] Robertson DM, Smith DC. Compressive strength of mandibular bone as a function of microstructure and strain rate. J Biomech. 1978;11:455-71.
[104] Behiri JC, Bonfield W. Fracture mechanics of bone--the effects of density, specimen thickness and crack velocity on longitudinal fracture. J Biomech. 1984;17:25-34.

[105] Evans GP, Behiri JC, Vaughan LC, Bonfield W. The response of equine cortical bone to loading at strain rates experienced in vivo by the galloping horse. Equine Vet J. 1992;24:125-8.
[106] Pithioux M, Subit D, Chabrand P. Comparison of compact bone failure under two different loading rates: experimental and modelling approaches. Med Eng Phys. 2004;26:647-53.
[107] Yamashita J, Li X, Furman BR, Rawls HR, Wang X, Agrawal CM. Collagen and bone viscoelasticity: a dynamic mechanical analysis. J Biomed Mater Res. 2002;63:31-6.
[108] Hansen U, Zioupos P, Simpson R, Currey JD, Hynd D. The effect of strain rate on the mechanical properties of human cortical bone. J Biomech Eng. 2008;130:011011.
[109] Boyde A, Bianco P, Portigliatti Barbos M, Ascenzi A. Collagen orientation in compact bone: I. A new method for the determination of the proportion of collagen parallel to the plane of compact bone sections. Metab Bone Dis Relat Res. 1984;5:299-307.
[110] Portigliatti Barbos M, Bianco P, Ascenzi A, Boyde A. Collagen orientation in compact bone: II. Distribution of lamellae in the whole of the human femoral shaft with reference to its mechanical properties. Metab Bone Dis Relat Res. 1984;5:309-15.
[111] Reilly GC, Currey JD. The development of microcracking and failure in bone depends on the loading mode to which it is adapted. J Exp Biol. 1999;202:543-52.
[112] Rubin CT, Lanyon LE. Limb mechanics as a function of speed and gait: a study of functional strains in the radius and tibia of horse and dog. J Exp Biol. 1982;101:187-211.
[113] Biewener AA, Thomason J, Goodship A, Lanyon LE. Bone stress in the horse forelimb during locomotion at different gaits: a comparison of two experimental methods. J Biomech. 1983;16:565-76.
[114] Riggs CM, Lanyon LE, Boyde A. Functional associations between collagen fibre orientation and locomotor strain direction in cortical bone of the equine radius. Anat Embryol (Berl). 1993;187:231-8.
[115] Fratzl P, Schreiber S, Boyde A. Characterization of bone mineral crystals in horse radius by small-angle X-ray scattering. Calcif Tissue Int. 1996;58:341-6.
[116] Evans FG. Relations between the microscopic structure and tensile strength of human bone. Acta Anat (Basel). 1958;35:285-301.
[117] Kotani Y, Cunningham BW, Parker LM, Kanayama M, McAfee PC. Static and fatigue biomechanical properties of anterior thoracolumbar instrumentation systems. A synthetic testing model. Spine (Phila Pa 1976). 1999;24:1406-13.

[118] Weaver JK, Chalmers J. Cancellous bone: its strength and changes with aging and an evaluation of some methods for measuring its mineral content. J Bone Joint Surg Am. 1966;48:289-98.
[119] Galante J, Rostoker W, Ray RD. Physical properties of trabecular bone. Calcif Tissue Res. 1970;5:236-46.
[120] Kleerekoper M, Villanueva AR, Stanciu J, Rao DS, Parfitt AM. The role of three-dimensional trabecular microstructure in the pathogenesis of vertebral compression fractures. Calcif Tissue Int. 1985;37:594-7.
[121] Davidson JS, Brown DJ, Barnes SN, Bruce CE. Simple treatment for torus fractures of the distal radius. J Bone Joint Surg Br. 2001;83:1173-5.
[122] van der Meulen MC, Jepsen KJ, Mikic B. Understanding bone strength: size isn't everything. Bone. 2001;29:101-4.
[123] Donnelly E. Methods for assessing bone quality: a review. Clin Orthop Relat Res. 2011;469:2128-38.
[124] Khan Y. Encyclopedia of Biomedical Engineering. 2019;1:537-45.
[125] I Hofinger, M Oechsner, HA Bahr, Swain M. Modified four-point bending specimen for determining the interface fracture energy for thin, brittle layers. International Journal of Fracture. 1998;92:213-20.
[126] Hodgskinson R, Currey JD, Evans GP. Hardness, an indicator of the mechanical competence of cancellous bone. J Orthop Res. 1989;7:754-8.
[127] Hansma P, Turner P, Drake B, Yurtsev E, Proctor A, Mathews P, et al. The bone diagnostic instrument II: indentation distance increase. Rev Sci Instrum. 2008;79:064303.
[128] Oliver Cw, Pharr GM. An improved technique for determining hardness and elastic modulus using load and displacement sensing indentation experiments. Journal of materials research. 1992;7.
[129] Kazakia GJ, Majumdar S. New imaging technologies in the diagnosis of osteoporosis. Rev Endocr Metab Disord. 2006;7:67-74.
[130] Hrenikoff A. Solution of problems of elasticity by the framework method. Journal of Applied Mechanics. 1941;8:169-75.
[131] Courant R. Variational methods for the solution of problems of equilibrium and vibrations. Bulletin of the American Mathematical Society. 1943;49:1-23.
[132] Chevalier Y, Pahr D, Allmer H, Charlebois M, Zysset P. Validation of a voxel-based FE method for prediction of the uniaxial apparent modulus of human trabecular bone using macroscopic mechanical tests and nanoindentation. J Biomech. 2007;40:3333-40.

[133] Weidenreich F. Das Knochengewehe. Mollendorf's Handbuch der microskopischenAnatomie des Menchen. 1930;11:391-520.
[134] Schmidt WJ. Grenzsheiden der Lakunen und Kittlinien des Knochengewebes. Zellforsch. 1959;50:275-96.
[135] Philipson B. Composition of Cement Lines in Bone. The Journal of Histochemistry and Cytochemistry. 1964;13:270-81.
[136] Parfitt MA. The physiologic and clinical significance of bone histomorphometric data. Bone histomorphometry: techniques and interpretation. 1983:143-223.
[137] Zhou H, Chernecky R, Davies JE. Deposition of cement at reversal lines in rat femoral bone. J Bone Miner Res. 1994;9:367-74.
[138] Dong X, Zhang N, Guo XE. Interfacial strength of cement lines in human cortical bone. MCB-TECH Science Press. 2005;2:63.
[139] Bigley RF, Griffin LV, Christensen L, Vandenbosch R. Osteon interfacial strength and histomorphometry of equine cortical bone. Journal of biomechanics. 2006;39:1629-40.
[140] Krishnamoorthy A, Mercy J, Vineeth K, M S. Delamination Analysis of Carbon Fiber Reinforced Plastic (CFRP) Composite plates by Thermo graphic technique. Materials today: Proceedings. 2014;2:3132-39.
[141] Favre J, Jacques D. Stress transfer by shear in carbon fibre model composites. Journal of Materials Science. 1990;25:1372-80.
[142] Phillips D. Interfacial bonding and the toughness of carbon fibre reinforced glass and glass-ceramics. Journal of Materials Science. 1974;9:1847-54.
[143] Harris B, Beaumont PWR, de Ferran EM. Strength and fracture toughness of carbon fibre polyester composites. Journal of Materials Science. 1971;6.
[144] Fantner GE, Rabinovych O, Schitter G, Thurner P, Kindt JH, Finch MM, et al. Hierarchical interconnections in the nano-composite material bone: Fibrillar cross-links resist fracture on several length scales. Composites Science and Technology. 2006;66:1205-11.
[145] Guidelines for preclinical evaluation and clinical trials in osteoporosis. World Health Organization Geneva. 1998.
[146] Leng H, Dong X, Wang X. Progressive post-yield behavior of human cortical bone in compression for middle-aged and elderly groups. Journal of biomechanics. 2009;42.
[147] Zioupos P, Kirchner H, Peterlik H, 2020. Ageing bone fractures: The case of a ductile to brittle transition that shifts with age. Bone, 131, p.115176. Ageing bone fractures: The case of a ductile to brittle transition that shifts with age. Bone. 2020;131:2-8.

[148] Sink EL, Gralla J, Repine M. Complications of pediatric femur fractures treated with titanium elastic nails: a comparison of fracture types. J Pediatr Orthop. 2005;25:577-80.
[149] Saikia K, Bhuyan S, Bhattacharya T, Saikia S. Titanium elastic nailing in femoral diaphyseal fractures of children in 6-16 years of age. Indian J Orthop. 2007;41:381-5.
[150] Cohen H, Kugel C, May H, Medlej B, Stein D, Slon V, et al. The impact velocity and bone fracture pattern: Forensic perspective. Forensic Sci Int. 2016;266:54-62.
[151] Alms M. Fracture mechanics. J Bone Joint Surg Br. 1961;43-B:162-6.
[152] Carter DR, Schwab GH, Spengler DM. Tensile fracture of cancellous bone. Acta Orthop Scand. 1980;51:733-41.
[153] Johner R, Wruhs O. Classification of tibial shaft fractures and correlation with results after rigid internal fixation. Clin Orthop Relat Res. 1983:7-25.
[154] Rixford E. Theory and Treatment of Spiral Fractures. Ann Surg. 1925;81:368-73.
[155] Wang X, Bank RA, TeKoppele JM, Hubbard GB, Athanasiou KA, Agrawal CM. Effect of collagen denaturation on the toughness of bone. Clin Orthop Relat Res. 2000:228-39.
[156] Turner CH. Bone strength: current concepts. Ann N Y Acad Sci. 2006;1068:429-46.
[157] Currey JD. The mechanical consequences of variation in the mineral content of bone. Journal of biomechanics. 1969;2:1-11.
[158] Currey JD. The relationship between the stiffness and the mineral content of bone. J Biomech. 1969;2:477-80.
[159] Vose GP, Kubala AL. Bone strength—its relationship to x-ray-determined ash content. Human Biology. 1959;31:261-70.
[160] Portigliatti Barbos M, Bianco P, Ascenzi A. Distribution of osteonic and interstitial components in the human femoral shaft with reference to structure, calcification and mechanical properties. Acta Anat (Basel). 1983;115:178-86.
[161] Ascenzi A, Boyde A, Portigliatti Barbos M, Carando S. Micro-biomechanics vs macro-biomechanics in cortical bone. A micromechanical investigation of femurs deformed by bending. J Biomech. 1987;20:1045-53.
[162] Portigliatti-Barbos M, Carando S, Ascenzi A, Boyde A. On the structural symmetry of human femurs. Bone. 1987;8:165-9.
[163] Carando S, Portigliatti Barbos M, Ascenzi A, Boyde A. Orientation of collagen in human tibial and fibular shaft and possible correlation with mechanical properties. Bone. 1989;10:139-42.
[164] Burstein AH, Zika JM, Heiple KG, Klein L. Contribution of collagen and mineral to the elastic-plastic properties of bone. J Bone Joint Surg Am. 1975;57:956-61.

[165] Martin RB, Boardman DL. The effects of collagen fiber orientation, porosity, density, and mineralization on bovine cortical bone bending properties. J Biomech. 1993;26:1047-54.
[166] Landis WJ. The strength of a calcified tissue depends in part on the molecular structure and organization of its constituent mineral crystals in their organic matrix. Bone. 1995;16:533-44.
[167] Puustjarvi K, Nieminen J, Rasanen T, Hyttinen M, Helminen HJ, Kroger H, et al. Do more highly organized collagen fibrils increase bone mechanical strength in loss of mineral density after one-year running training? J Bone Miner Res. 1999;14:321-9.
[168] W G. Ueber f inktionell wichtige Anordnungsweisen der feineren and groeberen Bauelemente des Wirbeltierknochens . It . Spezieller Teil . I . Der Ban der Havers schen lamellensysteme and seine funktionelle Bedeutung. Arch Entwicklungsmechanik. 1905:187-322.
[169] Ascenzi A, Bonucci E. The tensile properties of single osteons. Anat Rec. 1967;158:375-86.
[170] Graham JS, Vomund AN, Phillips CL, Grandbois M. Structural changes in human type I collagen fibrils investigated by force spectroscopy. Exp Cell Res. 2004;299:335-42.
[171] Shen ZL, Dodge MR, Kahn H, Ballarini R, Eppell SJ. Stress-strain experiments on individual collagen fibrils. Biophys J. 2008;95:3956-63.
[172] Yang L, Fitie CF, van der Werf KO, Bennink ML, Dijkstra PJ, Feijen J. Mechanical properties of single electrospun collagen type I fibers. Biomaterials. 2008;29:955-62.
[173] Yang L, van der Werf KO, Fitie CF, Bennink ML, Dijkstra PJ, Feijen J. Mechanical properties of native and cross-linked type I collagen fibrils. Biophys J. 2008;94:2204-11.
[174] Oxlund H, Barckman M, Ortoft G, Andreassen TT. Reduced concentrations of collagen cross-links are associated with reduced strength of bone. Bone. 1995;17:365S-71S.
[175] Oxlund H, Christensen H, Seyer-Hansen M, Andreassen TT. Collagen deposition and mechanical strength of colon anastomoses and skin incisional wounds of rats. J Surg Res. 1996;66:25-30.
[176] Kovach IS AC, Richards-Kortum R, Wang X, Athanasiou KA. Laser-induced autofluorescence and fracture toughness of baboon cortical bone. Trans Orthop Res SOC. 1997:37.
[177] Wang X, Bank RA, TeKoppele JM, Agrawal CM. The role of collagen in determining bone mechanical properties. J Orthop Res. 2001;19:1021-6.

[178] Jonas J, Burns J, Abel EW, Cresswell MJ, Strain JJ, Paterson CR. Impaired mechanical strength of bone in experimental copper deficiency. Ann Nutr Metab. 1993;37:245-52.
[179] Lees S, Hanson D, Page E, Mook HA. Comparison of dosage-dependent effects of beta-aminopropionitrile, sodium fluoride, and hydrocortisone on selected physical properties of cortical bone. J Bone Miner Res. 1994;9:1377-89.
[180] Nalla RK, Kruzic JJ, Ritchie RO. On the origin of the toughness of mineralized tissue: microcracking or crack bridging? Bone. 2004;34:790-8.
[181] Vashishth D, Behiri JC, Bonfield W. Crack growth resistance in cortical bone: concept of microcrack toughening. J Biomech. 1997;30:763-9.
[182] Vashishth D, Tanner KE, Bonfield W. Experimental validation of a microcracking-based toughening mechanism for cortical bone. J Biomech. 2003;36:121-4.
[183] Wang X, Qian C. Prediction of microdamage formation using a mineral-collagen composite model of bone. J Biomech. 2006;39:595-602.
[184] Nalla RK, Kruzic JJ, Kinney JH, Ritchie RO. Effect of aging on the toughness of human cortical bone: evaluation by R-curves. Bone. 2004;35:1240-6.
[185] Kruzic JJ, Nalla RK, Kinney JH, Ritchie RO. Crack blunting, crack bridging and resistance-curve fracture mechanics in dentin: effect of hydration. Biomaterials. 2003;24:5209-21.
[186] Nalla RK, Kinney JH, Ritchie RO. Mechanistic fracture criteria for the failure of human cortical bone. Nat Mater. 2003;2:164-8.
[187] Pezzotti G, Sakakura S. Study of the toughening mechanisms in bone and biomimetic hydroxyapatite materials using Raman microprobe spectroscopy. J Biomed Mater Res A. 2003;65:229-36.
[188] Office for National Statistics. Overview of the UK population: August 2019. Retrieved April 2020 from https://wwwonsgovuk/peoplepopulationandcommunity/populationandmigration/populationestimates/articles/overviewoftheukpopulation/august2019. 2019.
[189] Wang X, Puram S. The toughness of cortical bone and its relationship with age. Ann Biomed Eng. 2004;32:123-35.
[190] Seeman E. Reduced bone formation and increased bone resorption: rational targets for the treatment of osteoporosis. Osteoporos Int. 2003;14 Suppl 3:S2-8.
[191] Yerramshetty JS, Lind C, Akkus O. The compositional and physicochemical homogeneity of male femoral cortex increases after the sixth decade. Bone. 2006;39:1236-43.

[192] Langdahl BL, Ralston SH, Grant SF, Eriksen EF. An Sp1 binding site polymorphism in the COLIA1 gene predicts osteoporotic fractures in both men and women. J Bone Miner Res. 1998;13:1384-9.
[193] Mann V, Hobson EE, Li B, Stewart TL, Grant SF, Robins SP, et al. A COL1A1 Sp1 binding site polymorphism predisposes to osteoporotic fracture by affecting bone density and quality. J Clin Invest. 2001;107:899-907.
[194] Kovach IS AC, Richards-Kortum R, Wang X, Athanasiou KA. Laser-induced autofluorescence and fracture toughness of baboon cortical hone. Trans Orthop Res Soc. 1997;22.
[195] Wang X, Shen X, Li X, Agrawal CM. Age-related changes in the collagen network and toughness of bone. Bone. 2002;31:1-7.
[196] Danielsen CC, Mosekilde L, Bollerslev J, Mosekilde L. Thermal stability of cortical bone collagen in relation to age in normal individuals and in individuals with osteopetrosis. Bone. 1994;15:91-6.
[197] Oxlund H, Mosekilde L, Ortoft G. Reduced concentration of collagen reducible cross links in human trabecular bone with respect to age and osteoporosis. Bone. 1996;19:479-84.
[198] Burr DB, Forwood MR, Fyhrie DP, Martin RB, Schaffler MB, Turner CH. Bone microdamage and skeletal fragility in osteoporotic and stress fractures. J Bone Miner Res. 1997;12:6-15.
[199] Grabner B, Landis WJ, Roschger P, Rinnerthaler S, Peterlik H, Klaushofer K, et al. Age- and genotype-dependence of bone material properties in the osteogenesis imperfecta murine model (oim). Bone. 2001;29:453-7.
[200] Reid SA, Boyde A. Changes in the mineral density distribution in human bone with age: image analysis using backscattered electrons in the SEM. J Bone Miner Res. 1987;2:13-22.
[201] Zagba-Mongalima G, Goret-Nicaise M, Dhem A. Age changes in human bone: a microradiographic and histological study of subperiosteal and periosteal calcifications. Gerontology. 1988;34:264-76.
[202] Ruff CB, Hayes WC. Age changes in geometry and mineral content of the lower limb bones. Ann Biomed Eng. 1984;12:573-84.
[203] Basle MF, Mauras Y, Audran M, Clochon P, Rebel A, Allain P. Concentration of bone elements in osteoporosis. J Bone Miner Res. 1990;5:41-7.
[204] Riggs BL, Melton LJ, 3rd. Involutional osteoporosis. N Engl J Med. 1986;314:1676-86.

[205] Kiebzak GM, Smith R, Gundberg CC, Howe JC, Sacktor B. Bone status of senescent male rats: chemical, morphometric, and mechanical analysis. J Bone Miner Res. 1988;3:37-45.
[206] Kiebzak GM, Smith R, Howe JC, Gundberg CM, Sacktor B. Bone status of senescent female rats: chemical, morphometric, and biomechanical analyses. J Bone Miner Res. 1988;3:439-46.
[207] Hruza Z, Wachtlova M. Diminution of bone blood flow and capillary network in rats during aging. J Gerontol. 1969;24:315-20.
[208] Brindley GW, Williams EA, Bronk JT, Meadows TH, Montgomery RJ, Smith SR, et al. Parathyroid hormone effects on skeletal exchangeable calcium and bone blood flow. Am J Physiol. 1988;255:H94-100.
[209] Matsushima N, Hikichi K. Age changes in the crystallinity of bone mineral and in the disorder of its crystal. Biochim Biophys Acta. 1989;992:155-9.
[210] Tonna EA. Electron microscopic study of bone surface changes during aging. The loss of cellular control and biofeedback. J Gerontol. 1978;33:163-77.
[211] Irving JT, LeBolt SA, Schneider EL. Ectopic bone formation and aging. Clin Orthop Relat Res. 1981:249-53.
[212] Nishimoto SK, Chang CH, Gendler E, Stryker WF, Nimni ME. The effect of aging on bone formation in rats: biochemical and histological evidence for decreased bone formation capacity. Calcif Tissue Int. 1985;37:617-24.
[213] Vernon-Roberts B, Pirie CJ. Healing trabecular microfractures in the bodies of lumbar vertebrae. Ann Rheum Dis. 1973;32:406-12.
[214] Sharpe WD. Age changes in human bone: an overview. Bull N Y Acad Med. 1979;55:757-73.
[215] Martin RB, Pickett JC, Zinaich S. Studies of skeletal remodeling in aging men. Clin Orthop Relat Res. 1980:268-82.
[216] Martin B. Aging and strength of bone as a structural material. Calcif Tissue Int. 1993;53 Suppl 1:S34-9; discussion S9-40.
[217] Zioupos P, Wang XT, Currey JD. The accumulation of fatigue microdamage in human cortical bone of two different ages in vitro. Clin Biomech (Bristol, Avon). 1996;11:365-75.
[218] Li GP, Zhang SD, Chen G, Chen H, Wang AM. Radiographic and histologic analyses of stress fracture in rabbit tibias. Am J Sports Med. 1985;13:285-94.
[219] Parfitt AM. The coupling of bone formation to bone resorption: a critical analysis of the concept and of its relevance to the pathogenesis of osteoporosis. Metab Bone Dis Relat Res. 1982;4:1-6.

[220] Ingram RT, Collazo-Clavell M, Tiegs R, Fitzpatrick LA. Paget's disease is associated with changes in the immunohistochemical distribution of noncollagenous matrix proteins in bone. J Clin Endocrinol Metab. 1996;81:1810-20.
[221] Martin RB, Lau ST, Mathews PV, Gibson VA, Stover SM. Collagen fiber organization is related to mechanical properties and remodeling in equine bone. A comparison of two methods. J Biomech. 1996;29:1515-21.
[222] Nyssen-Behets C, Duchesne PY, Dhem A. Structural changes with aging in cortical bone of the human tibia. Gerontology. 1997;43:316-25.
[223] Court-Brown CM, Caesar B. Epidemiology of adult fractures: A review. Injury. 2006;37:691-7.
[224] Carter DR, Hayes WC. The compressive behavior of bone as a two-phase porous structure. J Bone Joint Surg Am. 1977;59:954-62.
[225] Russo CR, Lauretani F, Bandinelli S, Bartali B, Di Iorio A, Volpato S, et al. Aging bone in men and women: beyond changes in bone mineral density. Osteoporosis international. 2003;14:531-38.
[226] Bailey DA, Faulkner RA, McKay HA. Growth, physical activity, and bone mineral acquisition. Exerc Sport Sci Rev. 1996;24:233-66.
[227] Judex S, Zernicke RF. High-impact exercise and growing bone: relation between high strain rates and enhanced bone formation. Journal of Applied Physiology. 2000;88:2183-91.
[228] Zernicke KC, Barnard RF, Li AF. Differential response of rat limb bones to strenuous exercise. Journal of Applied Physiology. 1991;70:554-60.
[229] Forwood MR, Parker AW. Repetitive loading, in vivo, of the tibiae and femora of rats: effects of repeated bouts of treadmill-running. Bone and mineral. 1991;13:35-46.
[230] Bradney M, Pearce G, Naughton G, Sullivan C, Bass S, Beck T, et al. Moderate exercise during growth in prepubertal boys: changes in bone mass, size, volumetric density, and bone strength: a controlled prospective study. Journal of Bone and Mineral Research. 1998;13:1814-21.
[231] Courteix DE, Lespessailles S, Peres SL, Obert PG, Benhamou CL. Effect of physical training on bone mineral density in prepubertal girls: a comparative study between impact-loading and non-impact-loading sports. Osteoporosis International. 1998;8:152-58.
[232] Lloyd T, Chinchilli VM, Johnson-Rollings N, Kieselhorst K, Eggli DF, Marcus R. Adult female hip bone density reflects teenage sports–exercise patterns but not teenage calcium intake. Pediatrics. 2000;106:40-4.

[233] Nilsson M, Ohlsson C, Mellström D, Lorentzon M. Sport-specific association between exercise loading and the density, geometry, and microstructure of weight-bearing bone in young adult men. Osteoporosis International. 2013;24:1613-22.
[234] Johnston CC, Slemenda CW. Peak bone mass, bone loss and risk of fracture. Osteoporosis international. 1994;4:43-5.
[235] Tai BL, Palmisano AC, Belmont B, Irwin TA, Holmes J, Shih AJ. Numerical evaluation of sequential bone drilling strategies based on thermal damage. Medical engineering & physics,. 2015;37:855-61.
[236] Ohman C, Baleani M, Pani C, Taddei F, Alberghini M, Viceconti M, et al. Compressive behaviour of child and adult cortical bone. Bone. 2011;49:769-76.
[237] Tanner JM, Whitehouse RH, Marshall WA, Healy MR. Assessment of Skeletal Maturity and Prediction of Adult Height. London Academic Press. 1975.
[238] Tanner J, Oshman D, Bahhage F, Healy M. Tanner-Whitehouse bone age reference values for North American children. The Journal of pediatrics. 1997;131:34-40.
[239] Bigot G, Bouzidi A, Rumelhart C, Martin-Rosset W. Evolution during growth of the mechanical properties of the cortical bone in equine cannon-bones. Med Eng Phys. 1996;18:79-87.
[240] Nafei A, Danielsen CC, Linde F, Hvid I. Properties of growing trabecular ovine bone. Part I: mechanical and physical properties. J Bone Joint Surg Br. 2000;82:910-20.
[241] Wang X, Shen X, Li X, Agrawal CM. Age-related changes in the collagen network and toughness of bone. Bone. 2002;31:1-7.
[242] Forman JL, de Dios, E., Symeonidis, I., Duart, J., Kerrigan, J. R., Salzar, R. S., Balasubramanian, S., Segui-Gomez, M., & Kent, R. W. Fracture tolerance related to skeletal development and aging throughout life: 3-point bending of human femurs. Paper presented at the IRCOBI Conference Proceedings,. 2012;Dublin, Ireland.
[243] Sai H, Iguchi G, Tobimatsu T, Takahashi K, Yoh K. Novel ultrasonic bone densitometry based on two longitudinal waves: significant correlation with pQCT measurement values and age-related changes in trabecular bone density, cortical thickness, and elastic modulus of trabecular bone in a normal Japanese population. Osteoporosis international. 2010;21:1781-90.
[244] Steiger P, Cummings SR, Black DM, Spencer NE, Genant HK. Age-related decrements in bone mineral density in women over 65. J Bone Miner Res. 1992;7:625-32.
[245] Campbell-Furtick M, Moore BJ, Overton TL, Phillips JL, Simon KJ, Gandhi RR, et al. Post-trauma mortality increase at age 60: a cutoff for defining elderly? The American Journal of Surgery. 2016;212:781-5.

[246] MacKenzie EJ, Rivara F, Jurkovich G, Nathens A, Frey K, Egleston B, et al. A national evaluation of the effect of trauma-center care on mortality. New England Journal of Medicine. 2006;354:366-78.
[247] Phillips S, Rond PC, Kelly SM, Swartz PD. The failure of triage criteria to identify geriatric patients with trauma: results from the Florida Trauma Triage Study. Journal of Trauma and Acute Care Surgery. 1996;40:278-83.
[248] Staudenmayer KL, Hsia RY, Mann NC, Spain DA, Newgard CD. Triage of elderly trauma patients: a population-based perspective. Journal of the American College of Surgeons. 2013;217:569-76.
[249] Nelson HD, Helfand M, Woolf SH, Allan JD. Screening for postmenopausal osteoporosis: a review of the evidence for the U.S. Preventive Services Task Force. Ann Intern Med. 2002;137:529-41.
[250] Schousboe JT, Ensrud KE, Nyman JA, Melton LJ, 3rd, Kane RL. Universal bone densitometry screening combined with alendronate therapy for those diagnosed with osteoporosis is highly cost-effective for elderly women. J Am Geriatr Soc. 2005;53:1697-704.
[251] Kanis JA, Oden A, Johnell O, Jonsson B, de Laet C, Dawson A. The burden of osteoporotic fractures: a method for setting intervention thresholds. Osteoporos Int. 2001;12:417-27.
[252] Oden A, McCloskey EV, Kanis JA, Harvey NC, Johansson H. Burden of high fracture probability worldwide: secular increases 2010-2040. Osteoporos Int. 2015;26:2243-8.
[253] Burge RT, Worley D, Johansen A, Bhattacharyya S, Bose U. The cost of osteoporotic fractures in the UK: projections for 2000–2020. Journal of Medical Economics,. 2001;4:51-62.
[254] Kanis JA. Assessment of fracture risk and its application to screening for postmenopausal osteoporosis: synopsis of a WHO report. WHO Study Group. Osteoporos Int. 1994;4:368-81.
[255] Schuit SC, van der Klift M, Weel AE, de Laet CE, Burger H, Seeman E, et al. Fracture incidence and association with bone mineral density in elderly men and women: the Rotterdam Study. Bone. 2004;34:195-202.
[256] Thurner PJ, Chen CG, Ionova-Martin S, Sun L, Harman A, Porter A, et al. Osteopontin deficiency increases bone fragility but preserves bone mass. Bone. 2010;46:1564-73.
[257] Ahlborg HG, Johnell O, Turner CH, Rannevik G, Karlsson MK. Bone loss and bone size after menopause. N Engl J Med. 2003;349:327-34.

[258] Kindblom JM, Lorentzon M, Norjavaara E, Hellqvist A, Nilsson S, Mellstrom D, et al. Pubertal timing predicts previous fractures and BMD in young adult men: the GOOD study. J Bone Miner Res. 2006;21:790-5.
[259] Lindsay R, Hart DM, Forrest C. Effect of a natural and artificial menopause on serum, urinary and erythrocyte magnesium. Clin Sci (Lond). 1980;58:255-7.
[260] Toussirot E, Royet O, Wendling D. [Aetiologic features of osteoporosis in male patients aged less than 50 years: study of 28 cases with a comparative series of 30 patients over the age of 50]. Rev Med Interne. 1998;19:479-85.
[261] Jarvinen TL, Sievanen H, Khan KM, Heinonen A, Kannus P. Shifting the focus in fracture prevention from osteoporosis to falls. BMJ. 2008;336:124-6.
[262] Kanis JA, Delmas P, Burckhardt P, Cooper C, Torgerson D. Guidelines for diagnosis and management of osteoporosis. The European Foundation for Osteoporosis and Bone Disease. Osteoporos Int. 1997;7:390-406.
[263] Kanis JA, Gluer CC. An update on the diagnosis and assessment of osteoporosis with densitometry. Committee of Scientific Advisors, International Osteoporosis Foundation. Osteoporos Int. 2000;11:192-202.
[264] Marshall D, Johnell O, Wedel H. Meta-analysis of how well measures of bone mineral density predict occurrence of osteoporotic fractures. BMJ. 1996;312:1254-9.
[265] Stone KL, Seeley DG, Lui LY, Cauley JA, Ensrud K, Browner WS, et al. BMD at multiple sites and risk of fracture of multiple types: long-term results from the Study of Osteoporotic Fractures. J Bone Miner Res. 2003;18:1947-54.
[266] Johnell O, Kanis JA, Oden A, Johansson H, De Laet C, Delmas P, et al. Predictive value of BMD for hip and other fractures. J Bone Miner Res. 2005;20:1185-94.
[267] Wang X, Sanyal A, Cawthon PM, Palermo L, Jekir M, Christensen J, et al. Prediction of new clinical vertebral fractures in elderly men using finite element analysis of CT scans. J Bone Miner Res. 2012;27:808-16.
[268] Anderson DE, Demissie S, Allaire BT, Bruno AG, Kopperdahl DL, Keaveny TM, et al. The associations between QCT-based vertebral bone measurements and prevalent vertebral fractures depend on the spinal locations of both bone measurement and fracture. Osteoporos Int. 2014;25:559-66.
[269] Shapiro JR, Stover ML, Burn VE, McKinstry MB, Burshell AL, Chipman SD, et al. An osteopenic nonfracture syndrome with features of mild osteogenesis imperfecta associated with the substitution of a cysteine for glycine at triple helix position 43 in the pro alpha 1(I) chain of type I collagen. J Clin Invest. 1992;89:567-73.

[270] Mesfin A, Nesterenko SO, Al-Hourani KG, Jain A, Sponseller PD. Management of hangman's fractures and a subaxial compression fracture in two children with osteogenesis imperfecta. J Surg Orthop Adv. 2013;22:326-9.
[271] Rauch F, Glorieux FH. Osteogenesis imperfecta. Lancet. 2004;363:1377-85.
[272] Byers PH. Osteogenesis imperfecta: perspectives and opportunities. Curr Opin Pediatr. 2000;12:603-9.
[273] Fratzl P, Paris O, Klaushofer K, Landis WJ. Bone mineralization in an osteogenesis imperfecta mouse model studied by small-angle x-ray scattering. J Clin Invest. 1996;97:396-402.
[274] Camacho NP, Hou L, Toledano TR, Ilg WA, Brayton CF, Raggio CL, et al. The material basis for reduced mechanical properties in oim mice bones. J Bone Miner Res. 1999;14:264-72.
[275] Rauch F, Travers R, Parfitt AM, Glorieux FH. Static and dynamic bone histomorphometry in children with osteogenesis imperfecta. Bone. 2000;26:581-9.
[276] Misof K, Landis WJ, Klaushofer K, Fratzl P. Collagen from the osteogenesis imperfecta mouse model (oim) shows reduced resistance against tensile stress. J Clin Invest. 1997;100:40-5.
[277] Wharton B, Bishop N. Rickets. Lancet. 2003;362:1389-400.
[278] Chapman T, Sugar N, Done S, Marasigan J, Wambold N, Feldman K. Fractures in infants and toddlers with rickets. Pediatr Radiol. 2010;40:1184-9.
[279] Thacher TD, Fischer PR, Pettifor JM. The effect of nutritional rickets on bone mineral density. J Clin Endocrinol Metab. 2014;99:4174-80.
[280] Subit D, Arregui C, Salzar R, J C. Pediatric, Adult and Elderly Bone Material Properties. IRCOBI Conference. 2013:760-9.
[281] Bowman SM, Zeind J, Gibson LJ, Hayes WC, McMahon TA. The tensile behavior of demineralized bovine cortical bone. J Biomech. 1996;29:1497-501.
[282] Shah KM, Goh JC, Karunanithy R, Low SL, Das De S, Bose K. Effect of decalcification on bone mineral content and bending strength of feline femur. Calcif Tissue Int. 1995;56:78-82.
[283] Hey CD, Stainsby G. The Enhanced Solubility of Collagen Following Alkaline Treatment. Biochim Biophys Acta. 1965;97:364-6.
[284] Amadasi A, Camici A, Porta D, Cucca L, Merli D, Milanese C, et al. Assessment of the Effects Exerted by Acid and Alkaline Solutions on Bone: Is Chemistry the Answer? J Forensic Sci. 2017;62:1297-303.

[285] Privalov PL. Stability of proteins. Proteins which do not present a single cooperative system. Adv Protein Chem. 1982;35:1-104.
[286] Yang H, Shu Z. The extraction of collagen protein from pigskin. Journal of Chemical and Pharmaceutical Research. 2014;6:683-7.
[287] Bi L, Li DC, Huang ZS, Yuan Z. Effects of sodium hydroxide, sodium hypochlorite, and gaseous hydrogen peroxide on the natural properties of cancellous bone. Artif Organs. 2013;37:629-36.
[288] Barzel US. The skeleton as an ion exchange system: implications for the role of acid-base imbalance in the genesis of osteoporosis. J Bone Miner Res. 1995;10:1431-6.
[289] Arnett TR. Extracellular pH regulates bone cell function. J Nutr. 2008;138:415S-8S.
[290] Arnett TR, Dempster DW. Effect of pH on bone resorption by rat osteoclasts in vitro. Endocrinology. 1986;119:119-24.
[291] Galloway TL, Johnston MJ, Starsiak MD, Silverman ED. A Unique Case of Increased 18F-FDG Metabolic Activity in the Soft Tissues of the Bilateral Upper Thighs Due to Immunizations in a Pediatric Patient. World J Nucl Med. 2017;16:59-61.
[292] Merck Research Labs. The Merck Index, Rahway NJ,. 1983;10th Edition.:1471.
[293] Davidson MK, Lindsey JR, Davis JK. Requirements and selection of an animal model. Isr J Med Sci. 1987;23:551-5.
[294] Nunamaker DM. Experimental models of fracture repair. Clin Orthop Relat Res. 1998:S56-65.
[295] Bergmann G, Graichen F, Rohlmann A. Hip joint forces in sheep. J Biomech. 1999;32:769-77.
[296] Newman E, Turner AS, Wark JD. The potential of sheep for the study of osteopenia: current status and comparison with other animal models. Bone. 1995;16:277S-84S.
[297] Arens D, Sigrist I, Alini M, Schawalder P, Schneider E, Egermann M. Seasonal changes in bone metabolism in sheep. Vet J. 2007;174:585-91.
[298] Aerssens J, Boonen S, Lowet G, Dequeker J. Interspecies differences in bone composition, density, and quality: potential implications for in vivo bone research. Endocrinology. 1998;139:663-70.
[299] Chu CR, Szczodry M, Bruno S. Animal models for cartilage regeneration and repair. Tissue Eng Part B Rev. 2010;16:105-15.
[300] Libbin RM, Rivera ME. Regeneration of growth plate cartilage induced in the neonatal rat hindlimb by reamputation. J Orthop Res. 1989;7:674-82.

[301] Moran CJ, Ramesh A, Brama PA, O'Byrne JM, O'Brien FJ, Levingstone TJ. The benefits and limitations of animal models for translational research in cartilage repair. J Exp Orthop. 2016;3:1.
[302] Alffram PA, Bauer GC. Epidemiology of fractures of the forearm. A biomechanical investigation of bone strength. J Bone Joint Surg Am. 1962;44-A:105-14.
[303] Salminen ST, Pihlajamaki HK, Avikainen VJ, Bostman OM. Population based epidemiologic and morphologic study of femoral shaft fractures. Clin Orthop Relat Res. 2000:241-9.
[304] Weiss RJ, Montgomery SM, Al Dabbagh Z, Jansson KA. National data of 6409 Swedish inpatients with femoral shaft fractures: stable incidence between 1998 and 2004. Injury. 2009;40:304-8.
[305] Bengner U, Ekbom T, Johnell O, Nilsson BE. Incidence of femoral and tibial shaft fractures. Epidemiology 1950-1983 in Malmo, Sweden. Acta Orthop Scand. 1990;61:251-4.
[306] Donaldson LJ, Cook A, Thomson RG. Incidence of fractures in a geographically defined population. J Epidemiol Community Health. 1990;44:241-5.
[307] Arneson TJ, Melton LJ, 3rd, Lewallen DG, O'Fallon WM. Epidemiology of diaphyseal and distal femoral fractures in Rochester, Minnesota, 1965-1984. Clin Orthop Relat Res. 1988:188-94.
[308] Singer BR, McLauchlan GJ, Robinson CM, Christie J. Epidemiology of fractures in 15,000 adults: the influence of age and gender. J Bone Joint Surg Br. 1998;80:243-8.
[309] Wolinsky PR, McCarty E, Shyr Y, Johnson K. Reamed intramedullary nailing of the femur: 551 cases. J Trauma. 1999;46:392-9.
[310] Nafei A, Teichert G, Mikkelsen SS, Hvid I. Femoral shaft fractures in children: an epidemiological study in a Danish urban population, 1977-86. J Pediatr Orthop. 1992;12:499-502.
[311] Fry K, Hoffer MM, Brink J. Femoral shaft fractures in brain-injured children. J Trauma. 1976;16:371-3.
[312] Hedlund R, Ahlbom A, Lindgren U. Hip fracture incidence in Stockholm 1972-1981. Acta Orthop Scand. 1986;57:30-4.
[313] Blakemore LC, Loder RT, Hensinger RN. Role of intentional abuse in children 1 to 5 years old with isolated femoral shaft fractures. J Pediatr Orthop. 1996;16:585-8.
[314] Hinton RY, Lincoln A, Crockett MM, Sponseller P, Smith G. Fractures of the femoral shaft in children. Incidence, mechanisms, and sociodemographic risk factors. J Bone Joint Surg Am. 1999;81:500-9.

[315] Heideken J, Svensson T, Blomqvist P, Haglund-Akerlind Y, Janarv PM. Incidence and trends in femur shaft fractures in Swedish children between 1987 and 2005. J Pediatr Orthop. 2011;31:512-9.
[316] A S, G L, C D, JA B, B S, MF. S. Clinical and functional outcomes of internal fixation of displaced pilon fractures. Clinical orthopaedics and related research. 1998;347:131-7.
[317] Kress T PD, Snider J, Fuller P, Psihigios J, Heck W, Frick S, Wasserman J. Fracture Patterns of Human Cadaver Long Bones. Paper presented at the International Research of Crash Biomechanics and Impact (IRCOBI). 1995;Brunnen, Switzerland.
[318] Cheong VS, Karunaratne A, Amis AA, Bull AMJ. Strain rate dependency of fractures of immature bone. J Mech Behav Biomed Mater. 2017;66:68-76.
[319] Hibbeler R. Mechanics of Materials. Prentice Hall. 2008.
[320] Anderson DD, Kilburg AT, Thomas TP, Marsh JL. Expedited CT-based methods for evaluating fracture severity to assess risk of post-traumatic osteoarthritis after articular fractures. The Iowa orthopaedic journal. 2016;36:46.
[321] Nafei A, Danielsen CC, Linde F, Hvid I. Properties of growing trabecular ovine bone. Part I: mechanical and physical properties. J Bone Joint Surg Br. 2000;82:910-20.
[322] Nafei A, Kabel J, Odgaard A, Linde F, Hvid I. Properties of growing trabecular ovine bone. Part II: architectural and mechanical properties. J Bone Joint Surg Br. 2000;82:921-7.
[323] van Haaren EH, van der Zwaard BC, van der Veen AJ, Heyligers IC, Wuisman PI, Smit TH. Effect of long-term preservation on the mechanical properties of cortical bone in goats. Acta Orthop. 2008;79:708-16.
[324] Topp T, Muller T, Huss S, Kann PH, Weihe E, Ruchholtz S, et al. Embalmed and fresh frozen human bones in orthopedic cadaveric studies: which bone is authentic and feasible? Acta Orthop. 2012;83:543-7.
[325] Alers JC, Krijtenburg PJ, Vissers KJ, van Dekken H. Effect of bone decalcification procedures on DNA in situ hybridization and comparative genomic hybridization. EDTA is highly preferable to a routinely used acid decalcifier. J Histochem Cytochem. 1999;47:703-10.
[326] FM S, GI B, J B, C T, MA W. Comparison of different decalcification methods using rat mandibles as a model. Journal of Histochemistry & Cytochemistry. 2017;65:705-22.
[327] Thorpe EJ, Bellomy BB, Sellers RF. Ultrasonic Decalcification of Bone. An Experimental and Clinical Study. J Bone Joint Surg Am. 1963;45:1257-9.
[328] Burr DB, Milgrom C, Fyhrie D, Forwood M, Nyska M, Finestone A, et al. In vivo measurement of human tibial strains during vigorous activity. Bone. 1996;18:405-10.

[329] Timoshenko SY, DH. Elements of strength of materials. Ed Van Nostrand, D. 1968.
[330] Melbourne. TRCsH. Clinical Practice Guidelines: Femoral Shaft Fractures. Site visited 2018: https://wwwrchorgau/clinicalguide/guideline_index/fractures/femoral_shaft_emergency/. 2011.
[331] National Institute of Clinical Excellence. Limb and joint fractures in hospital - NICE Pathways. Site Visited 2018: https://wwwniceorguk/guidance/. 2016.
[332] Landin LA. Fracture patterns in children. Analysis of 8,682 fractures with special reference to incidence, etiology and secular changes in a Swedish urban population 1950-1979. Acta Orthop Scand Suppl. 1983;202:1-109.
[333] Grunkemeier GL, Jin R. Receiver operating characteristic curve analysis of clinical risk models. Ann Thorac Surg. 2001;72:323-6.
[334] Landis JR, Koch GG. The measurement of observer agreement for categorical data. Biometrics. 1977;33:159-74.
[335] Yamada H, Evans FG. Strength of biological materials. 1970.
[336] Mizrahi J, Silva MJ, Keaveny TM, Edwards WT, Hayes WC. Finite-element stress analysis of the normal and osteoporotic lumbar vertebral body. Spine (Phila Pa 1976). 1993;18:2088-96.
[337] Zioupos P CJ. The extent of microcracking and the morphology of microcracks in damaged bone. Journal of Materials Science. 1994;29:978-86.
[338] Vose GP. The relation of microscopic mineralization to intrinsic bone strength. Anat Rec. 1962;144:31-6.
[339] Todoh M, Tadano S, B. G, Nishimoto M. Effect of gradual demineralization on the mineral fraction and mechanical properties of cortical bone. Journal of Biomechanical Science and Engineering. 2009;4:230-38.
[340] Rho JY, Zioupos P, Currey JD, Pharr GM. Microstructural elasticity and regional heterogeneity in human femoral bone of various ages examined by nano-indentation. J Biomech. 2002;35:189-98.
[341] Currey JD. The effect of porosity and mineral content on the Young's modulus of elasticity of compact bone. J Biomech. 1988;21:131-9.
[342] Schaffler MB, Burr DB. Stiffness of compact bone: effects of porosity and density. J Biomech. 1988;21:13-6.
[343] Currey JD. Physical characteristics affecting the tensile failure properties of compact bone. J Biomech. 1990;23:837-44.

[344] Les CM, Stover SM, Keyak JH, Taylor KT, Kaneps AJ. Stiff and strong compressive properties are associated with brittle post-yield behavior in equine compact bone material. J Orthop Res. 2002;20:607-14.
[345] Currey JD, Foreman J, Laketic I, Mitchell J, Pegg DE, Reilly GC. Effects of ionizing radiation on the mechanical properties of human bone. J Orthop Res. 1997;15:111-7.
[346] Gupta HS, Seto J, Wagermaier W, Zaslansky P, Boesecke P, Fratzl P. Cooperative deformation of mineral and collagen in bone at the nanoscale. Proc Natl Acad Sci U S A. 2006;103:17741-6.
[347] Gao H. Application of fracture mechanics concepts to hierarchical biomechanics of bone and bone-like materials. Int J Fracture. 2006;138:101-37.
[348] Hull D CT. An Introduction to composite materials. 1996:124.
[349] Knott L, Whitehead CC, Fleming RH, Bailey AJ. Biochemical changes in the collagenous matrix of osteoporotic avian bone. Biochem J. 1995;310 ( Pt 3):1045-51.
[350] Mashiba T, Hirano T, Turner CH, Forwood MR, Johnston CC, Burr DB. Suppressed bone turnover by bisphosphonates increases microdamage accumulation and reduces some biomechanical properties in dog rib. J Bone Miner Res. 2000;15:613-20.
[351] Ettinger B, Burr DB, Ritchie RO. Proposed pathogenesis for atypical femoral fractures: lessons from materials research. Bone. 2013;55:495-500.
[352] Sasaki S, Miyakoshi N, Hongo M, Kasukawa Y, Shimada Y. Low-energy diaphyseal femoral fractures associated with bisphosphonate use and severe curved femur: a case series. J Bone Miner Metab. 2012;30:561-7.
[353] Oh Y, Wakabayashi Y, Kurosa Y, Fujita K, Okawa A. Potential pathogenic mechanism for stress fractures of the bowed femoral shaft in the elderly: Mechanical analysis by the CT-based finite element method. Injury. 2014;45:1764-71.
[354] Smith CB, Smith DA. Relations between age, mineral density and mechanical properties of human femoral compacta. Acta Orthop Scand. 1976;47:496-502.
[355] Singer K, Edmondston S, Day R, Breidahl P, Price R. Prediction of thoracic and lumbar vertebral body compressive strength: correlations with bone mineral density and vertebral region. Bone. 1995;17:167-74.
[356] Dent CE, Smellie JM, Watson I. Studies in Osteopetrosis. Arch Dis Child. 1965;40:7-15.
[357] Ashman RB, Van Buskirk WC, Cowin SC, Sandborn PM, Wells MK, Rice JC. The mechanical properties of immature osteopetrotic bone. Calcified tissue international. 1985;37:73-6.

[358] Hasson D, Armstrong R. A ductile-to-brittle transition in bone? Journal of Materials Science. 1974;9.
[359] Currey JD. The design of mineralised hard tissues for their mechanical functions. J Exp Biol. 1999;202:3285-94.
[360] Allen MR, Gineyts E, Leeming DJ, Burr DB, Delmas PD. Bisphosphonates alter trabecular bone collagen cross-linking and isomerization in beagle dog vertebra. Osteoporos Int. 2008;19:329-37.
[361] Ma S, Goh EL, Jin A, Bhattacharya R, Boughton OR, Patel B, et al. Long-term effects of bisphosphonate therapy: perforations, microcracks and mechanical properties. Sci Rep. 2017;7:43399.
[362] Currey J. Bones: Structure and Mechanics. Princeton University Press ,Oxford,. 2002.
[363] Brear KCJ, Pond CM. Ontogenetic changes in the mechanical properties of the femur of the polar bear Ursus Maritimus. Journal of Zoology (London). 1990;222:49-58.
[364] Fakhry SM, Rutledge R, Dahners LE, Kessler D. Incidence, management, and outcome of femoral shaft fracture: a statewide population-based analysis of 2805 adult patients in a rural state. J Trauma. 1994;37:255-60; discussion 60-1.
[365] Enninghorst N, McDougall D, Evans JA, Sisak K, Balogh ZJ. Population-based epidemiology of femur shaft fractures. J Trauma Acute Care Surg. 2013;74:1516-20.
[366] Baxter-Jones AD, Faulkner RA, Forwood MR, Mirwald RL, Bailey DA. Bone mineral accrual from 8 to 30 years of age: an estimation of peak bone mass. J Bone Miner Res. 2011;26:1729-39.
[367] Arlot ME, Sornay-Rendu E, Garnero P, Vey-Marty B, Delmas PD. Apparent pre- and postmenopausal bone loss evaluated by DXA at different skeletal sites in women: the OFELY cohort. J Bone Miner Res. 1997;12:683-90.
[368] Adami S. Optimizing peak bone mass: what are the therapeutic possibilities? Osteoporos Int. 1994;4 Suppl 1:27-30.
[369] Pentecost RL, Murray RA, Brindley HH. Fatigue, Insufficiency, and Pathologic Fractures. JAMA. 1964;187:1001-4.
[370] Dunwoody J, Villaggio P. A theory for brittle fracture in compression. Continuum Mech Thermodyn. 1993:243-54.
[371] Zdenek P, Baiant l, Yuyin Xiang. Size effect in compression fracture: Splitting crack band propagation. Journal of Engineering Mechanics. 1997;123:167-72.
[372] Cooper KL, Beabout JW, Swee RG. Insufficiency fractures of the sacrum. Radiology. 1985;156:15-20.

[373] Plint AC, Perry JJ, Correll R, Gaboury I, Lawton L. A randomized, controlled trial of removable splinting versus casting for wrist buckle fractures in children. Pediatrics. 2006;117:691-7.
[374] Zanchetta JR, Plotkin H, Alvarez Filgueira ML. Bone mass in children: normative values for the 2-20-year-old population. Bone. 1995;16:393S-9S.
[375] Berteau JP, Gineyts E, Pithioux M, Baron C, Boivin G, Lasaygues P, et al. Ratio between mature and immature enzymatic cross-links correlates with post-yield cortical bone behavior: An insight into greenstick fractures of the child fibula. Bone. 2015;79:190-5.
[376] Berteau JP, Gineyts E, Pithioux M, Baron C, Boivin G, Lasaygues P, et al. Ratio between mature and immature enzymatic cross-links correlates with post-yield cortical bone behavior: An insight into greenstick fractures of the child fibula. Bone. 2015;79:190-5.
[377] McBride SH, Evans SF, Knothe Tate ML. Anisotropic mechanical properties of ovine femoral periosteum and the effects of cryopreservation. J Biomech. 2011;44:1954-9.
[378] Allen MR, Hock JM, Burr DB. Periosteum: biology, regulation, and response to osteoporosis therapies. Bone. 2004;35:1003-12.
[379] Hughston JC. Fractures of the femur in children. South Med J. 1960;53:299-304.
[380] Smith IO, Ren F, Baumann MJ, Case ED. Confocal laser scanning microscopy as a tool for imaging cancellous bone. J Biomed Mater Res B Appl Biomater. 2006;79:185-92.
[381] Bromage TG, Goldman HM, McFarlin SC, Warshaw J, Boyde A, Riggs CM. Circularly polarized light standards for investigations of collagen fiber orientation in bone. Anat Rec B New Anat. 2003;274:157-68.